

Cellular and Molecular Mechanisms of Corneal Inflammation and Wound Healing

By

Debjani Gagen, BA Biology

DISSERTATION

In partial fulfillment of requirements of the degree of

DOCTOR OF PHILOSOPHY

in

PHYSIOLOGICAL OPTICS

Presented to the

Graduate faculty

of the

College of Optometry

University of Houston

August, 2011

DEDICATION

This dissertation is dedicated to my mother, the late Dipika DasGupta, my father, Ramlal DasGupta, and my sister, Roni DasGupta. Thank you all for everything you have sacrificed for me. I owe my current and future success to your unconditional love and unwavering support.

ACKNOWLEDGEMENTS

I would like to begin by thanking my advisor, Dr. Alan Burns, for his continuous support, guidance, and encouragement over the last 10 years. I could not have come this far without his remarkable patience and outstanding teaching skills. Dr. Burns, it was a genuine honor to work with you and words can not express my gratitude to for taking me under your wing and being such an extraordinary advisor and friend.

I would also like to express my deepest appreciation to my committee members Dr. Rolando Rumbaut, Dr. Alison McDermott, and Dr. William Miller. To Dr. Rumbaut, thank you for your help and support throughout my time at Baylor and for excellent guidance and encouragement during my time as a graduate student at University of Houston College of Optometry. To Dr. Alison McDermott, thank you for motivating me to strive for excellence and being a wonderful role model for female scientists. To Dr. William Miller, thank you for taking the time to participate in my committee and you're your encouragement.

I would like to also thank Dr. Laura Frishman, for all her dedication to individual student success and to the graduate program at UHCO. Dr. Frishman, you are the foundation of the program I respect you immensely for the time and effort you put towards your students.

I would also like to thank Dr. C.Wayne Smith, without whom I would have never had the opportunity to work in a laboratory. Dr. Smith, you opened the door for my future and I will always be grateful for your kindness, encouragement, and friendship. I would like to thank and acknowledge the hard work, dedication, and constant support of Mrs. Evelyn Brown. Evelyn, you will always be my "lab mom". Finally, I would like to

thank the staff and students at UHCO and Baylor College of Medicine, Section of Leukocyte Biology, for their support and friendship.

DISSERTATION ABSTRACT

Purpose: Accidental or surgical-induced trauma (e.g., refractive surgery) to the corneal epithelium results in keratocyte death immediately below the wound. Subsequent recovery of keratocytes during healing often remains incomplete, even after many years. Keratocytes produce essential proteins that help maintain corneal stability and preserve corneal clarity, and incomplete keratocyte repopulation after injury can result in loss of normal corneal structure (e.g., keratectasia) and impaired vision. To date, very little is known about the mechanisms regulating keratocyte repopulation. In the mouse, central corneal epithelial abrasion not only evokes keratocyte death, but also neutrophil (PMN), platelet, and $\gamma\delta$ T cell recruitment out of the limbal vessels and into the stroma. This inflammatory cell recruitment is necessary for efficient epithelial cell and epithelial nerve recovery. CD18, ICAM-1, and P-selectin are adhesion molecules linked to the regulated recruitment of these inflammatory cells. The purpose of this Dissertation is to determine if the molecular mechanisms regulating inflammatory cell recruitment into the injured cornea are necessary for keratocyte repopulation following central epithelial abrasion.

Methods: A 2 mm diameter central epithelial region was mechanically debrided from corneas of male wild type C57Bl/6 (WT), CD18 mutant (hypomorphic), ICAM-1^{-/-}, TCR δ ^{-/-} (deficient in $\gamma\delta$ T cells) and P-selectin^{-/-} mice. Injured and uninjured corneas were prepared for transmission electron microscopy or immunofluorescence microscopy. PMN-keratocyte interactions, total PMN infiltration (per mm²), total and extravascular (EV) platelet accumulation (per mm²), and keratocyte repopulation were morphometrically analyzed using stereological methods. *In vitro* analyses, using cultured mouse keratocytes and extravasated PMNs, were performed to investigate PMN motility on keratocytes.

Results: Previously, it was determined that PMN CD18 mediated close surface contacts between the PMN and keratocyte. The current studies show keratocyte ICAM-1, a ligand for CD18, also mediates PMN-keratocyte surface contact, and contacts were significantly reduced in ICAM-1^{-/-} mice compared to WT ($21.5 \pm 3.0\%$ versus $39.9 \pm 3.5\%$, respectively), consistent with the idea that ICAM-1 binds to PMN CD18 to mediate the cell-cell close surface contact. Antibody blockade of PMN CD18 or keratocyte ICAM-1 markedly reduced PMN motility on keratocytes, *in vitro* (by 33% and 47.5%, respectively), suggesting CD18 and ICAM-1 play a functional role in promoting PMN migration on keratocytes. PMN and platelet recruitment were greatest in ICAM-1^{-/-} mice and, 4 days after corneal abrasion, anterior central (AC) keratocyte numbers returned to baseline, demonstrating ICAM-1 negatively regulates PMN infiltration and platelet accumulation. AC keratocyte repopulation in WT and CD18 mutant mice was significantly lower than their respective baseline counts (by 28% and 56%, respectively). There were no differences in PMN infiltration between WT and CD18 mutant mice but platelet accumulation was blunted in CD18 mutant mice, suggesting platelets, not PMNs, participate in keratocyte recovery. Previous studies show platelet P-selectin and $\gamma\delta$ T cells are required for efficient epithelial healing. AC keratocyte repopulation in P-selectin^{-/-} and TCR δ ^{-/-} mice only recovered to 31% and 23% of their baselines, respectively. However, infusion of WT platelets into P-selectin^{-/-} mice “rescued” keratocyte repopulation, bringing it back to P-selectin baseline values. Additionally, AC keratocyte repopulation in platelet-depleted WT mice recovered to only 29% of WT baseline.

Conclusion: Collectively, these data confirm platelet recruitment is necessary for efficient keratocyte recovery. Interestingly, EV platelet recruitment in TCR δ ^{-/-} mice was greater than WT (by 62%) although keratocyte repopulation was low; however, EV platelets in TCR δ ^{-/-} mice showed less evidence of shape change, suggesting they were less “activated” in the absence of $\gamma\delta$ T cells. The evidence provided in this Dissertation

demonstrates a role for adhesion molecules and inflammatory cells in mediating PMN-keratocyte interactions, facilitating PMN migration, regulating inflammatory cell recruitment, and promoting keratocyte repopulation following corneal epithelial abrasion. Collectively, the data suggest this inflammatory cascade is necessary for keratocyte recovery during wound healing.

TABLE OF CONTENTS

LIST OF TABLES.....	vi
LIST OF FIGURES AND LEGENDS.....	vii
APPENDIX FIGURE LIST.....	ix
ABBREVIATIONS.....	x
THE NEED FOR NEW TREATMENT OPTIONS TO PROMOTE CORNEAL WOUND	
HEALING: AN OVERVIEW.....	1
CHAPTER 1: INTRODUCTION	5
1.1 OVERVIEW OF THE CORNEA	5
1.1.1 Corneal Morphogenesis	5
1.1.2 Corneal Anatomy and Physiology.....	6
1.1.2.1 Corneal Layers	6
1.1.2.2 Corneal Innervation	7
1.1.2.3 Corneal Collagen.....	8
1.1.2.4 Keratocytes.....	9
1.1.3 General Paradigm of Inflammation	10
1.1.3.1 Immune Cells.....	12
1.1.3.1.1 Neutrophils	13
1.1.3.1.2 Platelets.....	15
1.1.3.1.3 $\gamma\delta$ T-cells	17
1.1.3.2 Adhesion Molecules That Facilitate Immune Cell Infiltration.....	18
1.1.3.2.1 CD18	18
1.1.3.2.2 ICAM-1	20
1.1.3.2.3 P-selectin.....	21
1.2 CORNEAL INFLAMMATION AND HEALING	22

1.3	KERATOCYTE DEATH.....	25
	CHAPTER 2: SPECIFIC AIMS	28
2.1	AIM 1: TO DETERMINE IF ICAM-1 MEDIATES CLOSE SURFACE CONTACTS BETWEEN NEUTROPHILS AND KERATOCYTES FOLLOWING CORNEAL EPITHELIAL ABRASION IN THE MOUSE.....	28
2.2	AIM 2: TO DETERMINE IF CD18 AND ICAM-1 FACILITATE NEUTROPHIL MOTILITY ON THE SURFACE OF MOUSE KERATOCYTES.....	31
2.3	AIM 3: TO DETERMINE IF CD18 AND ICAM-1 REGULATE NEUTROPHIL INFILTRATION AND PLATELET ACCUMULATION FOLLOWING CORNEAL EPITHELIAL ABRASION IN THE MOUSE.....	32
2.4	AIM 4: TO DETERMINE IF PMNS AND/OR PLATELETS ARE NECESSARY FOR KERATOCYTE REPOPULATION FOLLOWING CORNEAL EPITHELIAL ABRASION IN THE MOUSE.....	35
	CHAPTER 3: METHODS	39
3.1	ANIMALS	39
3.1.1	Corneal Epithelial Abrasion Model.....	40
3.1.2	Wound Protocol.....	42
3.2	CELL CULTURE	43
3.2.1	Cover Slip Preparation	43
3.2.2	Keratocyte Isolation.....	44
3.2.3	Mouse PMN Isolation	46
3.2.4	Determining PMN Migration Velocity	47
3.2.5	Cardiac Puncture.....	48

3.2.6	Platelet Isolation	48
3.3	IMMUNOHISTOCHEMISTRY	49
3.3.1	Characterization of Cultured Keratocytes	49
3.3.2	Preparation of Corneas for PMN and Platelet Analyses.....	50
3.3.3	Characterization of ICAM-1 Expression on Whole-Mount Corneas.....	51
3.3.4	IL-22R (receptor) Staining on Corneal Keratocytes	52
3.3.5	Systemic and Topical Application of Recombinant (r)IL-22	52
3.3.6	Corneal Immunostaining for Keratocyte Repopulation.....	53
3.4	MORPHOMETRIC ANALYSES OF IMMUNOSTAINED WHOLE-MOUNT CORNEAS	53
3.4.1	Whole-Mount Corneal Analyses Parameters	53
3.4.2	PMN Infiltration.....	53
3.4.3	Platelet Accumulation	54
3.4.4	Keratocyte Repopulation	55
3.5	ELECTRON MICROSCOPY	56
3.5.1	Tissue processing	56
3.5.1.1	Close Surface Contact Studies	56
3.5.1.2	WT Mouse Anterior Central Keratocyte Repopulation	57
3.5.1.3	Morphometric Analysis.....	57
3.5.1.4	Corneal Thickness Measurements.....	59
3.6	STATISTICAL ANALYSIS.....	61
3.6.1	PMN-keratocyte close surface contact	61
3.6.2	PMN infiltration, platelet accumulation, and keratocyte repopulation	61
CHAPTER 4:	RESULTS	62

4.1	AIM 1: TO DETERMINE IF ICAM-1 MEDIATES CLOSE SURFACE CONTACTS BETWEEN NEUTROPHILS AND KERATOCYTES FOLLOWING CORNEAL EPITHELIAL ABRASION IN THE MOUSE.....	62
4.1.1	Paralimbal keratocyte phenotype is retained after central epithelial abrasion	62
4.1.2	ICAM-1 expression on mouse keratocytes	62
4.1.3	Morphometric Analysis	63
4.2	AIM 2: TO DETERMINE IF CD18 AND ICAM-1 FACILITATE NEUTROPHIL MOTILITY ON THE SURFACE OF MOUSE KERATOCYTES.....	67
4.2.1	Characterization of Cultured Keratocytes	67
4.2.2	In Vitro Analysis.....	67
4.3	AIM 3: TO DETERMINE IF CD18 AND ICAM-1 REGULATE NEUTROPHIL INFILTRATION AND PLATELET ACCUMULATION FOLLOWING CORNEAL EPITHELIAL ABRASION IN THE MOUSE.....	69
4.3.1	PMNs Infiltration Following Corneal Epithelial Abrasion.....	69
4.3.2	Platelet Accumulation Following Corneal Epithelial Abrasion.....	71
4.4	AIM 4: TO DETERMINE IF PMNS AND/OR PLATELETS ARE NECESSARY FOR KERATOCYTE REPOPULATION FOLLOWING CORNEAL EPITHELIAL ABRASION IN THE MOUSE.....	74
4.4.1	Analysis of Keratocyte Recovery in WT Mice	74
4.4.2	Keratocyte recovery in CD18 ^{mutant} and ICAM-1 ^{-/-} mice.....	75
4.4.3	Keratocyte Recovery in Platelet-Depleted WT Mice	77
4.4.4	Keratocyte repopulation in TCR δ ^{-/-} and P-selectin mice.....	77
4.4.5	Platelet Infusion restores keratocyte repopulation in P-selectin ^{-/-} mice.....	78
4.4.6	Characterization of IL-22R on Keratocytes and Vessels.....	79

4.4.7	Application of rIL-22 Does Not Rescue Keratocyte Repopulation	80
CHAPTER 5: DISCUSSION.....		81
5.1	AIM 1: TO DETERMINE IF ICAM-1 MEDIATES CLOSE SURFACE CONTACTS BETWEEN NEUTROPHILS AND KERATOCYTES FOLLOWING CORNEAL EPITHELIAL ABRASION IN THE MOUSE.....	81
5.2	AIM 2: TO DETERMINE IF CD18 AND ICAM-1 FACILITATE NEUTROPHIL MOTILITY ON THE SURFACE OF MOUSE KERATOCYTES.....	85
5.3	AIM 3: TO DETERMINE IF CD18 AND ICAM-1 REGULATE NEUTROPHIL INFILTRATION AND PLATELET ACCUMULATION FOLLOWING CORNEAL EPITHELIAL ABRASION IN THE MOUSE.....	87
5.4	AIM 4: TO DETERMINE IF PMNS AND/OR PLATELETS ARE NECESSARY FOR KERATOCYTE REPOPULATION FOLLOWING CORNEAL EPITHELIAL ABRASION IN THE MOUSE.....	91
CHAPTER 6: GENERAL CONCLUSION.....		99
CHAPTER 7: FUTURE DIRECTION FOR KERATOCYTE REPOPULATION STUDIES		106
REFERENCES.....		111

LIST OF TABLES	163
Table 1: Platelet adhesion molecules and their associated ligands on PMNs and vascular endothelial cells.....	163
Table 2: List of primary, secondary antibodies, isotype controls used.....	164
Table 3: Percent of PMN Surface in Close Contact (≤ 25 nm) with Keratocytes or Collagen in the Paralimbal Region of Injured Cornea	166
Table 4: Percent of PMN Surface in Close Contact (≤ 25 nm) with Neighboring PMN(s) or Associated with Interlamellar Space (% Sv> 25 nm).....	167
Table 5: Total PMN numbers in the cornea as assessed by the area under the curve....	168
Table 6: Wild type anterior keratocyte network recovery.....	169
Table 7: Relationship between PMN infiltration, platelet accumulation, and keratocyte repopulation	170

LIST OF FIGURES AND LEGENDS	171
Figure 1: Interaction between PMN CD18 and ICAM-1 (found on vascular endothelium and keratocyte)	171
Figure 2: Diagram of the division of corneal regions	172
Figure 3: Eighteen hour Algerbrush injury versus Golf Club Spud injury in WT mice	173
Figure 4: Mouse cultured keratocytes.....	175
Figure 5: Tracking PMN migration over cultured mouse keratocytes	176
Figure 6: Morphometric number estimation grid for PMN density analyses.....	177
Figure 7: Morphometric number estimation grid for platelet density analyses	178
Figure 8: Morphometric analysis of keratocyte repopulation	180
Figure 9: Morphometric analysis of PMN-keratocyte close surface interactions.....	181
Figure 10: Paralimbal keratocyte ICAM-1immunostaining	183
Figure 11: TEM of PMN-keratocyte close surface contacts in WT and ICAM-1 ^{-/-} mice	185
Figure 12: Keratocyte network surface-to-volume ratio (Sv) in WT and ICAM-1 ^{-/-} mice....	187
Figure 13: Keratocyte network surface area (SA) in WT and ICAM-1 ^{-/-} mice.....	188
Figure 14: Stromal thickness in WT and ICAM-1 ^{-/-} mice.....	189
Figure 15: KSFM cultured mouse keratocytes retain their phenotype in culture.....	190
Figure 16: PMN migration on cultured mouse keratocytes.....	191
Figure 17: Kinetics of WT, CD18 ^{mutant} , and ICAM-1 ^{-/-} PMN infiltration following corneal epithelial abrasion with the Algerbrush	192
Figure 18: Kinetics of PMN infiltration in ICAM-1 ^{-/-} mice following diamond blade injury .	193
Figure 19: Kinetics of platelet infiltration following corneal epithelial abrasion with the Algerbrush.....	194
Figure 20: WT anterior central keratocyte repopulation	196
Figure 21: Keratocyte repopulation following corneal epithelial abrasion in WT, ICAM-1 ^{-/-} , and CD18 ^{mutant} mice.....	197

Figure 22: Anterior central keratocyte repopulation in platelet-depletion WT mice	199
Figure 23: Four day anterior central keratocyte repopulation in TCR $\delta^{-/-}$ mice	200
Figure 24: Anterior central keratocyte repopulation in P-selectin $^{-/-}$ mice.....	201
Figure 25: WT platelet infusion into P-selectin $^{-/-}$ mice	202
Figure 26: WT platelet infusion into WT mice.....	203
Figure 27: Twenty-four hour extravascular platelet density in WT and TCR $\delta^{-/-}$ mice	204
Figure 28: WT keratocyte IL-22R staining.....	205
Figure 29: IL-22R staining at the corneal limbal region	206
Figure 30: JAM-C protein and mRNA expression on cultured mouse keratocytes	207
Figure 31: Inflammation induces endothelial cell activation and inflammatory cell infiltration	208
Figure 32: Unactivated appearance of TCR $\delta^{-/-}$ platelets.....	209
Figure 33: Thy1.2 Positive Stromal Cells in ICAM-1 $^{-/-}$ Mice.....	210

APPENDIX FIGURE LIST	212
Figure I: Cross section of mammal cornea	212
Figure II: CD18 expression on WT and CD18 hypomorphic mutant PMN infiltrating the cornea 36 hours after injury	213
Figure III: Morphometric Analysis of Platelet Density: Intra-observer Comparisons	214
Figure IV: WT central corneal basal epithelial cell densities before and after epithelial abrasion	215

ABBREVIATIONS

μl.....	Microliter
μg.....	Microgram
AAO	American Academy of Ophthalmology
ALDH3A1.....	Aldehyde dehydrogenase (3A1)
APC.....	Allophycocyanin
AUC.....	Area under the curve
BSA.....	Bovine serum albumin
CD.....	Cluster of differentiation
DIC.....	Differential interference contrast
DISC.....	Death inducing signaling complex
E.....	Embryonic (day)
FADD.....	Fas-associated death domain
FBS.....	Fetal bovine serum
FITC.....	Fluorescein isothiocyanate
FLIP.....	FLICE-inhibitory protein
GAG.....	Glycosaminoglycan
GP.....	Glycoprotein
h.....	Hour(s)
HBSS.....	Hank's balanced salt solution
ICAM.....	Intercellular adhesion molecule
Ig.....	Immunoglobulin

IL.....	Interleukin
JAM.....	Junctional adhesion molecules
KSFM.....	Keratinocyte serum free media
LASIK.....	Laser-assisted <i>in situ</i> keratomileusis
mg.....	Milligram
MHC.....	Major histocompatibility complex
ml.....	Milliliter
Mo.....	Mouse
OCT.....	Optical Coherence Tomography
PBS.....	Phosphate buffered saline
PE.....	Phycoerythrin
PECAM.....	Platelet-endothelial cell adhesion molecule
PDGF.....	Platelet-derived growth factor
PMN.....	Polymorphonuclear (cell); PMN
PN.....	Post natal (day)
PRK.....	Photorefractive keratectomy
r.....	Recombinant (protein)
R.....	Receptor
SA.....	Surface area
SEM.....	Standard error of mean
SLRP.....	Small leucine rich protein
Sv.....	Surface-to-volume
TCR.....	T-cell receptor

TGF β	Transforming growth factor β
VVO.....	Vasiculo-vacular organelle
WT.....	Wild type

The Need for New Treatment Options to Promote Corneal Wound Healing: An Overview

The overall goal of this Dissertation is to investigate cellular and molecular mechanisms that play a role in corneal inflammation and wound healing. Understandably, there are numerous mechanisms participating in this inflammatory event but the Dissertation will specifically focus on the contributions of inflammatory cells neutrophils, platelets, $\gamma\delta$ T cells, and adhesion molecules CD18, ICAM-1, and P-selectin. This overview is intended to provide a general rationale for the studies performed in this Dissertation.

The intricate composition of the human cornea lays the foundation for its refractive properties, providing an optically transparent medium which grants us visual clarity. A breach in the corneal structure induced by physical trauma, environmental factors, or biological agents may result in sustained corneal damage. The prevalence of eye injuries in the United States is high (Klopfer, Tielsch et al. 1992; McGwin and Owsley 2005; Li, Burns et al. 2007; AAO 2008) and the American Academy of Ophthalmology recently reported that eye injuries are the second leading cause of blindness in the United States (AAO 2008). According to the report, approximately 2.5 million eye injuries occur annually and nearly 50,000 of all eye injuries result in loss of vision. Additionally, prolonged use and in compliant contact lens wear can cause immediate damage to the epithelium, long-term damage to the endothelium, and stromal edema (Bergmanson and Chu 1982). Because the cornea is continuously exposed to environmental factors (allergens, climate conditions) throughout the day, it is also susceptible to environmental stress which, in turn, can cause epithelial dessication resulting in dry eye. Furthermore, like all tissue, the cornea is susceptible to viral, bacterial, or fungal infection, resulting in keratitis (Jones 1958; Thygeson and Spencer

1973; Lemp 2008). To prevent vision loss caused by corneal injuries, the mechanisms promoting efficient corneal healing must be thoroughly understood and exploited to ensure the preservation and stability of the corneal ultrastructure.

In addition to environmental factors, popular refractive surgical procedures can severely compromise the corneal ultrastructure. Laser *in situ* keratomileusis, commonly referred to as LASIK, remains one of the most common surgical procedures performed worldwide and currently is the most popular refractive surgery for myopic corrections (Sekundo, Bonicke et al. 2003; Kempen, Mitchell et al. 2004; O'Doherty, O'Keeffe et al. 2006; Solomon, Fernandez de Castro et al. 2009; Kuo 2011). The procedure creates a corneal flap (including epithelial cells and anterior stroma) that is essentially flipped over during the correction process and then replaced over the reconstructed stroma. But even as the short-term outcomes of LASIK appear beneficial to visual acuity, emerging complications warrant further investigation of its safety and efficacy, (Jacobs and Taravella 2002; Bailey, Mitchell et al. 2003; Arevalo 2004; Schallhorn, Amesbury et al. 2006; Sutton and Kim 2010). One such complication is keratectasia following LASIK, a vision-impairing condition defined by a thinning and steepening protrusion of the cornea (Twa, Nichols et al. 2004; Kanellopoulos and Binder 2010; Khachikian and Belin 2010). While the prevalence of keratectasia is low (occurring in <1% of patients), this number only accounts for documented cases (Kennedy, Bourne et al. 1986; Randleman, Russell et al. 2003; Binder, Lindstrom et al. 2005). Keratectasia also can occur after photorefractive keratectomy (PRK), although it is observed even less frequently than in patients undergoing LASIK (Kim, Choi et al. 2006; Randleman, Caster et al. 2006; Leccisotti 2007). PRK, the first form of refractive surgery, ablates corneal epithelial cells with a laser prior to stroma reconstruction. Regardless if the onset of keratectasia results from LASIK or PRK, it is most important to recognize that the progression of this condition significantly alters the corneal ultrastructure and can ultimately compromise

corneal biomechanical properties (Comaish and Lawless 2002; Dupps and Wilson 2006). While corneal cross-linking may help to manage keratectasia after refractive surgery, there is currently no cure for keratectasia and the only treatment option is corneal transplant (Twa, Nichols et al. 2004; Kymionis, Portaliou et al. 2011).

Following tissue damage, the immediate biological response is inflammation, characterized by an infiltration of immune cells to the injured site (Arturson 1980; Entman, Michael et al. 1991; Burns, Takei et al. 1994; Ley 1996; Galkina and Ley 2009; Guan, Pritts et al. 2010; Ferraccioli and Gremese 2011; Snelgrove, Godlee et al. 2011; Weill, Cela et al. 2011). Inflammation is a necessary precursor for subsequent wound healing. In fact, patients with weakened immune responses show delayed or diminished healing abilities (Anderson, Schmalstieg et al. 1985; Etzioni 1994; Twigg, Soliman et al. 1999; Uzel, Kleiner et al. 2001; Gu, Bauer et al. 2004). Although the cornea is considered an immune privileged tissue, injury and disease does indeed elicit an inflammatory response (O'Brien, Li et al. 1998; Hamrah, Liu et al. 2003; Belmonte, Acosta et al. 2004; Burns, Li et al. 2005; Li, Burns et al. 2006a; Li, Burns et al. 2006b; Li, Rumbaut et al. 2006c; Li, Burns et al. 2007; Chinnery, Carlson et al. 2009; Li, Burns et al. 2011), where the nature of the inciting stimulus defines the severity of the inflammatory response and its consequences to healing. While excessive inflammatory cell infiltration may exacerbate corneal injury and delay healing, suppressing inflammation impairs corneal wound healing (Rudner, Kernacki et al. 2000; Vij, Roberts et al. 2005; Li, Burns et al. 2006b; Molesworth-Kenyon, Yin et al. 2008; Tarabishy, Aldabagh et al. 2008; Byeseda, Burns et al. 2009), . In the context of refractive surgery, topical anti-inflammatory agents, such as corticosteroids, are administered during and following LASIK and PRK procedures to prevent fibrotic scarring. NSAIDs are administered at later times and are used to provide analgesic effects. However studies suggest these drugs have sustained effects on cellular regeneration and may delay or

hinder recovery (Shah and Wilson ; Srinivasan and Kulkarni 1981; Waterbury, Kunysz et al. 1987; Rask, Jensen et al. 1995; Park and Kim 1996) . To date, the advantages and disadvantages of corneal inflammation following injury have not been well characterized and only a few laboratories examine the role of injury-associated inflammation during corneal healing (Saika, Shiraishi et al. 2000; Burns, Li et al. 2005; Vij, Roberts et al. 2005; Li, Burns et al. 2006a; Carlson, Lin et al. 2007; Byeseda, Burns et al. 2009; Hayashi, Call et al. 2010). Hence, a thorough investigation of corneal inflammation is required to discern its benefits from its disadvantages with respect to wound healing.

Corneal injury is clearly a high risk factor to vision loss and of major concern to ophthalmologists. Severe corneal ultrastructural damage, as in keratectasia, can inflict long lasting damage and may require corneal transplantation (Javadi and Feizi 2010). However, graft rejection remains a risk factor associated with this invasive procedure (Kucumen, Yenerel et al. 2008). A plausible alternative is devising therapeutic treatments to promote corneal regeneration but this requires a thorough understanding of the molecular mechanisms involved in corneal inflammation and wound healing.

This dissertation investigates the role of inflammatory cells and associated adhesion molecules in advancing keratocyte recovery during corneal healing. These studies seek to understand the basic concepts assisting and inhibiting corneal inflammation and their advantages and disadvantages to wound healing with the hope of providing better insight into the corneal inflammatory response. Such knowledge will encourage advancements in drug therapy aimed at to promoting efficient healing and the preservation of sight as well as reduce long-term costs for patients and clinicians.

CHAPTER 1: INTRODUCTION

1.1 *Overview of the Cornea*

A corneal cross-section EM micrograph and cartoon is provided as reference for this chapter (Appendices Figure I).

1.1.1 *Corneal Morphogenesis*

Human corneal development begins around 5 weeks embryonic (E) stage with a layer of ectoderm covering the lens. This primitive epithelium stratifies by 7 weeks and separates from the lens. Immediately following separation, neural crest-derived mesenchymal cells migrate into the void space, laying the foundation for the corneal endothelium. This initial migration is followed by a second wave of neural crest-derived mesenchymal cells, filling in the space between the epithelium and endothelium. These cells become the stromal keratocytes. Thus, while epithelial cells derive from ectodermal lineage, keratocytes and corneal endothelial cells originate from neural crest-derived mesenchymal cells (O'Rahilly 1975; Hay 1980; Barishak 1992; Zieske 2004; Forrester, Dick et al. 2008).

A mouse model was used to do all corneal wound healing studies in this Dissertation (discussed in section 1.2), so it is also important to briefly mention the stages of corneal development in the mouse. The sequence of developmental processes does not differ from that of humans, but in the mouse, the cornea begins to form between E11- E14, when the ectoderm layer covering the lens (which forms the primitive epithelium) is first detected. Neural crest cell migration occurs in a similar manner as in humans, forming both the corneal endothelium and keratocytes (Pei and Rhodin 1971; Collinson, Hill et al. 2004). Additionally, innervation is detected by E12.5 in the mouse cornea (McKenna and Lwigale 2011). It is important to note that eyelid opening in mice

does not occur until post natal (PN) day 12, and between PN1 and PN56 the mouse corneal continues to develop (Song, Lee et al. 2003; Beecher, Chakravarti et al. 2006; Hanlon, Patel et al. 2011).

1.1.2 Corneal Anatomy and Physiology

This section provides general overview of human corneal anatomy and physiology. However, because a mouse model is used for inflammation and wound healing studies, the mouse corneal anatomy will be briefly addressed and will be specified as mouse corneal anatomy and/or physiology when addressed.

1.1.2.1 Corneal Layers

The human ocular surface is covered by a thin, mucin-rich tear fluid. This film provides additional nutrients to the corneal epithelial cells (primary nutrient source comes from the aqueous humor) and serves as a first line of defense against pathogens (Fullard and Snyder 1990; van Setten, Schultz et al. 1994; Bron and Tiffany 1998; Haynes, Tighe et al. 1999; McDermott 2004; Tiffany 2008). Furthermore, the lipid composition of the tear film smoothens and stabilizes the curvature of the corneal surface and allows for optimal refractive properties (Tutt, Bradley et al. 2000; Bron, Tiffany et al. 2004; Montes-Mico, Alio et al. 2004). The topmost layer is the stratified epithelium, consisting of a basal cell monolayer, 2-3 wing cell layers, and 2-3 superficial cell layers (DeMonte and Kim 2011). The stratified arrangement of epithelial cells offers further protection to the cornea from foreign pathogens, providing numerous mechanisms to detect and destroy unknown exogenous and endogenous agents (McDermott, Redfern et al. 2003; Redfern, Reins et al. 2011). In addition, the epithelial cells regulate tear fluid transport into the cornea and actively maintain corneal homeostasis (Yang, Reinach et al. 2000; Hamann 2002; Levin and Verkman 2006).

Below the epithelial cells is the acellular Bowman's layer (a.k.a. Anterior Limiting Lamina-ALL), acting primarily as a barrier between the epithelium and the stroma (Wilson and Hong 2000b), the third and largest corneal layer. The stroma supports the majority of ultrastructural components which help maintain corneal clarity. The stroma will be the focus of the dissertation and will be discussed in detail below. Beneath the stroma is another acellular layer called Posterior Limiting Lamina, or PLL, (a.k.a Descemet's membrane), thought to function as the basement membrane for the final corneal layer, the endothelial monolayer, which regulates anterior chamber fluid exchange in the stroma (Hamann 2002; Kuang, Yiming et al. 2004; Srinivas 2010).

1.1.2.2 Corneal Innervation

The cornea is the one of the most innervated tissues in the human body. Corneal sensory nerves derive from the ophthalmic branch of the trigeminal ganglia, with each neuron supporting up to 3000 nerve endings (Muller, Marfurt et al. 2003). Additionally, sympathetic nerves from the superior cervical ganglia innervate the cornea. Innervation begins at the periphery, where large trunked fibers enter from the limbal region, thinning and branching as they radially extend upwards toward the corneal apex. These thicker stromal branches give rise to finer fibers reaching the basal epithelium, forming the sub basal nerve plexus and extends into the super epithelial nerve plexi (Yu and Rosenblatt 2007). Nerve axon fiber bundles are unsheathed by myelin, which is rapidly lost as the bundles enter the stroma (Muller, Vrensen et al. 1997; Nagano, Nakamura et al. 2003), leaving only Schwann cells to unsheathe the nerve (Muller, Pels et al. 1996).

1.1.2.3 Corneal Collagen

The stroma is comprised primarily of collagen fibrils which are packed tightly into lamellae. Collagen lamellae are organized in a stratified, orthogonal arrangement in the posterior stroma and assume a more randomized, swirled pattern towards the anterior stroma. Of the 26 identified collagen types, 22 are associated with the eye and of those 12 exist in the cornea (Knupp, Pinali et al. 2009; Bueno, Gualda et al. 2011). The primary collagen type constituting the stroma is collagen Type I, although Types IV and V are also present in smaller amounts (Zimmermann, Trueb et al. 1986; Birk, Fitch et al. 1990; Gordon, Foley et al. 1994; Khoshnoodi, Pedchenko et al. 2008). Type I collagen lays the structural foundation for the cornea (Hassell and Birk ; Birk, Fitch et al. 1986) while Type V collagen regulates fibril diameter size and fibrillogenesis (Birk, Fitch et al. 1990; Wenstrup, Florer et al. 2004). In contrast, Type IV collagen, typically located in basal lamina, is non-fibrillar and serves to hold together the other two types to form larger fibrils (Zimmermann, Trueb et al. 1986; Hudson, Reeders et al. 1993; Ljubimov, Burgeson et al. 1995). The arrangement, diameter, and homogenous distribution of collagen fibers play an important role in maintaining corneal clarity (Hassell and Birk ; Goldman and Benedek 1967; Maurice 1970). In 1957, Maurice proposed the lattice theory of corneal transparency, hypothesizing that scattered light diverging off of incident light was destroyed by interference of their own wavelengths, due to the nature of collagen fibril diameter and spacing (Maurice 1970). Goldman and Benedek took into account the irregular arrangement of the Bowman's layer (ALL) collagen fibrils and suggested corneal transparency resulted from the inability of large wavelengths of visible light to overcome the small fibril diameter and spacing, which results in very small fluctuations in the corneal refractive index over very small distances (Goldman and Benedek 1967).

Collagen fibrils are decorated with a variety of proteoglycans (i.e., proteoglycans are interdispersed among and connected to collagen fibrils). Proteoglycans are heavily glycosylated proteins belonging to the small leucine-rich proteoglycan (SLRP) family (Hassell and Birk). Proteoglycans contain glycosaminoglycan (GAG) side chains, heavily sulphated disaccharide units, attached to a specific core protein. The two classes of stromal GAGs are keratan sulphates and dermatan sulphates. Keratocan, lumican, and mimecan are the three key keratan sulphate proteoglycans while the proteoglycan decorin is associated with dermatan sulphate GAGs (Funderburgh, Caterson et al. 1987; Funderburgh and Conrad 1990; Funderburgh, Hevelone et al. 1998). Proteoglycans make a critical contribution to corneal strength and transparency by maintaining fibril spacing (Hassell and Birk ; Funderburgh, Caterson et al. 1987; Funderburgh and Conrad 1990; Chakravarti, Magnuson et al. 1998; Funderburgh, Hevelone et al. 1998), forming the basis of corneal transparency (Chakravarti, Magnuson et al. 1998; Funderburgh, Hevelone et al. 1998; Carlson, Liu et al. 2005). Additionally, proteoglycans play an important role in inflammation, cellular migration, leukocyte adhesion, and regulation of growth factor activities (Hassell and Birk ; Schonherr, Sunderkotter et al. 2004; Vij, Roberts et al. 2005; Carlson, Lin et al. 2007; Carlson, Sun et al. 2010; Hayashi, Call et al. 2010; Mohan, Gupta et al. 2010; Mohan, Tovey et al. 2011).

1.1.2.4 Keratocytes

Embedded between the collagen lamellae are the corneal stromal cells, the keratocytes. As described earlier, keratocytes are neural crest-derived mesenchymal cells and in the normal cornea, they are typically referred to as “quiescent” cells, even though they actively produce and secrete essential extracellular matrix components. Morphologically, keratocytes are flat, stellate cells with slender dendritic-like processes.

These processes interconnect with processes of neighboring keratocytes via gap junctions (Jester, Barry et al. 1994; Watsky 1995; Lakshman, Kim et al. 2010), thereby forming a network within the stroma. Keratocytes are directly responsible for the synthesis and secretion of corneal collagen and proteoglycans (Birk, Fitch et al. 1988; Beales, Funderburgh et al. 1999). In addition, they produce and store corneal crystallins, aldehyde dehydrogenase 3A1/1A1 and transketolase, soluble enzyme/proteins which protect against ultraviolet rays and oxidative stress, participate in corneal metabolic activities, and most importantly contribute to the maintenance of corneal transparency (Jester, Moller-Pedersen et al. 1999; Stramer and Fini 2004).

Keratocytes have the ability to differentiate in the presence of growth factors. If the stroma is breeched during injury, growth factors from tears, such as TGF β , and cytokines, such as IL-1 β , released by epithelial cells and infiltrating leukocytes, transform the “quiescent” phenotype into repair phenotype cells, fibroblasts, then myofibroblasts (Jester, Petroll et al. 1995; Fini 1999; Wilson 2002; Jester and Ho-Chang 2003; Pei, Sherry et al. 2004; Jester, Budge et al. 2005; Kaur, Chaurasia et al. 2009). However, the current studies use an epithelial abrasion injury model (Sections 1.2 and 3.2.5), which is a non-penetrating injury, and does not result in mass differentiation of peripheral keratocytes into the repair phenotypes.

1.1.3 General Paradigm of Inflammation

The cornea is susceptible to a variety of injuries. Whether these injuries are caused by physical trauma (abrasion, refractive surgery), environmental stress (dry eye), infections (microbial), or genetic mutations (Fuch’s dystrophy), to varying degrees, they all result in corneal inflammation and death or damage to corneal cells (Rudner, Kernacki et al. 2000; Wilson, Mohan et al. 2002; Erie, Patel et al. 2003; Klintworth 2003;

Zhao and Nagasaki 2004; Redfern, Reins et al. 2011). This section will briefly review corneal inflammation and participating inflammatory cells in detail.

To understand the mechanisms involved in corneal inflammation, it is first important to understand the general paradigm of inflammation. The five cardinal signs of inflammation are redness (*rubor*), increased heat (*calor*), swelling (*tumor*), pain (*dolor*), loss of function (*functio laesa*) (1-4, described by Celsus, ca 30 BC–38 AD; the last added by Galen, ca 129 – 199/217 AD). Upon injury, vascular endothelial cells produce chemokines and cytokines, acute phase proteins, which facilitate inflammatory cells recruitment to the site of injury. Chemokines are chemical attractants that direct the migration of cells in a specific path. Chemokines are subdivided into four families: C, CC, CxC, and Cx₃C chemokines. The CC and CxC are most abundant (Laing and Secombes 2004), of which Interleukin-8 (IL-8) plays a dominant role in human leukocyte recruitment. Cytokines are immunomodulating proteins secreted by leukocytes (monocytes and granulocytes) and inflamed endothelial cells. Cytokines can be subdivided into pro-inflammatory and anti-inflammatory groups. Examples of pro-inflammatory cytokines are IL-1, IL-6, TNF, INF γ , and examples of anti-inflammatory cytokines are IL-4, IL-10, IL-11, and IL-13 (Dinarello 2000; Opal and DePalo 2000). While these are classical examples, several cytokines have both pro- and anti-inflammatory effects. Pro-inflammatory cytokines and chemokines work to recruit leukocytes and upregulate inflammatory and endothelial cell surface adhesion molecules during inflammation while anti-inflammatory cytokines maintain control over proinflammatory activities and help to modulate inflammatory reactions.

Leukocyte recruitment occurs in a multi-step paradigm, initiated by rolling and capture of leukocytes via P-selectin, E-selectin, and L-selectin interactions (Bevilacqua and Nelson 1993; Erban 1993; Bevilacqua, Nelson et al. 1994; Ley, Bullard et al. 1995). This is followed by firm adhesion of leukocytes onto the endothelium. Firm adhesion is

predominantly mediated by the $\beta 2$ integrin, CD18 (Smith, Marlin et al. 1989; Diamond and Springer 1993; Lynam, Sklar et al. 1998; Wang and Doerschuk 2002). There are four CD18 family members, CD11a/CD18 (LFA-1), CD11b/CD18 (Mac-1), CD11c/CD18, and CD11d/CD18. CD11a and CD11b/CD18 play critical roles in PMN firm adhesion and the process of their activation will be further discussed below. Following firm adhesion, at which time PMNs are capable of crawling on the surface of endothelial cells using adhesion molecules and their receptors, PMNs transmigrate out of the vessels into the extravascular region. The process of transmigration is also facilitated by leukocyte and endothelial adhesion molecules through CD18 as well as CD31 (PECAM) and the JAM family of adhesion molecules, specifically JAM-A and JAM-C (Muller, Weigl et al. 1993; Diacovo, Roth et al. 1996; Vestweber 2002; Chavakis, Keiper et al. 2004).

Platelets are small, anucleate, inflammatory cells that are best known for their roles in thrombosis. However, platelets also play an integral role during inflammation by facilitating PMN recruitment, activation, and rolling. Platelet surface adhesion molecules (discussed below) can associate with ligands expressed on vascular endothelial cells and PMN to facilitate the aforementioned functions (Erban 1993; Varki 1994; Asa, Raycroft et al. 1995; Evangelista, Manarini et al. 1996; Evangelista, Manarini et al. 1999; Rivera, Lozano et al. 2000; Simon, Chen et al. 2000; Wang, Sakuma et al. 2005; Xiao, Goldsmith et al. 2006; Xu, Zhang et al. 2007; Lam, Burns et al. 2011). Additionally, platelets are major contributors to wound healing and as corneal wound healing is an important aspect of this dissertation, the role of platelets during recovery will be discussed in detail later and throughout the document.

1.1.3.1 Immune Cells

This section is meant to provide a general overview of inflammatory cells involved in corneal inflammation and relevant to this Dissertation. It is not meant as a

detailed review of neutrophils, platelets, or $\gamma\delta$ T cells. For further information and detailed descriptions of mechanisms involved in neutrophil, platelet, and $\gamma\delta$ T cell production, activation, and their involvement in healing, the reader is referred to the reviews cited in the descriptions below.

1.1.3.1.1 Neutrophils

During inflammation, neutrophils are the first leukocytes to infiltrate the injured tissue, often serving as the first line of defense against foreign pathogens. Neutrophils are myeloid-lineage hematopoietic cells and are also called polymorphonuclear cells (PMNs) due to their multi-lobed nuclei. PMN production occurs in the bone marrow, arising from hematopoietic stem cells. These stem cells differentiate into the myeloid lineage or lymphoid lineage, depending on the stimuli provided. All myeloid leukocytes arise from a common myeloid progenitor cell but PMNs are formed specifically from myeloblasts that have differentiated into neutrophil promyelocytes, followed by neutrophil myelocytes, and finally neutrophil metamyelocytes before maturing into PMNs (Cartwright, Athens et al. 1964; Fittschen, Parmley et al. 1988). In the absence of inflammation, circulating PMN counts in humans range from $2.5 - 7.5 \times 10^9$ cells per ml and in mice, $\geq 0.3 - 2.0 \times 10^6$ cells per ml. Unactivated PMNs are medium-sized leukocytes, measuring roughly 6-10 μm in diameter, although this changes dramatically upon activation and transmigration (Burns, Smith et al. 2003; Li, Rumbaut et al. 2006c). Previously it was thought that circulating PMNs had a life span of several hours (Dancey, Deubelbeiss et al. 1976; Suratt, Young et al. 2001; Basu, Hodgson et al. 2002) but recent studies suggest a circulating half life up to 5 days in humans and 12 hours in mice (Pillay, den Braber et al. 2010).

PMNs play a critical role during inflammation, migrating to the site of injury through processes of chemotaxis (migration towards a chemical gradient) and haptotaxis

(directional migration). Their migration is dependent on chemokine and cytokines released by both inflammatory cells and resident cells at or near the site of injury. Once PMNs have infiltrated the injured and/or infected area, they phagocytize bacteria and necrotic cells. PMNs are one of three granulocytes, and contain primary, secondary, and tertiary granules. Primary granules, also termed azurophilic granules, contain proteolytic enzymes, such as myeloperoxidase, elastase, and antimicrobial defensins, among other proteins. Secondary granules contain lactoferrin and cathelicidin and tertiary granules contain cathepsin and gelatinase. All of these serve as antimicrobial agents or pathogen degrading enzymes to clear the inflamed tissue of foreign bodies as well as damaged resident cells (Faurschou and Borregaard 2003; Borregaard, Sorensen et al. 2007).

PMN transmigration out of vessels and their emigration through the extravascular tissue are well documented events (Arfors, Lundberg et al. 1987; Smith, Marlin et al. 1989; Geng, Bevilacqua et al. 1990; Jones, Abbassi et al. 1993; Carlos and Harlan 1994; Guyer, Moore et al. 1996; Ley 1996; Burns, Walker et al. 1997; Feng, Nagy et al. 1998; Lynam, Sklar et al. 1998; Oberyszyn, Conti et al. 1998; Ley 2001; Piccardoni, Sideri et al. 2001; Burns, Smith et al. 2003). PMNs, like all leukocytes, express the $\beta 2$ surface integrin CD18. CD18 is upregulated on the surface of activated PMNs and is a key player in PMN adhesion, transmigration, and motility. It also participates in PMN signal transduction and apoptosis (Smith, Rothlein et al. 1988; Diamond and Springer 1993; Burns and Doerschuk 1994; Coxon, Rieu et al. 1996; Diacovo, Roth et al. 1996; Wang and Doerschuk 2002; Li, Burns et al. 2006a; El Kebir, Jozsef et al. 2008) and will be discussed further in Section 1.1.3.2.1.

The contribution of PMNs to corneal epithelial wound healing has been duly outlined by Li and colleagues (Li, Burns et al. 2006a). This Dissertation will determine

whether PMNs also contribute to keratocyte repopulation following corneal epithelial abrasion in the mouse.

1.1.3.1.2 Platelets

Platelets are small, discoid-shaped, anucleate inflammatory cells that are commonly associated with thrombotic responses (Gonzalez-Villalva, Falcon-Rodriguez et al. ; Firkin 1963; David-Ferreira 1964; Rumbaut 2005). The normal circulating platelet count in humans is approximately $150 - 400 \times 10^9 \mu\text{l}^{-1}$ with an average lifespan of 8-10 days (Kamath, Blann et al. 2001; Rumbaut and Thiagarajan 2010). Platelets are the smallest intact inflammatory cells, averaging approximately 2 μm in size. Their discoid shape is retained by a band of microtubules running longitudinally along the sides of the cell (Behnke 1970). Platelets are formed from fragments of cytoplasm released by platelet precursor cells, megakaryocytes (Behnke and Forer 1998; Hartwig and Italiano 2003). Megakaryocytes are highly granulated hematopoietic cells that are formed and reside in the bone marrow. As megakaryocytes mature, they synthesize and package a variety of proteins within granules. Upon platelet production, granules from megakaryocyte cytoplasmic fragments are retained within the newly formed platelets; hence platelets are abundant in granules (Behnke and Forer 1998).

There are three types of platelet granules: 1) α granules, 2) δ granules (dense bodies), and 3) λ granules (primary lysosomes). The majority of granules in platelets are α granules, averaging 50-80 per platelet. Alpha granules primarily contain platelet adhesion proteins, which support platelet interactions with other platelets, leukocytes, endothelial cells, and ECM components (Harrison and Cramer 1993). Platelet dense bodies exist in fewer numbers, averaging 3-8 per platelet, and contain serotonin, ADP, ATP, inorganic phosphates, calcium and other divalent cations (McNicol and Israels 1999). Lysosomes are membrane-bound, enzyme-containing organelles found in

platelets and other cells (Dell'Angelica, Mullins et al. 2000). These granules are characterized by their acidic interior and lysosomal membrane markers (Polasek 2005).

Platelets express adhesion molecules that assist in signal transduction, aggregation, hemostasis, and adhesion during inflammation (Bevilacqua and Nelson 1993; Furie and Furie 1995; Evangelista, Manarini et al. 1996; George 2000; Kamath, Blann et al. 2001; Piccardoni, Sideri et al. 2001; Ehlers, Ustinov et al. 2003; Smith 2008; Senzel, Gnatenko et al. 2009). With respect to adhesion and inflammation, platelets are capable of interacting with other platelets, endothelial cells, and leukocytes. Some platelet adhesion molecules relevant to adhesion during inflammation and their counter-receptors are listed in Table 1.

Platelet adhesion during inflammation and exposure to extracellular matrix components promotes their activation. The process of platelet activation involves structural and molecular changes associated with a change in cell shape involving the extension of pseudopods and further upregulation of adhesion molecules facilitating the associations with other platelets (aggregation), endothelial cells, and leukocytes. Finally, platelet activation results in degranulation and release of granular contents into the extracellular/extravascular region during inflammation (White and Estensen 1972; Kamath, Blann et al. 2001; Rumbaut and Thiagarajan 2010).

In addition to maintaining hemostasis by forming clots to control vascular ruptures, platelets play important roles in wound healing, primarily facilitated by their release of growth factors (Servold 1991; Imanishi, Kamiyama et al. 2000; Rozman and Bolta 2007; Smyth, McEver et al. 2009; Nurden 2011). With respect to corneal inflammation, platelets are required for efficient epithelial healing (Li, Rumbaut et al. 2006c). The role of platelets in keratocyte repopulation will be evaluated in detail in this Dissertation.

1.1.3.1.3 $\gamma\delta$ T-cells

Gamma delta ($\gamma\delta$) T cells are a small subpopulation of T cells (< 5% of circulating T cells, <0.9% total thymocytes) distinguished by their $\gamma\delta$ T cell receptor ($\gamma\delta$ TCR) (Lanier and Weiss 1986; Parker, Groh et al. 1990; Allison, Winter et al. 2001). Like $\alpha\beta$ T cells, $\gamma\delta$ T cells develop in the thymus, arising from a common CD4⁺/CD8⁺ precursor as $\alpha\beta$ T cells. During the various stages of T cell development, gene rearrangement at the TCR β , TCR γ , or TCR δ gene loci differentiates cells expressing pre-($\alpha\beta$)TCR from those expressing $\gamma\delta$ TCR, demonstrating $\gamma\delta$ T cell development precedes that of $\alpha\beta$ T cells (Livak, Tourigny et al. 1999; Ciofani and Zuniga-Pflucker 2010). $\gamma\delta$ T cells are located in mucosa-associated epithelial tissue, and perform immunoregulatory functions to maintain tissue homeostasis (Bonneville, O'Brien et al. 2010; Macleod and Havran 2011). To this extent, $\gamma\delta$ T cells perform effector functions such as eliminating diseased cells through association with CD95 (FAS), modulating inflammation by production of pro- and anti-inflammatory cytokines, and secreting growth factors to promote cellular proliferation and tissue regeneration (Parker, Groh et al. 1990; Huber 2000; Roessner, Wolfe et al. 2003; Braun, Ferrick et al. 2008; Deknuydt, Scotet et al. 2009; Bonneville, O'Brien et al. 2010; Ma, Lancto et al. 2010)

In 1993, Itohara and colleagues developed a $\gamma\delta$ T cell-deficient mouse (TCR $\delta^{-/-}$) (Itohara, Mombaerts et al. 1993). These knockout mice were generated by disrupting the TCR δ gene segment, resulting in the complete loss of T cells expressing TCR $\gamma\delta$ chains. However development and quantity of T cells expressing TCR $\alpha\beta$ chains remained unaffected. The TCR $\delta^{-/-}$ mice provide a unique opportunity to investigate the modulatory role of $\gamma\delta$ T cells during corneal inflammation and healing, specifically to examine whether their recruitment promotes efficient keratocyte repopulation following corneal epithelial abrasion.

1.1.3.2 Adhesion Molecules That Facilitate Immune Cell Infiltration

This section is meant to provide a general overview of three adhesion molecules associated with the inflammatory cells discussed above. They are involved in corneal inflammation and relevant to this Dissertation. It is not a detailed review of CD18, ICAM-1, or P-selectin. For detailed descriptions of these adhesion molecules, the reader is referred to the reviews cited in the descriptions below.

1.1.3.2.1 CD18

The $\beta 2$ integrin CD18 is a leukocyte-specific adhesion molecule that plays an important role in leukocyte recruitment to sites of inflammation (Smith, Rothlein et al. 1988; Arnaout 1990; Wilson, Ballantyne et al. 1993; Walzog, Scharffetter-Kochanek et al. 1999; Li, Burns et al. 2006a). CD18 is comprised of $\alpha\beta$ heterodimers expressed on the surface of leukocytes. The four members in the $\beta 2$ integrin family are as follows: 1) CD11a/CD18 (lymphocyte function-associated antigen-1; $\alpha_L\beta 2$; LFA-1), 2) CD11b/CD18 (macrophage antigen-1; $\alpha_M\beta 2$; Mac-1), 3) CD11c/CD18 (p150,95), and CD11d/CD18 ($\alpha_D\beta 2$) and participate in leukocyte signaling, activation, migration, and even apoptosis (Anderson, Schmalstieg et al. 1985; Smith, Rothlein et al. 1988; Arnaout 1990; Diamond, Garcia-Aguilar et al. 1993; Coxon, Rieu et al. 1996; Walzog, Scharffetter-Kochanek et al. 1999; El Kebir, Jozsef et al. 2008; Sarantos, Zhang et al. 2008). LFA-1 and Mac-1 are expressed on virtually all myeloid cells while CD11c and CD11d are associated primarily with antigen presenting cells and monocytes, with the exception of CD11c expression on some activated lymphocytes (Krensky, Sanchez-Madrid et al. 1983; Diamond, Alon et al. 1995; Gahmberg and Fagerholm 2002).

Leukocyte activation is a necessary precursor to adhesion and transmigration and occurs through chemokine and cytokine-mediated conformational changes and upregulation of the $\beta 2$ integrins (Albelda, Smith et al. 1994). Integrin expression is low

and evenly distributed in unactivated leukocytes but activation results in elevated surface expression and clustering (Arnaout 1990; Albelda, Smith et al. 1994; Gahmberg and Fagerholm 2002), increasing integrin avidity to interact with its ligands (due to integrin rearrangement) and affinity to bind with a ligand (Kucik 2002).

The most extensively studied CD11/CD18 members are LFA-1 and Mac-1, both recognizing separate binding domains on the endothelial ligand, ICAM-1 (discussed below, Section 1.1.3.2.2) (Krensky, Sanchez-Madrid et al. 1983; Anderson, Schmalstieg et al. 1985; Dustin and Springer 1988; Kishimoto, Jutila et al. 1989; Smith, Marlin et al. 1989; Diamond, Staunton et al. 1990; Diamond, Staunton et al. 1991; Diamond and Springer 1993; Huang and Springer 1995; Diacovo, Roth et al. 1996; Sarantos, Zhang et al. 2008). These associations are considered critical for leukocyte emigration as evidenced by inhibition of PMN adhesion and transmigration after blocking LFA-1 or Mac-1 (Dustin and Springer 1988; Smith, Marlin et al. 1989; Diamond, Staunton et al. 1990; Diamond, Staunton et al. 1991; Burns, Walker et al. 1997). CD18-ICAM-1 associations are known to transduce bi-directional signaling to the PMN and cell expressing ICAM-1, stimulating upregulation of ICAM-1 and other cell surface receptors, secretion of growth factors and cytokines, amplifying antigen presentation on surface of leukocytes, and possibly promoting cellular regeneration through the MAP Kinase pathway (Hubbard and Rothlein 2000). Additionally, LFA-1 also associates with the endothelial adhesion molecule, ICAM-2 (Dustin and Springer 1988; Smith, Marlin et al. 1989; Ley 1996). Also, Mac-1 has several other binding partners, including platelet GP1b α and endothelial JAM-C, both of which are relevant to this Dissertation (Diamond, Staunton et al. 1990; Diamond, Staunton et al. 1991; Diamond, Garcia-Aguilar et al. 1993; Diamond and Springer 1993; Diamond, Alon et al. 1995; Simon, Chen et al. 2000; Ehlers, Ustinov et al. 2003; Wang, Sakuma et al. 2005; Langer and Chavakis 2009).

Leukocyte Adhesion Deficiency (LAD) I is a disease characterized by a defect in the expression of CD11/CD18 and/or other leukocyte adhesion molecules, commonly resulting in recurring infection, soft tissue necrosis, and peripheral blood neutrophilia (Fischer, Lisowska-Grospierre et al. 1988; Etzioni 1994; Gu, Bauer et al. 2004; Gazit, Mory et al. 2010). It has been diagnosed in hundreds of patients and can be treated with early therapy (Uzel, Kleiner et al. 2001). Hypomorphic CD18^{mutant} mice were generated to study the structural and functional mechanisms regulating CD18-related deficiencies (Wilson, Ballantyne et al. 1993; Walzog, Scharffetter-Kochanek et al. 1999) and are used in this Dissertation to determine the relative contribution of CD18 to PMN extravasation and platelet accumulation during corneal inflammation and keratocyte repopulation during wound healing.

1.1.3.2.2 ICAM-1

Intercellular adhesion molecule-1 (ICAM-1) is a 5-domain transmembrane glycoprotein and is a structurally related member of the immunoglobulin (Ig) supergene family. ICAM-1 spans the cell membrane and has 5 extracellular domains and a short cytosolic tail (Albelda, Smith et al. 1994; Hubbard and Rothlein 2000). ICAM-1 is constitutively expressed at low levels on vascular endothelial cells, some mononuclear cells, as well as other cell types (Rothlein, Dustin et al. 1986; Burns, Takei et al. 1994; Brake, Smith et al. 2006). With respect to the cornea, low expression of ICAM-1 is found on corneal epithelial cells and keratocytes and this expression increases as a result of cytokine stimulation, injury, or infection (Pavilack, Elner et al. 1992; Hobden, Masinick et al. 1995; Yannariello-brown, Hallberg et al. 1998; Hobden, Masinick-McClellan et al. 1999; Hobden 2003; Kumagai, Fukuda et al. 2003; Byeseda, Burns et al. 2009).

ICAM-1 associates with LFA-1 at domain 1 and Mac-1 at domain 3 (Figure 1). These interactions allow for signal transduction between leukocytes and cells expressing

ICAM-1, promoting additional upregulation of ICAM-1 and growth factors (Hubbard and Rothlein 2000). However, the primary function of ICAM-1 is to promote leukocyte firm adhesion, transmigration, and trafficking during inflammation by associating with leukocyte LFA-1 and Mac-1 (Dustin and Springer 1988; Diamond, Staunton et al. 1991; Lynam, Sklar et al. 1998; Byeseda, Burns et al. 2009). Hence, ICAM-1 is required for efficient wound healing as evidenced by delayed and/or diminished leukocyte recruitment and delayed healing ICAM-1^{-/-} mice (Smith, Entman et al. 1991; Robker, Collins et al. 2004; Brake, Smith et al. 2006; Sumagin and Sarelius 2006; Byeseda, Burns et al. 2009).

1.1.3.2.3 P-selectin

P-selectin is an adhesion molecule that belongs to the Selectin family of adhesion molecules. P-selectin is stored in platelet α granules and Weibel-Palade bodies of endothelial cells. Cytokines and other stimulants released during inflammation promotes the P-selectin translocation to the cells' surface, allowing for leukocyte-endothelial cell and leukocyte-platelet interactions (Stenberg, McEver et al. 1985; Bonfanti, Furie et al. 1989; Larsen, Celi et al. 1989; McEver, Beckstead et al. 1989; Koedam, Cramer et al. 1992; Burns, Bowden et al. 1999; Evangelista, Manarini et al. 1999).

Selectin family members are most commonly associated with leukocyte rolling and capture on vascular endothelial cells (Jones, Abbassi et al. 1993; Nolte, Schmid et al. 1994; Ley, Bullard et al. 1995; Massberg, Enders et al. 1998) but are also linked to PMN aggregation, adhesion, and transmigration (Geng, Bevilacqua et al. 1990; Diacovo, Roth et al. 1996; Guyer, Moore et al. 1996; Burns, Bowden et al. 1999; Lam, Burns et al. 2011). Specifically, platelet P-selectin binds with leukocyte P-selectin glycoprotein-1 (PSGL-1) and Sialyl Lewis^x carbohydrates, and endothelial von Willebrand factor to

facilitate these functions (Bevilacqua and Nelson 1993; Nash 1994; Varki 1994; Asa, Raycroft et al. 1995; Guyer, Moore et al. 1996; Ikeda, Ueyama et al. 1999; Langer and Chavakis 2009). Additionally, P-selectin participates in platelet aggregation and accumulation during inflammation (Ikeda, Ueyama et al. 1999; Li, Rumbaut et al. 2006c). Because of its key role in facilitating leukocyte infiltration and platelet accumulation, P-selectin is required for efficient wound healing. Studies on P-selectin^{-/-} mice show delayed inflammatory cell recruitment and accumulation, and incomplete wound healing in the absence of P-selectin (Kanwar, Smith et al. 1998; Li, Rumbaut et al. 2006c; Naik-Mathuria, Gay et al. 2008).

1.2 Corneal Inflammation and Healing

The cornea is considered an immune-privileged tissue because of its avascular nature, even though it harbors resident leukocytes (discussed below). However, physical injury to the cornea (i.e. epithelial abrasion) profoundly alters its ultrastructure, causing stromal swelling, redistribution of resident leukocytes, death of keratocytes, and the infiltration of inflammatory cells. Corneal inflammation involves a series of complex events which results in the extravasation of inflammatory cells out of the limbal vessels and into the extravascular stromal environment. The removal of epithelium also causes nerve fibers to degenerate and keratocytes below the region of injury to die (Wilson, He et al. 1996a; Zieske, Guimaraes et al. 2001; Zhao and Nagasaki 2004; Li, Burns et al. 2011). Keratocyte death is discussed further in the following section (Section 1.3). Corneal nerves in the epithelium release substance P as a result of injury and substance P is known to stimulate epithelial IL-8 release in humans and MIP-2 in mice. IL-8 and its murine ortholog, MIP-2, are chemokines secreted by vascular endothelial cells upon injury and play a role in PMN recruitment. Additionally, substance P promotes vascular dilation, secretion of cytokines, and activation of leukocyte adhesion molecules

(Laurenzi, Persson et al. 1990; Baluk, Bowden et al. 1997; Castagliuolo, Keates et al. 1998; Xavier, Isowa et al. 1999; Tran, Lausch et al. 2000; Tran, Ritchie et al. 2000). Although these mechanisms have not been directly linked to the initiation of inflammation following epithelial abrasion, given these exact events transpire at the onset of inflammation, it is reasonable to suggest substance P release activates the onset of corneal inflammation following epithelial abrasion.

Injury induces secretion of chemokines and cytokines by limbal endothelial cells and uninjured epithelial cells and keratocytes. Chemokine production by vascular endothelial cells promotes leukocyte recruitment (Fernandez and Lolis 2002; Laing and Secombes 2004), which in turn, secrete cytokines (Dinarello 2000). Wilson and colleagues have proposed the cytokine interleukin (IL)-1, secreted by corneal epithelial cells in addition to leukocytes, is the master regulator of corneal inflammation and wound healing by modulating inflammation and keratocyte apoptosis during inflammation stimulating the production of growth factors to facilitate wound healing (Wilson, He et al. 1994; Wilson, He et al. 1996a; Wilson, Li et al. 1996b; Wilson and Esposito 2009). Additionally, IL-1 is secreted by keratocytes (Wilson, Mohan et al. 2001).

During inflammation, neutrophils (PMNs) are the first leukocytes to transmigrate out of the limbal vasculature and into the stroma where they interact with collagen and peripheral keratocytes as they migrate towards the site of injury (O'Brien, Li et al. 1998; Burns, Li et al. 2005; Li, Burns et al. 2006b; Petrescu, Larry et al. 2007; Byeseda, Burns et al. 2009; Gagen, Laubinger et al. 2010). As previously described, PMN transmigration out of vessels is facilitated by a series of adhesion molecule interactions, involving selectins and integrins (Ley 1996). During corneal inflammation, Li and colleagues demonstrated that PMN $\beta 2$ integrin CD18 facilitates influx of PMN into the stroma (Li, Burns et al. 2006a). ICAM-1 is a known ligand for CD18 and the influence of ICAM-1 in PMN infiltration will also be discussed in this Dissertation. Additionally,

platelets infiltrate the limbal stroma during inflammation (Li, Rumbaut et al. 2006c; Li, Burns et al. 2007; Li, Burns et al. 2011; Li, Burns et al. 2011). Platelets express surface adhesion molecules which associate with PMN, endothelial or other platelet adhesion molecules. These interactions promote signaling events that initiate leukocyte activation, adhesion, and cellular differentiation and proliferation. It is even suggested that platelets promote PMN transmigration during inflammation (Diacovo, Roth et al. 1996; Evangelista, Manarini et al. 1996; Bennett, Berger et al. 2009; Lam, Burns et al. 2011). However, the specific mechanisms mediating platelet transmigration are still unclear, and although this Dissertation will not seek to elucidate these specific mechanisms, possible adhesion molecule-mediated and adhesion molecule-independent mechanisms of platelet extravasation will be discussed. During corneal inflammation, $\gamma\delta$ T cells enter the stroma (Li, Burns et al. 2007). $\gamma\delta$ T cells serve multiple functions in general wound healing, from secreting cytokines to promoting leukocyte infiltration to regulating the immune response (Hayday and Tigelaar 2003; Braun, Ferrick et al. 2008; Molesworth-Kenyon, Yin et al. 2008; Deknuydt, Scotet et al. 2009; Bonneville, O'Brien et al. 2010; Ma, Lancto et al. 2010). Byeseda *et al.* demonstrated that recruitment of corneal epithelial $\gamma\delta$ T cells into the cornea is facilitated by epithelial ICAM-1 and preventing their recruitment significantly delays epithelial wound closure (Li, Burns et al. 2007; Byeseda, Burns et al. 2009).

The human and mouse corneas harbor a resident population of myeloid lineage antigen presenting dendritic cells (O'Brien, Li et al. 1998; Hamrah, Zhang et al. 2002; Hamrah, Huq et al. 2003; Hamrah, Liu et al. 2003; Chinnery, Ruitenberg et al. 2007; Hamrah and Dana 2007; Mayer, Irschick et al. 2007; Chinnery, Carlson et al. 2009). Subpopulations of dendritic cells, called Langerhans' cells (after Paul Langerhans, the man who discovered them in skin epidermis (Sakula 1988)), reside in the corneal basal epithelium. These Langerin positive cells are clearly distinguished from other dendritic

cells (DCs) by the presence of specific Birbeck granules. Additionally, there are also resident DCs that are Langerin positive but are not Langerhans' cells (Valladeau, Ravel et al. 2000; Hamrah, Zhang et al. 2002; Lau, Chu et al. 2008; Thepaut, Valladeau et al. 2009; Hattori, Chauhan et al. 2011). In the uninjured cornea, these cells reside primarily along the peripheral and paracentral regions (Mayer, Irschick et al. 2007). Corneal dendritic cells are dispersed throughout the cornea, with immature cells being more central and mature cells more peripheral; macrophages reside throughout the posterior stroma (Hamrah, Liu et al. 2003; Mayer, Irschick et al. 2007). Corneal injury induces immature dendritic cells to migrate to the periphery as mature DCs migrate towards the center (Hamrah, Huq et al. 2003). Macrophage numbers increase as a result of inflammation, possibly due to monocyte infiltration (personal communication with Drs. C.W. Smith and Z. Li, Baylor College of Medicine). Macrophages and DCs are classical antigen presenting cells and phagocytose pathogens and present them via Major Histocompatibility Complex (MHC) II to T cells. Multiple mechanisms of defense, such as antimicrobial peptides and toll-like receptors, also work to protect the cornea against pathogens (McDermott 2004; Redfern, Reins et al. 2011). However, because this Dissertation is based on a non-infectious injury model (pathogen-independent inflammation), these defense mechanisms will not be discussed.

1.3 *Keratocyte Death*

In addition to eliciting corneal inflammation, central epithelial abrasion results in anterior keratocyte death, immediately below the injury (Wilson, He et al. 1996a; Zieske, Guimaraes et al. 2001; Zhao and Nagasaki 2004; Burns, Li et al. 2005; Li, Burns et al. 2006a; Li, Burns et al. 2006b; Li, Rumbaut et al. 2006c; Li, Burns et al. 2007; Petrescu, Larry et al. 2007; Byeseda, Burns et al. 2009; Gagen, Laubinger et al. 2010; Li, Burns et al. 2011). Current evidence suggests that early keratocyte death occurs primarily

through apoptosis (Wilson, He et al. 1996a; Wilson, Mohan et al. 2002; Ambrosio, Karajose et al. 2009) but necrotic cells are also observed as a result of epithelial abrasion (Mohan, Hutcheon et al. 2003; Wilson, Chaurasia et al. 2007). This phenomenon is extensively documented in post-refractive surgery patients and studies have shown that keratocytes never return to baseline, even many years after surgery (Wilson, Mohan et al. 2001; Mitooka, Ramirez et al. 2002; Erie, Patel et al. 2003; Ivarsen, Laurberg et al. 2004; Patel, Erie et al. 2007).

Wilson and colleagues have extensively studied mechanisms involved in keratocyte death and they propose the interleukin-1 (IL-1 α , β) system, cytokines released primarily from epithelial cells, but also from keratocytes, as well as the Fas/Fas ligand system, released by damaged epithelial cells, are responsible for keratocyte apoptosis. Keratocytes express receptors for IL-1 and Fas and their studies showed apoptosis occurred between minutes, *in vivo* and days, *in vitro* (Wilson, He et al. 1996a; Mohan, Liang et al. 1997). Necrosis, an “accidental” form of cell death, may occur as somewhat of a side-effect of apoptosis. Caspase 8, a protein involved in the initiation and execution of apoptosis through the extrinsic pathway, also can regulate the induction of necrosis. Briefly, extrinsic signaling ligands triggers the recruitment of the death-induced signaling complex (DISC), which consists of Caspase 8, FADD (Fas-associated death domain), and FLIP (FLICE-inhibitory protein). This tri-protein complex suppresses a necrosis pathway by preventing a necrosome complex formation. This is also a three-protein complex and its pathway is inhibited by a stable DISC complex. However, the absence (mutation, disassembly, degradation) of the DISC complex triggers the activation of the necrosis pathway (involving a necrosome complex) while inhibiting the apoptosis pathway (Krueger, Baumann et al. 2001; Screaton, Kiessling et al. 2003; Peter 2011). Thus, both apoptosis and necrosis may be involved in keratocyte death due to epithelial abrasion. Keratocytes produce essential extracellular matrix components,

such as collagen, proteoglycans, and corneal crystallins, which are all important for preserving the corneal ultrastructure and maintaining corneal clarity. Following corneal injury, keratocyte recovery is critical for supporting good vision.

It is established that effective healing requires an efficient inflammatory response, which involves PMNs, platelets, and $\gamma\delta$ T cell recruitment. Furthermore, these cells have been shown to promote corneal epithelial healing and nerve regeneration (Li, Burns et al. 2006a; Li, Burns et al. 2006b; Li, Rumbaut et al. 2006c; Li, Burns et al. 2007; Li, Burns et al. 2011). Clearly, inflammation is essential for corneal healing and these cells and their associated adhesion molecules play an integral role in promoting healing of corneal epithelial cells and nerves.

Thus, this dissertation hypothesizes that PMNs, platelets, their associated adhesion molecules (CD18, ICAM-1, and P-selectin), and $\gamma\delta$ T cells can also contribute to keratocyte repopulation. The goals of this dissertation are to elucidate the cellular and molecular mechanisms that 1) mediate PMN-keratocyte interactions and facilitate PMN and platelet infiltration during inflammation and 2) promote keratocyte repopulation during wound healing.

CHAPTER 2: SPECIFIC AIMS

2.1 Aim 1: To Determine if ICAM-1 Mediates Close Surface Contacts Between Neutrophils and Keratocytes Following Corneal Epithelial Abrasion in the Mouse

Corneal epithelial abrasion, resulting from physical damage or refractive surgery, elicits an inflammatory response (O'Brien, Li et al. 1998; Wilson, Mohan et al. 2001; Hamrah, Liu et al. 2003; Belmonte, Acosta et al. 2004; Burns, Li et al. 2005; Li, Burns et al. 2006a; Li, Burns et al. 2006b; Pearlman, Johnson et al. 2008; Chinnery, Carlson et al. 2009) characterized by an acute recruitment of neutrophils (PMNs) into the stroma (Wilson, Mohan et al. 2001; Burns, Li et al. 2005; Li, Burns et al. 2006a; Li, Burns et al. 2006b). Li and colleagues showed PMN emigration from limbal vessels is facilitated by leukocyte-specific Beta (β)-2 integrin, CD18. Furthermore, they showed that the total absence of CD18, or absence of specific CD18 family members (CD11a/CD18-LFA-1 or CD11b/CD18-Mac-1), not only delayed entry of PMNs into the stroma but also significantly delayed wound closure (Li, Burns et al. 2006a; Li, Burns et al. 2006b).

PMN transendothelial migration in the systemic circulation is well known to be regulated by CD18 integrins (Carlos and Harlan 1994; Jaeschke and Smith 1997; Ley 2001; Phillipson, Heit et al. 2006). Most recently, in response to central corneal epithelial abrasion, we identified a novel extravascular role for CD18 during PMN migration through the corneal interstitium (Petrescu, Larry et al. 2007). We observed that PMNs preferentially infiltrate the anterior stroma and migrate within the interlamellar spaces where they make close surface contacts with the surrounding collagen and paralimbal keratocytes. Close contact with keratocytes requires CD18 while contact with collagen does not. It is well known that keratocytes form a cellular network and we suggested keratocytes function as a "cellular highway" for CD18-dependent PMN migration within

the stroma. The identity of the CD18-ligand expressed on the keratocyte was not determined.

It is well established that endothelial intercellular adhesion molecule-1 (ICAM-1) plays a key role during inflammation, serving as a ligand for CD18 integrins and thereby facilitating PMN recruitment (Burns, Takei et al. 1994; Ley 1996; Oberyszyn, Conti et al. 1998; Moreland, Fuhrman et al. 2002; Brake, Smith et al. 2006). ICAM-1 is a five-domain transmembrane glycoprotein that binds to PMN integrin CD11a/CD18 at domain one and CD11b/CD18 at domain three (Smith, Marlin et al. 1989; Diamond, Garcia-Aguilar et al. 1993; Huang and Springer 1995; Lynam, Sklar et al. 1998; Roebuck and Finnegan 1999). *In vitro* and *in vivo* studies of the cornea show that ICAM-1 is expressed on epithelial cells (Hobden, Masinick et al. 1995; Yannariello-brown, Hallberg et al. 1998; Kumagai, Fukuda et al. 2003; Li, Burns et al. 2007; Liang, Brignole-Baudouin et al. 2007; Byeseda, Burns et al. 2009), keratocytes (Pavilack, Elner et al. 1992; Hobden, Masinick et al. 1995; Seo, Gebhardt et al. 2001; Kumagai, Fukuda et al. 2003; Liang, Brignole-Baudouin et al. 2007), and endothelial cells (Elner, Elner et al. 1991; Pavilack, Elner et al. 1992; Hobden, Masinick et al. 1995). We and others have observed increased ICAM-1 staining on mouse corneal epithelial cells following epithelial abrasion or *Pseudomonas* infection (Hobden, Masinick et al. 1995; Li, Burns et al. 2006b; Li, Burns et al. 2007; Byeseda, Burns et al. 2009). With respect to the corneal keratocyte, *in vitro* studies of human corneal explants show increased levels of ICAM-1 staining after cytokine treatment (Pavilack, Elner et al. 1992). In the mouse, baseline immunostaining for keratocyte ICAM-1 reportedly increases *in vivo* after *Pseudomonas* infection (Hobden, Masinick et al. 1995) but whether it increases after simple epithelial abrasion is unknown. Furthermore, it remains to be determined if ICAM-1 expression on mouse keratocytes mediates PMN close surface contact with keratocytes.

The purpose of this study is to evaluate the relative contribution of ICAM-1 to PMN stromal migration by determining if close surface contact between migrating PMNs and stromal keratocytes is ICAM-1-dependent.

2.2 *Aim 2: To Determine if CD18 and ICAM-1 Facilitate Neutrophil Motility on the Surface of Mouse Keratocytes*

Acute inflammation induced by corneal epithelial abrasion elicits PMN extravasation into the stroma (Burns, Li et al. 2005; Li, Burns et al. 2006a; Li, Burns et al. 2006b; Li, Rumbaut et al. 2006c; Li, Burns et al. 2007; Petrescu, Larry et al. 2007; Byeseda, Burns et al. 2009; Li, Burns et al. 2011). As PMNs enter the corneal stroma, they preferentially migrate through the anterior stroma during early inflammation. During migration, PMNs make close surface contact with paralimbal keratocytes and previous studies showed that close surface contacts between these cells is mediated by the adhesion molecule CD18 (Petrescu, Larry et al. 2007).

Inflammatory stimuli cause conformational changes and upregulation of PMN CD18 and increase ICAM-1 expression on endothelial cells. Thus, extravasated PMNs have increased CD18 expression (Kishimoto, Jutila et al. 1989; Griffin, Spertini et al. 1990; Crockett-Torabi, Sulenbarger et al. 1995). . Furthermore, it is well established that PMN-CD18 forms adhesive contacts with endothelial-ICAM-1 to facilitate PMN motility over endothelial monolayers (Smith, Marlin et al. 1989; Carlos and Harlan 1994). Whether these intravascular functional features of CD18 and ICAM-1 also translate into an extravascular functional role for these adhesion molecules in facilitating PMN migration over keratocytes is unknown, but keratocytes can express ICAM-1 (Pavilack, Elner et al. 1992; Kumagai, Fukuda et al. 2003).

The purpose of Aim 2 is to determine whether CD18 and ICAM-1 serve functional roles in facilitating PMN migration through the paralimbal stroma.

2.3 *Aim 3: To Determine if CD18 and ICAM-1 Regulate Neutrophil Infiltration and Platelet Accumulation Following Corneal Epithelial Abrasion in the Mouse*

Corneal epithelial abrasion results in PMN and platelet infiltration into the cornea (Burns, Li et al. 2005; Li, Burns et al. 2006a; Li, Burns et al. 2006b; Li, Rumbaut et al. 2006c; Li, Burns et al. 2007; Petrescu, Larry et al. 2007; Byeseda, Burns et al. 2009; Li, Burns et al. 2011). While PMNs are capable of migration through the stroma, platelet accumulation is confined to the vicinity of the limbus, a region peripheral and immediately adjacent to the cornea, along the corneal-scleral interface (Figure 2). The kinetics of PMN and platelet infiltration was previously described by Li and colleagues (Li, Burns et al. 2006a). However, the epithelial injury in those studies was created using either a diamond blade or golf club spud while the studies in this Dissertation use the Algerbrush to debride the epithelium. There are substantial qualitative differences between the two injury models, making it necessary to reassess of the kinetics of inflammatory cell recruitment following an Algerbrush injury (Figure 3).

Leukocyte specific CD18 is a $\beta 2$ integrin that has four family members, two of which, CD11a/CD18 (LFA-1) and CD11b/CD18 (Mac-1), play integral roles in leukocyte firm adhesion and facilitate transmigration out of the vasculature (Smith, Marlin et al. 1989; Diamond, Staunton et al. 1991; Diamond and Springer 1993; Burns, Simon et al. 1996; Ley 1996; Lynam, Sklar et al. 1998; Smith 2008). The absence or reduced expression of CD18 inhibits leukocyte infiltration, suppresses inflammation, and delays wound healing. The pathology of this phenotype is most notable in a condition called Leukocyte Adhesion Deficiency (LAD-I), where mutations in the $\beta 2$ integrin CD18 results in reduced leukocyte emigration to the site of infection, thus increasing vulnerability to infection and disease (Etzioni and Alon 2004; Helmus, Denecke et al. 2006; Movahedi, Entezari et al. 2007). This illustrates the importance of inflammation in aiding the healing process. While previous corneal inflammation studies used CD18 null mice,

which replicate extreme LAD conditions, the studies in this Dissertation use CD18 hypomorphic mutants, which are functionally analogous to the moderate form of LAD (Wilson, Ballantyne et al. 1993) (See section 3.1). Baseline PMN CD18 expression in these mice is significantly lower than in WT C57Bl/6 mice and while there is upregulation of CD18 in activated PMNs, the expression remains significantly lower than CD18 expression in activated WT PMNs.

ICAM-1 is a five-domain transmembrane glycoprotein and known ligand for CD18 (Roebuck and Finnegan 1999). ICAM-1 is expressed on vascular endothelial cells and corneal epithelial cells, corneal endothelial cells, and keratocytes (Elner, Elner et al. 1991; Pavilack, Elner et al. 1992; Hobden, Masinick et al. 1995; Yannariello-brown, Hallberg et al. 1998; Seo, Gebhardt et al. 2001; Kumagai, Fukuda et al. 2003; Li, Burns et al. 2007; Liang, Brignole-Baudouin et al. 2007; Byeseda, Burns et al. 2009). Figure 1 is a cartoon depicting the interactions between CD18 and ICAM-1, where PMN LFA-1 associates with domain 1 on ICAM-1 and PMN Mac-1 associates with domain-3 (Dustin and Springer 1988; Diamond, Staunton et al. 1990). This association mediates firm adhesion of PMN on the surface of endothelial cells at the “intravascular level” and mediates close surface contacts between PMNs and stromal keratocytes at the extravascular level (Burns, Li et al. 2005; Petrescu, Larry et al. 2007; Gagen, Laubinger et al. 2010).

Platelets are small, granulated, anucleate inflammatory cells (Firkin 1963; George 2000; Blair and Flaumenhaft 2009). Li *et al* showed platelet accumulation was coincident with PMN infiltration into the cornea. Platelets play an important role in the healing process and platelet depletion studies in mouse cornea showed delayed epithelial healing (Li, Rumbaut et al. 2006c; Li, Burns et al. 2007). However, platelet depletion also reduces PMN infiltration and vice versa. Taken together with the

coincident recruitment of PMNs and platelets, it is difficult to determine whether PMNs or platelets or both are required for wound healing.

The studies in Aim 3 will determine whether adhesion molecules CD18 and ICAM-1 regulate PMN infiltration and migration in the cornea and platelet accumulation at the limbus in the Algerbrush-induced corneal epithelial abrasion model. Elucidating these molecular mechanisms mediating inflammatory infiltration in this injury model will

- 1) substantiate the Algerbrush injury model for future corneal inflammation studies and
- 2) provide further insight on the contribution of these adhesion molecules in subsequent corneal wound healing.

2.4 Aim 4: To Determine if PMNs and/or Platelets are Necessary for Keratocyte Repopulation Following Corneal Epithelial Abrasion in the Mouse

Keratocytes are resident corneal stromal cells which actively synthesize essential extracellular matrix components, such as collagen, proteoglycans, and corneal crystallins, in order to sustain corneal clarity and preserve the corneal ultrastructure (Hassell and Birk ; Goldman and Benedek 1967; Maurice 1970; Zimmermann, Trueb et al. 1986; Birk, Fitch et al. 1988; Fitch, Birk et al. 1991; Funderburgh, Funderburgh et al. 1996; Chakravarti, Magnuson et al. 1998; Beales, Funderburgh et al. 1999; Jester, Moller-Pedersen et al. 1999; Chakravarti, Petroll et al. 2000; Ihanamaki, Pelliniemi et al. 2004; Carlson, Liu et al. 2005; Jester 2008). Mechanical injury to the cornea, occurring from non-penetrating epithelial abrasion or refractive surgery (LASIK, PRK), can result in the death of anterior keratocytes, below the region of injury. While corneal epithelial recovery is rapid (Srinivasan 1982; Saika, Shiraishi et al. 2000; Wilson, Mohan et al. 2001; Li, Burns et al. 2006a; Li, Burns et al. 2006b; Li, Rumbaut et al. 2006c; Li, Burns et al. 2007), keratocyte recovery is delayed (Zieske, Guimaraes et al. 2001) and post-operative case studies show that keratocyte numbers do not return to normal levels years after surgery (Helena, Baerveldt et al. 1998; Wilson, Mohan et al. 2001; Erie, Patel et al. 2003; Ivarsen, Laurberg et al. 2004; Patel, Erie et al. 2007). Because keratocytes play an essential role in maintaining corneal integrity, their loss can lead to profound ultrastructural damage. In fact, many studies report a high risk for corneal ectasia in patients after LASIK associated with unusually low anterior keratocyte density (Comaish and Lawless 2002; Khachikian and Belin 2010; Hodge, Lawless et al. 2011; Peinado, Pinero et al. 2011). While the mechanisms involved in keratocyte loss are extensively studied (Wilson, He et al. 1996a; Mohan, Liang et al. 1997; Helena, Baerveldt et al. 1998; Wilson and Kim 1998; Kim, Rabinowitz et al. 1999; Mohan, Kim et al. 2000; Wilson 2002; Mohan, Hutcheon et al. 2003; Wilson, Mohan et al. 2003a; Ambrosio,

Kara-Jose et al. 2009), very little is known about keratocyte recovery. Thus, elucidating the cellular and molecular mechanisms promoting keratocyte recovery is critical for minimizing corneal damage following mechanical injury.

PMNs and platelets are required for effective wound healing and a delay or deficiency in their infiltration leads to impaired healing (Li, Rumbaut et al. 2006c; Li, Burns et al. 2007; Burmeister, Hartwig et al. 2009; Smyth, McEver et al. 2009; Nurden 2011; Ravari, Hamidi-Almadari et al. 2011). Both inflammatory cell types contain growth factors that contribute to cell proliferation and tissue regeneration (Servold 1991; Smyth, McEver et al. 2009; Li, Burns et al. 2011). Furthermore, the life saving benefits of platelet transfusion therapy have been understood and practiced for decades (Ferraris, Ferraris et al. 2007; Blumberg, Heal et al. 2010; Spiess 2010). In the cornea, platelet extracts improve epithelial healing but cause stromal cells (keratocytes) to differentiate into myofibroblasts, a phenotype associated with corneal haze (Geremicca, Fonte et al. ; Kamiyama, Iguchi et al. 1998; Imanishi, Kamiyama et al. 2000; Matsuo, Ohkohchi et al. 2008). Using mice deficient in gamma delta ($\gamma\delta$) T cells and P-selectin, Li and colleagues previously demonstrated that reduced platelet accumulation at the limbal stroma hindered subsequent healing (Li, Rumbaut et al. 2006c; Li, Burns et al. 2007), suggesting that efficient infiltrating platelet accumulation is required for effective healing.

Gamma delta ($\gamma\delta$) T cells play a role in platelet recruitment into tissue. This small subpopulation of T cells can be distinguished from the $\alpha\beta$ T cell subtype by their $\gamma\delta$ T cell receptor ($\gamma\delta$ TCR) (Allison, Winter et al. 2001). $\gamma\delta$ T cells have diverse functions, from maintaining homeostasis by behaving as an effector T cell, to modulating inflammation by producing pro-inflammatory cytokines, to assisting in epithelial healing (Bonneville, O'Brien et al. 2010; Macleod and Havran 2011). With respect to cytokine production, $\gamma\delta$ T cells secrete pro-inflammatory cytokines IL-17 and IL-22 (Deknuydt, Scotet et al. 2009; Ma, Lancto et al. 2010; Ness-Schwickerath, Jin et al. 2010; Li, Burns

et al. 2011; Li, Burns et al. 2011). These cytokines have been shown to induce vascular permeability and cellular migration, regulate inflammatory cell infiltration, and promote tissue repair and wound healing (Wolk, Witte et al. ; Boniface, Bernard et al. 2005; Braun, Ferrick et al. 2008; Roussel, Houle et al. 2010). Indeed, Li and colleagues showed $\gamma\delta$ T cell and platelet numbers are reduced when anti-IL-17 or anti-IL-22 is topically or systemically administered to WT mice and platelet recruitment in TCR $\delta^{-/-}$ mice is restored after recombinant (r)IL-17 or rIL-22 treatment, confirming their previous hypothesis that $\gamma\delta$ T cells play an important role in platelet recruitment to the limbal stroma (Li, Burns et al. 2007; Li, Burns et al. 2011; Li, Burns et al. 2011).

In addition to $\gamma\delta$ T cells, platelet infiltration into tissue is mediated by other cellular and molecular mechanisms (Feng, Nagy et al. 1998; Rumbaut 2005; Ruggeri and Mendolicchio 2007; Bennett, Berger et al. 2009; Rivera, Lozano et al. 2009). One well characterized mechanism involves the cell surface adhesion molecule, P-selectin. P-selectin belongs to the Selectin family of adhesion molecules and is expressed on activated platelets and inflamed vascular endothelium (Stenberg, McEver et al. 1985; Bonfanti, Furie et al. 1989; Larsen, Celi et al. 1989; McEver, Beckstead et al. 1989; Koedam, Cramer et al. 1992; McEver 1995). During inflammatory cell infiltration, P-selectin facilitates associations between PMNs, platelets, and endothelial cells through a variety of receptor-co-receptor interactions (Nash 1994; Varki 1994; Asa, Raycroft et al. 1995; Furie and Furie 1995; Ma, Plow et al. 2004; Lam, Burns et al. 2011). *In vivo* studies using P-selectin $^{-/-}$ mice showed inefficient platelet recruitment and healing after ischemia/reperfusion injury (Massberg, Enders et al. 1998) and reduced limbal platelet accumulation and delayed wound closure after corneal epithelial abrasion (Li, Rumbaut et al. 2006c). In the cornea, transfusion of WT platelets, which express P-selectin, into P-selectin $^{-/-}$ mice restored corneal epithelial recovery (Li, Rumbaut et al. 2006c), demonstrating a positive regulatory role for platelet P-selectin in corneal healing.

Aim three investigated the kinetics of PMN infiltration and migration and platelet accumulation following corneal epithelial abrasion. Corneal epithelial healing and the participation of inflammatory cells and associated adhesion molecules during epithelial recovery are well characterized (Li, Burns et al. 2006a; Li, Burns et al. 2006b; Li, Rumbaut et al. 2006c; Byeseda, Burns et al. 2009). However, the cellular and molecular mechanisms driving keratocyte repopulation have yet to be resolved. The purpose of Aim 4 is to determine whether PMNs and/or platelets also contribute to keratocyte repopulation following corneal epithelial abrasion using an Algerbrush.

CHAPTER 3: METHODS

3.1 *Animals*

Male ICAM-1^{-/-} mice and P-selection^{-/-} mice were housed and backcrossed at least 10 generations with C57Bl/6 mice at Baylor college of Medicine (Li, Rumbaut et al. 2006c; Byeseda, Burns et al. 2009). Male C57Bl/6 wild type (WT) mice, CD18 hypomorphic mutant mice (B6.129S7-*Itgb2*^{tm1Bay}), TCR δ ^{-/-} mice (B6.129P27-*Tcrd*^{41Mom}), and a separate set of P-selectin^{-/-} mice (B6.129S7-*Itgb2*^{tm1Bay}) were purchased from Jackson Laboratory (Bar Harbor, ME). All mice were and bred at Baylor College of Medicine animal housing facilities.

The CD18^{mutant} mice were originally created at Baylor College of Medicine by Arthur Beaudet's laboratory (Wilson, Ballantyne et al. 1993). These mutant mice express baseline levels of the β 2 integrin CD18 but this expression is < 2% of WT baseline CD18 expression. While PMA stimulation increased CD18 expression on PMNs of mutant mice, this also remains significantly lower than that of CD18 in PMA-stimulated WT mice (only 16% of WT).

Female mice were not used for these studies because the estrous cycle in female mice alter their hormone levels and may affect the inflammatory response (Walmer, Wrona et al. 1992; Gaillard and Spinedi 1998; Tibbetts, Conneely et al. 1999). Preliminary observations by Dr. Zhijie Li (Baylor College of Medicine) showed significant differences in peak PMN infiltration time between male and female WT mice. Hence, to reduce variability, only male mice were used for these studies.

For *in vitro* experiments, corneas from 30-50 mice, ages 2 to 7 weeks, were pooled per experiment. For *in vivo* wound healing studies, 400 mice, ages 6 to 12 weeks, were used. All animals were treated according to the guidelines described in the

ARVO Statement for the Use of Animals in Ophthalmic and Vision Research, Baylor College of Medicine Animal Care and Use Committee policy, and Animal Care and Use Policies of the University of Houston.

3.1.1 *Corneal Epithelial Abrasion Model*

The corneal epithelial abrasion injury model has been used for over a decade to evaluate corneal inflammation, epithelial healing, stromal recovery, and keratocyte death and repopulation (Szerenyi, Wang et al. 1994; Wilson, He et al. 1996a; Zieske, Guimaraes et al. 2001; Zhao and Nagasaki 2004; Burns, Li et al. 2005; Li, Burns et al. 2006a; Li, Burns et al. 2006b; Li, Rumbaut et al. 2006c; Li, Burns et al. 2007; Petrescu, Larry et al. 2007; Byeseda, Burns et al. 2009; Gagen, Laubinger et al. 2010; Li, Burns et al. 2011; Li, Burns et al. 2011). This model is more similar to PRK than LASIK in that PRK requires the complete removal of the epithelial sheet prior to stromal ablation while LASIK leaves an epithelial and stromal flap intact to cover the ablated stromal region post-surgery (Lindstrom, Sher et al. 1991; Lindstrom, Hardten et al. 1997). However, both procedures result in substantial keratocyte loss and incomplete recovery (Erie, McLaren et al. 2005).

Various instruments are used to abrade the epithelium, such as scalpels, spatulas, diamond blade (Accutome, Malvern, PA), the Algerbrush II (Alger Equipment Co., Inc., Lago Vista, TX), and the golf club spud for refractive surgery (Accutome, Malvern, PA). It is taken for granted that the same injury created with different instruments will yield similar results. This was initially confirmed by Li and Byeseda, who were able to reproduce similar kinetics of inflammatory cell recruitment and rate of epithelial wound closure (in WT mice) following abrasion with either a diamond blade or a golf club spud (Li, Burns et al. 2006a; Li, Burns et al. 2006b; Li, Rumbaut et al. 2006c;

Li, Burns et al. 2007; Byeseda, Burns et al. 2009; Li, Burns et al. 2011; Li, Burns et al. 2011). Their results were initially considered the basis of corneal inflammation studies presented in this dissertation and the injury technique of a 2 mm diameter wound was adapted for the Algerbrush II (See Methods, Section 3.2.5). Clinically, the Algerbrush II is used by Ophthalmologists and Optometrists to remove rust rings left by foreign bodies removed from the ocular surface. Additionally, the Algerbrush is a useful tool for studying corneal inflammation and healing (Sharma, He et al. 2003; Gronert, Maheshwari et al. 2005; Lam, Burns et al. 2011). The Algerbrush II creates a smooth and reproducible injury, without disrupting the epithelial basement membrane (Sharma, He et al. 2003), undocumented personal observations). This is evidenced by the lack of the myofibroblasts phenotype in mouse corneas injured using the Algerbrush II. It is the disruption of the epithelial basement membrane allows TGF β to enter the stroma and induce keratocyte differentiation into myofibroblasts. Thus, the Algerbrush, rather than alternative Ophthalmology tools (i.e. golf club spud, scalpel, diamond blade), was used to debride the epithelium. However, following quantitation of inflammatory cell infiltration (in WT and knockout mice) after epithelial abrasion with the Algerbrush II, it was evident the two models were not equivalent.

Figure 3 illustrates the differences in inflammatory cell recruitment between a golf club spud versus the Algerbrush II 18 hours after injury. It is clear there are far fewer PMNs and platelets in the Algerbrush II injury versus the golf club spud injured cornea. Only the right cornea was injured in the wound model used in the present studies in contrast to the bilateral injuries performed by Li and colleagues. This was a possible explanation for the profound differences in inflammatory cell infiltration between the two models. The bilateral injury may enhance the inflammatory response, resulting in a vigorous PMN and platelet infiltration compared to the unilateral injury model. Therefore, WT mice and TCR $\delta^{-/-}$ mice were injured bilaterally, the right cornea using the Algerbrush

II and the left cornea using the golf club spud by Dr. Zhijie Li (Baylor College of Medicine). Eighteen hours after injury, a time point between peak PMN infiltration times in the two injury models, corneas were harvested and fixed by Dr. Li. From that point, all corneas were immunostained to detect PMNs and platelets, as described below (Section 3.3). Remarkable differences were observed in both PMN and platelet infiltration between the injury models. PMN infiltration after Algerbrush injury appeared less at the limbus, paralimbus, and center (Figure 3 A-C, E-G). PMN infiltration in TCR $\delta^{-/-}$ mice did not appear different between the two injury methods (Figure 3 I-K, M-O) but platelet numbers were markedly greater in the Algerbrush injured cornea (Figure 3 L,P). These results provide compelling evidence for injury-specific inflammatory response, thus the kinetics of inflammatory cell infiltration was re-evaluated in these studies (See Results, Section 4.3.1).

3.1.2 Wound Protocol

Two different anesthetics were used to sedate the mice for survival injuries, as per each institution's animal protocol. Pentobarbital (50 mg/kg body weight; Nembutal; Ovation Pharmaceuticals, Deerfield, IL) was used at Baylor College of Medicine and Ketamine (100 mg/kg)/Xylazine (10 mg/kg) (K/X) cocktail was used at the University of Houston. Ketamine has been demonstrated to have anti-inflammatory properties and Xylazine can exacerbate inflammation by promoting edema (Amouzadeh, Sangiah et al. 1991; Li, Chou et al. 1997; Helmer, Cui et al. 2003). Because these are the only approved anesthetics at UHCO, the K/X cocktail was only used to study WT keratocyte network surface area and surface-to-volume ratio 4 weeks post-injury (see section 3.5.1.2), in hopes the negative effects of the K/X would not affect the late time point results. A 2 mm diameter trephine was used to demarcate the central epithelial region of the right eye and the epithelium within the demarcated region was mechanically

removed using an Algerbrush II (Alger Equipment Co., Inc., Lago Vista, TX) under a dissecting microscope. Epithelial demarcation using the trephine may contribute to inflammation, but this was not independently investigated. Only right corneas were injured for all experiments. Uninjured right corneas were obtained from separate sets of mice of each genotype for all baseline measurements.

3.1.3 Genotyping

Tails were cut immediately after mice were humanely sacrificed and corneas were harvested. Tails were kept in -20° C for genotyping. The following primers were used to genotype knockout mice: 5'-AGG ACA GCA AGG GGG AGG ATT-3' (mutant primer oIMR0019) and 5'-GAG CGG CAG AGC AAA AGA AGC-3' (common primer oIMR0018) for ICAM-1^{-/-} genotyping; 5'-CTT GGG TGG AGA GGC TAT TC-3' (mutant forward primer oIMR6916) and 5'-AGG TGA GAT GAC AGG AGA TC-3' (mutant reverse primer oIMR6917) for TCR δ ^{-/-} genotyping, 5'-CTG AAT GAA CTG CAG GAC GA-3' (mutant forward primer oIMR0158) and 5'-ATA CTT TCT CGG CAG GAG CA-3' (mutant reverse primer oIMR0159) for P-selectin^{-/-} genotyping. PMNs in corneas of CD18 hypomorphic mutant mice were stained for CD18 expression to show these mice still expressed CD18 (Appendices Figure II). The level of CD18 expression was not quantified as the original paper determined this (Wilson, Ballantyne et al. 1993).

3.2 Cell Culture

3.2.1 Cover Slip Preparation

Inside a tissue culture hood, 24 mm diameter glass cover slips (Fisher Scientific, Pittsburgh, PA) were centrally placed within single wells of 6-well plates (35 mm diameter) (VWR, Randor, PA). Cover slips were coated with 250-350 μ l of sterile 1%

gelatin (BD Difco, Lawrence, KS) and incubated for 30 minutes at 37° C. Wells were subsequently flooded with 2 ml of 0.5% glutaraldehyde (from 50% EM grade stock, Electron Microscopy Sciences, Hatsfield, PA). Cover slips were incubated for 30 minutes at room temperature. Glutaraldehyde was removed and the cover slips were washed 3 times with 1X phosphate buffered saline, without calcium and magnesium (pH 7.2) (Invitrogen Life Technologies, Carlsbad, CA). Cover slips were incubated in 1 mM of glycine for 30 minutes, at room temperature, washed 3 times with PBS, and wells were filled with Keratinocyte Serum Free Medium (KSFM) (Invitrogen Life Technologies, Carlsbad, CA). Cover slips were kept at 37° C for 2 hours up to 24 hours, to acclimate with the serum free medium. Prior to cell seeding, the media was aspirated completely so the cell suspension would not flow over into the well.

3.2.2 Keratocyte Isolation

WT, CD18^{mutant}, and ICAM-1^{-/-} mice were humanely euthanized using Isoflurane inhalation followed by cervical dislocation. Corneas were dissected and put into PBS-glucose (pH 7.2, with calcium, magnesium, and 2% glucose), Penicillin/Streptomycin, and Amphotericin B (Invitrogen Life Technologies, Carlsbad, CA). Corneas were transferred to a laminar flow tissue culture hood and further washed three times in PBS-glucose (plus Penicillin/Streptomycin and Amphotericin B). Corneas were pooled together in a 100 mm diameter sterile petri dish and minced using two size 11 disposable scalpels (Sklar Instruments, West Chester, PA). Corneal tissue was transferred to a 15 ml test tube with sterile-filtered Collagenase Type 1(1.25 mg/ml) (Worthington Biochemical Corporation, Lakewood, NJ) in PBS/glucose. The test tube was placed on a tube rotator and the tissue was digested for 16 hours at 37° C. All subsequent procedures were performed inside a tissue culture hood. Following digest, the sample was centrifuged at 1000 rpm for 10 minutes at room temperature, to pellet the digest.

The collagenase was immediately aspirated and the digested sample was washed three times (by centrifuging for five minutes per wash at 1000 rpm, room temperature) in sterile-filtered PBS (pH 7.2) with 4% 20 mM EDTA and 1% BSA. This solution will be referred to as Keratocyte Isolation (KI) buffer. The digested sample was strained through a 40 μ m nylon mesh pre-separation filter (Miltenyi Biotech, Auburn, CA) in KI buffer and washed by centrifugation (1000 rpm, room temperature) three times. Because the corneal epithelium and endothelium were not removed prior to digestion, the cell pellet contained a mix of epithelial, stromal (keratocytes), and endothelial cells. Corneal keratocytes were purified using monoclonal anti-mouse CD324 (E-cadherin) (eBioscience, San Diego, CA) to label corneal epithelial cells and rat anti-human CD321 (JAM-A, specificity to human and mouse JAM-A) (GenWay Biotech, San Diego, CA) to label corneal epithelial cells and limbal and corneal endothelial cells (Chen, Ebihara et al. 2007; Kang, Wang et al. 2007). The antibodies were used at a final concentration of 10 μ g/ml, in 100-200 μ l cell suspension, in KI buffer, and incubated for 10 minutes at room temperature. Following one wash, cells resuspended with KI buffer containing goat anti-rat IgG secondary antibodies conjugated with ferritin particles for 15 minutes at room temperature (MACS Cell Separation system, Miltenyi Biotech, Auburn, CA). Cells were washed once, as previously described, and resuspended in 1 ml of KI buffer. The cell suspension was then passed through the MACS MS metal-matrix column suspended on a magnet so the matrix aligns with the magnet. All CD324 and CD321 positive cells remained within the magnetic column while all other cells, presumably keratocytes and resident leukocytes, were in the negative fraction flowing out of the column. The columns were washed twice more with KI buffer and the eluate was centrifuged to pellet the isolated cells. The KI buffer was aspirated and the cells were washed once in KSFM (Kawakita, Espana et al. 2006) containing pen/strep and Amphotericin B. Cells were finally resuspended in KSFM (in a total volume of 250-300

µl per cover slip). Dry cover slips were seeded with the appropriate volume of cell suspension and placed in an incubator at 37° C. After 2 hours, the wells containing the cover slips were gently flooded from the side with 2 ml KSFM, making sure each cover slip was completely covered. The medium was changed every two days and cells were allowed to attach and spread over 4 to 10 days prior to use in functional analysis assays. Figure 4 shows images of cultured mouse keratocytes 3 and 7 days after incubation. Additionally, resident corneal leukocytes were likely harvested during isolation but because of their low density (qualitative observations) and inability to divide under unstimulated conditions, resident corneal leukocytes were not deemed high risk factors for contamination. A separate batch of cultured cells was grown in the presence of 10% FBS in KSFM to promote myofibroblast differentiation and used as a positive myofibroblast control culture (Figure 15).

3.2.3 Mouse PMN Isolation

Three percent thioglycollate (Sigma-Aldrich, Fluka, St. Louis, MO), an enriched broth medium, was intraperitoneally (IP) injected into WT mice to induce peritonitis. The peritoneal cavity was lavaged using PBS, 4 hours post injection, to collect extravasated PMNs. Briefly, 4-6 ml of PBS was injected into the peritoneal cavity following humane euthanization, as previously described. The peritoneal cavity was gently massaged and the abdominal skin was bluntly dissected to expose the muscle. A 19 or 16 gauge needle was inserted into the peritoneal cavity and fluid containing PMNs was allowed to drain through the needle into a 50 ml conical tube. This process was repeated three times to collect maximum numbers of PMNs (Savige, Saverymuttu et al. 1984; Segal, Kuhns et al. 2002). Peritoneal fluid from three mice was pooled for one isolation gradient. The cell suspension was washed once in 0.9% NaCl and resuspended in 2 ml of 1X Hank's Buffered Saline Solution (HBSS), with phenol red, and 2mM EDTA (pH 7.2-

7.4). PMNs were isolated using a three-step Percoll gradient. A 1-part RediGrad Percoll (Amersham Biosciences, GE Healthcare Bio-Sciences Corporation, Piscataway, NJ) to 10 parts sterile 10X HBSS, without phenol red, was prepared to generate 100% Percoll. This was used as stock to prepare subsequent percoll dilutions. Seventy-five percent, 67%, and 52% dilutions of the stock percoll were prepared using HBSS (1X), with phenol red. The dilutions were carefully overlaid in 2 ml aliquots in a 15 ml conical tube, with the greatest density (75%) at the bottom and the lowest density (52%) at the top. The HBSS/EDTA cell suspension was carefully layered on top of the gradient and the preparation was centrifuged at 2800 rpm for 30 minutes, at room temperature. The gradient separated PMNs to the 67%-75% interface and other mononuclear cells (lymphocytes and monocytes) to the 52%-67% interface. The gradient fluid was aspirated through half of the 67% layer. A 10mm syringe attached with a 19 gauge angio-catheter needle (BD Bioscience, Franklin Lakes, NJ) was used to carefully remove the PMN-containing gradient fraction. The fraction was washed in PBS with 2% glucose (pH 7.2), cell numbers were quantified using a hemacytometer, and resuspended in PBS-glucose (warmed to 37° C) at 10^7 PMNs/ml.

3.2.4 *Determining PMN Migration Velocity*

Cultured mouse keratocytes were stimulated in rMolL-1 β made up at 10 U/ml in fresh KSFM. The stimulation times per cover slip were staggered every 30 minutes and the cells were incubated for 4 hours at 37° C. Each cover slip was washed 3 times in warm PBS/2% glucose and placed in a Muntz adhesion chamber (Smith, Rothlein et al. 1988; Smith, Marlin et al. 1989; Burns, Bowden et al. 1999). An O-ring was placed in the chamber, to contain warm PBS/2% glucose (37° C). The set-up was transferred to the DeltaVision Spectris light microscope with a heating chamber set to 37° C. All recordings were done on the DeltaVision Core light microscope with differential

interference contrast (DIC) imaging. Isolated extravascular PMNs (final concentration of 10^6 PMNs/ml) were added to rMolL-1 β stimulated keratocytes and baseline PMN migration was recorded for 5 minutes using time-lapse DIC imaging. After 5 minutes, blocking antibodies against CD18 (clone GAME46) or ICAM-1 (CD54, clone YN-1) were added at a final concentrations of 10 μ g/ml (Simon, Chambers et al. 1992). PMN migration was recorded for an additional 5 minutes. The recordings were analyzed and PMN velocity was determined by following the changes in the distance an individual PMN traveled over cultured keratocytes during the 10 minute period. These studies helped elucidate whether the addition of blocking antibodies to CD18 or ICAM-1 affected PMN migration velocity. Figure 5 shows frames tracking WT PMNs on WT keratocytes over the course of time. Non-immune rat IgG was used as a negative control for both anti-CD18 (GAME46) and anti-ICAM-1 (YN-1). At least 5 cells were analyzed per condition and one cover slip was considered as n=1.

3.2.5 Cardiac Puncture

Under Isoflurane anesthesia, fore and hind limbs of WT mice were extended and pinned at four sides using 16 gauge needles, and the thoracic region was aseptically cleaned using 70% ethanol. Peripheral blood (0.9 ml) was drawn by cardiac puncture into a syringe with containing 0.1 ml ACD anticoagulant (acid-citrate-dextrose, Sigma-Aldrich, St. Louis, MO), taking care not to introduce air into the syringe during collection. Blood from 3-4 donor WT mice was pooled to isolate platelets for a single recipient P-selectin^{-/-} mouse.

3.2.6 Platelet Isolation

An established method of platelet isolation, which minimizes platelet activation, was used to isolate platelets from WT donor mice (Rumbaut, Bellera et al. 2006; Li,

Rumbaut et al. 2006c). Whole blood was centrifuged at 260g for 8 minutes, to separate the red blood cells from the plasma. The top plasma layer was collected and centrifuged at 740 g for 10 minutes to pellet platelets. The supernatant was aspirated and the platelet pellet was gently resuspended in 500 μ l of PBS (Sigma-Aldrich, St. Louis, MO) and allowed to rest at room temperature for up to 30 minutes, at which time platelet numbers were counted using a hemacytometer. Platelets were resuspended at volume of 10^6 platelets/ μ l and 200 μ l of this suspension (representing 10% of circulating platelets) was injected into the tail vein of anesthetized recipient P-selectin^{-/-} mice, immediately before corneal epithelial abrasion. In a separate set of experiments, the same platelet suspension volume was injected into WT mice.

3.3 *Immunohistochemistry*

3.3.1 *Characterization of Cultured Keratocytes*

Cultured cells were immunostained with phycoerythrin (PE)-conjugated anti-mouse CD34 and a rabbit serum raised against keratocan antibody (generous gift from Dr. C.Y. Liu, University of Miami School of Medicine, Miami, FL). CD34 is a hematopoietic precursor marker and a positive keratocyte marker and keratocan is a KS proteoglycan synthesized and secreted by keratocytes (Kawakita, Espana et al. 2005; Sosnova, Bradl et al. 2005; Liu, Zhang et al. 2010). FITC conjugated α -smooth muscle actin (Sigma-Aldrich, St. Louis, MO) a myofibroblast marker (Jester, Petroll et al. 1995), was used to determine whether the cultured cells had differentiated into myofibroblasts during isolation and incubation. A separate batch of cultured cells were grown in the presence of 10% fetal bovine serum (FBS) in KSFM to promote myofibroblast differentiation and used as a positive control.

3.3.2 Preparation of Corneas for PMN and Platelet Analyses

Following corneal abrasion, WT, ICAM-1^{-/-}, and CD18^{mutant} mice were humanely euthanized (using Isoflurane inhalation followed by cervical dislocation) in 6 hour intervals, through 48 hours ($n=4$ to 6 corneas per time point, for each genotype). Mice used for PMN infiltration experiments were injured at the same time, on the same day, and each mouse was considered $n = 1$. Experiments for a given time point were not repeated on another day for these studies. For platelet accumulation studies, all injuries for a given time point were performed at the same time, on the same day, and each mouse was considered $n = 1$. A second set of WT and ICAM-1^{-/-} mice ($n = 5$ per genotype) were injured and the injury and the results were found to be highly reproducible.

Uninjured and injured right corneas from these mice were excised and fixed in 2% paraformaldehyde (Tousimus Research Corporation, Rockville, MD) in phosphate buffered saline (PBS, pH 7.2) for 60 minutes at 4° C, blocked for 30 minutes in PBS with 2% BSA, and permeabilized for 30 minutes with 0.1% Triton-X. All corneas were then incubated overnight at 4° C with PE conjugated anti-CD41 (GP2b, BD Bioscience, Pharmingen, San Jose, CA) antibody to label platelets, FITC conjugated Ly6-G antibody to detect PMNs (Fleming, Fleming et al. 1993; Daley, Thomay et al. 2008) (BD Bioscience, Pharmingen, San Jose, CA), APC conjugated anti-CD31 (PECAM-1, BD Bioscience, Pharmingen, San Jose, CA) to stain for limbal vessels, and DAPI (4',6-diamidino-2-phenylindole, Sigma, St. Louis, MO) to detect nuclei. Following overnight incubations, corneas were washed three times in PBS and radial cuts were made from the peripheral edge to the paracentral region. Corneas were mounted in AIRVOL mounting media (Celanese, Dallas, TX) or Prolong Gold self-curing mounting media (Invitrogen, Carlsbad, CA), and imaged with the DeltaVision Core inverted light microscope (Applied Precision, Issaquah, WA).

3.3.3 Characterization of ICAM-1 Expression on Whole-Mount Corneas

For histological studies, WT and ICAM-1^{-/-} mice were humanely euthanized (1-chloro-2,2,2-trifluoroethylidifluoromethyl ether-Isofluorane inhalation followed by cervical dislocation) and the eyes were enucleated. Corneas were excised from ICAM-1^{-/-} and WT mice and incubated in 20mM EDTA at 37° C for 30 minutes to loosen and permit easy removal of the corneal epithelium. The corneal epithelium was removed to allow better antibody penetration into corneas. Corneas were fixed in 2% paraformaldehyde in 0.1M phosphate buffered saline (PBS, pH 7.2) at 4° C for 60 minutes, blocked with PBS with 2% bovine serum albumin (BSA), and permeabilized with 0.1% Triton-X. Radial cuts were made from the peripheral edge to the paracentral region. Uninjured and 12 hour injured corneas (a time point when PMN stromal infiltration is underway;(Li, Rumbaut et al. 2006c)) were incubated with unconjugated rabbit anti-ALDH3A1 antibody (Santa Cruz Biotechnology, Inc., Santa Cruz, CA) overnight at 4° C. All corneas were washed three times with PBS/2% BSA and incubated overnight with goat-anti-rabbit Cy5 conjugated secondary IgG (Abcam, San Francisco, CA) to identify ALDH3A1-positive keratocytes, PE conjugated anti-ICAM-1 antibody (clone YN-1, Abcam, San Francisco, CA) to evaluate ICAM-1 expression on keratocytes, FITC conjugated Ly6-G antibody to detect PMNs (BD Bioscience, Pharmingen, San Jose, CA), and DAPI (4',6-diamidino-2-phenylindole, Sigma, St. Louis, MO) to detect nuclei. Separate 12 hour injured corneas were stained with a PE conjugated antibody against Thy1.2 (Ishihara, Hou et al. 1987)(BD Bioscience, Pharmingen, San Jose, CA), a fibroblast marker, and FITC conjugated antibody against α -smooth muscle actin, a myofibroblast marker (Jester, Petroll et al. 1995; Yoshida, Shimmura et al. 2005)(Sigma, St. Louis, MO). A third set of uninjured and injured corneas served as control for non-specific antibody staining and was incubated with the appropriate isotype matched non-immune IgG antibodies. All

corneas were mounted in AIRVOL mounting media (Celanese, Dallas, TX). Images through the full thickness of the paralimbal corneal region, immediately central and adjacent to the limbus, were obtained using a DeltaVision Core inverted microscope (Applied Precision, Issaquah, WA) and processed using SoftWorx software.

3.3.4 *IL-22R (receptor) Staining on Corneal Keratocytes*

Uninjured and 24h injured right corneas were harvested from male WT, ICAM-1^{-/-}, and TCR δ ^{-/-} mice and incubated in PBS with 20 mM EDTA to strip off the epithelium (Section 3.3.3). Radial cuts were made from the periphery into the center, taking care not to cut through the tissue. Corneas were processed for immunostaining, as previously described, and dual-stained with either APC-conjugated rat anti-mouse CD31, a positive limbal endothelial cell marker and PE rat anti-mouse IL-22R antibody (R&D Systems, Minneapolis, MN). Separate corneas were stained with non-immune rat IgG2a and APC CD31 as negative controls. The nuclear stain DAPI was also included during incubation with antibodies. Corneas were stained overnight at 4° C, washed 3 times in PBS and mounted in AIRVOL. The DeltaVision Core microscope was used to evaluate IL-22r staining on the limbal endothelium and keratocytes.

3.3.5 *Systemic and Topical Application of Recombinant (r)IL-22*

Recombinant (r)IL-22 (R&D Systems, Minneapolis, MN) was injected (IP) into male TCR δ ^{-/-} mice and right corneas were injured 24h later. Right corneas of a second set of TCR δ ^{-/-} mice were injured and rIL-22 was topically administered every 6 hours over a 24 hour period. Injured corneas were harvested 4 days later and anterior central keratocyte numbers were morphometrically analyzed, (Section 3.4.4).

3.3.6 Corneal Immunostaining for Keratocyte Repopulation

Following euthanization, right corneas from uninjured and injured WT, ICAM-1^{-/-}, and CD18^{mutant} mice ($n=5$ mice per time point, for each genotype) were excised, fixed in 2% paraformaldehyde in phosphate buffered saline (PBS, pH 7.2) for 60 minutes at 4° C, blocked for 30 minutes in PBS with 2% BSA, and permeabilized for 30 minutes with 0.1% Triton-X. All corneas were incubated with a FITC cocktail of leukocyte-specific antibodies (Table 2) and DAPI. Following overnight incubation, corneas were washed, cut radially from the periphery to the paracentral region, mounted in AIRVOL mounting media, and imaged with the DeltaVision Core microscope. Mice used for each time point were injured at the same time, on the same day, and each mouse was considered $n = 1$.

3.4 Morphometric Analyses of Immunostained Whole-Mount Corneas

3.4.1 Whole-Mount Corneal Analyses Parameters

For all whole-mount immunostain corneal analyses, the central corneal region for individual corneas was calculated using specific x- and y-coordinates obtained from the edge of the corneal endothelial monolayer at four directly opposite and perpendicular poles on the DeltaVision Core microscope. Limbal and paralimbal images of individual corneas were taken at these opposite, perpendicular poles and central regions were imaged at the calculated center.

3.4.2 PMN Infiltration

Images were obtained through the full thickness of four limbal and paralimbal regions and a single central corneal region, as described above. A morphometric number estimation 9-square grid (625 μm^2 /square) was overlaid upon the single panel

$2.72 \times 10^4 \mu\text{m}^2$ image (Figure 6). Only FITC conjugated Ly6G positive PMN nuclei falling within the grid squares or on the accepted frame lines, but not on forbidden frame lines, were counted, through the thickness of the image stack. PMN density, expressed in PMNs/mm², was calculated using the formula $[(\sum P/5625)/2.72 \times 10^4] \times 10^6$, where P=PMNs, 5625 (μm^2) is the total area of the 9 squares, and $2.72 \times 10^4 (\mu\text{m}^2)$ represents the image area.

3.4.3 Platelet Accumulation

A nine panel image was acquired through the thickness of the limbal vessels at 40X magnification using the DeltaVision Core microscope. The images were post-processed into $2.25 \times 10^5 \mu\text{m}^2$ montages using the Softworx software (Applied Precision, Issaquah, WA). Digital images were analyzed in Adobe Photoshop (Adobe Systems Inc., San Jose, CA) after randomly casting a 60-square (10×6 , $3211 \mu\text{m}^2/\text{square}$) morphometric number estimation grid (Figure 7) over the montage. The grid squares were oriented perpendicular to the major axis of the limbal vessels. Only CD41 positive platelets, greater than $2 \mu\text{m}$ diameter, were counted for the analyses. Within platelet aggregates, a $2 \mu\text{m}$ diameter region was considered an individual platelet and total numbers of $2 \mu\text{m}$ areas within these aggregates were estimated. Only platelets falling within the grid boxes or on the accepted lines of the grid boxes were counted. Platelets/mm² was calculated by using the formula $[(\sum C / \sum S)/3211] \times 10^6$, where C is platelet counts and S is squares completely falling within the montage region.

A second observer analyzed platelet accumulation (see section 3.3.2) in the second group of 24 hour injured WT mice to confirm whether there were inter-observer differences using the morphometric number estimation grid for platelet accumulation analyses (Appendices Figure III).

3.4.4 Keratocyte Repopulation

The two most reliable keratocyte-specific markers are keratocan, a corneal-specific proteoglycan synthesized and secreted by keratocytes, and aldehyde dehydrogenase (ALDH) 3A1, a corneal crystallin also synthesized by keratocytes (Jester, Moller-Pedersen et al. 1999; Jester 2008). Since keratocan is secreted throughout the stroma, it can not be used to detect individual keratocytes by immunohistochemistry. ALDH3A1 staining is localized to the cell body but the amount of ALDH present within individual keratocytes varies considerably, also making it an unreliable marker for accurate individual keratocyte counts. Stramer *et al.* demonstrated that the monoclonal antibody 3G5, a microvascular pericyte marker, positively stains keratocytes in a variety of species except mouse (Stramer, Kwok et al. 2004). Trying to obtain accurate measurements of keratocyte numbers in uninjured and injured mouse corneas using these antibodies was not feasible. Thus, to assess individual keratocyte counts, we stained for all corneal leukocytes using the FITC cocktail of leukocyte-specific antibodies (Ly6G, GR1, CD3e, $\gamma\delta$ TCR, CD45, CD18, F4/80) and DAPI (see Immunohistochemistry Methods above and Table 2). Along with resident keratocytes, the uninjured cornea harbors a resident population of dendritic cells and macrophages (Hamrah, Zhang et al. 2002; Hamrah, Huq et al. 2003; Chinnery, Ruitenberg et al. 2007; Chinnery, Humphries et al. 2008), while many other leukocytes infiltrate the injured cornea (Hamrah, Liu et al. 2003; Li, Burns et al. 2006a; Li, Rumbaut et al. 2006c; Li, Burns et al. 2007). A morphometric number estimation box ($1.56 \times 10^4 \mu\text{m}^2$) was used to count only non FITC-labeled (DAPI-stained) cell nuclei falling within the frame of the estimation box or on the accepted lines (Figure 8), through the thickness of the stroma. All FITC-labeled cells or non-FITC-labeled (DAPI-stained) nuclei falling on the forbidden lines were excluded from the counts. Central and paralimbal keratocyte numbers were analyzed for uninjured and 1, 4, 14, and 28 day injured corneas. Uninjured keratocyte

numbers were analyzed to establish baseline. One day (24 hours) after epithelial abrasion, central basal epithelial cells cover the original wound region (Appendices Figures IV B). Furthermore, Zieske and colleagues showed keratocyte recovery occurs at a slower rate following epithelial abrasion in the rat but this was not established using the mouse animal model (Zieske, Guimaraes et al. 2001) Hence, the first injured time point evaluated was 1 day to determine whether keratocyte repopulation begins early in the mouse model of corneal epithelial abrasion. Four days post injury, central basal epithelial cell density appears similar to uninjured basal cell density (Appendices Figure IV A and C). Li and colleagues showed that WT mouse epithelium is fully re-stratified by 4 days, as well (Li, Burns et al. 2007). This was the primary rational for choosing to evaluate keratocyte repopulation at 4 days post-injury. To observe keratocyte repopulation over an extended period of time, 14 days (2 weeks) was chosen as the third time point to observe. Finally, repopulation was evaluated 28 days (4 weeks) post-injury, to determine whether a longer healing time promoted greater repopulation or if keratocyte numbers remained low even after lengthy recovery period, as they remain low years after refractive surgery.

3.5 *Electron Microscopy*

3.5.1 *Tissue processing*

3.5.1.1 *Close Surface Contact Studies*

Whole uninjured and injured mouse eyes were fixed in 0.1 M sodium cacodylate buffer (pH 7.2) containing 2.5% glutaraldehyde for 2 hours at room temperature. Fixed eyes were rinsed in 0.1 M sodium cacodylate buffer and stored at 4° C until further

processing. Corneas, with the limbus intact, were carefully excised from the whole eye and cut into four equal-sized quadrants. These quadrants were post-fixed in 1% tannic acid for 5 minutes and transferred to 1% osmium tetroxide. Specimens were then dehydrated through an acetone series and embedded in resin (EMbed-812, Electron Microscopy Sciences, Hatfield, PA). Thin plastic sections (80 to 100 nm) were cut and imaged on a JEOL 200CX (Tokyo, Japan) electron microscope or a Tecnai G² Spirit BioTWIN (FEI Company, Hillsboro, OR) electron microscope.

3.5.1.2 WT Mouse Anterior Central Keratocyte Repopulation

Uninjured, 4, and 28 day injured WT mouse eyes (n=5 per time point) were enucleated and processed for EM using the PELCO BioWave Pro vacuum-assisted microwave (Ted Pella, Inc., Redding, CA) as previously described (ref-Hanlon *et al*). Briefly, whole eyeballs were fixed in 0.1 M sodium cacodylate buffer (pH 7.2) containing 2.5% glutaraldehyde for 6-8 minutes in the microwave with 1-3 minute intervals of alcohol dehydrations and water rinses. Corneas were carefully excised from the whole eye, cut into halves, and embedded in resin (EMbed-812, Electron Microscopy Sciences, Hatfield, PA). Thin plastic sections (80 to 100 nm) were cut and imaged on a Tecnai G² Spirit BioTWIN (FEI Company, Hillsboro, OR) electron microscope.

3.5.1.3 Morphometric Analysis

Morphometric analyses using stereological techniques were performed, as previously described (Petrescu, Larry et al. 2007), to quantify the percentage of PMN membrane in close contact with stromal structures (keratocytes, other PMNs and collagen) and determine keratocyte network size and surface area. Stereology, a well-established technique, is used for analyzing two-dimensional images (e.g., tissue sections) to obtain unbiased and accurate estimates of geometrical features including

feature number, length, surface area, and volume. It has been used extensively over the past 40 years in the study of biological structures (Weibel 1981; Michel and Cruz-Orive 1988; Anderson, Stitt et al. 1994; Howard and Reed 1998; Mahon, Anderson et al. 2004; Schmitz and Hof 2005; Petrescu, Larry et al. 2007; Gibbons, Illigens et al. 2009; Knust, Ochs et al. 2009), including the cornea (Petrescu, Larry et al. 2007) and retina (Anderson, Stitt et al. 1994; Mahon, Anderson et al. 2004). Briefly, electron micrographs were recorded from the anterior and posterior paralimbal regions. To avoid observer sampling bias, systematic uniform random sampling (SURS) (Howard and Reed 1998; Petrescu, Larry et al. 2007) of PMNs, keratocytes, and collagen lamellae were obtained by imaging the paralimbal corneal region in a rasterized pattern. Digital images were analyzed in Adobe Photoshop (Adobe Systems Inc., San Jose, CA) using a cycloid grid. The grid consisted of a sinusoidal wave pattern with regularly spaced target points which were randomly cast over the digital images using the layer function in Photoshop; the orientation of the grid was fixed in a direction perpendicular to the direction of the collagen lamellae (Figure 9) to account for the anisotropic properties of the corneal stroma.

Cycloid grid lines intersecting the PMN plasma membrane at PMN-keratocyte or PMN-collagen associations where the membrane-membrane or membrane-collagen separation was ≤ 25 nm were recorded as close contact (Figure 9). This value defines the predicted length of an integrin-ligand association required to mediate cell adhesion (Springer 1990). Distances greater than 25 nm were considered as PMN association with interlamellar space. Grid target points falling within the PMN body were also recorded (Figure 9). Grid lines intersecting the keratocyte membrane and grid target points falling within the keratocyte cell body were recorded for morphometric analysis of the keratocyte network (Figure 9). The ratio between lines on the cycloid grid intersecting the surface of a cell and the target points on the grid which lie within the cell

body was used to calculate cell surface density, or Sv (surface-to-volume ratio). Using an established formula (Howard and Reed 1998; Petrescu, Larry et al. 2007), $S_v = (2 \cdot \Sigma I) / (l \cdot p \cdot \Sigma P)$, where I is defined by the number of times the cycloid lines intersect the interface of PMN-keratocyte, PMN-collagen, and PMN-PMN interactions or PMN-interlamellar space associations and P is the number of cycloid grid points within the PMN body, the amount of PMN surface (i.e. percentage of Sv) in contact with keratocytes, collagen, with neighboring PMNs, or associated with interlamellar space was acquired. Sv is an indirect measure of shape; thus, the same formula can be used to obtain an estimate of keratocyte network shape (Sv). Keratocyte network surface area (SA) can then be derived by multiplying Sv by the volume of the paralimbal stromal keratocytes. To obtain the volume of the paralimbal stromal keratocytes, the number of grid target points falling on keratocytes is divided by the number of points falling on the stroma. This ratio is then multiplied by the known reference volume of the paralimbal corneal stroma which is obtained by multiplying the paralimbal width of 530 μm (Petrescu, Larry et al. 2007) by the thickness of the paralimbal stroma (see below). For keratocyte recovery studies, the volume calculation is based on the area of the central region, determined to have a 0.4 mm diameter at 40X magnification using a light microscope, multiplied by the average *in vivo* thickness of the paralimbal stroma of 35 μm , as measured by the Spectralis Spectral Domain OCT (SD-OCT) instrument (Heidelberg Engineering, Dossenheim, Germany) (Hanlon 2011).

3.5.1.4 Corneal Thickness Measurements

Thick cross sections (0.5 μm) from corneas prepared for electron microscopy were stained with 1% toluidine blue O and examined by light microscopy using a 40X objective. For each cornea, three separate perpendicular measurements, laterally

separated by 50 μm , were made from the basement membrane of the epithelium to the top of Descemet's membrane at the paralimbal region of the corneal cross section. The mean measurement was reported as the corneal paralimbal stromal thickness.

3.6 Statistical Analysis

3.6.1 PMN-keratocyte close surface contact

Data analyses were performed using one-way analysis of variance (ANOVA) followed by a Newman-Keuls Multiple Comparison post test. A p value <0.05 was considered significant. Data are reported as means \pm SEM.

3.6.2 PMN infiltration, platelet accumulation, and keratocyte repopulation

Data were analyzed using one-way analysis of variance (ANOVA) followed by a Newman-Keuls Multiple Comparison post test for keratocyte Sv and SA. Two-way ANOVA followed by Bonferroni post test was used to analyze kinetics of PMN infiltration, platelet accumulation, and keratocyte recovery. A p value <0.05 was considered significant. Data are reported as means \pm SEM.

CHAPTER 4: RESULTS

4.1 Aim 1: To Determine if ICAM-1 Mediates Close Surface Contacts Between Neutrophils and Keratocytes Following Corneal Epithelial Abrasion in the Mouse

4.1.1 Paralimbal keratocyte phenotype is retained after central epithelial abrasion

The corneal crystallin aldehyde dehydrogenase (ALDH) 3A1 is a marker for undifferentiated mammalian keratocytes (Stagos, Chen et al. ; Yoshida, Shimmura et al. 2005; Jester 2008) and is not present in keratocytes that have differentiated into fibroblasts and myofibroblasts. Paralimbal stromal cells from uninjured and injured WT and ICAM-1^{-/-} corneas stained positively with anti-ALDH3A1 antibody (Figure 10 B, F, J, and N). In addition, uninjured and injured WT and ICAM-1^{-/-} corneas incubated with antibodies against Thy1.2 (fibroblast marker) and α -smooth muscle actin (myofibroblast marker) did not show staining on any stromal cells within the paralimbus (data not shown). Collectively, the data suggest epithelial abrasion does not cause keratocyte differentiation during the first 12 hours post-injury.

4.1.2 ICAM-1 expression on mouse keratocytes

ICAM-1 expression is upregulated on keratocytes during corneal infections, as demonstrated in rabbits and mice (Pavilack, Elner et al. 1992; Seo, Gebhardt et al. 2001; Liang, Brignole-Baudouin et al. 2007). However, to our knowledge, the expression of ICAM-1 on mouse keratocytes following epithelial abrasion has not been reported. PE conjugated antibody against mouse ICAM-1 (clone YN-1) was used to determine the relative expression of ICAM-1 on uninjured and 12 hour injured WT corneal keratocytes. Uninjured and 12 hour injured ICAM-1^{-/-} corneas were also incubated with the YN-1

antibody to confirm the absence of ICAM-1 in the knockout genotype. To validate that ICAM-1-positive cells were indeed keratocytes, all corneas were dual-stained with ALDH3A1. Immunostaining of uninjured WT corneas revealed that ICAM-1 was expressed at baseline levels (Figure 10 C) on ALDH3A1 positive keratocytes (Figure 10 B and D). The intensity of ICAM-1 staining was markedly increased on ALDH3A1 positive WT keratocytes 12 hours post-injury (Figure 10 F-H), suggesting keratocyte ICAM-1 protein is upregulated after epithelial debridement. Furthermore, PMNs in the stroma were found in close proximity to paralimbal keratocytes (Figure 10 E-H). As expected, neither the uninjured nor the 12 hour injured ICAM-1^{-/-} corneas stained positively for ICAM-1 (Figure 10 K and O, respectively), whereas PMNs were readily detected in the ICAM-1^{-/-} corneal stroma 12 hour after injury (Figure 10 M-P). Non-specific antibody binding using appropriate non-immune antibodies was negligible (data not shown). Thus, we confirm that stromal paralimbal keratocytes in the mouse stain positively for ICAM-1 and show for the first time that keratocyte ICAM-1 staining increases after simple epithelial abrasion.

4.1.3 Morphometric Analysis

Following corneal epithelial abrasion, PMNs preferentially infiltrate the anterior aspect of the stroma as early as 6 hours and by 12 hours there is a substantial influx of PMNs into the WT cornea (Li, Burns et al. 2006a). PMNs first enter the paralimbal region of the cornea, the area immediately central and adjacent to the limbus (Petrescu, Larry et al. 2007). Previously, Li and colleagues showed that although peak limbal PMN infiltration is delayed by 6 hours in ICAM-1^{-/-} mice compared to WT mice, both genotypes have substantial PMN infiltration 12 hours after epithelial abrasion (Li, Rumbaut et al. 2006c). Moreover, in this study, electron micrographs clearly demonstrate the presence of PMNs in both WT and ICAM-1^{-/-} mouse paralimbal stroma

12 hours after injury (Figure 11 A-D). In the paralimbal stroma of the WT corneas, PMNs made close surface contact with both stromal collagen and keratocytes (Figure 11 A-B). In contrast, PMNs migrating through the stroma of ICAM-1^{-/-} corneas appeared to have fewer close contacts with keratocytes, but remained in close contact with collagen (Figure 11 C-D).

Table 3 summarizes the morphometric results of PMN close surface contact with keratocytes and collagen in the presence and absence of ICAM-1. Twelve hours after injury, in the presence of ICAM-1 on the surface of keratocytes (WT corneas), ~ 50% of the PMN surface was in close contact with surrounding collagen while ~ 40% of the PMN surface was in close contact with a neighboring keratocyte (Table 3). These results agree with our previous findings in WT corneas 6 hours after injury and show that as a PMN migrates through the interlamellar space in the paralimbal cornea, approximately half of its surface contacts collagen while the remainder of its surface is in close contact with keratocytes (Petrescu, Larry et al. 2007). In the ICAM-1^{-/-} corneas, ~ 60% of the PMN surface came into close contact with collagen (Table 3). This estimation was not statistically different from that of WT. However, PMN-keratocyte interactions in ICAM-1^{-/-} corneas were significantly reduced by 50% compared to WT estimates ($p < 0.05$; Table 3). Infiltrating PMNs also encounter neighboring PMNs and interlamellar space while migrating through the stroma. These interactions account for the remaining PMN associations within the stroma (Table 4). As expected, PMN associations with interlamellar space (where the distance between the PMN membrane and the nearest cell membrane or collagen fibril is >25 nm) increase significantly in ICAM-1^{-/-} corneas while PMN-keratocyte surface contacts decrease, consistent with the idea that PMN close surface contact with keratocytes is dependent on ICAM-1 (Petrescu, Larry et al. 2007).

To exclude the possibility that the reduction in PMN contact with keratocytes observed in ICAM-1^{-/-} mice was due to some factor other than a lack of ICAM-1, it was necessary to verify that the keratocyte network shape, amount of keratocyte network surface area, and degree of stromal swelling (edema) was comparable in ICAM-1^{-/-} and WT mice. Any or all of these factors could impose changes in the keratocyte-stromal environment that could result in decreased PMN contact with keratocytes, independent of a contribution from ICAM-1.

First it was determined if there were any differences in keratocyte network shape. An indirect estimate of keratocyte network shape is given by its surface-to-volume ratio (Sv). Morphometric analysis of Sv (see methods section 3.5.1.3) showed that there was no difference in keratocyte network shape prior to injury (baseline) in the anterior or posterior aspect of the cornea for WT and ICAM-1^{-/-} mice (Figure 12 A; p=0.2741). Moreover, twelve hours after injury, when PMNs are migrating within the paralimbal stroma, the keratocyte Sv ratio was not different between genotypes (Figure 12 B; p=0.5119). Hence, in ICAM-1^{-/-} mice, there are no mouse strain-specific changes in keratocyte network shape after injury that could account for the reduction in PMN surface contact with keratocytes.

Keratocyte network surface area (SA) is the amount of surface available on the network itself with which a PMN can closely associate. A mouse strain-specific decrease in network SA as a result of injury could potentially explain a reduction in PMN-keratocyte close surface contact observed in the absence of ICAM-1. At baseline levels, there was no difference between anterior or posterior keratocyte network SA within a given genotype and no difference between the two mouse genotypes of mice (Figure 13 A; p=0.3765). Similarly, 12 hours post injury when PMNs are migrating, there was no strain-specific difference in network SA for anterior and posterior paralimbal keratocytes within a genotype and no difference between genotypes (Figure 13 B; p=0.4452).

Hence, in ICAM-1^{-/-} mice, there are no mouse strain-specific changes in keratocyte network SA that could account for the reduction in PMN-keratocyte close surface interactions.

Finally, corneal epithelial abrasion in the mouse can result in stromal edema (Petrescu, Larry et al. 2007). Corneal swelling is associated with interlamellar separation and if swelling was more severe in the ICAM-1^{-/-} mice, it could result in less PMN contact with keratocytes. Since our analysis focused solely on the paralimbal region, which was not directly injured, we wanted to verify whether edema extended into the paralimbus and whether there was any difference in corneal swelling between WT and ICAM-1^{-/-} mice. Our results show that there was no significant difference in total stromal thickness between uninjured and 12 hour injured WT and ICAM-1^{-/-} corneas in the paralimbal region (Figure 14; $p=0.3301$). Hence, paralimbal stromal edema is not a prominent feature of WT or ICAM-1^{-/-} corneas at 12 hours post-injury. Moreover, enhanced stromal edema in ICAM-1^{-/-} mice is not a reasonable explanation for the reduction of PMN and paralimbal keratocyte close surface contact.

4.2 Aim 2: To Determine if CD18 and ICAM-1 Facilitate Neutrophil Motility on the Surface of Mouse Keratocytes

4.2.1 Characterization of Cultured Keratocytes

Prior to functional analyses using cultured cells, the phenotype of the cultures needed to be positively characterized. There are three major corneal cells types, epithelial cells, keratocytes, and endothelial cells. Negative selection was used to isolate epithelial and endothelial cells from the culture. Resident corneal leukocytes, such as limbal PMNs, dendritic cells, and macrophages, are present in low density and are unable to divide, thus were not considered during the isolation. The panel of antibodies used to characterize the cultured cells is listed in Table 2. Figure 15 A-B shows that cultured cells were positive for CD34 and keratocan, consistent with other reports of characteristic markers expressed by keratocytes (Sosnova, Bradl et al. 2005). Figure 15 C demonstrates these cells did not differentiate into the myofibroblast phenotype as they do not stain positive for α SMA, a myofibroblast marker. Cultured cells grown in the presence of 10% FBS differentiated into myofibroblasts and were used as positive myofibroblast controls (Figure 15 D).

4.2.2 In Vitro Analysis

PMNs coming into contact with keratocytes *in vivo* have transmigrated out of the limbus and have an activated phenotype most prominently characterized by shedding of PMN L-selectin and up-regulation of CD18 (Kishimoto, Jutila et al. 1989; Griffin, Spertini et al. 1990; Crockett-Torabi, Sulenbarger et al. 1995). To simulate the *in vivo* phenotype, extravasated PMNs, rather than peripheral blood PMNs, were added to IL-1 stimulated cultured keratocytes and their movement was recorded over a 5 minute period, to

assess baseline migration velocity. Average baseline velocity of extravasated PMNs crawling on the surface of keratocytes was 5.91 ± 0.41 $\mu\text{m}/\text{min}$ (Figure 16).

Five minutes after recording baseline motility, blocking antibody GAME46 (anti-CD18, 10 $\mu\text{g}/\text{ml}$) was added to the culture and allowed to dissipate. Analysis of PMN migration velocity 5 minutes after adding GAME46 showed velocity was reduced by 33% from baseline. After a similar baseline assessment of PMN motility, YN-1 was added to a separate set of cultured keratocytes. Assessment of PMN migration velocity after YN-1 also showed a significant reduction of 47.5% compared to baseline. These results indicate that CD18 and ICAM-1 in part facilitate PMN motility on cultured keratocytes. Migration velocity in non-immune rat IgG-treated samples was not different from baseline velocity ($p = 0.4474$), thus these data were combined with control data.

4.3 *Aim 3: To Determine if CD18 and ICAM-1 Regulate Neutrophil Infiltration and Platelet Accumulation Following Corneal Epithelial Abrasion in the Mouse*

4.3.1 *PMNs Infiltration Following Corneal Epithelial Abrasion*

Corneal epithelial abrasion elicits an acute inflammatory response whereby PMNs transmigrate out of limbal vessels, infiltrate the limbal stroma, and emigrate through the cornea (O'Brien, Li et al. 1998; Burns, Li et al. 2005; Li, Burns et al. 2006b; Petrescu, Larry et al. 2007). During the course of their migration, PMNs travel from the limbal stroma through the paralimbus, where they come into contact with uninjured paralimbal keratocytes (Petrescu, Larry et al. 2007), and eventually reach the central injured region. Using the scalpel blade, Li and colleagues documented the kinetics of PMN migration after epithelial abrasion (Li, Burns et al. 2006b). As previously evidenced, there is a large difference in the inflammatory response between the golf club spud injury versus the Algerbrush injury (Figure 3), suggesting the kinetics of PMN migration following a scalpel injury was also not relevant for the Algerbrush injury model. Thus, it was necessary to determine the kinetics of PMN migration in the Algerbrush-induced injury model. In contrast to the bi-phasic PMN infiltration response at the limbus reported by Li and colleagues, the Algerbrush-induced injury generated a single, delayed PMN infiltration peak (36h) at the limbal region in WT mice (Figure 17 A). Although there are less paralimbal PMNs at any given time, PMN density at the paralimbus is not different from that of the limbus (Figure 17 B and C) and collectively, the data suggest that once PMNs extravasate, they rapidly migrate through the paralimbus, where viable keratocytes reside, to reach the central site of injury.

The $\beta 2$ integrin CD18 and its known ligand ICAM-1 play an important role in PMN extravasation in a variety of tissues (Smith, Marlin et al. 1989; Diamond, Staunton et al. 1990; Carlos and Harlan 1994; Burns, Simon et al. 1996; Oberyshyn, Conti et al. 1998;

Moreland, Fuhrman et al. 2002). Li and colleagues previously showed that the absence of CD18 delays PMN extravasation following epithelial abrasion using a diamond blade (Li, Burns et al. 2006a). Furthermore, unpublished data using the diamond blade injury shows a delay in PMN influx when ICAM-1 is absent (Figure 18) (Courtesy of Dr. Z. Li, Baylor College of Medicine). Because the injury models showed differences in WT PMN response, the purpose of these experiments was to determine if CD18 and ICAM-1 also contribute to PMN infiltration following an Algerbrush injury. For the first 12 hours after injury, there were no differences in infiltrating PMNs at the limbal stroma among WT, ICAM-1^{-/-}, and CD18^{mutant} mice (Figure 17). Furthermore, the overall kinetics of limbal PMN infiltration in CD18^{mutant} mice were not different from that of WT mice and both demonstrate peak PMN accumulation 36 hours after injury. While these results are different from the published data (Li, Burns et al. 2006a) the hypomorphic mutation of CD18^{mutant} mice used for these studies may explain the differences in early and coincident patterns of PMN infiltration (Wilson, Ballantyne et al. 1993). The differences in injury technique may also additionally contribute to the early PMN response observed in the CD18^{mutant} mice.

At the paralimbus, 2-way ANOVA analysis did not show differences between WT and CD18^{mutant} PMN density, up to 48h ($p > 0.05$). Additionally, central PMN density was comparable to that of WT, suggesting that CD18 does not contribute to PMN extravasation. PMN density in WT and CD18^{mutant} mice reduces by 48 hours, indicating the resolution of inflammation in both genotypes.

There was also no noticeable delay in PMN infiltration at the limbus in ICAM-1^{-/-} mice but one can argue that this may be due to ICAM-1-independent mechanisms of PMN transmigration, such as PMN CD11a/CD18 (LFA-1) binding to ICAM-2 to promote PMN extravasation (Dustin and Springer 1988; Smith, Marlin et al. 1989; Ley 1996). Additionally, the method of injury may again play a role in the different response

between published data (Li, Burns et al. 2006a; Li, Burns et al. 2006b; Li, Rumbaut et al. 2006c; Li, Burns et al. 2007; Li, Burns et al. 2011) and these results. Remarkably, by 18 hours, PMN density in ICAM-1^{-/-} mice significantly increases, not only at the limbus but also in the paralimbal and central regions of the stroma and peaks 24 hours after abrasion (Figure 17). Table 5 shows the estimated area under the curve for each region evaluated. The area under the curve (AUC) provides an estimate of the total numbers of the variable being evaluated over time, in this case PMN numbers. Others have used it to determine the total increase or decrease of a variable over time (Le Floch, Escuyer et al. 1990). The area under the curve (mm²) is significantly greater in paralimbal and central regions of ICAM-1^{-/-} mice, suggesting there are more infiltrating PMNs in the corneas of these mice after epithelial abrasion. Moreover, PMN numbers in the center remain significantly higher in ICAM-1^{-/-} mice at 48 hours compared to WT and CD18^{mutant} mice (by 90% and 99%, respectively), implying that resolution of inflammation takes longer in the absence of ICAM-1. No differences in AUC are observed between WT and CD18^{mutant} mice in any regions evaluated.

4.3.2 Platelet Accumulation Following Corneal Epithelial Abrasion

In addition to PMN infiltration, platelets also enter the limbal stroma following epithelial abrasion. The presence of platelets during corneal inflammation has been shown to promote epithelial recovery and nerve regeneration (Li, Rumbaut et al. 2006c; Li, Burns et al. 2011), possibly through the release of growth factors. Thus it is possible that platelet infiltration may promote keratocyte recovery. However, prior to determining whether platelets contribute to keratocyte repopulation following epithelial abrasion, it was necessary to determine molecular mechanisms facilitating platelet recruitment into the limbal stroma. Li and colleagues showed that CD18 and ICAM-1 regulate numbers of PMNs entering the stroma so it is possible that these molecules may regulate

infiltrating platelet numbers following epithelial abrasion. Platelet density (platelets/mm²) was calculated to determine if platelet accumulation at the limbal stroma required CD18 and ICAM-1. Figure 19 shows that total platelet accumulation (platelets inside and outside of limbal vessels) in WT, ICAM-1^{-/-}, and CD18^{mutant} mice. Platelets density was not statistically different among WT, ICAM-1^{-/-}, and CD18^{mutant} mice up to 12 hours post injury and within this time platelet accumulation was coincident with PMN infiltration. Eighteen hours after injury, while platelets in WT and CD18^{mutant} mice remained low, total platelets in ICAM-1^{-/-} mice increased suddenly and significantly, peaked at 24 hours and remained elevated through 36 hours (Figure 19 A).

Total platelet density in WT mice peaked 24h post injury but still was significantly lower than 24 hour platelet numbers in ICAM-1^{-/-} mice and WT platelets returned to baseline values immediately at 30 hours after injury, and remained at baseline through 48 hours. Total platelet density in CD18^{mutant} mice was consistently low through 48 hours (Figure 19 A), suggesting CD18 played a role in platelet recruitment to the limbal vessels and stroma.

Total limbal platelet recruitment does not differentiate between platelets that are inside of vessels versus those that are outside of vessels. Therefore, extravascular platelets (those only outside of vessels) were analyzed separately in WT, ICAM-1^{-/-}, and CD18^{mutant} mice. It is well established that platelets become activated upon encountering extravascular tissue (Firkin 1963; George 2000; Kamath, Blann et al. 2001; Smith and Weyrich 2011) and their activation results in degranulation and release of growth factors (Firkin 1963; George 2000; Kamath, Blann et al. 2001; Stellos and Gawaz 2007; Blair and Flaumenhaft 2009), which in turn may support keratocyte repopulation. Figure 19 B (and C) shows extravascular platelet accumulation in WT, ICAM-1^{-/-}, and CD18^{mutant} mice. The pattern of extravascular platelet accumulation mimics that of total platelet response, whereby peak accumulation 24 hours after injury occurs in WT and ICAM-1^{-/-}

mice. Again, significantly greater platelet numbers are observed in the absence of ICAM-1 (Figure 19) and peak in accumulation in ICAM-1^{-/-} mice exceeds WT peak accumulation by 44%. Interestingly, in CD18^{mutant} mice, extravascular platelet accumulation is significantly depressed, suggesting that vascular CD18 is required for platelets to efficiently extravasate out of limbal vessels (Figure 19 B and C). Collectively, the data show that extravascular platelet accumulation is positively regulated by the β 2 integrin CD18 but negatively regulated by its binding partner ICAM-1.

To determine if there were inter-observer reliability in the analyses of platelet accumulation, a second observer analyzed platelet density in a second set of uninjured and 24 hour-injured WT and ICAM-1^{-/-} mice. The results showed no difference in the results between the two observers for the time points observed (Appendices Figure III). This demonstrates that the analyses is reproducible.

4.4 Aim 4: To Determine if PMNs and/or Platelets are Necessary for Keratocyte Repopulation Following Corneal Epithelial Abrasion in the Mouse

4.4.1 Analysis of Keratocyte Recovery in WT Mice

Epithelial abrasion results in anterior keratocyte death (Szerenyi, Wang et al. 1994; Wilson, He et al. 1996a; Zieske, Guimaraes et al. 2001; Mohan, Hutcheon et al. 2003; Zhao and Nagasaki 2004), predominantly below the region of injury. In WT mice, anterior central keratocytes were markedly reduced 24 hours after epithelial abrasion (Figure 20). Four days post injury, a time when the epithelium has completely re-stratified (Li, Burns et al. 2007), anterior central keratocytes in WT mice rapidly repopulated the central anterior stroma, but this recovery was incomplete, and reached only 72% of uninjured baseline numbers. Over time, anterior central keratocyte numbers in WT mice did not increase and remained at 72% of baseline, up to 28 days post-injury. These findings of anterior central keratocyte repopulation are consistent with reports of reduced anterior central keratocyte density in humans following refractive surgery (Helena, Baerveldt et al. 1998; Ivarsen, Laurberg et al. 2004; Patel, Erie et al. 2007).

A reduction in keratocytes was also observed in the anterior paralimbal region 24 hours after injury but posterior central and paralimbal keratocytes numbers were unaffected by the injury (Figure 21, red line). However, posterior paralimbal keratocyte numbers increased significantly at 14 days (Figure 21, red line), suggesting that keratocyte proliferation may occur at the posterior periphery.

Keratocytes extend dendritic-like processes which associate with neighboring keratocytes through gap junctions, thus forming keratocyte networks within the stroma (Jester, Barry et al. 1994; Lakshman, Kim et al. 2010). It is possible that the reduction in anterior central keratocytes after injury results from changes occurring to the keratocyte network during repopulation. For example, once repopulating keratocytes migrate into

the anterior central stroma and interconnect with neighboring keratocytes, a stop signal can be generated to inhibit further proliferation and/or cell migration. If this occurs early during healing, it may result in fewer anterior central keratocyte numbers. But it is also possible that these cells compensate for their reduction in numbers by increasing cell size, so to completely occupy the stromal area left void as a result of keratocyte death. Thus, fewer cells would be required to establish a network size comparable to the uninjured keratocyte network. Ultrastructural stereology was used to evaluate the keratocyte network and estimate geometric parameters such as network surface-to-volume ratio (Sv) and network surface area (SA). Differences in keratocyte network Sv between uninjured and injured corneas is indicative of network shape changes and differences in SA designates changes to the overall network size. Table 6 shows the estimated keratocyte network surface-to-volume ratio (Sv) and surface area (SA) of uninjured and 28 day-injured WT corneas. There were no differences observed in anterior or posterior central keratocyte network Sv between the two time points, demonstrating that keratocyte network shape was restored by 28 days post injury. In contrast, anterior central keratocyte network SA recovered to only 66% of baseline, significantly lower than uninjured central keratocyte network SA. Posterior central SA recovered to baseline by 28 days. Anterior and posterior paralimbal keratocyte network SA and Sv did not change between 0 day and 28 days after injury (Table 6).

4.4.2 *Keratocyte recovery in CD18^{mutant} and ICAM-1^{-/-} mice*

As previously demonstrated, platelet accumulation is regulated by adhesion molecules CD18 and ICAM-1, positively and negatively, respectively, in the Algerbrush injury model. Platelet accumulation at the limbus has been shown to promote corneal epithelial healing and nerve regeneration (Li, Rumbaut et al. 2006c; Li, Burns et al. 2011). To determine if limbal platelet accumulation affects keratocyte repopulation,

keratocyte recovery was evaluated in CD18^{mutant} and ICAM-1^{-/-} mice. If in fact platelets contribute to keratocyte repopulation, one would expect depressed repopulation in CD18^{mutant} mice and enhanced repopulation in ICAM-1^{-/-} mice. Figure 21 shows the kinetics of anterior central keratocyte repopulation of CD18^{mutant} (green line) and ICAM-1^{-/-} mice (blue line) compared to WT. Baseline numbers are not different among the three genotypes and 1 day after injury, keratocytes numbers in all are significantly reduced as a result of death. While the initial reduction is followed by recovery at 4 days, the absence of ICAM-1 significantly enhances keratocyte repopulation where keratocyte numbers return to baseline levels and even exceed baseline counts 28 days after injury. In contrast, keratocyte repopulation in CD18^{mutant} mice recover only to 44% of its respective baseline 4 days post injury and remains significantly blunted up to 28 days following epithelial abrasion. Considering that extravascular platelet accumulation in CD18^{mutant} mice was markedly low while extravascular platelet accumulation in ICAM-1^{-/-} mice significantly exceeded that of WT, these studies suggest enhanced platelet accumulation at the limbus advances anterior central keratocyte repopulation.

Interestingly, 4 days after injury, posterior central keratocyte numbers in ICAM-1^{-/-} mice also increase significantly, but return to baseline values by 14 days, and remain constant up to 28 days after abrasion (Figure 21). However, increases in either anterior or posterior paralimbal keratocyte numbers in ICAM-1^{-/-} mice are not observed at 4 days. Keratocyte numbers may increase in these paralimbal regions between 1 and 4 days and rapidly migrate into the central regions by 4 days, contributing to the increased 4 day anterior and posterior keratocyte numbers. Alternatively, posterior keratocytes may proliferate and migrate vertically and restore anterior central keratocyte numbers, although vertical migration is highly unlikely due to the complicated architecture of corneal collagen lamellae (Birk, Fitch et al. 1986; Knupp, Pinali et al. 2009; Lakshman,

Kim et al. 2010). In CD18^{mutant} mice, posterior central and anterior and posterior paralimbal keratocyte counts were not different from baseline values through 28 days (Figure 21), consistent with the idea that efficient keratocyte repopulation requires enhanced platelet accumulation at the limbal stroma.

4.4.3 *Keratocyte Recovery in Platelet-Depleted WT Mice*

To further establish a role for platelets in keratocyte repopulation, anterior central keratocyte nuclei counts were analyzed in platelet-depleted (anti-CD42) WT mice (Figure 22). Platelet depletion using anti-GP1b α antibody (IP injection) significantly reduces circulating platelet numbers ($\leq 10\%$) up to 4 days (Nieswandt, Bergmeier et al. 2000). The depletion of platelets significantly hampers anterior central keratocyte repopulation, by 71% compared to uninjured and 60% compared to 4 day injured anterior central keratocyte counts. This study, in concordance with the adhesion molecule-mediated platelet accumulation studies, suggests an important role for platelets in keratocyte repopulation, demonstrating that enhanced platelet accumulation is associated with effective keratocyte repopulation following corneal epithelial abrasion.

4.4.4 *Keratocyte repopulation in TCR δ ^{-/-} and P-selectin mice*

P-selectin and $\gamma\delta$ T cell deficient mice were used to further investigate a role for platelets in keratocyte repopulation. Recent studies showed that platelet accumulation at the limbal stroma is reduced (compared to WT) in the absence of $\gamma\delta$ T cells and the platelet adhesion molecule P-selectin and epithelial healing is delayed in these knockout mice (Li, Rumbaut et al. 2006c; Li, Burns et al. 2007; Li, Burns et al. 2011; Li, Burns et al. 2011). If indeed platelets are required for efficient keratocyte repopulation, one would expect impaired keratocyte recovery in these mice. Indeed, anterior central keratocyte repopulation was significantly lower in TCR δ ^{-/-} mice 4 days after injury, reaching only ~23% of baseline TCR δ ^{-/-} anterior central keratocyte numbers (Figure 23). The absence

of P-selectin also significantly hindered keratocyte repopulation (Figure 24), where 4-day repopulation reached only ~31% of its respective baseline.

4.4.5 *Platelet Infusion restores keratocyte repopulation in P-selectin^{-/-} mice*

Li and colleagues previously showed that infusion of WT platelets into P-selectin^{-/-} mice restored accumulating limbal platelet numbers during inflammation, demonstrating that platelet P-selectin, rather than endothelial cell P-selectin, facilitated extravasation of platelets (Li, Rumbaut et al. 2006c). Isolated WT mouse platelets were injected into P-selectin^{-/-} mice to determine whether restoration of platelets in P-selectin^{-/-} mice would rescue anterior central keratocyte repopulation. Li and colleagues have demonstrated this procedure increases limbal platelet accumulation and shifts the peak accumulation time closer towards that of WT mice (Li, Rumbaut et al. 2006c). Figure 25 shows WT platelet infusion into P-selectin^{-/-} mice restored P-selectin^{-/-} anterior central keratocytes to baseline values and both baseline and platelet-treated keratocyte numbers were markedly higher (69 % and 59%, respectively) than untreated 4-day keratocyte numbers.

WT platelet infusion into P-selectin^{-/-} mice rescued their keratocyte repopulation to baseline, but anterior central keratocyte repopulation in untreated WT mice only reached 72% of baseline. Hence, it could be rationalized that WT anterior central keratocyte numbers could be restored to baseline by transfusing WT mice with WT platelets. However, WT platelet infusion into WT mice did not rescue anterior central keratocyte repopulation (Figure 26), suggesting a 10% boost in platelet numbers does not enhance keratocyte repopulation if platelet accumulation prior to treatment was normal.

Interestingly, extravascular platelet density was significantly higher in TCR δ ^{-/-} mice compared to WT mice, 24 hours after injury (Figure 27), suggesting platelet

recruitment does not require $\gamma\delta$ T cells. However, preliminary observations show a remarkable difference in platelet morphology between WT and TCR $\delta^{-/-}$ mice. While the platelets outside of the vessels in WT corneas appear pleomorphic, presumably activated, platelets in TCR $\delta^{-/-}$ mice appear more rounded and whole, although they are outside of vessels and in the presence of extracellular matrix components (Figure 32). This novel observation suggests perhaps $\gamma\delta$ T cells are required for activation of platelets, possibly through cytokine release. Results for platelet density in P-selectin $^{-/-}$ are not presented because P-selectin $^{-/-}$ mice used for these specific studies were incorrectly bred and became heterozygous.

4.4.6 *Characterization of IL-22R on Keratocytes and Vessels*

$\gamma\delta$ T cells produce cytokines IL-17 and IL-22, which modulate platelet activation and help regulate the balance between inflammation and homeostasis (Liang, Tan et al. 2006; Braun, Ferrick et al. 2008; Molesworth-Kenyon, Yin et al. 2008; Deknuydt, Scotet et al. 2009; Ness-Schwickerath, Jin et al. 2010; Roussel, Houle et al. 2010; Li, Burns et al. 2011; Li, Burns et al. 2011; Maione, Cicala et al. 2011); (Ren, Hu et al. ; Trifari and Spits ; Boniface, Bernard et al. 2005; Liang, Nickerson-Nutter et al. 2010; Ma, Lancto et al. 2010). Fibroblast-like cells express both IL-17 and IL-22 receptors (Kehlen, Thiele et al. 2002; Boniface, Bernard et al. 2005). Because corneal keratocytes are fibroblast-like, WT mouse corneas were stained with IL-22R. While there was no baseline expression of IL-22R in paralimbal keratocytes of uninjured mice, IL-22R staining was detected on paralimbal keratocytes 24 hours post-injury (Figure 28). IL-22 plays a role in mediating vascular permeability (Wolk, Witte et al. ; Kebir, Kreymborg et al. 2007) so IL-22R expression was also examined at the limbus. APC-conjugated rat-anti-mouse CD31 was used to positively identify the limbal vessels. Surprisingly, IL-22R expression was not detected on CD31-labeled limbal endothelial cells (Figure 29). Instead, IL-22R-

positive staining was detected on CD31⁺ vessels, presumably lymphatic vessels which have low or no CD31 expression (Ruddell, Mezquita et al. 2003; Cao, Lim et al. 2011) (Figure 29 C). The lymphatics participate in clearance of excess fluid and debris from injured tissue (D'Amico and Alitalo 2010) and may require IL-22 to enhance endothelial permeability. These findings suggest IL-22 may not regulate inflammatory cell infiltration out of vessels but may directly promote keratocyte repopulation by binding to keratocyte IL-22R, perhaps by inducing regeneration and migration as it has been shown to do in other tissue (Ren, Hu et al. ; Boniface, Bernard et al. 2005; Liang, Nickerson-Nutter et al. 2010). This was investigated in the following experiment.

4.4.7 Application of rIL-22 Does Not Rescue Keratocyte Repopulation

Since IL-22R was expressed on paralimbal keratocytes, it was important to determine whether treating TCR $\delta^{-/-}$ mice enhances anterior central keratocyte repopulation. Previously, Li and colleagues showed systemic or topical treatment with rIL-17 or rIL-22 restored epithelial wound closure rate in TCR $\delta^{-/-}$ mice (Li, Burns et al. 2011; Li, Burns et al. 2011). Both systemic administration (tail vein injection) and topical application of rIL-22 showed no increase in anterior central keratocyte numbers 4 days post injury, confirming that IL-22 did not directly contribute to keratocyte repopulation following epithelial abrasion. However, whether keratocytes or CD31⁺ limbal vessels express IL-17R or whether treatment with rIL-17 promotes keratocyte repopulation remains to be determined.

CHAPTER 5: DISCUSSION

5.1 *Aim 1: To Determine if ICAM-1 Mediates Close Surface Contacts Between Neutrophils and Keratocytes Following Corneal Epithelial Abrasion in the Mouse*

The purpose of this study was 1) to confirm that ICAM-1 is expressed on mouse keratocytes in our epithelial debridement model and 2) to determine if ICAM-1 contributes to PMN-keratocyte close surface contact during the corneal inflammatory response. In our model of injury, epithelial abrasion is a non-stromal penetrating injury associated with an acute corneal inflammatory response (Li, Burns et al. 2006a; Li, Burns et al. 2006b; Li, Rumbaut et al. 2006c; Li, Burns et al. 2007; Petrescu, Larry et al. 2007) and death of underlying central keratocytes (Wilson, S. E., et al., 1996, Zhao, J. & Nagasaki, T., 2004, Zieske, J. D., et al., 2001). However, at least for the first 12 hours post-injury, keratocytes in the paralimbus, a region distal to the site of injury, remain viable and do not express fibroblast or myofibroblast differentiation markers (Thy1.2 or alpha smooth muscle actin, respectively), but do express ALDH3A1 (Figure 10), a marker for undifferentiated mammalian keratocytes (Stagos, Chen et al. ; Yoshida, Shimmura et al. 2005; Jester 2008). Immunostaining for ICAM-1 reveals baseline ICAM-1 expression on uninjured mouse keratocytes, and 12 hours after injury the intensity of the ICAM-1 staining increases. Others have reported low expression of keratocyte ICAM-1 in mice (Hobden, Masinick et al. 1995) and this expression increases following LPS stimulation (Seo, Gebhardt et al. 2001) or bacterial infection (Hobden, Masinick et al. 1995). We now report that ICAM-1 expression also increases on mouse keratocytes following central corneal epithelial abrasion, an injury not associated with bacterial infection. More importantly, our studies with ICAM-1^{-/-} mice show that PMN close surface contact with paralimbal keratocytes is significantly reduced in the absence of keratocyte ICAM-1.

ICAM-1 has a well defined “intravascular” role in regulating PMN recruitment at sites of inflammation (Carlos and Harlan 1994; Ley 1996; Jaeschke and Smith 1997; Oberyszyn, Conti et al. 1998; Ley 2001; Moreland, Fuhrman et al. 2002; Brake, Smith et al. 2006; Phillipson, Heit et al. 2006). Specifically, the association of endothelial ICAM-1 and PMN CD18 allows for firm adhesion of PMNs to the blood vessel wall, a pre-requisite for efficient transendothelial migration (Ley 1996; Jaeschke and Smith 1997; Oberyszyn, Conti et al. 1998; Ley 2001; Moreland, Fuhrman et al. 2002; Phillipson, Heit et al. 2006). We now provide data showing that ICAM-1 also has an “extravascular” role in regulating PMN contact with corneal keratocytes. Our observation of increased keratocyte ICAM-1 expression during the corneal inflammatory process is consistent with the view that the binding of the leukocyte Beta-2 integrin (CD18) with keratocyte ICAM-1 facilitates PMN surface interactions with keratocytes. This finding is in line with an earlier study using excised human corneas which documented ICAM-1 staining on keratocytes and speculated stromal ICAM-1 may play a role in leukocyte localization (Pavilack, Elner et al. 1992). Our ultrastructural stereologic findings are consistent with this concept and show that PMN close contact with stromal keratocytes is dependent upon the presence of ICAM-1.

In our previous study (Petrescu, Larry et al. 2007), using the same corneal epithelial abrasion model, we found that in the absence of CD18, PMN-keratocyte interactions are reduced by 75% from that of WT. Utilizing the same wounding technique, we also see a significant reduction in PMN-keratocyte interactions in the absence of ICAM-1 (50% of WT). The reduction in surface contact by 50% as opposed to 75% as seen with the CD18^{mutant} mice suggests the possible involvement of an additional CD18 ligand during PMN contact with paralimbal keratocytes. JAM-C is an adhesion molecule that also interacts with Cd11b/CD18 (Mac-1) during intravascular PMN transendothelial migration (Chavakis, Keiper et al. 2004). Morris *et al.* identified

JAM-C expression on cultured human corneal fibroblasts (Morris, Tawil et al. 2006) and we have identified JAM-C mRNA expression on freshly isolated mouse keratocytes and staining for JAM-C is evident on cultured mouse keratocytes (Figure 30). Whether JAM-C is expressed on mouse keratocytes *in vivo*, and whether its expression pattern is altered by inflammation associated with epithelial abrasion remains to be determined.

Recent reports show the association of endothelial ICAM-1 with PMN CD18 triggers outside-in signaling events promoting sustained PMN adhesion to vascular endothelium (Wang and Doerschuk 2002) and directing PMN transmigration at sites of inflammation (Sarantos, Zhang et al. 2008). Conceivably, this integrin-ligand binding may also trigger similar signaling events outside the limbal vasculature, through extravascular keratocyte ICAM-1 and extravasated PMN CD18 binding. While the existence of such signaling in the corneal stroma remains to be shown, Aim 4 results suggest ICAM-1 negatively regulates keratocyte repopulation following epithelial abrasion (Section 4.4.2). In our injury model, there is complete loss of keratocytes from the central anterior stroma directly beneath the site of injury. Keratocytes in the posterior central stroma do not appear to die. Keratocyte repopulation of the central anterior stroma occurs within 4 days post-injury and, in the absence of ICAM-1, the number of anterior central keratocytes recovers completely while WT anterior central keratocyte numbers fail to return to normal levels. Whether CD18-dependent PMN binding to keratocyte ICAM-1 promotes paralimbal keratocyte signaling events that negatively regulate the recovery of anterior central keratocytes remains to be determined.

In summary, the data show keratocyte ICAM-1 serves a novel extravascular role as a mediator of cell-cell contact, enabling PMNs to make close surface contact with keratocytes. This observation is entirely consistent with our previous finding that PMN contact with keratocytes also requires CD18. The fact that CD18 and ICAM-1 are well

established receptor/ligand partners makes it reasonable to consider these two molecules as complementary partners of extravascular PMN adhesion to keratocytes. The addition of keratocyte ICAM-1 to the original concept that PMNs utilize CD18 to closely associate with the keratocyte network adds a new level of understanding to leukocyte recruitment in the injured cornea.

5.2 Aim 2: To Determine if CD18 and ICAM-1 Facilitate Neutrophil Motility on the Surface of Mouse Keratocytes

Aim 2 sought to determine whether CD18 and ICAM-1 played a functional role in facilitating PMN motility on cultured keratocytes. *In vitro* analyses demonstrate roles for CD18 and ICAM-1 as mediators of PMN migration on keratocytes, evidenced by significant reductions in migration velocity after treatment with blocking antibodies against CD18 (GAME46) and ICAM-1 (YN-1). Recently, Petrescu and colleagues showed an extravascular role for PMN CD18 in mediating close surface contacts with corneal keratocytes (Petrescu, Larry et al. 2007). Similarly, Aim 1 showed that ICAM-1 is also required to maintain close contacts between PMNs and keratocytes (Gagen, Laubinger et al. 2010). These findings raised the possibility of functional necessity of these adhesion molecules in the cornea. Burns and colleagues previously demonstrated a novel extravascular role for CD18 in mediating PMN motility on lung fibroblasts (Burns, Simon et al. 1996). This early study made plausible the notion of functional extravascular roles for CD18 and ICAM-1 in the cornea.

Although blocking either CD18 or ICAM-1 significantly reduces PMN migration velocity, neither reduction is greater than 50% of baseline. ICAM-1 can only associate with PMN CD11a/CD18 and CD11b/CD18 (Smith, Marlin et al. 1989; Diamond, Staunton et al. 1990; Carlos and Harlan 1994; Huang and Springer 1995; Lynam, Sklar et al. 1998; Roebuck and Finnegan 1999), yet blocking CD18 only partially reduces PMN motility. This suggests that additional mechanisms may contribute to migration of PMNs *in vitro*. One such molecular mechanism is CD18 interaction with JAM-C. JAM-C is a junctional adhesion molecule that associates with Mac-1 (CD11b/CD18) (Chavakis, Keiper et al. 2004). JAM-C mRNA is expressed in isolated keratocytes and JAM-C protein is expressed on cultured keratocytes (Figure 30). JAM-C association with Mac-

1 could account for a reduction rather than a complete inhibition of PMN migration on keratocytes when ICAM-1 is blocked.

It must be considered that *in vitro* observations of PMN motility on keratocytes are based on “2-dimensional” analyses when physiologically keratocytes exist in a “3-dimensional” environment. Keratocytes are embedded within layers of collagen lamella and bind to extracellular matrix components through $\beta 1$ and $\beta 3$ integrins (Stepp 2006) and epithelial abrasion causes stromal edema. As demonstrated by Petrescu *et al* (Petrescu, Larry et al. 2007), and explained in Aim 1 of this Dissertation, PMNs must crawl the through interlamellar space, making contact with both keratocytes and collagen, as they migrate towards the site of injury (Burns, Li et al. 2005; Petrescu, Larry et al. 2007; Gagen, Laubinger et al. 2010). PMNs additionally express $\beta 1$ and $\beta 3$ integrins, which are also able to bind to stromal matrix components (Smith 2008). The collagen component, a substantial stromal element, is absent in the *in vitro* model and assessing PMN motility *in vivo* may produce different results. In fact, following epithelial abrasion with a diamond blade, Li *et al.* showed a rapid PMN migration to the central corneal region in CD18 null mice (Li, Burns et al. 2006a).

While *in vitro* analysis demonstrates a functional role for CD18 and ICAM-1 in facilitating PMN motility on cultured keratocytes, it is clear that other mechanisms must also participate in PMN motility through the stroma. Further functional studies must also be done to substantiate the involvement of all possible molecular mechanisms promoting PMN motility on keratocytes. Most importantly, while *in vitro* analysis provides a means to selectively study specific adhesion molecules, *in vivo* assessment of these molecular mechanisms is needed to put them into proper physiologic context.

5.3 *Aim 3: To Determine if CD18 and ICAM-1 Regulate Neutrophil Infiltration and Platelet Accumulation Following Corneal Epithelial Abrasion in the Mouse*

The purpose of Aim 3 was to determine if adhesion molecules CD18 and ICAM-1 regulate 1) PMN infiltration and migration and 2) platelet accumulation at the limbus. First, in the present studies, early PMN recruitment (between 0 hour and 12 hours) appears not to be regulated by CD18 or ICAM-1, evidenced by coincident PMN infiltration at the limbus with WT PMNs (Figure 17). However, the CD18^{mutant} mice were hypomorphic mutations, expressing low levels of CD18 (Wilson, Ballantyne et al. 1993) and this may contribute to early PMN recruitment. Early recruitment of PMNs in ICAM-1^{-/-} mice may be attributed to ICAM-2 interactions with PMN LFA-1 (Hobden, Masinick-McClellan et al. 1999; Hobden 2003). ICAM-2 association with LFA-1 has been shown to modulate PMN emigration in the cornea and cremaster, raising the possibility that ICAM-2-mediate PMN infiltration in the absence of ICAM-1 (Hobden, Masinick et al. 1995; Huang and Springer 1995; Hobden, Masinick-McClellan et al. 1999; Hobden 2003). Second, platelet accumulation at the limbus is positively regulated by CD18 and negatively regulated by ICAM-1. While the reduction in CD18 markedly diminished extravascular platelet accumulation, the absence of ICAM-1 significantly enhanced extravascular platelet numbers.

Together, the PMN infiltration and platelet accumulation data demonstrate that the degree of inflammation modulates the degree of inflammatory cell infiltration. Enhanced inflammation in ICAM-1^{-/-} mice, substantiated by increased PMN infiltration, may also be explained by ICAM-2 mediated events. Feng and colleagues previously showed that PMN and platelet emigration occurs via transendothelial mechanisms, whereby these cells are transported across the vessels by large endothelial cell vacuoles (Feng, Nagy et al. 1998; Feng, Nagy et al. 1998). The same group demonstrated that VEGF stimulation increases cytoplasmic vesicle-like formations in the

endothelium called vasiculo-vacular organelles (VVO), structures that comprised of multiple vesicles and vacuoles and are capable of large macromolecular transport (Feng, Nagy et al. 1996). PMNs contain VEGF, a growth factor which increases vascular permeability and promotes the formation of VVOs (Feng, Nagy et al. 1996; Barrientos, Stojadinovic et al. 2008; Matsuo, Ohkohchi et al. 2008; Smyth, McEver et al. 2009; Li, Burns et al. 2011). ICAM-2 signaling activates Rac-mediated angiogenesis and Rac-1 synergistically associates with VEGF to enhance embryonic angiogenesis (Hoang, Nagy et al. 2011; Roberts 2011). While no angiogenesis is observed in ICAM-1^{-/-} mice during wound healing (see Aim 4), these publications support an indirect relationship between ICAM-2, VEGF, and VVO formation, substantiating the proposal that early and enhanced endothelial activation is mediated by ICAM-2-signaling events.

These reports are consistent with unpublished observations by Dr. David Walker (University of British Columbia, Vancouver, British Columbia, Canada). He found that elevated inflammatory responses can exacerbate the structural integrity of vascular endothelial cells, whereby the cells develop large (1-2 μ m) transcellular pores (personal communication between Dr. Alan Burns and Dr. David Walker). Preliminary evidence of VVO generation in inflamed WT limbal endothelial cells show abundant vacuole-like structures at the apical and basal surfaces of the inflamed endothelium which are absent on the resting cells (Figure 31). The inflamed endothelium looks ruffled, with multiple cytoplasmic projections at the apical and basal surfaces. Finally, PMNs, platelets, and even RBCs, are observed in the extravascular region of the inflamed tissue, consistent with the idea that these cells may have access to transcellular pores.

It is well known that platelet-PMN associations are mediated by multiple adhesion molecules. Relevant interactions are summarized in Table 1. Of those listed, the strongest association occurs between PMN CD11b/CD18 (Mac-1) and platelet GP1b α , a platelet surface glycoprotein (Diamond, Garcia-Aguilar et al. 1993; Simon,

Chen et al. 2000; Ehlers, Ustinov et al. 2003; Wang, Sakuma et al. 2005). Because CD18 expression on the hypomorphic mutants is significantly lower than WT, one would expect the binding affinity of platelets to PMNs through CD18 family members (LFA-1 to platelet ICAM-2, Mac-1 with platelet GP1b α and JAM-C) to be reduced. This lack or reduction in platelet binding to PMNs may explain low platelet recruitment in the hypomorphic CD18^{mutant} mice after abrasion. In ICAM-1^{-/-} mice, ICAM-2 binding to LFA-1 possibly mediates PMN-endothelial interactions. This leaves PMN Mac-1 free to associate with platelet GP1b α . Thus, it is conceivable that platelet-GP1b α binding with PMN-Mac-1 allows for the coincident emigration observed in ICAM-1^{-/-} mice. This coupled with enhanced PMN recruitment may explain enhanced platelet recruitment in ICAM-1^{-/-} mice.

The negative regulatory role of ICAM-1 is the novel observation in these studies. While it is widely accepted that ICAM-1 is required for inflammatory cell recruitment (i.e., its absence delays inflammatory cell infiltration), the findings of this Dissertation clearly demonstrate that platelet and PMN recruitment are enhanced in the absence of ICAM-1, in this injury model. This brings up a possible mechanism which may prevent efficient PMN and platelet extravasation. Human PMNs express ICAM-1 (Elsner, Sach et al. 1995; Mandi, Nagy et al. 1997; Wang, Sexton et al. 1997) and it is suggested that mouse PMNs may also express ICAM-1 (personal correspondence between Dr. Alan Burns, UHCO, and Dr. C.W. Smith, Baylor College of Medicine). It is feasible that ICAM-1-fibrinogen binding in WT mice can cause PMN-PMN interactions and possible aggregation. PMN clustering may occlude vessels, possibly averting inflammatory cell infiltration (PMNs and platelets) into the injured cornea. Because both WT and CD18^{mutant} mice PMNs could express ICAM-1, this may be one explanation for significantly lower extravasated PMN numbers observed in these genotypes compared to ICAM-1^{-/-} mice.

Aim 3 provides evidence that a heightened inflammatory response enhances inflammatory cell recruitment. While enhanced inflammation can exacerbate healing, PMNs and platelets also promote healing in various tissues, including the cornea (Rudner, Kernacki et al. 2000; Molesworth-Kenyon, Yin et al. 2008; Tarabishy, Aldabagh et al. 2008). With respect to the cornea, the absence of PMNs or platelets delays epithelial closure and nerve regeneration. Epithelial abrasion also causes death of keratocytes and Aim 4 investigates whether PMNs and platelets are required for efficient keratocyte repopulation.

While the proposed mechanisms of PMN and platelet infiltration in this injury model is beyond the scope of this dissertation, further investigation driving these cellular and molecular interactions during inflammation is warranted.

5.4 Aim 4: To Determine if PMNs and/or Platelets are Necessary for Keratocyte Repopulation Following Corneal Epithelial Abrasion in the Mouse

The goal of Aim 4 was to determine whether inflammatory cells promote keratocyte repopulation following corneal epithelial abrasion. The PMN and platelet extravasation results in Aim 3 provided evidence that efficient keratocyte repopulation depended on the degree of inflammation. This is supported by observations showing complete keratocyte repopulation in ICAM-1^{-/-} mice, where inflammation was enhanced, and incomplete repopulation in WT and CD18^{mutant} mice, where PMN and platelet infiltration was significantly lower compared to ICAM-1^{-/-} mice.

Anterior central keratocyte repopulation was the focus of this study since there is significant keratocyte loss below the injury as a result of death. This loss is akin to keratocyte loss after extensive contact lens wear and refractive surgery (PRK and LASIK) and anterior central keratocyte repopulation in WT mice mirrors keratocyte repopulation after refractive surgery because both are incomplete (Wilson 1998; Mitooka, Ramirez et al. 2002; Bourne 2003; Patel, Erie et al. 2007; Ambrosio, Kara-Jose et al. 2009). Contact lens wear also reduces endothelial cell density but viable endothelial cells compensate for the loss by increasing in size (Bourne 2003). The keratocyte network does not appear to increase in size to compensate for cell loss in the anterior stroma. Morphometric analyses show a proportional decrease between keratocyte network size (SA) and numbers (nuclei counts) by 4 days and up to 28 days post injury in WT mice. This suggests there is a small window of opportunity for cell proliferation and migration into the anterior central stroma. In adhesion molecule deficient mice, the degree of keratocyte repopulation appears to be dependent on the degree of platelet accumulation and not PMN infiltration. ICAM-1^{-/-} mice showed a greater inflammatory response in this injury model and PMN and platelet recruitment were coincidental through 48 hours, in stark contrast to the kinetics of platelet

accumulation in WT and CD18^{mutant} mice. While this implies coincident recruitment of PMNs and platelets may facilitate efficient keratocyte repopulation, normal PMN recruitment (compared to WT), blunted platelet accumulation, and depressed keratocyte repopulation in CD18^{mutant} mice suggests platelets alone contribute to keratocyte recovery. Because the CD18^{mutant} mice expressed the β 2 integrin CD18, albeit at significantly lower levels than WT (Wilson, Ballantyne et al. 1993), these mice provide a unique opportunity to study the accumulation of platelets into the cornea independent of PMN infiltration. Platelet depletion studies further support the findings that platelets contribute to keratocyte repopulation.

Collectively, the data show both early and enhanced platelet accumulation is required for anterior central keratocyte repopulation to return baseline numbers (Table 6). As previously suggested, a small window of opportunity exists for cellular migration and proliferation, and may be determined by the kinetics of platelet accumulation. The initial increase of platelet accumulation in ICAM-1^{-/-} mice occurs at 18 hours but whether this is the critical time point for stimulating keratocyte repopulation remains unclear, since platelet accumulation in ICAM-1^{-/-} mice remains elevated through 48 hours.

Extravascular platelets become activated as they come into contact with extracellular matrix components, resulting in their degranulation and release of growth factors (Firkin 1963; Kainoh, Ikeda et al. 1992; George 2000; Kamath, Blann et al. 2001; Smith and Weyrich 2011). Platelet growth factors can promote cellular differentiation, regeneration, and proliferation (Servold 1991; Kamiyama, Iguchi et al. 1998; Imanishi, Kamiyama et al. 2000; Baldwin and Marshall 2002; Barrientos, Stojadinovic et al. 2008) and addition of recombinant growth factors associated with platelets enhance keratocyte DNA synthesis *in vitro* (Etheredge, Kane et al. 2009). Thus, it seems plausible for growth factors released by limbal stromal platelets to promote anterior paralimbal keratocytes, which do not die as a result of central epithelial abrasion (Petrescu, Larry et

al. 2007; Gagen, Laubinger et al. 2010), to proliferate and migrate into the central stroma.

The human and mouse limbus harbor resident stem cells (Thoft, Wiley et al. 1989; Du, Funderburgh et al. 2005; Charukamnoetkanok 2006; McGowan, Edelhauser et al. 2007; Polisetty, Fatima et al. 2008; Takacs, Toth et al. 2009) and platelets accumulate within this limbal region, possibly releasing growth factors as they degranulate over time. It is known that stem cell differentiation is triggered by growth factors (Bocelli-Tyndall, Zajac et al. ; Arsenijevic and Weiss 1998), supporting a possibility for limbal stem cell differentiation into new keratocytes. Additionally, growth factors stimulate differentiation of resident corneal cells. Growth factors, such as transforming growth factor (TGF)- β and platelet-derived growth factor (PDGF), have been shown to cause keratocyte differentiation and the same growth factors are stored in platelet α granules (Imanishi, Kamiyama et al. 2000; Baldwin and Marshall 2002; Rozman and Bolta 2007; Barrientos, Stojadinovic et al. 2008) . Topical application of platelet extracts, used to promote epithelial recovery, also cause keratocyte differentiation (Geremicca, Fonte et al. ; Kamiyama, Iguchi et al. 1998; Matsuo, Ohkohchi et al. 2008). Thus, it is plausible that large numbers of platelets accumulating at the limbal stroma, as in ICAM-1^{-/-} mice, may release large amounts of growth factors and initiate peripheral keratocyte differentiation. In fact, preliminary observations found Thy1.2 positive stromal cells in the central stroma of ICAM-1^{-/-} mice as early as 42 hours after injury (Figure 33 B) but not at the paralimbus (not shown). Thy1.2 (CD90.2) is one possible marker used to identify fibroblasts and identifies nerves as well (Ishihara, Hou et al. 1987; Pei, Sherry et al. 2004; Yu and Rosenblatt 2007). Preliminary observations show that Thy1.2 positive cells were not present in paralimbal (not shown) or central stroma at 24 hours (Figure 33 A), suggesting differentiated cell migration begins after 24 hours. If this Thy1.2 positive cells are indeed differentiated keratocytes, these

observations would suggest keratocyte differentiation, and their possible migration, occurs between 24 and 42 hours after injury. Fibroblasts are capable of migration (Kong, Majeska et al. 2011; Meier, Scharl et al. 2011), but it is unknown whether these Thy1.2 positive cells can migrate. By 4 days, there appears to be fewer Thy1.2 positive cells in the center and by 4 weeks these cells are no longer detected (Figure 33). These observations raise the possibility that these Thy1.2 positive cells may transform back into the keratocyte phenotype. While it has been demonstrated that fibroblasts can transform into keratocyte *in vitro* (Fini 1999), whether fibroblasts are capable of “de-differentiating” into keratocytes *in vivo* is currently unknown and beyond the scope of this Dissertation. However, it is possible that modulated infiltration and clearance of platelets by physiological mechanisms instead of a bolus application allows regulation of keratocyte differentiation and results in timely “de-differentiation”, if this in fact is the mechanism by which keratocytes repopulate the anterior stroma.

Remarkably, there was an unexpected boost, but no keratocyte death, in the posterior central stroma of ICAM-1^{-/-} mice. Taken together with keratocyte recovery in all regions (Figures 21), the data suggest an early wave of posterior cellular proliferation, possibly resulting from growth factor stimulation. It is unknown whether this increase was a direct effect of enhanced platelet accumulation in ICAM-1^{-/-} mice or a phenomenon that also occurs in WT and CD18^{mutant} mice but was left unrecorded due to the time points observed. However, other studies on keratocyte recovery in rats reported similar findings of increased posterior cell proliferation (Zieske, Guimaraes et al. 2001), suggesting differences in anterior-posterior keratocyte proliferation capabilities. Hindeman and colleagues showed posterior corneal keratocytes proliferate at a higher rate than anterior keratocytes *in vitro* (Hindman, Swanton et al. 2010). Recent studies indicate there is a second corneal stem cell niche in the posterior region of the limbus, at the trabecular meshwork (Whikehart, Parikh et al. 2005; McGowan, Edelhauser et al.

2007). Although these studies suggest these posterior stem cells contribute to corneal endothelial repair, these stem cells may also contribute to the sudden increase in posterior central keratocytes. Whether posterior keratocyte proliferation directly affects anterior keratocyte repopulation is currently unknown. While it is difficult to imagine how new keratocytes would migrate vertically through the stromal matrix to repopulate the anterior stroma, stromal reorganization during inflammation could play an important role in keratocyte distribution during wound healing.

In addition to promoting cell differentiation and proliferation, growth factors such as VEGF are implicated in promoting angiogenesis. Thus, one would expect early signs of corneal angiogenesis in ICAM-1^{-/-} mice due to enhanced recruitment of PMNs and platelets, both of which contain VEGF (Firkin 1963; George 2000; Blair and Flaumenhaft 2009; Smyth, McEver et al. 2009; Li, Burns et al. 2011). However, CD31 positive vessel staining was not detected in ICAM-1^{-/-} mice beyond the limbal region.

Using diamond blade injury models of mouse corneal epithelial abrasion, Li and colleagues showed that platelet accumulation was poor in TCR δ ^{-/-} and P-selectin^{-/-} mice (Li, Rumbaut et al. 2006c; Li, Burns et al. 2007). If platelets were indeed important for keratocyte repopulation, one would expect impaired keratocyte repopulation in mice lacking $\gamma\delta$ T cells and P-selectin. Therefore, to further substantiate a role for platelets in keratocyte repopulation, TCR δ ^{-/-} and P-selectin^{-/-} mice were used to show reduced platelet accumulation results in impaired anterior central keratocyte repopulation. These studies suggest platelets promote keratocyte repopulation, directly supported by observations of poor keratocyte recovery in P-selectin^{-/-} mice, with low platelet accumulation, and complete keratocyte recovery with the addition of P-selectin-expressing WT platelets. Unexpectedly, platelet numbers in TCR δ ^{-/-} mice were not different from WT. Initially, these contradictory results suggested platelets did not contribute to keratocyte repopulation. However, the observational findings of

morphologically “unactivated”-appearing extravasated platelets in TCR $\delta^{-/-}$ mice (Figure 32) suggests $\gamma\delta$ T cells may be required for platelet activation rather than recruitment, which is entirely consistent with the hypothesis that platelets are required for efficient keratocyte repopulation.

$\gamma\delta$ T cells produce cytokines IL-17 and IL-22 (Braun, Ferrick et al. 2008; Ness-Schwickerath, Jin et al. 2010; Li, Burns et al. 2011), both of which promote tissue regeneration (Li, Burns et al. 2011; Li, Burns et al. 2011). Additionally, IL-17 induces platelet activation via ADP and IL-22 modulates circulating platelet numbers (Liang, Nickerson-Nutter et al. 2010; Maione, Cicala et al. 2011). Maione showed that IL-17 induces platelet activation via ADP and collagen alone was inadequate to achieve similar activation without the presence of IL-17 (Maione, Cicala et al. 2011). IL-22 modulates circulating platelet numbers during acute phase response and, in part, facilitates resolution of inflammation, and assists to reinstate homeostasis (Liang, Nickerson-Nutter et al. 2010). The absence of $\gamma\delta$ T cells would eliminate these mechanisms of platelet activation.

$\gamma\delta$ T cell numbers in P-selectin $^{-/-}$ mice are not different than in WT mice but platelet numbers are still low in P-selectin $^{-/-}$ mice and keratocyte repopulation is impaired, suggesting, 1) $\gamma\delta$ T cells alone are not sufficient for platelet recruitment, and 2) P-selectin is required for platelet accumulation. Conversely, P-selectin is expressed on platelets of TCR $\delta^{-/-}$ mice hence may accommodate platelet accumulation outside of the limbal vessels. Yet the “inactivated” shape of platelets in these mice (Figure 32) suggests that activation signaling mechanisms are absent. Without $\gamma\delta$ T cells to produce IL-17 or IL-22, platelets may not achieve the degree of activation necessary to degranulate and release growth factors, even when exposed to collagen (Maione, Cicala et al. 2011).

Interestingly, preliminary observations also reveal increased central PMN accumulation in $\text{TCR}\delta^{-/-}$ mice at 18 hours (Figure 3) and PMNs are detected as late as 4 days post injury (observational data, not shown). This is one possible explanation for why the addition of rIL-22 did not rescue keratocyte repopulation but rescued epithelial healing in $\text{TCR}\delta^{-/-}$ mice (Li, Burns et al. 2011). Proteolytic enzymes released by PMNs can damage tissue, especially if there is excess PMN accumulation (Dyugovskaya and Polyakov 2010). This too can contribute to depressed keratocyte repopulation in $\text{TCR}\delta^{-/-}$ mice. In fact, corneal epithelial healing is severely compromised in $\text{Mac-1}^{-/-}$ mice because of their inability to resolve inflammation via PMN clearance (Li, Burns et al. 2006b) .

Even though IL-22 may not directly modulate keratocyte migration or proliferation, one important function of IL-22 is to assist in resolving inflammation by enhancing permeability (Liang, Nickerson-Nutter et al. 2010). Positive IL-22R staining on CD31^{+} vessels in the limbal region suggests the lymphatic vessels express IL-22R during inflammation (Figure 29). As previously discussed, lymphatic vessels express low levels of CD31 in other tissue (D'Amico and Alitalo 2010) and immunostaining corneas for CD31 and LYVE-1, a lymphatic marker, shows no CD31 expression on LYVE-1 positive vessels (Ruddell, Mezquita et al. 2003). Lymphatic vessels clear excess fluid and debris, and possibly leukocytes, from injured tissue (D'Amico and Alitalo 2010). Without IL-22 release and binding to IL-22R on these $\text{CD31}^{-}/\text{IL-22R}^{+}$ vessels, signaling to promote enhanced permeability may not occur, if indeed these are lymphatic vessels, thus compromising their function to remove cellular debris, or clear inflammatory cells, during inflammation.

Hence, both P-selectin and $\gamma\delta$ T cells are required to facilitate keratocyte repopulation. The former through promoting platelet extravasation in the presence of $\gamma\delta$ T cells and the latter possibly through the secretion of cytokines IL-17 and IL-22, which

play important roles in modulating inflammation (Trifari and Spits ; Boniface, Bernard et al. 2005; Liang, Tan et al. 2006; Braun, Ferrick et al. 2008; Molesworth-Kenyon, Yin et al. 2008; Deknuydt, Scotet et al. 2009; Roussel, Houle et al. 2010; Maione, Cicala et al. 2011). While much remains to be investigated with regards to IL-22 and IL-17-mediated keratocyte repopulation, it is clear that P-selectin and $\gamma\delta$ T cells are required for corneal wound healing following epithelial abrasion.

Collectively, these data provide evidence for a novel negative regulatory role for the adhesion molecule ICAM-1 in recruiting inflammatory cells during corneal inflammation and a positive role for platelets in promoting enhanced keratocyte repopulation during wound healing. While these studies showed platelets are important for keratocyte repopulation, it should be noted that studies evaluating epithelial healing or nerve regeneration using the Algerbrush-induced injury model were not performed. Hence, it is still unclear whether platelets have the same effect on epithelial and nerve healing in this model and these studies warrant investigation.

CHAPTER 6: GENERAL CONCLUSION

Keratocytes are corneal stromal cells that produce the collagens, proteoglycans, and crystallins which help maintain corneal strength, curvature, and clarity. The loss of these cells may possibly alter corneal biomechanical properties, which in turn can severely compromise quality of vision (Dupps and Wilson 2006). Keratocyte loss can occur as a result of incomppliance with contact lens wearing or using rigid contact lenses (Bergmanson and Chu 1982; Patel, McLaren et al. 2002; Lema, Duran et al. 2008). Prolonged contact lens wear also causes sustained corneal inflammation and sustained inflammation can exacerbate injury and significantly delay wound healing (Li, Burns et al. 2006b; Lema, Sobrino et al. 2009). Additionally, long-term contact lens wear can cause considerable corneal endothelial cell loss. However, neighboring endothelial cells can compensate for cell loss by enlargening, a condition termed polymegethism (Bourne 2003). In contrast, keratocytes do not appear to increase in size to compensate for cell loss. Keratocyte death also occurs after refractive surgery (LASIK and PRK) and these cells do not recover to normal levels as do epithelial cells (Helena, Baerveldt et al. 1998; Kim, Shah et al. 1998; Mitooka, Ramirez et al. 2002). Loss and incomplete recovery of keratocytes may cause significant post-surgical complications such as Keratectasia, a condition characterized by the protrusion of the corneal apex (Comaish and Lawless 2002; Twa, Nichols et al. 2004; Khachikian and Belin 2010; Hodge, Lawless et al. 2011). Many studies found that keratocyte density in refractive surgery-induced keratectasia was significantly lower than keratocyte density in normal, un-operated corneas (Mitooka, Ramirez et al. 2002; Erie, Nau et al. 2004; Ali Javadi, Kanavi et al. 2009; Javadi and Feizi 2010). While these findings do not directly demonstrate that low keratocyte density causes keratectasia, it is logical to assume that loss of keratocytes, cells which produce necessary structural components for maintaining and preserving corneal integrity, can

lead to these extreme cases of corneal disfigurement. Indeed, a similar corneal protrusion occurs in Kerataconic (Kc) patients and without rigid lens or surgery, Kc patients eventually lose their vision. Furthermore, keratocyte density in Kc corneas is significantly lower than normal corneas, as are post-LASIK or post-PRK corneas (Erie, Patel et al. 2002; Binder, Lindstrom et al. 2005; Ali Javadi, Kanavi et al. 2009). Hence, understanding the mechanisms promoting keratocyte repopulation is important for preventing the possibility of vision loss.

Corneal epithelial abrasion also causes death of keratocytes, below the region of injury and is a useful model for studying keratocyte repopulation during wound healing (Wilson, He et al. 1996a; Zieske, Guimaraes et al. 2001; Wilson, Mohan et al. 2002; Zhao and Nagasaki 2004). Epithelial abrasion also elicits an inflammatory response, resulting in PMN, platelet, and $\gamma\delta$ T cell infiltration into the limbal stroma and emigration of PMNs into the corneal stroma (Burns, Li et al. 2005; Li, Burns et al. 2006a; Li, Burns et al. 2006b; Li, Rumbaut et al. 2006c; Li, Burns et al. 2007; Petrescu, Larry et al. 2007; Byeseda, Burns et al. 2009; Gagen, Laubinger et al. 2010; Li, Burns et al. 2011; Li, Burns et al. 2011). Li and colleagues demonstrated the importance of PMNs, platelets, and $\gamma\delta$ T cells in epithelial recovery and nerve regeneration (Li, Burns et al. 2006a; Li, Rumbaut et al. 2006c; Li, Burns et al. 2007). However, there is no supporting literature demonstrating the effects of these inflammatory cells on keratocyte repopulation after corneal abrasion. The purpose of this Dissertation was to investigate the cellular and molecular mechanisms of corneal inflammation and wound healing with a specific interest in PMN interactions with keratocytes and the roles of PMNs, platelets, and $\gamma\delta$ T cells in promoting keratocyte repopulation.

The results show that PMN interaction with keratocytes is regulated by keratocyte ICAM-1, an adhesion molecule that can associate with the $\beta 2$ integrin CD18 expressed on the surface of PMNs. It is highly likely that PMNs use the intact keratocyte

network (at the paralimbal stroma) as a cellular highway to migrate towards the wound region. Evidence for this theory is presented by a significant reduction in PMN motility on keratocytes after blocking either CD18 or ICAM-1, *in vitro*. With respect to keratocyte repopulation, PMNs however do not influence their efficient recovery, as PMN numbers in CD18^{mutant} and WT mice are not different. However, platelets do significantly influence keratocyte repopulation. The absence of ICAM-1 enhances both PMN infiltration and platelet accumulation and keratocyte repopulation after epithelial abrasion in ICAM-1^{-/-} mice recovers to baseline numbers as early as 4 days post injury. Furthermore, depletion of platelets diminishes keratocyte repopulation in WT mice but platelet infusion into P-selectin^{-/-} mice restores keratocyte repopulation. Finally, while it is clear that $\gamma\delta$ T cells alone are not sufficient for promoting efficient keratocyte repopulation, they may indirectly assist keratocyte recovery by secreting cytokines (IL-17 and IL-22) that are essential for platelet activation and tissue regeneration (Liang, Tan et al. 2006; Liang, Nickerson-Nutter et al. 2010; Maione, Cicala et al. 2011).

While other studies show coincident recruitment of PMNs and platelets throughout the course the corneal inflammatory response (Li, Rumbaut et al. 2006c; Li, Burns et al. 2007), the studies presented in this Dissertation suggests otherwise, except in the case of ICAM-1^{-/-} mice. Coincident arrival of PMNs and platelets is observed in all three genotypes only during the first 12 hours after injury but their course is altered in WT and CD18^{mutant} mice soon after. However, PMNs and platelets in ICAM-1^{-/-} mice indeed display simultaneous influx and clearance through the 48 hours of inflammation observed for these studies. This may be due to the elevated levels of stromal $\gamma\delta$ T cells in ICAM-1^{-/-} mice. Studies by Li and colleagues showed that both PMN infiltration and platelet accumulation require $\gamma\delta$ T cells. While this may not hold true for WT mice in Algerbrush injury model, it may follow accordingly in ICAM-1^{-/-} mice. Byeseda demonstrated elevated stromal $\gamma\delta$ T cells in ICAM-1^{-/-} mice, significantly higher than in

WT (Byeseda, Burns et al. 2009). Interestingly, the sudden increase in stroma of $\gamma\delta$ T cell numbers occurs at 18 hours post injury, the time when enhanced PMN and platelet numbers are first observed in the present studies. As well, message for the cytokine CCL20, a potent attractant of $\gamma\delta$ T cells (Li, Burns et al. 2011), is elevated in injured corneas of ICAM-1^{-/-} mice (personal communication with Dr. CW Smith, Baylor College of Medicine). $\gamma\delta$ T cells produce and secrete IL-17 and IL-22, cytokines associated with the modulation of inflammation, vessel permeability, platelet activation, and tissue regeneration (Ren, Hu et al. ; Trifari and Spits ; Boniface, Bernard et al. 2005; Liang, Tan et al. 2006; Braun, Ferrick et al. 2008; Deknuydt, Scotet et al. 2009; Liang, Nickerson-Nutter et al. 2010; Roussel, Houle et al. 2010; Li, Burns et al. 2011; Li, Burns et al. 2011; Maione, Cicala et al. 2011). Thus, while it is true that $\gamma\delta$ T cells do not directly influence keratocyte repopulation, in high numbers, they appear to be the master regulators of corneal inflammation, indirectly contributing to keratocyte recovery. However, the reason CCL20 mRNA levels, and subsequently stromal $\gamma\delta$ T cell numbers, are enhanced in ICAM-1^{-/-} mice is currently unknown. Furthermore, CCL20 protein levels have not been determined in any genotypes studied. These questions warrant further investigation.

The PMN infiltration responses between WT and CD18^{mutant} mice were not different, possibly because of the hypomorphic mutation of CD18^{mutant} mice. Yet platelet accumulation in WT mice peaked 24 hours after injury but remained severely low in CD18^{mutant} mice. Reasons for this disparity are unclear but may involve mechanisms by which platelets associate with PMNs and/or the condition of the limbal endothelium during the course of inflammation. First, while the low expression of CD18 may allow early PMN emigration in hypomorphic CD18^{mutant} mice, the avidity and affinity of the Mac-1 component to bind with platelet GP1b α may be too low to allow platelets to associate with PMNs, if indeed this mechanism of platelet extravasation occurs in the

cornea. Second, increased transcellular pores may arise in the vascular endothelium of WT mice by 24 hours. These pores range between 1-2 μm in size, large enough to facilitate platelet transport but not PMN transport. Further investigation is required to discern whether either of these possibilities is responsible for the different responses of PMN versus platelet extravasation between WT and CD18^{mutant} mice. However, keratocyte repopulation in WT mice was greater than that of CD18^{mutant} mice, possibly as a consequence of the 24 hour peak in platelet accumulation, which would imply that platelets play an important role in keratocyte repopulation following corneal epithelial abrasion. PMNs do not contribute to keratocyte repopulation, as evidenced by the near identical kinetics of PMN recruitment in WT and CD18^{mutant} mice.

These studies suggest that an accelerated inflammatory response, followed by prompt clearance, promotes stromal cell recovery. With regards to resolution of inflammation, the eventual fate of the infiltrating inflammatory cells is currently unclear. Recently the half life of resting human PMNs has been re-evaluated and it appears to be days rather than hours as previously thought (Pillay, den Braber et al. 2010). Whether this longer half life applies to activated PMNs is unknown. The half life of mouse PMNs was not different from what has previously been reported (Basu, Hodgson et al. 2002; Pillay, den Braber et al. 2010). PMN and platelet numbers reduced by 48 hours, which is essential for proper healing to occur, as prolonged inflammation can further exacerbate the injury (Rudner, Kernacki et al. 2000; Vij, Roberts et al. 2005; Li, Rumbaut et al. 2006c; Molesworth-Kenyon, Yin et al. 2008; Tarabishy, Aldabagh et al. 2008). It is likely that infiltrating and resident macrophages engulf apoptotic PMNs over time, but given the high density of PMNs in this wound model, this would be a difficult feat to accomplish over a 48 hour time frame, albeit feasible, depending on the kinetics and density of macrophage infiltration in this injury model. Platelets remain at the vicinity of the limbal stroma, where lymphatic vessels intertwine with the limbal vessels (Cursiefen,

Schlotzer-Schrehardt et al. 2002; Hos, Bachmann et al. 2008). Lymphatic vessels are the body's "drainage" system, clearing fluid from tissue back into the circulation and may clear inflammatory cell debris (i.e. platelet microparticles and degranulated PMNs) during tissue healing (D'Amico and Alitalo 2010). PMN migration in the corneal stroma occurs over the keratocyte network and is possibly mediated by the interactions between keratocyte ICAM-1 and PMN CD18 (Petrescu, Larry et al. 2007; Gagen, Laubinger et al. 2010). When central keratocytes are not available for PMN associations, after epithelial abrasion, PMNs can use $\beta 1$ and $\beta 3$ integrins to associate with collagen components (Stepp 2006). If PMNs can utilize these associations to migrate within the corneal stroma, they may be capable of migrating back towards the corneal periphery using the same association during the time when inflammation is beginning to resolve. If this is the case, PMN clearance may also occur through lymphatic vessels as well.

Furthermore, recent evidence shows that PMNs can migrate back into blood vessels in a "reverse" migration process (Yoo and Huttenlocher 2011). Even in ICAM-1^{-/-} mice, where enhanced inflammation occurs, the release of IL-22 by $\gamma\delta$ T cells may possibly impact the rate of inflammatory cell clearance. As previously explained in Section 5.5, the cytokine IL-22 can enhance vascular permeability (Liang, Nickerson-Nutter et al. 2010) and IL-22 staining detected on CD31⁺ vessels found the region of the limbus. These are presumably lymphatic vessels (Figure 29C). Increased stromal $\gamma\delta$ T cells numbers in ICAM-1^{-/-} mice (Byeseda, Burns et al. 2009) may result in elevated IL-22 levels and this could result in increased lymphatic vessel permeability, thereby accommodating the clearance of large amounts of inflammatory cells that had accumulated in the corneas of ICAM-1^{-/-} mice. Thus, numerous mechanisms may participate in resolution of inflammation, allowing for effective cellular regeneration and tissue healing.

This Dissertation demonstrated the important effects of a robust acute corneal inflammatory response for subsequent wound healing. Infiltration and accumulation of inflammatory cells is essential for epithelial healing, nerve regeneration and, as now evidenced, keratocyte repopulation. Key participants include PMNs, platelets, and the associated adhesion molecules, CD18 and P-selectin. Additionally, intravascular ICAM-1 contributes significantly by inhibiting enhanced inflammatory cell infiltration, suggesting a negative regulatory role for ICAM-1 in facilitating PMN infiltration and platelet accumulation. ICAM-1 also plays an extravascular role by mediating close surface contacts with PMN, in all probability through keratocyte ICAM-1 and PMN CD18 associations, possibly even facilitating PMN motility over the keratocyte network. Timing and density of limbal platelet accumulation is essential for keratocyte repopulation. Early accumulation of high platelet numbers (between 18 - 24 hours) appears to be most beneficial to keratocyte repopulation. As previously described, stem cells reside within the limbal region (Thoft, Wiley et al. 1989; McGowan, Edelhauser et al. 2007; Polisetty, Fatima et al. 2008; Takacs, Toth et al. 2009) and early stimulation of these cells by platelet growth factors may enhance their differentiation into stromal cells. Alternatively, paralimbal keratocytes may also proliferate *in vivo* following stimulation by growth factors, as they have been shown to do *in vitro* (Etheredge, Kane et al. 2009). Cytokines released by $\gamma\delta$ T cells regulate inflammation, modulate platelet and PMN recruitment, stimulate platelet activation, and assist in resolution of inflammation. Thus, $\gamma\delta$ T cells may serve as the master regulators of corneal inflammation and wound healing. Collectively, the Dissertation demonstrates the important cellular and molecular mechanisms influencing corneal inflammation and promoting corneal wound healing.

CHAPTER 7: FUTURE DIRECTION FOR KERATOCYTE REPOPULATION STUDIES

These studies have determined 1) keratocyte ICAM-1 regulates extravascular associations between keratocytes and PMNs in the corneal stroma, 2) PMN CD18 and keratocyte ICAM-1 facilitates PMN motility on keratocytes, *in vitro* 3) PMN CD18 and vascular endothelial ICAM-1 modulate the influx of PMNs and platelets in to the limbal stroma, 4) platelets promote keratocyte repopulation, and 5) $\gamma\delta$ T cells may be the master regulators of corneal inflammation and wound healing but do not directly influence keratocyte repopulation. While multiple future studies can stem from these novel findings, a few of the most feasible and direct future studies will be outlined.

The kinetics of keratocyte repopulation following epithelial abrasion is similar to keratocyte repopulation observed post refractive surgery, where cells never return to baseline. Consequences of incomplete recovery may include development of ectasia and impaired vision. Since keratocytes produce essential components for maintaining corneal clarity, studies designed to promote their full recovery are important to pursue.

The evidence provided in this Dissertation suggests ICAM-1 plays a negative regulatory role in platelet and PMN infiltration where its absence enhanced PMN infiltration, platelet accumulation, and keratocyte repopulation. While the first instinct would be to try blocking ICAM-1 in injured WT mice and observe the inflammatory cell and keratocyte repopulation kinetics, it should be remembered that ICAM-1 is ubiquitously expressed (Dustin, Rothlein et al. 2011) and systemic administration of a blocking antibody to ICAM-1 (YN-1) would result in functional inhibition of ICAM-1 throughout other systems. Topical application of an anti-ICAM antibody to the cornea following injury may allow it to dissipate and bind to limbal endothelial ICAM-1 but it would also bind with keratocyte ICAM-1 and possibly inhibit PMN emigration to the site of injury. These *in vivo* blocking studies (using GAME46 and YN-1) are currently

underway in Dr. Alan Burns' laboratory. Still, blocking ICAM-1 would not be a direction to pursue, in as far as therapeutic application to enhance keratocyte repopulation.

Clearly when there are more platelets (ICAM-1^{-/-} mice), or even a slight boost in platelets (WT mice) by 24 hours (Figure 19), keratocyte repopulation is enhanced to varying degrees (Figure 21). The cytokine CCL20 is abundantly expressed in corneas of ICAM-1^{-/-} mice. This cytokine is known to attract $\gamma\delta$ T cells and indeed ICAM-1^{-/-} mice have elevated stromal $\gamma\delta$ T cells (Li, Burns et al. 2011). $\gamma\delta$ T cells secrete IL-17, a cytokine responsible, in part, for platelet activation, and IL-22 a cytokine that modulates circulating platelet numbers and vessel dilation (Liang, Nickerson-Nutter et al. 2010; Maione, Cicala et al. 2011). Enhanced platelet recruitment in ICAM-1^{-/-} mice may be linked to $\gamma\delta$ T cells and the cytokines IL-17 and IL-22. These are the key experiments to pursue in order to elucidate mechanisms promoting keratocyte repopulation.

Inhibiting $\gamma\delta$ T cell influx into ICAM-1^{-/-} mice after corneal epithelial abrasion would determine whether $\gamma\delta$ T cells indeed boost the inflammatory response, promoting greater PMN infiltration and platelet accumulation. This can be accomplished by systemic administration of a $\gamma\delta$ T cell sequestering antibody, clone GL3 (Li, Burns et al. 2007) into ICAM-1^{-/-} mice. The sequestration of $\gamma\delta$ T cells diminishes inflammatory cell infiltration, as shown by Li *et al.*, using WT mice (Li, Burns et al. 2007), and theoretically should result in depressed anterior central keratocyte repopulation in ICAM-1^{-/-} mice.

Systemic administration and topical application of rIL-22 did not rescue keratocyte repopulation even though keratocytes express IL-22R (Figure 28). This makes sense because while IL-22 may modulate platelets in circulation, it may not promote platelet extravasation and does not stimulate platelet activation. However IL-17 is known to promote platelet aggregation (Maione, Cicala et al. 2011). The Smith and Li group showed that rIL-17 administration rescued nerve regeneration (Li, Burns et al. 2011). To determine whether IL-17 plays a role in keratocyte repopulation, possibly by

activating platelets, rIL-17 should be systemically or topically administered to WT and TCR $\delta^{-/-}$ mice and keratocyte repopulation 4 days post injury should be evaluated. Because WT mice showed incomplete keratocyte repopulation, this experiment may determine if IL-17 enhances WT keratocyte recovery. Alternatively, administration of IL-17 antibody into ICAM-1 $^{-/-}$ mice should inhibit platelet activation (even in the presence of collagen (Maione, Cicala et al. 2011)), possibly depressing keratocyte repopulation, thus providing further insight into mechanisms promoting keratocyte recovery.

$\gamma\delta$ T cell recruitment is facilitated by CCL20. It would be important, as well as interesting, to see whether CCL20 application onto injured WT corneas also restored keratocyte repopulation back to baseline but recruiting more $\gamma\delta$ T cells. While WT platelet infusion into WT mice was not productive for enhancing keratocyte repopulation, cytokine stimulation to physiologically recruit larger numbers of cells, rather than introducing cells from a relatively external source, may enhance keratocyte repopulation in WT mice.

While understanding the mechanisms promoting keratocyte differentiation allows for development of therapeutic remedies to promote keratocyte repopulation following epithelial abrasion, or after refractive surgery, elucidating the source of repopulating keratocytes is just as important. The limbal vessels harbor resident stem cells (Thoft, Wiley et al. 1989; Collinson, Chanas et al. 2004; Charukamnoetkanok 2006; Polisetty, Fatima et al. 2008; Davies, Chui et al. 2009; Holan, Pokorna et al. 2010) and these may be a source of newly differentiated keratocytes. Furthermore, uninjured paralimbal keratocytes may proliferate and migrate to replenish the anterior stroma of keratocytes. In addition to discovering limbal stem cells, the proliferative properties of keratocytes have been investigated *in vitro* (Etheredge, Kane et al. 2009; Hindman, Swanton et al. 2010). However if differentiated stem cells or proliferating paralimbal keratocytes repopulate the anterior stroma, they must migrate from the periphery to the center. It is

not known whether the keratocyte phenotype can migrate individually or as a network, although the latter seems highly unlikely. However, the differentiated “repair” phenotypes, fibroblasts or myofibroblasts, have migratory capabilities (Kong, Majeska et al. 2011; Meier, Scharl et al. 2011) and may repopulate the stromal region void of keratocytes. While these phenotypes are not desirable for maintaining visual clarity, they may be a likely source of new keratocytes. Fini described cytokine regulation of repair phenotypes may allow de-differentiation of the fibrotic cells back into the quiescent keratocyte phenotype *in vitro* (Fini 1999). Preliminary observations show Thy1.2 positive cells in ICAM-1^{-/-} as early as 42 hours after injury but this staining is no longer detected by 4 weeks (Figure 33). Thus, it is worth quantifying these cells over time and comparing the differentiation rate between WT and ICAM-1^{-/-} mice to determine whether increased differentiated keratocytes promote keratocyte repopulation. Elucidating the mechanisms involved in the de-differentiation process would be beyond the scope of cellular and molecular mechanisms involved in keratocyte repopulation.

Clearance of inflammatory cells is very important for proper healing to occur. Prolonged existence of PMNs in the tissue can cause further tissue damage and prevent wound healing (Li, Burns et al. 2006b). Tracking labeled PMNs would help elucidate the fate of PMNs during the resolution of corneal inflammation. Without generating transgenic mice to conduct these experiments, isolated peripheral blood PMNs from enhanced green fluorescent protein (EGFP) WT mice or isolated carboxyfluorescein diacetate, succinimidyl ester (CFSE)-labeled peripheral blood PMNs from WT mice can be injected via tail vein 2 hours after injury, a time when PMN infiltration is first observed. CFSE passively diffuses through cells and as intracellular esterases cleave the acetate groups, a green fluorescence is emitted and sustained for a prolonged period of time. Early injection of isolated PMNs will allow tracking of infiltrating PMNs. Corneas can be harvested at 6 hour intervals from an uninjured time through a 48 hour time course.

Subsequent injections may not be ideal as newly extravasating labeled PMN would be indistinguishable from early injected PMNs. However, these studies would be dependent on the numbers of labeled PMNs getting out of the circulation through the limbal vessels.

While many tangential experiments can stem from these corneal inflammation and keratocyte repopulation studies, the essential experiments to pursue are those directly linking enhanced platelet recruitment to complete keratocyte recovery, as outlined earlier in this chapter. The key is manipulating the inflammatory response to allow for physiologically enhanced but controlled platelet accumulation. Elucidating these mechanisms will enable the advancement of therapeutic treatments to promote keratocyte repopulation after injury or refractive surgery.

REFERENCES

- AAO (2008). Eye injuries: Recent data and trends in the united states, AAO website.
Available at <http://www.aao.org/newsroom/guide/upload/Eye-Injuries-BkgrnderLongVersFinal-I.pdf>.
- Albelda, S. M., C. W. Smith, et al. (1994). "Adhesion molecules and inflammatory injury." FASEB J 8(8): 504-512.
- Ali Javadi, M., M. R. Kanavi, et al. (2009). "Comparison of keratocyte density between keratoconus, post-laser in situ keratomileusis keratectasia, and uncomplicated post-laser in situ keratomileusis cases. A confocal scan study." Cornea 28(7): 774-779.
- Allison, T. J., C. C. Winter, et al. (2001). "Structure of a human gammadelta T-cell antigen receptor." Nature 411(6839): 820-824.
- Ambrosio, R., Jr., N. Kara-Jose, et al. (2009). "Early keratocyte apoptosis after epithelial scrape injury in the human cornea." Exp Eye Res 89(4): 597-599.
- Amouzadeh, H. R., S. Sangiah, et al. (1991). "Xylazine-induced pulmonary edema in rats." Toxicol Appl Pharmacol 108(3): 417-427.
- Anderson, D. C., F. C. Schmalstieg, et al. (1985). "Leukocyte LFA-1, OKM1, p150,95 deficiency syndrome: functional and biosynthetic studies of three kindreds." Fed Proc 44(10): 2671-2677.
- Anderson, H. R., A. W. Stitt, et al. (1994). "Estimation of the surface area and volume of the retinal capillary basement membrane using the stereologic method of vertical sections." Anal Quant Cytol Histol 16(4): 253-260.

- Arevalo, J. F. (2004). "Retinal complications after laser-assisted in situ keratomileusis (LASIK)." Curr Opin Ophthalmol 15(3): 184-191.
- Arfors, K. E., C. Lundberg, et al. (1987). "A monoclonal antibody to the membrane glycoprotein complex CD18 inhibits polymorphonuclear leukocyte accumulation and plasma leakage in vivo." Blood 69(1): 338-340.
- Arnaout, M. A. (1990). "Structure and function of the leukocyte adhesion molecules CD11/CD18." Blood 75(5): 1037-1050.
- Arsenijevic, Y. and S. Weiss (1998). "Insulin-like growth factor-I is a differentiation factor for postmitotic CNS stem cell-derived neuronal precursors: distinct actions from those of brain-derived neurotrophic factor." J Neurosci 18(6): 2118-2128.
- Arturson, G. (1980). "Pathophysiology of the burn wound." Ann Chir Gynaecol 69(5): 178-190.
- Asa, D., L. Raycroft, et al. (1995). "The P-selectin glycoprotein ligand functions as a common human leukocyte ligand for P- and E-selectins." J Biol Chem 270(19): 11662-11670.
- Bailey, M. D., G. L. Mitchell, et al. (2003). "Patient satisfaction and visual symptoms after laser in situ keratomileusis." Ophthalmology 110(7): 1371-1378.
- Baldwin, H. C. and J. Marshall (2002). "Growth factors in corneal wound healing following refractive surgery: A review." Acta Ophthalmol Scand 80(3): 238-247.
- Baluk, P., J. J. Bowden, et al. (1997). "Upregulation of substance P receptors in angiogenesis associated with chronic airway inflammation in rats." Am J Physiol 273(3 Pt 1): L565-571.

- Barishak, Y. R. (1992). "Embryology of the eye and its adnexae." Dev Ophthalmol 24: 1-142.
- Barrientos, S., O. Stojadinovic, et al. (2008). "Growth factors and cytokines in wound healing." Wound Repair Regen 16(5): 585-601.
- Basu, S., G. Hodgson, et al. (2002). "Evaluation of role of G-CSF in the production, survival, and release of neutrophils from bone marrow into circulation." Blood 100(3): 854-861.
- Beales, M. P., J. L. Funderburgh, et al. (1999). "Proteoglycan synthesis by bovine keratocytes and corneal fibroblasts: maintenance of the keratocyte phenotype in culture." Invest Ophthalmol Vis Sci 40(8): 1658-1663.
- Beecher, N., S. Chakravarti, et al. (2006). "Neonatal development of the corneal stroma in wild-type and lumican-null mice." Invest Ophthalmol Vis Sci 47(1): 146-150.
- Behnke, O. (1970). "A comparative study of microtubules of disk-shaped blood cells." J Ultrastruct Res 31(1): 61-75.
- Behnke, O. and A. Forer (1998). "From megakaryocytes to platelets: platelet morphogenesis takes place in the bloodstream." Eur J Haematol Suppl 61: 3-23.
- Belmonte, C., M. C. Acosta, et al. (2004). "Neural basis of sensation in intact and injured corneas." Exp Eye Res 78(3): 513-525.
- Bennett, J. S., B. W. Berger, et al. (2009). "The structure and function of platelet integrins." J Thromb Haemost 7 Suppl 1: 200-205.
- Bergmanson, J. P. and L. W. Chu (1982). "Corneal response to rigid contact lens wear." Br J Ophthalmol 66(10): 667-675.

- Bevilacqua, M. P. and R. M. Nelson (1993). "Selectins." J Clin Invest 91(2): 379-387.
- Bevilacqua, M. P., R. M. Nelson, et al. (1994). "Endothelial-leukocyte adhesion molecules in human disease." Annu Rev Med 45: 361-378.
- Binder, P. S., R. L. Lindstrom, et al. (2005). "Keratoconus and corneal ectasia after LASIK." J Refract Surg 21(6): 749-752.
- Birk, D. E., J. M. Fitch, et al. (1990). "Collagen fibrillogenesis in vitro: interaction of types I and V collagen regulates fibril diameter." J Cell Sci 95 (Pt 4): 649-657.
- Birk, D. E., J. M. Fitch, et al. (1988). "Collagen type I and type V are present in the same fibril in the avian corneal stroma." J Cell Biol 106(3): 999-1008.
- Birk, D. E., J. M. Fitch, et al. (1986). "Organization of collagen types I and V in the embryonic chicken cornea." Invest Ophthalmol Vis Sci 27(10): 1470-1477.
- Blair, P. and R. Flaumenhaft (2009). "Platelet alpha-granules: basic biology and clinical correlates." Blood Rev 23(4): 177-189.
- Blumberg, N., J. M. Heal, et al. (2010). "Platelet transfusions: trigger, dose, benefits, and risks." F1000 Med Rep 2: 5.
- Bocelli-Tyndall, C., P. Zajac, et al. "FGF-2 and PDGF, but not Platelet Lysate (PL), induce proliferation dependent, functional MHC-classII antigen in human mesenchymal stem cells (hMSC)." Arthritis Rheum.
- Bonfanti, R., B. C. Furie, et al. (1989). "PADGEM (GMP140) is a component of Weibel-Palade bodies of human endothelial cells." Blood 73(5): 1109-1112.

- Boniface, K., F. X. Bernard, et al. (2005). "IL-22 inhibits epidermal differentiation and induces proinflammatory gene expression and migration of human keratinocytes." J Immunol 174(6): 3695-3702.
- Bonneville, M., R. L. O'Brien, et al. (2010). "Gammadelta T cell effector functions: a blend of innate programming and acquired plasticity." Nat Rev Immunol 10(7): 467-478.
- Borregaard, N., O. E. Sorensen, et al. (2007). "Neutrophil granules: a library of innate immunity proteins." Trends Immunol 28(8): 340-345.
- Bourne, W. M. (2003). "Biology of the corneal endothelium in health and disease." Eye (Lond) 17(8): 912-918.
- Brake, D. K., E. O. Smith, et al. (2006). "ICAM-1 expression in adipose tissue: effects of diet-induced obesity in mice." Am J Physiol Cell Physiol 291(6): C1232-1239.
- Braun, R. K., C. Ferrick, et al. (2008). "IL-17 producing gammadelta T cells are required for a controlled inflammatory response after bleomycin-induced lung injury." Inflammation 31(3): 167-179.
- Bron, A. J. and J. M. Tiffany (1998). "The meibomian glands and tear film lipids. Structure, function, and control." Adv Exp Med Biol 438: 281-295.
- Bron, A. J., J. M. Tiffany, et al. (2004). "Functional aspects of the tear film lipid layer." Exp Eye Res 78(3): 347-360.
- Bueno, J. M., E. J. Gualda, et al. (2011). "Analysis of corneal stroma organization with wavefront optimized nonlinear microscopy." Cornea 30(6): 692-701.

- Burmeister, S. L., D. Hartwig, et al. (2009). "Effect of various platelet preparations on retinal muller cells." Invest Ophthalmol Vis Sci 50(10): 4881-4886.
- Burns, A. R., R. A. Bowden, et al. (1999). "P-selectin mediates neutrophil adhesion to endothelial cell borders." J Leukoc Biol 65(3): 299-306.
- Burns, A. R. and C. M. Doerschuk (1994). "Quantitation of L-selectin and CD18 expression on rabbit neutrophils during CD18-independent and CD18-dependent emigration in the lung." J Immunol 153(7): 3177-3188.
- Burns, A. R., Z. Li, et al. (2005). "Neutrophil migration in the wounded cornea: the role of the keratocyte." Ocul Surf 3(4 Suppl): S173-176.
- Burns, A. R., S. I. Simon, et al. (1996). "Chemotactic factors stimulate CD18-dependent canine neutrophil adherence and motility on lung fibroblasts." J Immunol 156(9): 3389-3401.
- Burns, A. R., C. W. Smith, et al. (2003). "Unique structural features that influence neutrophil emigration into the lung." Physiol Rev 83(2): 309-336.
- Burns, A. R., F. Takei, et al. (1994). "Quantitation of ICAM-1 expression in mouse lung during pneumonia." J Immunol 153(7): 3189-3198.
- Burns, A. R., D. C. Walker, et al. (1997). "Neutrophil transendothelial migration is independent of tight junctions and occurs preferentially at tricellular corners." J Immunol 159(6): 2893-2903.
- Byeseda, S. E., A. R. Burns, et al. (2009). "ICAM-1 is necessary for epithelial recruitment of gammadelta T cells and efficient corneal wound healing." Am J Pathol 175(2): 571-579.

- Cao, R., S. Lim, et al. (2011). "Mouse corneal lymphangiogenesis model." Nat Protoc 6(6): 817-826.
- Carlos, T. M. and J. M. Harlan (1994). "Leukocyte-endothelial adhesion molecules." Blood 84(7): 2068-2101.
- Carlson, E. C., M. Lin, et al. (2007). "Keratocan and lumican regulate neutrophil infiltration and corneal clarity in lipopolysaccharide-induced keratitis by direct interaction with CXCL1." J Biol Chem 282(49): 35502-35509.
- Carlson, E. C., C. Y. Liu, et al. (2005). "Keratocan, a cornea-specific keratan sulfate proteoglycan, is regulated by lumican." J Biol Chem 280(27): 25541-25547.
- Carlson, E. C., Y. Sun, et al. (2010). "Regulation of corneal inflammation by neutrophil-dependent cleavage of keratan sulfate proteoglycans as a model for breakdown of the chemokine gradient." J Leukoc Biol 88(3): 517-522.
- Cartwright, G. E., J. W. Athens, et al. (1964). "THE KINETICS OF GRANULOPOIESIS IN NORMAL MAN." Blood 24: 780-803.
- Castagliuolo, I., A. C. Keates, et al. (1998). "Clostridium difficile toxin A stimulates macrophage-inflammatory protein-2 production in rat intestinal epithelial cells." J Immunol 160(12): 6039-6045.
- Chakravarti, S., T. Magnuson, et al. (1998). "Lumican regulates collagen fibril assembly: skin fragility and corneal opacity in the absence of lumican." J Cell Biol 141(5): 1277-1286.

- Chakravarti, S., W. M. Petroll, et al. (2000). "Corneal opacity in lumican-null mice: defects in collagen fibril structure and packing in the posterior stroma." Invest Ophthalmol Vis Sci 41(11): 3365-3373.
- Charukamnoetkanok, P. (2006). "Corneal stem cells: bridging the knowledge gap." Semin Ophthalmol 21(1): 1-7.
- Chavakis, T., T. Keiper, et al. (2004). "The junctional adhesion molecule-C promotes neutrophil transendothelial migration in vitro and in vivo." J Biol Chem 279(53): 55602-55608.
- Chen, L., N. Ebihara, et al. (2007). "Expression and distribution of junctional adhesion molecule-1 in the human cornea." Jpn J Ophthalmol 51(6): 405-411.
- Chinnery, H. R., E. C. Carlson, et al. (2009). "Bone marrow chimeras and c-fms conditional ablation (Mafia) mice reveal an essential role for resident myeloid cells in lipopolysaccharide/TLR4-induced corneal inflammation." J Immunol 182(5): 2738-2744.
- Chinnery, H. R., T. Humphries, et al. (2008). "Turnover of bone marrow-derived cells in the irradiated mouse cornea." Immunology 125(4): 541-548.
- Chinnery, H. R., M. J. Ruitenberg, et al. (2007). "The chemokine receptor CX3CR1 mediates homing of MHC class II-positive cells to the normal mouse corneal epithelium." Invest Ophthalmol Vis Sci 48(4): 1568-1574.
- Ciofani, M. and J. C. Zuniga-Pflucker (2010). "Determining gammadelta versus alphass T cell development." Nat Rev Immunol 10(9): 657-663.

- Collinson, J. M., S. A. Chanas, et al. (2004). "Corneal development, limbal stem cell function, and corneal epithelial cell migration in the Pax6(+/-) mouse." Invest Ophthalmol Vis Sci 45(4): 1101-1108.
- Collinson, J. M., R. E. Hill, et al. (2004). "Analysis of mouse eye development with chimeras and mosaics." Int J Dev Biol 48(8-9): 793-804.
- Comaish, I. F. and M. A. Lawless (2002). "Progressive post-LASIK keratectasia: biomechanical instability or chronic disease process?" J Cataract Refract Surg 28(12): 2206-2213.
- Coxon, A., P. Rieu, et al. (1996). "A novel role for the beta 2 integrin CD11b/CD18 in neutrophil apoptosis: a homeostatic mechanism in inflammation." Immunity 5(6): 653-666.
- Crockett-Torabi, E., B. Sulenbarger, et al. (1995). "Activation of human neutrophils through L-selectin and Mac-1 molecules." J Immunol 154(5): 2291-2302.
- Cursiefen, C., U. Schlotzer-Schrehardt, et al. (2002). "Lymphatic vessels in vascularized human corneas: immunohistochemical investigation using LYVE-1 and podoplanin." Invest Ophthalmol Vis Sci 43(7): 2127-2135.
- D'Amico, G. and K. Alitalo (2010). "Inside bloody lymphatics." Blood 116(4): 512-513.
- Daley, J. M., A. A. Thomay, et al. (2008). "Use of Ly6G-specific monoclonal antibody to deplete neutrophils in mice." J Leukoc Biol 83(1): 64-70.
- Dancey, J. T., K. A. Deubelbeiss, et al. (1976). "Neutrophil kinetics in man." J Clin Invest 58(3): 705-715.

- David-Ferreira, J. F. (1964). "The blood platelet: electron microscopic studies." Int Rev Cytol 17: 99-148.
- Davies, S. B., J. Chui, et al. (2009). "Stem cell activity in the developing human cornea." Stem Cells 27(11): 2781-2792.
- Deknuydt, F., E. Scotet, et al. (2009). "Modulation of inflammation through IL-17 production by gammadelta T cells: mandatory in the mouse, dispensable in humans?" Immunol Lett 127(1): 8-12.
- Dell'Angelica, E. C., C. Mullins, et al. (2000). "Lysosome-related organelles." FASEB J 14(10): 1265-1278.
- DelMonte, D. W. and T. Kim (2011). "Anatomy and physiology of the cornea." J Cataract Refract Surg 37(3): 588-598.
- Diacovo, T. G., S. J. Roth, et al. (1996). "Neutrophil rolling, arrest, and transmigration across activated, surface-adherent platelets via sequential action of P-selectin and the beta 2-integrin CD11b/CD18." Blood 88(1): 146-157.
- Diamond, M. S., R. Alon, et al. (1995). "Heparin is an adhesive ligand for the leukocyte integrin Mac-1 (CD11b/CD1)." J Cell Biol 130(6): 1473-1482.
- Diamond, M. S., J. Garcia-Aguilar, et al. (1993). "The I domain is a major recognition site on the leukocyte integrin Mac-1 (CD11b/CD18) for four distinct adhesion ligands." J Cell Biol 120(4): 1031-1043.
- Diamond, M. S. and T. A. Springer (1993). "A subpopulation of Mac-1 (CD11b/CD18) molecules mediates neutrophil adhesion to ICAM-1 and fibrinogen." J Cell Biol 120(2): 545-556.

- Diamond, M. S., D. E. Staunton, et al. (1990). "ICAM-1 (CD54): a counter-receptor for Mac-1 (CD11b/CD18)." J Cell Biol 111(6 Pt 2): 3129-3139.
- Diamond, M. S., D. E. Staunton, et al. (1991). "Binding of the integrin Mac-1 (CD11b/CD18) to the third immunoglobulin-like domain of ICAM-1 (CD54) and its regulation by glycosylation." Cell 65(6): 961-971.
- Dinarello, C. A. (2000). "Proinflammatory cytokines." Chest 118(2): 503-508.
- Du, Y., M. L. Funderburgh, et al. (2005). "Multipotent stem cells in human corneal stroma." Stem Cells 23(9): 1266-1275.
- Dupps, W. J., Jr. and S. E. Wilson (2006). "Biomechanics and wound healing in the cornea." Exp Eye Res 83(4): 709-720.
- Dustin, M. L., R. Rothlein, et al. (2011). "Induction by IL 1 and interferon-gamma: tissue distribution, biochemistry, and function of a natural adherence molecule (ICAM-1). J. Immunol. 1986. 137: 245-254." J Immunol 186(9): 5024-5033.
- Dustin, M. L. and T. A. Springer (1988). "Lymphocyte function-associated antigen-1 (LFA-1) interaction with intercellular adhesion molecule-1 (ICAM-1) is one of at least three mechanisms for lymphocyte adhesion to cultured endothelial cells." J Cell Biol 107(1): 321-331.
- Dyugovskaya, L. and A. Polyakov (2010). "Neutrophil apoptosis and hypoxia." Fiziol Zh 56(5): 115-124.
- Ehlers, R., V. Ustinov, et al. (2003). "Targeting platelet-leukocyte interactions: identification of the integrin Mac-1 binding site for the platelet counter receptor glycoprotein Ibalpha." J Exp Med 198(7): 1077-1088.

- El Kebir, D., L. Jozsef, et al. (2008). "Myeloperoxidase delays neutrophil apoptosis through CD11b/CD18 integrins and prolongs inflammation." Circ Res 103(4): 352-359.
- Elner, V. M., S. G. Elner, et al. (1991). "Intercellular adhesion molecule-1 in human corneal endothelium. Modulation and function." Am J Pathol 138(3): 525-536.
- Elsner, J., M. Sach, et al. (1995). "Synthesis and surface expression of ICAM-1 in polymorphonuclear neutrophilic leukocytes in normal subjects and during inflammatory disease." Immunobiology 193(5): 456-464.
- Entman, M. L., L. Michael, et al. (1991). "Inflammation in the course of early myocardial ischemia." FASEB J 5(11): 2529-2537.
- Erban, J. K. (1993). "P-selectin and wound healing." Behring Inst Mitt(92): 248-257.
- Erie, J. C., J. W. McLaren, et al. (2005). "Long-term corneal keratocyte deficits after photorefractive keratectomy and laser in situ keratomileusis." Trans Am Ophthalmol Soc 103: 56-66; discussion 67-58.
- Erie, J. C., C. B. Nau, et al. (2004). "Long-term keratocyte deficits in the corneal stroma after LASIK." Ophthalmology 111(7): 1356-1361.
- Erie, J. C., S. V. Patel, et al. (2003). "Keratocyte density in the human cornea after photorefractive keratectomy." Arch Ophthalmol 121(6): 770-776.
- Erie, J. C., S. V. Patel, et al. (2002). "Keratocyte density in keratoconus. A confocal microscopy study(a)." Am J Ophthalmol 134(5): 689-695.

- Etheredge, L., B. P. Kane, et al. (2009). "The effect of growth factor signaling on keratocytes in vitro and its relationship to the phases of stromal wound repair." Invest Ophthalmol Vis Sci 50(7): 3128-3136.
- Etzioni, A. (1994). "Adhesion molecule deficiencies and their clinical significance." Cell Adhes Commun 2(3): 257-260.
- Etzioni, A. and R. Alon (2004). "Leukocyte adhesion deficiency III: a group of integrin activation defects in hematopoietic lineage cells." Curr Opin Allergy Clin Immunol 4(6): 485-490.
- Evangelista, V., S. Manarini, et al. (1996). "Platelet/polymorphonuclear leukocyte interaction in dynamic conditions: evidence of adhesion cascade and cross talk between P-selectin and the beta 2 integrin CD11b/CD18." Blood 88(11): 4183-4194.
- Evangelista, V., S. Manarini, et al. (1999). "Platelet/polymorphonuclear leukocyte interaction: P-selectin triggers protein-tyrosine phosphorylation-dependent CD11b/CD18 adhesion: role of PSGL-1 as a signaling molecule." Blood 93(3): 876-885.
- Faurschou, M. and N. Borregaard (2003). "Neutrophil granules and secretory vesicles in inflammation." Microbes Infect 5(14): 1317-1327.
- Feng, D., J. A. Nagy, et al. (1996). "Vesiculo-vacuolar organelles and the regulation of venule permeability to macromolecules by vascular permeability factor, histamine, and serotonin." J Exp Med 183(5): 1981-1986.
- Feng, D., J. A. Nagy, et al. (1998). "Neutrophils emigrate from venules by a transendothelial cell pathway in response to FMLP." J Exp Med 187(6): 903-915.

- Feng, D., J. A. Nagy, et al. (1998). "Platelets exit venules by a transcellular pathway at sites of F-met peptide-induced acute inflammation in guinea pigs." Int Arch Allergy Immunol 116(3): 188-195.
- Fernandez, E. J. and E. Lolis (2002). "Structure, function, and inhibition of chemokines." Annu Rev Pharmacol Toxicol 42: 469-499.
- Ferraccioli, G. F. and E. Gremese (2011). "Adiposity, joint and systemic inflammation: the additional risk of having a metabolic syndrome in rheumatoid arthritis." Swiss Med Wkly 141: w13211.
- Ferraris, V. A., S. P. Ferraris, et al. (2007). "Perioperative blood transfusion and blood conservation in cardiac surgery: the Society of Thoracic Surgeons and The Society of Cardiovascular Anesthesiologists clinical practice guideline." Ann Thorac Surg 83(5 Suppl): S27-86.
- Fini, M. E. (1999). "Keratocyte and fibroblast phenotypes in the repairing cornea." Prog Retin Eye Res 18(4): 529-551.
- Firkin, B. G. (1963). "The Platelet." Australas Ann Med 12: 261-274.
- Fischer, A., B. Lisowska-Grospierre, et al. (1988). "Leukocyte adhesion deficiency: molecular basis and functional consequences." Immunodeficiency Rev 1(1): 39-54.
- Fitch, J. M., D. E. Birk, et al. (1991). "Stromal assemblies containing collagen types IV and VI and fibronectin in the developing embryonic avian cornea." Dev Biol 144(2): 379-391.
- Fittschen, C., R. T. Parmley, et al. (1988). "Morphometry of feline neutrophil granule genesis." Am J Anat 181(2): 195-202.

- Fleming, T. J., M. L. Fleming, et al. (1993). "Selective expression of Ly-6G on myeloid lineage cells in mouse bone marrow. RB6-8C5 mAb to granulocyte-differentiation antigen (Gr-1) detects members of the Ly-6 family." J Immunol 151(5): 2399-2408.
- Forrester, J. V., A. D. Dick, et al. (2008). The Eye: Basic Sciences in Practice. Philadelphia, Elsevier.
- Fullard, R. J. and C. Snyder (1990). "Protein levels in nonstimulated and stimulated tears of normal human subjects." Invest Ophthalmol Vis Sci 31(6): 1119-1126.
- Funderburgh, J. L., B. Caterson, et al. (1987). "Distribution of proteoglycans antigenically related to corneal keratan sulfate proteoglycan." J Biol Chem 262(24): 11634-11640.
- Funderburgh, J. L. and G. W. Conrad (1990). "Isoforms of corneal keratan sulfate proteoglycan." J Biol Chem 265(14): 8297-8303.
- Funderburgh, J. L., M. L. Funderburgh, et al. (1996). "Synthesis of corneal keratan sulfate proteoglycans by bovine keratocytes in vitro." J Biol Chem 271(49): 31431-31436.
- Funderburgh, J. L., N. D. Hevelone, et al. (1998). "Decorin and biglycan of normal and pathologic human corneas." Invest Ophthalmol Vis Sci 39(10): 1957-1964.
- Furie, B. and B. C. Furie (1995). "The molecular basis of platelet and endothelial cell interaction with neutrophils and monocytes: role of P-selectin and the P-selectin ligand, PSGL-1." Thromb Haemost 74(1): 224-227.

- Gagen, D., S. Laubinger, et al. (2010). "ICAM-1 mediates surface contact between neutrophils and keratocytes following corneal epithelial abrasion in the mouse." Exp Eye Res 91(5): 9.
- Gahmberg, C. G. and S. Fagerholm (2002). "Activation of leukocyte beta2-integrins." Vox Sang 83 Suppl 1: 355-358.
- Gaillard, R. C. and E. Spinedi (1998). "Sex- and stress-steroids interactions and the immune system: evidence for a neuroendocrine-immunological sexual dimorphism." Domest Anim Endocrinol 15(5): 345-352.
- Galkina, E. and K. Ley (2009). "Immune and inflammatory mechanisms of atherosclerosis (*)." Annu Rev Immunol 27: 165-197.
- Gazit, Y., A. Mory, et al. (2010). "Leukocyte adhesion deficiency type II: long-term follow-up and review of the literature." J Clin Immunol 30(2): 308-313.
- Geng, J. G., M. P. Bevilacqua, et al. (1990). "Rapid neutrophil adhesion to activated endothelium mediated by GMP-140." Nature 343(6260): 757-760.
- George, J. N. (2000). "Platelets." Lancet 355(9214): 1531-1539.
- Geremicca, W., C. Fonte, et al. "Blood components for topical use in tissue regeneration: evaluation of corneal lesions treated with platelet lysate and considerations on repair mechanisms." Blood Transfus 8(2): 107-112.
- Gibbons, C. H., B. M. Illigens, et al. (2009). "Quantification of sweat gland innervation: a clinical-pathologic correlation." Neurology 72(17): 1479-1486.

- Goldman, J. N. and G. B. Benedek (1967). "The relationship between morphology and transparency in the nonswelling corneal stroma of the shark." Invest Ophthalmol 6(6): 574-600.
- Gonzalez-Villalva, A. E., C. I. Falcon-Rodriguez, et al. "[Signaling pathways involved in megakaryopoiesis]." Gac Med Mex 146(2): 136-143.
- Gordon, M. K., J. W. Foley, et al. (1994). "Type V collagen and Bowman's membrane. Quantitation of mRNA in corneal epithelium and stroma." J Biol Chem 269(40): 24959-24966.
- Griffin, J. D., O. Spertini, et al. (1990). "Granulocyte-macrophage colony-stimulating factor and other cytokines regulate surface expression of the leukocyte adhesion molecule-1 on human neutrophils, monocytes, and their precursors." J Immunol 145(2): 576-584.
- Gronert, K., N. Maheshwari, et al. (2005). "A role for the mouse 12/15-lipoxygenase pathway in promoting epithelial wound healing and host defense." J Biol Chem 280(15): 15267-15278.
- Gu, Y. C., T. R. Bauer, Jr., et al. (2004). "The genetic immunodeficiency disease, leukocyte adhesion deficiency, in humans, dogs, cattle, and mice." Comp Med 54(4): 363-372.
- Guan, Y. F., T. A. Pritts, et al. (2010). "Ischemic post-conditioning to counteract intestinal ischemia/reperfusion injury." World J Gastrointest Pathophysiol 1(4): 137-143.
- Guyer, D. A., K. L. Moore, et al. (1996). "P-selectin glycoprotein ligand-1 (PSGL-1) is a ligand for L-selectin in neutrophil aggregation." Blood 88(7): 2415-2421.

- Hamann, S. (2002). "Molecular mechanisms of water transport in the eye." Int Rev Cytol 215: 395-431.
- Hamrah, P. and M. R. Dana (2007). "Corneal antigen-presenting cells." Chem Immunol Allergy 92: 58-70.
- Hamrah, P., S. O. Huq, et al. (2003). "Corneal immunity is mediated by heterogeneous population of antigen-presenting cells." J Leukoc Biol 74(2): 172-178.
- Hamrah, P., Y. Liu, et al. (2003). "Alterations in corneal stromal dendritic cell phenotype and distribution in inflammation." Arch Ophthalmol 121(8): 1132-1140.
- Hamrah, P., Y. Liu, et al. (2003). "The corneal stroma is endowed with a significant number of resident dendritic cells." Invest Ophthalmol Vis Sci 44(2): 581-589.
- Hamrah, P., Q. Zhang, et al. (2002). "Novel characterization of MHC class II-negative population of resident corneal Langerhans cell-type dendritic cells." Invest Ophthalmol Vis Sci 43(3): 639-646.
- Hanlon, S. (2011). "Assessment of postnatal corneal development in the C57BL/6 mouse using spectral domain optical coherence tomography and microwave-assisted histology." Exp Eye Res In Press.
- Hanlon, S. D., N. B. Patel, et al. (2011). "Assessment of postnatal corneal development in the C57BL/6 mouse using spectral domain optical coherence tomography and microwave-assisted histology." Exp Eye Res.
- Harrison, P. and E. M. Cramer (1993). "Platelet alpha-granules." Blood Rev 7(1): 52-62.
- Hartwig, J. and J. Italiano, Jr. (2003). "The birth of the platelet." J Thromb Haemost 1(7): 1580-1586.

- Hassell, J. R. and D. E. Birk "The molecular basis of corneal transparency." Exp Eye Res 91(3): 326-335.
- Hattori, T., S. K. Chauhan, et al. (2011). "Characterization of langerin-expressing dendritic cell subsets in the normal cornea." Invest Ophthalmol Vis Sci 52(7): 4598-4604.
- Hay, E. D. (1980). "Development of the vertebrate cornea." Int Rev Cytol 63: 263-322.
- Hayashi, Y., M. K. Call, et al. (2010). "Lumican is required for neutrophil extravasation following corneal injury and wound healing." J Cell Sci 123(Pt 17): 2987-2995.
- Hayday, A. and R. Tigelaar (2003). "Immunoregulation in the tissues by gammadelta T cells." Nat Rev Immunol 3(3): 233-242.
- Haynes, R. J., P. J. Tighe, et al. (1999). "Antimicrobial defensin peptides of the human ocular surface." Br J Ophthalmol 83(6): 737-741.
- Helena, M. C., F. Baerveldt, et al. (1998). "Keratocyte apoptosis after corneal surgery." Invest Ophthalmol Vis Sci 39(2): 276-283.
- Helmer, K. S., Y. Cui, et al. (2003). "Ketamine/xylazine attenuates LPS-induced iNOS expression in various rat tissues." J Surg Res 112(1): 70-78.
- Helmus, Y., J. Denecke, et al. (2006). "Leukocyte adhesion deficiency II patients with a dual defect of the GDP-fucose transporter." Blood 107(10): 3959-3966.
- Hindman, H. B., J. N. Swanton, et al. (2010). "Differences in the TGF- β 1-induced profibrotic response of anterior and posterior corneal keratocytes in vitro." Invest Ophthalmol Vis Sci 51(4): 1935-1942.

- Hoang, M. V., J. A. Nagy, et al. (2011). "Active Rac1 improves pathologic VEGF neovessel architecture and reduces vascular leak: mechanistic similarities with angiopoietin-1." Blood 117(5): 1751-1760.
- Hobden, J. A. (2003). "Intercellular adhesion molecule-2 (ICAM-2) and *Pseudomonas aeruginosa* ocular infection." DNA Cell Biol 22(10): 649-655.
- Hobden, J. A., S. Masinick-McClellan, et al. (1999). "*Pseudomonas aeruginosa* keratitis in knockout mice deficient in intercellular adhesion molecule 1." Infect Immun 67(2): 972-975.
- Hobden, J. A., S. A. Masinick, et al. (1995). "Aged mice fail to upregulate ICAM-1 after *Pseudomonas aeruginosa* corneal infection." Invest Ophthalmol Vis Sci 36(6): 1107-1114.
- Hodge, C., M. Lawless, et al. (2011). "Keratectasia following LASIK in a patient with uncomplicated PRK in the fellow eye." J Cataract Refract Surg 37(3): 603-607.
- Holan, V., K. Pokorna, et al. (2010). "Immunoregulatory properties of mouse limbal stem cells." J Immunol 184(4): 2124-2129.
- Hos, D., B. Bachmann, et al. (2008). "Age-related changes in murine limbal lymphatic vessels and corneal lymphangiogenesis." Exp Eye Res 87(5): 427-432.
- Howard, C. and M. Reed (1998). Unbiased Stereology-Three-Dimensional Measurements in Microscopy. New York, Springer-Verlag.
- Huang, C. and T. A. Springer (1995). "A binding interface on the I domain of lymphocyte function-associated antigen-1 (LFA-1) required for specific interaction with intercellular adhesion molecule 1 (ICAM-1)." J Biol Chem 270(32): 19008-19016.

- Hubbard, A. K. and R. Rothlein (2000). "Intercellular adhesion molecule-1 (ICAM-1) expression and cell signaling cascades." Free Radic Biol Med 28(9): 1379-1386.
- Huber, S. A. (2000). "T cells expressing the gamma delta T cell receptor induce apoptosis in cardiac myocytes." Cardiovasc Res 45(3): 579-587.
- Hudson, B. G., S. T. Reeders, et al. (1993). "Type IV collagen: structure, gene organization, and role in human diseases. Molecular basis of Goodpasture and Alport syndromes and diffuse leiomyomatosis." J Biol Chem 268(35): 26033-26036.
- Ihanamaki, T., L. J. Pelliniemi, et al. (2004). "Collagens and collagen-related matrix components in the human and mouse eye." Prog Retin Eye Res 23(4): 403-434.
- Ikeda, H., T. Ueyama, et al. (1999). "Adhesive interaction between P-selectin and sialyl Lewis(x) plays an important role in recurrent coronary arterial thrombosis in dogs." Arterioscler Thromb Vasc Biol 19(4): 1083-1090.
- Imanishi, J., K. Kamiyama, et al. (2000). "Growth factors: importance in wound healing and maintenance of transparency of the cornea." Prog Retin Eye Res 19(1): 113-129.
- Ishihara, A., Y. Hou, et al. (1987). "The Thy-1 antigen exhibits rapid lateral diffusion in the plasma membrane of rodent lymphoid cells and fibroblasts." Proc Natl Acad Sci U S A 84(5): 1290-1293.
- Itohara, S., P. Mombaerts, et al. (1993). "T cell receptor delta gene mutant mice: independent generation of alpha beta T cells and programmed rearrangements of gamma delta TCR genes." Cell 72(3): 337-348.

- Ivarsen, A., T. Laurberg, et al. (2004). "Role of keratocyte loss on corneal wound repair after LASIK." Invest Ophthalmol Vis Sci 45(10): 3499-3506.
- Jacobs, J. M. and M. J. Taravella (2002). "Incidence of intraoperative flap complications in laser in situ keratomileusis." J Cataract Refract Surg 28(1): 23-28.
- Jaeschke, H. and C. W. Smith (1997). "Cell adhesion and migration. III. Leukocyte adhesion and transmigration in the liver vasculature." Am J Physiol 273(6 Pt 1): G1169-1173.
- Javadi, M. A. and S. Feizi (2010). "Deep anterior lamellar keratoplasty using the big-bubble technique for keratectasia after laser in situ keratomileusis." J Cataract Refract Surg 36(7): 1156-1160.
- Jester, J. V. (2008). "Corneal crystallins and the development of cellular transparency." Semin Cell Dev Biol 19(2): 82-93.
- Jester, J. V., P. A. Barry, et al. (1994). "Corneal keratocytes: in situ and in vitro organization of cytoskeletal contractile proteins." Invest Ophthalmol Vis Sci 35(2): 730-743.
- Jester, J. V., A. Budge, et al. (2005). "Corneal keratocytes: phenotypic and species differences in abundant protein expression and in vitro light-scattering." Invest Ophthalmol Vis Sci 46(7): 2369-2378.
- Jester, J. V. and J. Ho-Chang (2003). "Modulation of cultured corneal keratocyte phenotype by growth factors/cytokines control in vitro contractility and extracellular matrix contraction." Exp Eye Res 77(5): 581-592.

- Jester, J. V., T. Moller-Pedersen, et al. (1999). "The cellular basis of corneal transparency: evidence for 'corneal crystallins'." J Cell Sci 112 (Pt 5): 613-622.
- Jester, J. V., W. M. Petroll, et al. (1995). "Expression of alpha-smooth muscle (alpha-SM) actin during corneal stromal wound healing." Invest Ophthalmol Vis Sci 36(5): 809-819.
- Jones, B. R. (1958). "The clinical features of viral keratitis and a concept of their pathogenesis." Proc R Soc Med 51(11): 917-924.
- Jones, D. A., O. Abbassi, et al. (1993). "P-selectin mediates neutrophil rolling on histamine-stimulated endothelial cells." Biophys J 65(4): 1560-1569.
- Kainoh, M., Y. Ikeda, et al. (1992). "Glycoprotein Ia/IIa-mediated activation-dependent platelet adhesion to collagen." Thromb Res 65(2): 165-176.
- Kamath, S., A. D. Blann, et al. (2001). "Platelet activation: assessment and quantification." Eur Heart J 22(17): 1561-1571.
- Kamiyama, K., I. Iguchi, et al. (1998). "Effects of PDGF on the migration of rabbit corneal fibroblasts and epithelial cells." Cornea 17(3): 315-325.
- Kanellopoulos, A. J. and P. S. Binder (2010). "Management of Corneal Ectasia After LASIK with Combined, Same-Day, Topography-Guided Partial Transepithelial PRK and Collagen Cross-Linking: The Athens Protocol." J Refract Surg: 1-9.
- Kang, L. I., Y. Wang, et al. (2007). "Deletion of JAM-A causes morphological defects in the corneal epithelium." Int J Biochem Cell Biol 39(3): 576-585.

- Kanwar, S., C. W. Smith, et al. (1998). "An absolute requirement for P-selectin in ischemia/reperfusion-induced leukocyte recruitment in cremaster muscle." Microcirculation 5(4): 281-287.
- Kaur, H., S. S. Chaurasia, et al. (2009). "Corneal stroma PDGF blockade and myofibroblast development." Exp Eye Res 88(5): 960-965.
- Kawakita, T., E. M. Espana, et al. (2005). "Keratocan expression of murine keratocytes is maintained on amniotic membrane by down-regulating transforming growth factor-beta signaling." J Biol Chem 280(29): 27085-27092.
- Kawakita, T., E. M. Espana, et al. (2006). "Preservation and expansion of the primate keratocyte phenotype by downregulating TGF-beta signaling in a low-calcium, serum-free medium." Invest Ophthalmol Vis Sci 47(5): 1918-1927.
- Kebir, H., K. Kreymborg, et al. (2007). "Human TH17 lymphocytes promote blood-brain barrier disruption and central nervous system inflammation." Nat Med 13(10): 1173-1175.
- Kehlen, A., K. Thiele, et al. (2002). "Expression, modulation and signalling of IL-17 receptor in fibroblast-like synoviocytes of patients with rheumatoid arthritis." Clin Exp Immunol 127(3): 539-546.
- Kempen, J. H., P. Mitchell, et al. (2004). "The prevalence of refractive errors among adults in the United States, Western Europe, and Australia." Arch Ophthalmol 122(4): 495-505.
- Kennedy, R. H., W. M. Bourne, et al. (1986). "A 48-year clinical and epidemiologic study of keratoconus." Am J Ophthalmol 101(3): 267-273.

- Khachikian, S. S. and M. W. Belin (2010). "Bilateral corneal ectasia after laser in situ keratomileusis." J Cataract Refract Surg 36(11): 2015; author reply 2015-2016.
- Khoshnoodi, J., V. Pedchenko, et al. (2008). "Mammalian collagen IV." Microsc Res Tech 71(5): 357-370.
- Kim, H., J. S. Choi, et al. (2006). "Corneal ectasia after PRK: clinicopathologic case report." Cornea 25(7): 845-848.
- Kim, W. J., Y. S. Rabinowitz, et al. (1999). "Keratocyte apoptosis associated with keratoconus." Exp Eye Res 69(5): 475-481.
- Kim, W. J., S. Shah, et al. (1998). "Differences in keratocyte apoptosis following transepithelial and laser-scrape photorefractive keratectomy in rabbits." J Refract Surg 14(5): 526-533.
- Kishimoto, T. K., M. A. Jutila, et al. (1989). "Neutrophil Mac-1 and MEL-14 adhesion proteins inversely regulated by chemotactic factors." Science 245(4923): 1238-1241.
- Klintworth, G. K. (2003). "The molecular genetics of the corneal dystrophies--current status." Front Biosci 8: d687-713.
- Klopfer, J., J. M. Tielsch, et al. (1992). "Ocular trauma in the United States. Eye injuries resulting in hospitalization, 1984 through 1987." Arch Ophthalmol 110(6): 838-842.
- Knupp, C., C. Pinali, et al. (2009). "The architecture of the cornea and structural basis of its transparency." Adv Protein Chem Struct Biol 78: 25-49.

- Knust, J., M. Ochs, et al. (2009). "Stereological estimates of alveolar number and size and capillary length and surface area in mice lungs." Anat Rec (Hoboken) 292(1): 113-122.
- Koedam, J. A., E. M. Cramer, et al. (1992). "P-selectin, a granule membrane protein of platelets and endothelial cells, follows the regulated secretory pathway in AtT-20 cells." J Cell Biol 116(3): 617-625.
- Kong, Q., R. J. Majeska, et al. (2011). "Migration of connective tissue-derived cells is mediated by ultra-low concentration gradient fields of EGF." Exp Cell Res 317(11): 1491-1502.
- Krensky, A. M., F. Sanchez-Madrid, et al. (1983). "The functional significance, distribution, and structure of LFA-1, LFA-2, and LFA-3: cell surface antigens associated with CTL-target interactions." J Immunol 131(2): 611-616.
- Krueger, A., S. Baumann, et al. (2001). "FLICE-inhibitory proteins: regulators of death receptor-mediated apoptosis." Mol Cell Biol 21(24): 8247-8254.
- Kuang, K., M. Yiming, et al. (2004). "Fluid transport across cultured layers of corneal endothelium from aquaporin-1 null mice." Exp Eye Res 78(4): 791-798.
- Kucik, D. F. (2002). "Rearrangement of integrins in avidity regulation by leukocytes." Immunol Res 26(1-3): 199-206.
- Kucumen, R. B., N. M. Yenerel, et al. (2008). "Penetrating keratoplasty for corneal ectasia after laser in situ keratomileusis." Eur J Ophthalmol 18(5): 695-702.

- Kumagai, N., K. Fukuda, et al. (2003). "Expression of functional ICAM-1 on cultured human keratocytes induced by tumor necrosis factor-alpha." Jpn J Ophthalmol 47(2): 134-141.
- Kuo, I. C. (2011). "Trends in refractive surgery at an academic center: 2007-2009." BMC Ophthalmol 11(1): 11.
- Kymionis, G. D., D. M. Portaliou, et al. (2011). "Management of post laser in situ keratomileusis ectasia with simultaneous topography guided photorefractive keratectomy and collagen cross-linking." Open Ophthalmol J 5: 11-13.
- Laing, K. J. and C. J. Secombes (2004). "Chemokines." Dev Comp Immunol 28(5): 443-460.
- Lakshman, N., A. Kim, et al. (2010). "Characterization of corneal keratocyte morphology and mechanical activity within 3-D collagen matrices." Exp Eye Res 90(2): 350-359.
- Lam, F. W., A. R. Burns, et al. (2011). "Platelets enhance neutrophil transendothelial migration via P-selectin glycoprotein ligand-1." Am J Physiol Heart Circ Physiol 300(2): H468-475.
- Langer, H. F. and T. Chavakis (2009). "Leukocyte-endothelial interactions in inflammation." J Cell Mol Med 13(7): 1211-1220.
- Lanier, L. L. and A. Weiss (1986). "Presence of Ti (WT31) negative T lymphocytes in normal blood and thymus." Nature 324(6094): 268-270.

- Larsen, E., A. Celi, et al. (1989). "PADGEM protein: a receptor that mediates the interaction of activated platelets with neutrophils and monocytes." Cell 59(2): 305-312.
- Lau, S. K., P. G. Chu, et al. (2008). "Immunohistochemical expression of Langerin in Langerhans cell histiocytosis and non-Langerhans cell histiocytic disorders." Am J Surg Pathol 32(4): 615-619.
- Laurenzi, M. A., M. A. Persson, et al. (1990). "The neuropeptide substance P stimulates production of interleukin 1 in human blood monocytes: activated cells are preferentially influenced by the neuropeptide." Scand J Immunol 31(4): 529-533.
- Le Floch, J. P., P. Escuyer, et al. (1990). "Blood glucose area under the curve. Methodological aspects." Diabetes Care 13(2): 172-175.
- Leccisotti, A. (2007). "Corneal ectasia after photorefractive keratectomy." Graefes Arch Clin Exp Ophthalmol 245(6): 869-875.
- Lema, I., J. A. Duran, et al. (2008). "Inflammatory response to contact lenses in patients with keratoconus compared with myopic subjects." Cornea 27(7): 758-763.
- Lema, I., T. Sobrino, et al. (2009). "Subclinical keratoconus and inflammatory molecules from tears." Br J Ophthalmol 93(6): 820-824.
- Lemp, M. A. (2008). "Advances in understanding and managing dry eye disease." Am J Ophthalmol 146(3): 350-356.
- Levin, M. H. and A. S. Verkman (2006). "Aquaporin-3-dependent cell migration and proliferation during corneal re-epithelialization." Invest Ophthalmol Vis Sci 47(10): 4365-4372.

- Ley, K. (1996). "Molecular mechanisms of leukocyte recruitment in the inflammatory process." Cardiovasc Res 32(4): 733-742.
- Ley, K. (2001). "Pathways and bottlenecks in the web of inflammatory adhesion molecules and chemoattractants." Immunol Res 24(1): 87-95.
- Ley, K., D. C. Bullard, et al. (1995). "Sequential contribution of L- and P-selectin to leukocyte rolling in vivo." J Exp Med 181(2): 669-675.
- Li, C. Y., T. C. Chou, et al. (1997). "Ketamine inhibits nitric oxide synthase in lipopolysaccharide-treated rat alveolar macrophages." Can J Anaesth 44(9): 989-995.
- Li, Z., A. R. Burns, et al. (2011). "CCL20, $\gamma\delta$ T cells, and IL-22 in corneal epithelial healing." FASEB J.
- Li, Z., A. R. Burns, et al. (2011). "IL-17 and VEGF are necessary for efficient corneal nerve regeneration." Am J Pathol 178(3): 1106-1116.
- Li, Z., A. R. Burns, et al. (2007). "gamma delta T cells are necessary for platelet and neutrophil accumulation in limbal vessels and efficient epithelial repair after corneal abrasion." Am J Pathol 171(3): 838-845.
- Li, Z., A. R. Burns, et al. (2006a). "Two waves of neutrophil emigration in response to corneal epithelial abrasion: distinct adhesion molecule requirements." Invest Ophthalmol Vis Sci 47(5): 1947-1955.
- Li, Z., A. R. Burns, et al. (2006b). "Lymphocyte function-associated antigen-1-dependent inhibition of corneal wound healing." Am J Pathol 169(5): 1590-1600.

- Li, Z., R. E. Rumbaut, et al. (2006c). "Platelet response to corneal abrasion is necessary for acute inflammation and efficient re-epithelialization." Invest Ophthalmol Vis Sci 47(11): 4794-4802.
- Liang, H., F. Brignole-Baudouin, et al. (2007). "LPS-stimulated inflammation and apoptosis in corneal injury models." Mol Vis 13: 1169-1180.
- Liang, S. C., C. Nickerson-Nutter, et al. (2010). "IL-22 induces an acute-phase response." J Immunol 185(9): 5531-5538.
- Liang, S. C., X. Y. Tan, et al. (2006). "Interleukin (IL)-22 and IL-17 are coexpressed by Th17 cells and cooperatively enhance expression of antimicrobial peptides." J Exp Med 203(10): 2271-2279.
- Lindstrom, R. L., D. R. Hardten, et al. (1997). "Laser In Situ keratomileusis (LASIK) for the treatment of low moderate, and high myopia." Trans Am Ophthalmol Soc 95: 285-296; discussion 296-306.
- Lindstrom, R. L., N. A. Sher, et al. (1991). "Use of the 193-NM excimer laser for myopic photorefractive keratectomy in sighted eyes: a multicenter study." Trans Am Ophthalmol Soc 89: 155-172; discussion 172-182.
- Liu, H., J. Zhang, et al. (2010). "Cell therapy of congenital corneal diseases with umbilical mesenchymal stem cells: lumican null mice." PLoS One 5(5): e10707.
- Livak, F., M. Tourigny, et al. (1999). "Characterization of TCR gene rearrangements during adult murine T cell development." J Immunol 162(5): 2575-2580.

- Ljubimov, A. V., R. E. Burgeson, et al. (1995). "Human corneal basement membrane heterogeneity: topographical differences in the expression of type IV collagen and laminin isoforms." Lab Invest 72(4): 461-473.
- Lynam, E., L. A. Sklar, et al. (1998). "Beta2-integrins mediate stable adhesion in collisional interactions between neutrophils and ICAM-1-expressing cells." J Leukoc Biol 64(5): 622-630.
- Ma, S. D., C. A. Lancto, et al. (2010). "Expression and regulation of IL-22 by bovine peripheral blood gamma/delta T cells." Gene 451(1-2): 6-14.
- Ma, Y. Q., E. F. Plow, et al. (2004). "P-selectin binding to P-selectin glycoprotein ligand-1 induces an intermediate state of alphaMbeta2 activation and acts cooperatively with extracellular stimuli to support maximal adhesion of human neutrophils." Blood 104(8): 2549-2556.
- Macleod, A. S. and W. L. Havran (2011). "Functions of skin-resident gammadelta T cells." Cell Mol Life Sci.
- Mahon, G. J., H. R. Anderson, et al. (2004). "Chloroquine causes lysosomal dysfunction in neural retina and RPE: implications for retinopathy." Curr Eye Res 28(4): 277-284.
- Maione, F., C. Cicala, et al. (2011). "IL-17A increases ADP-induced platelet aggregation." Biochem Biophys Res Commun 408(4): 658-662.
- Mandi, Y., Z. Nagy, et al. (1997). "Effects of tumor necrosis factor and pentoxifylline on ICAM-1 expression on human polymorphonuclear granulocytes." Int Arch Allergy Immunol 114(4): 329-335.

- Massberg, S., G. Enders, et al. (1998). "Platelet-endothelial cell interactions during ischemia/reperfusion: the role of P-selectin." Blood 92(2): 507-515.
- Matsuo, R., N. Ohkohchi, et al. (2008). "Platelets Strongly Induce Hepatocyte Proliferation with IGF-1 and HGF In Vitro." J Surg Res 145(2): 279-286.
- Maurice, D. M. (1970). "The transparency of the corneal stroma." Vision Res 10(1): 107-108.
- Mayer, W. J., U. M. Irschick, et al. (2007). "Characterization of antigen-presenting cells in fresh and cultured human corneas using novel dendritic cell markers." Invest Ophthalmol Vis Sci 48(10): 4459-4467.
- McDermott, A. M. (2004). "Defensins and other antimicrobial peptides at the ocular surface." Ocul Surf 2(4): 229-247.
- McDermott, A. M., R. L. Redfern, et al. (2003). "Defensin expression by the cornea: multiple signalling pathways mediate IL-1beta stimulation of hBD-2 expression by human corneal epithelial cells." Invest Ophthalmol Vis Sci 44(5): 1859-1865.
- McEver, R. P. (1995). "Regulation of function and expression of P-selectin." Agents Actions Suppl 47: 117-119.
- McEver, R. P., J. H. Beckstead, et al. (1989). "GMP-140, a platelet alpha-granule membrane protein, is also synthesized by vascular endothelial cells and is localized in Weibel-Palade bodies." J Clin Invest 84(1): 92-99.
- McGowan, S. L., H. F. Edelhauser, et al. (2007). "Stem cell markers in the human posterior limbus and corneal endothelium of unwounded and wounded corneas." Mol Vis 13: 1984-2000.

- McGwin, G., Jr. and C. Owsley (2005). "Incidence of emergency department-treated eye injury in the United States." Arch Ophthalmol 123(5): 662-666.
- McKenna, C. C. and P. Y. Lwigale (2011). "Innervation of the mouse cornea during development." Invest Ophthalmol Vis Sci 52(1): 30-35.
- McNicol, A. and S. J. Israels (1999). "Platelet dense granules: structure, function and implications for haemostasis." Thromb Res 95(1): 1-18.
- Meier, J. K., M. Scharl, et al. (2011). "Specific differences in migratory function of myofibroblasts isolated from Crohn's disease fistulae and strictures." Inflamm Bowel Dis 17(1): 202-212.
- Michel, R. P. and L. M. Cruz-Orive (1988). "Application of the Cavalieri principle and vertical sections method to lung: estimation of volume and pleural surface area." J Microsc 150(Pt 2): 117-136.
- Mitooka, K., M. Ramirez, et al. (2002). "Keratocyte density of central human cornea after laser in situ keratomileusis." Am J Ophthalmol 133(3): 307-314.
- Mohan, R. R., R. Gupta, et al. (2010). "Decorin transfection suppresses profibrogenic genes and myofibroblast formation in human corneal fibroblasts." Exp Eye Res 91(2): 238-245.
- Mohan, R. R., A. E. Hutcheon, et al. (2003). "Apoptosis, necrosis, proliferation, and myofibroblast generation in the stroma following LASIK and PRK." Exp Eye Res 76(1): 71-87.
- Mohan, R. R., W. J. Kim, et al. (2000). "Defective keratocyte apoptosis in response to epithelial injury in stat 1 null mice." Exp Eye Res 70(4): 485-491.

- Mohan, R. R., Q. Liang, et al. (1997). "Apoptosis in the cornea: further characterization of Fas/Fas ligand system." Exp Eye Res 65(4): 575-589.
- Mohan, R. R., J. C. Tovey, et al. (2011). "Decorin biology, expression, function and therapy in the cornea." Curr Mol Med 11(2): 110-128.
- Molesworth-Kenyon, S. J., R. Yin, et al. (2008). "IL-17 receptor signaling influences virus-induced corneal inflammation." J Leukoc Biol 83(2): 401-408.
- Montes-Mico, R., J. L. Alio, et al. (2004). "Postblink changes in total and corneal ocular aberrations." Ophthalmology 111(4): 758-767.
- Moreland, J. G., R. M. Fuhrman, et al. (2002). "CD11b and intercellular adhesion molecule-1 are involved in pulmonary neutrophil recruitment in lipopolysaccharide-induced airway disease." Am J Respir Cell Mol Biol 27(4): 474-480.
- Morris, A. P., A. Tawil, et al. (2006). "Junctional Adhesion Molecules (JAMs) are differentially expressed in fibroblasts and co-localize with ZO-1 to adherens-like junctions." Cell Commun Adhes 13(4): 233-247.
- Movahedi, M., N. Entezari, et al. (2007). "Clinical and laboratory findings in Iranian patients with leukocyte adhesion deficiency (study of 15 cases)." J Clin Immunol 27(3): 302-307.
- Muller, L. J., C. F. Marfurt, et al. (2003). "Corneal nerves: structure, contents and function." Exp Eye Res 76(5): 521-542.
- Muller, L. J., L. Pels, et al. (1996). "Ultrastructural organization of human corneal nerves." Invest Ophthalmol Vis Sci 37(4): 476-488.

- Muller, L. J., G. F. Vrensen, et al. (1997). "Architecture of human corneal nerves." Invest Ophthalmol Vis Sci 38(5): 985-994.
- Muller, W. A., S. A. Weigl, et al. (1993). "PECAM-1 is required for transendothelial migration of leukocytes." J Exp Med 178(2): 449-460.
- Nagano, T., M. Nakamura, et al. (2003). "Effects of substance P and IGF-1 in corneal epithelial barrier function and wound healing in a rat model of neurotrophic keratopathy." Invest Ophthalmol Vis Sci 44(9): 3810-3815.
- Naik-Mathuria, B., A. N. Gay, et al. (2008). "Fetal wound healing using a genetically modified murine model: the contribution of P-selectin." J Pediatr Surg 43(4): 675-682.
- Nash, G. B. (1994). "Adhesion between neutrophils and platelets: a modulator of thrombotic and inflammatory events?" Thromb Res 74 Suppl 1: S3-11.
- Ness-Schwickerath, K. J., C. Jin, et al. (2010). "Cytokine requirements for the differentiation and expansion of IL-17A- and IL-22-producing human Vgamma2Vdelta2 T cells." J Immunol 184(12): 7268-7280.
- Nieswandt, B., W. Bergmeier, et al. (2000). "Identification of critical antigen-specific mechanisms in the development of immune thrombocytopenic purpura in mice." Blood 96(7): 2520-2527.
- Nolte, D., P. Schmid, et al. (1994). "Leukocyte rolling in venules of striated muscle and skin is mediated by P-selectin, not by L-selectin." Am J Physiol 267(4 Pt 2): H1637-1642.

- Nurden, A. T. (2011). "Platelets, inflammation and tissue regeneration." Thromb Haemost 105 Suppl 1: S13-33.
- O'Brien, T. P., Q. Li, et al. (1998). "Inflammatory response in the early stages of wound healing after excimer laser keratectomy." Arch Ophthalmol 116(11): 1470-1474.
- O'Doherty, M., M. O'Keeffe, et al. (2006). "Five year follow up of laser in situ keratomileusis for all levels of myopia." Br J Ophthalmol 90(1): 20-23.
- O'Rahilly, R. (1975). "The prenatal development of the human eye." Exp Eye Res 21(2): 93-112.
- Oberyszyn, T. M., C. J. Conti, et al. (1998). "Beta2 integrin/ICAM-1 adhesion molecule interactions in cutaneous inflammation and tumor promotion." Carcinogenesis 19(3): 445-455.
- Opal, S. M. and V. A. DePalo (2000). "Anti-inflammatory cytokines." Chest 117(4): 1162-1172.
- Park, S. C. and J. H. Kim (1996). "Effect of steroids and nonsteroidal anti-inflammatory agents on stromal wound healing following excimer laser keratectomy in rabbits." Ophthalmic Surg Lasers 27(5 Suppl): S481-486.
- Parker, C. M., V. Groh, et al. (1990). "Evidence for extrathymic changes in the T cell receptor gamma/delta repertoire." J Exp Med 171(5): 1597-1612.
- Patel, S. V., J. C. Erie, et al. (2007). "Keratocyte and subbasal nerve density after penetrating keratoplasty." Trans Am Ophthalmol Soc 105: 180-189; discussion 189-190.

- Patel, S. V., J. W. McLaren, et al. (2002). "Confocal microscopy in vivo in corneas of long-term contact lens wearers." Invest Ophthalmol Vis Sci 43(4): 995-1003.
- Pavilack, M. A., V. M. Elner, et al. (1992). "Differential expression of human corneal and perilimbal ICAM-1 by inflammatory cytokines." Invest Ophthalmol Vis Sci 33(3): 564-573.
- Pearlman, E., A. Johnson, et al. (2008). "Toll-like receptors at the ocular surface." Ocul Surf 6(3): 108-116.
- Pei, Y., D. M. Sherry, et al. (2004). "Thy-1 distinguishes human corneal fibroblasts and myofibroblasts from keratocytes." Exp Eye Res 79(5): 705-712.
- Pei, Y. F. and J. A. Rhodin (1971). "Electron microscopic study of the development of the mouse corneal epithelium." Invest Ophthalmol 10(11): 811-825.
- Peinado, T. F., D. P. Pinero, et al. (2011). "Correlation of both corneal surfaces in corneal ectasia after myopic LASIK." Optom Vis Sci 88(4): E539-542.
- Peter, M. E. (2011). "Programmed cell death: Apoptosis meets necrosis." Nature 471(7338): 310-312.
- Petrescu, M. S., C. L. Larry, et al. (2007). "Neutrophil interactions with keratocytes during corneal epithelial wound healing: a role for CD18 integrins." Invest Ophthalmol Vis Sci 48(11): 5023-5029.
- Phillipson, M., B. Heit, et al. (2006). "Intraluminal crawling of neutrophils to emigration sites: a molecularly distinct process from adhesion in the recruitment cascade." J Exp Med 203(12): 2569-2575.

- Piccardoni, P., R. Sideri, et al. (2001). "Platelet/polymorphonuclear leukocyte adhesion: a new role for SRC kinases in Mac-1 adhesive function triggered by P-selectin." Blood 98(1): 108-116.
- Pillay, J., I. den Braber, et al. (2010). "In vivo labeling with $2H_2O$ reveals a human neutrophil lifespan of 5.4 days." Blood 116(4): 625-627.
- Polasek, J. (2005). "Platelet secretory granules or secretory lysosomes?" Platelets 16(8): 500-501.
- Polisetty, N., A. Fatima, et al. (2008). "Mesenchymal cells from limbal stroma of human eye." Mol Vis 14: 431-442.
- Randleman, J. B., A. I. Caster, et al. (2006). "Corneal ectasia after photorefractive keratectomy." J Cataract Refract Surg 32(8): 1395-1398.
- Randleman, J. B., B. Russell, et al. (2003). "Risk factors and prognosis for corneal ectasia after LASIK." Ophthalmology 110(2): 267-275.
- Rask, R., P. K. Jensen, et al. (1995). "Healing velocity of corneal epithelium evaluated by computer. The effect of topical steroid." Acta Ophthalmol Scand 73(2): 162-165.
- Ravari, H., D. Hamidi-Almadari, et al. (2011). "Treatment of non-healing wounds with autologous bone marrow cells, platelets, fibrin glue and collagen matrix." Cytotherapy.
- Redfern, R. L., R. Y. Reins, et al. (2011). "Toll-like receptor activation modulates antimicrobial peptide expression by ocular surface cells." Exp Eye Res 92(3): 209-220.

- Ren, X., B. Hu, et al. "IL-22 is involved in liver regeneration after hepatectomy." Am J Physiol Gastrointest Liver Physiol 298(1): G74-80.
- Rivera, J., M. L. Lozano, et al. (2000). "Platelet GP Ib/IX/V complex: physiological role." J Physiol Biochem 56(4): 355-365.
- Rivera, J., M. L. Lozano, et al. (2009). "Platelet receptors and signaling in the dynamics of thrombus formation." Haematologica 94(5): 700-711.
- Roberts, D. D. (2011). "Activate Rac to rescue new vessels." Blood 117(5): 1444-1445.
- Robker, R. L., R. G. Collins, et al. (2004). "Leukocyte migration in adipose tissue of mice null for ICAM-1 and Mac-1 adhesion receptors." Obes Res 12(6): 936-940.
- Roebuck, K. A. and A. Finnegan (1999). "Regulation of intercellular adhesion molecule-1 (CD54) gene expression." J Leukoc Biol 66(6): 876-888.
- Roessner, K., J. Wolfe, et al. (2003). "High expression of Fas ligand by synovial fluid-derived gamma delta T cells in Lyme arthritis." J Immunol 170(5): 2702-2710.
- Rothlein, R., M. L. Dustin, et al. (1986). "A human intercellular adhesion molecule (ICAM-1) distinct from LFA-1." J Immunol 137(4): 1270-1274.
- Roussel, L., F. Houle, et al. (2010). "IL-17 promotes p38 MAPK-dependent endothelial activation enhancing neutrophil recruitment to sites of inflammation." J Immunol 184(8): 4531-4537.
- Rozman, P. and Z. Bolta (2007). "Use of platelet growth factors in treating wounds and soft-tissue injuries." Acta Dermatovenereol Alp Panonica Adriat 16(4): 156-165.

- Ruddell, A., P. Mezquita, et al. (2003). "B lymphocyte-specific c-Myc expression stimulates early and functional expansion of the vasculature and lymphatics during lymphomagenesis." Am J Pathol 163(6): 2233-2245.
- Rudner, X. L., K. A. Kernacki, et al. (2000). "Prolonged elevation of IL-1 in *Pseudomonas aeruginosa* ocular infection regulates macrophage-inflammatory protein-2 production, polymorphonuclear neutrophil persistence, and corneal perforation." J Immunol 164(12): 6576-6582.
- Ruggeri, Z. M. and G. L. Mendolicchio (2007). "Adhesion mechanisms in platelet function." Circ Res 100(12): 1673-1685.
- Rumbaut, R. E. (2005). "Platelet-microvessel interactions." Microcirculation 12(3): 233-234.
- Rumbaut, R. E., R. V. Bellera, et al. (2006). "Endotoxin enhances microvascular thrombosis in mouse cremaster venules via a TLR4-dependent, neutrophil-independent mechanism." Am J Physiol Heart Circ Physiol 290(4): H1671-1679.
- Rumbaut, R. E. and P. Thiagarajan (2010).
- Saika, S., A. Shiraishi, et al. (2000). "Role of lumican in the corneal epithelium during wound healing." J Biol Chem 275(4): 2607-2612.
- Sakula, A. (1988). "Paul Langerhans (1847-1888): a centenary tribute." J R Soc Med 81(7): 414-415.
- Sarantos, M. R., H. Zhang, et al. (2008). "Transmigration of neutrophils across inflamed endothelium is signaled through LFA-1 and Src family kinase." J Immunol 181(12): 8660-8669.

- Savige, J. A., S. H. Saverymuttu, et al. (1984). "A functional comparison of Indium-111 labelled elicited peripheral blood neutrophils and peritoneal neutrophils in the rat." Clin Exp Immunol 58(3): 737-744.
- Schallhorn, S. C., E. C. Amesbury, et al. (2006). "Avoidance, recognition, and management of LASIK complications." Am J Ophthalmol 141(4): 733-739.
- Schmitz, C. and P. R. Hof (2005). "Design-based stereology in neuroscience." Neuroscience 130(4): 813-831.
- Schönherr, E., C. Sunderkotter, et al. (2004). "Decorin deficiency leads to impaired angiogenesis in injured mouse cornea." J Vasc Res 41(6): 499-508.
- Screaton, R. A., S. Kiessling, et al. (2003). "Fas-associated death domain protein interacts with methyl-CpG binding domain protein 4: a potential link between genome surveillance and apoptosis." Proc Natl Acad Sci U S A 100(9): 5211-5216.
- Segal, B. H., D. B. Kuhns, et al. (2002). "Thioglycollate peritonitis in mice lacking C5, 5-lipoxygenase, or p47(phox): complement, leukotrienes, and reactive oxidants in acute inflammation." J Leukoc Biol 71(3): 410-416.
- Sekundo, W., K. Bonicke, et al. (2003). "Six-year follow-up of laser in situ keratomileusis for moderate and extreme myopia using a first-generation excimer laser and microkeratome." J Cataract Refract Surg 29(6): 1152-1158.
- Senzel, L., D. V. Gnatenko, et al. (2009). "The platelet proteome." Curr Opin Hematol 16(5): 329-333.

- Seo, S. K., B. M. Gebhardt, et al. (2001). "Murine keratocytes function as antigen-presenting cells." Eur J Immunol 31(11): 3318-3328.
- Servold, S. A. (1991). "Growth factor impact on wound healing." Clin Podiatr Med Surg 8(4): 937-953.
- Shah, R. A. and S. E. Wilson "Use of mitomycin-C for phototherapeutic keratectomy and photorefractive keratectomy surgery." Curr Opin Ophthalmol 21(4): 269-273.
- Sharma, G. D., J. He, et al. (2003). "p38 and ERK1/2 coordinate cellular migration and proliferation in epithelial wound healing: evidence of cross-talk activation between MAP kinase cascades." J Biol Chem 278(24): 21989-21997.
- Simon, D. I., Z. Chen, et al. (2000). "Platelet glycoprotein Iba1 is a counterreceptor for the leukocyte integrin Mac-1 (CD11b/CD18)." J Exp Med 192(2): 193-204.
- Simon, S. I., J. D. Chambers, et al. (1992). "Neutrophil aggregation is beta 2-integrin- and L-selectin-dependent in blood and isolated cells." J Immunol 149(8): 2765-2771.
- Smith, C. W. (2008). "3. Adhesion molecules and receptors." J Allergy Clin Immunol 121(2 Suppl): S375-379; quiz S414.
- Smith, C. W., M. L. Entman, et al. (1991). "Adherence of neutrophils to canine cardiac myocytes in vitro is dependent on intercellular adhesion molecule-1." J Clin Invest 88(4): 1216-1223.

- Smith, C. W., S. D. Marlin, et al. (1989). "Cooperative interactions of LFA-1 and Mac-1 with intercellular adhesion molecule-1 in facilitating adherence and transendothelial migration of human neutrophils in vitro." J Clin Invest 83(6): 2008-2017.
- Smith, C. W., R. Rothlein, et al. (1988). "Recognition of an endothelial determinant for CD 18-dependent human neutrophil adherence and transendothelial migration." J Clin Invest 82(5): 1746-1756.
- Smith, T. L. and A. S. Weyrich (2011). "Platelets as central mediators of systemic inflammatory responses." Thromb Res 127(5): 391-394.
- Smyth, S. S., R. P. McEver, et al. (2009). "Platelet functions beyond hemostasis." J Thromb Haemost 7(11): 1759-1766.
- Snelgrove, R. J., A. Godlee, et al. (2011). "Airway immune homeostasis and implications for influenza-induced inflammation." Trends Immunol.
- Solomon, K. D., L. E. Fernandez de Castro, et al. (2009). "LASIK world literature review: quality of life and patient satisfaction." Ophthalmology 116(4): 691-701.
- Song, J., Y. G. Lee, et al. (2003). "Neonatal corneal stromal development in the normal and lumican-deficient mouse." Invest Ophthalmol Vis Sci 44(2): 548-557.
- Sosnova, M., M. Bradl, et al. (2005). "CD34+ corneal stromal cells are bone marrow-derived and express hemopoietic stem cell markers." Stem Cells 23(4): 507-515.
- Spiess, B. D. (2010). "Platelet transfusions: the science behind safety, risks and appropriate applications." Best Pract Res Clin Anaesthesiol 24(1): 65-83.

- Springer, T. A. (1990). "Adhesion receptors of the immune system." Nature 346(6283): 425-434.
- Srinivas, S. P. (2010). "Dynamic regulation of barrier integrity of the corneal endothelium." Optom Vis Sci 87(4): E239-254.
- Srinivasan, B. D. (1982). "Corneal reepithelialization and anti-inflammatory agents." Trans Am Ophthalmol Soc 80: 758-822.
- Srinivasan, B. D. and P. S. Kulkarni (1981). "Polymorphonuclear leukocyte response. Inhibition following corneal epithelial denudation by steroidal and nonsteroidal anti-inflammatory agents." Arch Ophthalmol 99(6): 1085-1089.
- Stagos, D., Y. Chen, et al. "Corneal aldehyde dehydrogenases: multiple functions and novel nuclear localization." Brain Res Bull 81(2-3): 211-218.
- Stellos, K. and M. Gawaz (2007). "Platelet interaction with progenitor cells: potential implications for regenerative medicine." Thromb Haemost 98(5): 922-929.
- Stenberg, P. E., R. P. McEver, et al. (1985). "A platelet alpha-granule membrane protein (GMP-140) is expressed on the plasma membrane after activation." J Cell Biol 101(3): 880-886.
- Stepp, M. A. (2006). "Corneal integrins and their functions." Exp Eye Res 83(1): 3-15.
- Stramer, B. M. and M. E. Fini (2004). "Uncoupling keratocyte loss of corneal crystallin from markers of fibrotic repair." Invest Ophthalmol Vis Sci 45(11): 4010-4015.
- Stramer, B. M., M. G. Kwok, et al. (2004). "Monoclonal antibody (3G5)-defined ganglioside: cell surface marker of corneal keratocytes." Invest Ophthalmol Vis Sci 45(3): 807-812.

- Sumagin, R. and I. H. Sarelius (2006). "TNF-alpha activation of arterioles and venules alters distribution and levels of ICAM-1 and affects leukocyte-endothelial cell interactions." Am J Physiol Heart Circ Physiol 291(5): H2116-2125.
- Suratt, B. T., S. K. Young, et al. (2001). "Neutrophil maturation and activation determine anatomic site of clearance from circulation." Am J Physiol Lung Cell Mol Physiol 281(4): L913-921.
- Sutton, G. L. and P. Kim (2010). "Laser in situ keratomileusis in 2010 - a review." Clin Experiment Ophthalmol 38(2): 192-210.
- Szerenyi, K. D., X. Wang, et al. (1994). "Keratocyte loss and repopulation of anterior corneal stroma after de-epithelialization." Arch Ophthalmol 112(7): 973-976.
- Takacs, L., E. Toth, et al. (2009). "Stem cells of the adult cornea: from cytometric markers to therapeutic applications." Cytometry A 75(1): 54-66.
- Tarabishy, A. B., B. Aldabagh, et al. (2008). "MyD88 regulation of Fusarium keratitis is dependent on TLR4 and IL-1R1 but not TLR2." J Immunol 181(1): 593-600.
- Thepaut, M., J. Valladeau, et al. (2009). "Structural studies of langerin and Birbeck granule: a macromolecular organization model." Biochemistry 48(12): 2684-2698.
- Thoft, R. A., L. A. Wiley, et al. (1989). "The multipotential cells of the limbus." Eye (Lond) 3 (Pt 2): 109-113.
- Thygeson, P. and W. H. Spencer (1973). "The changing character of infectious corneal disease: emerging opportunistic microbial forms (1928-1973)." Trans Am Ophthalmol Soc 71: 246-253.

- Tibbetts, T. A., O. M. Conneely, et al. (1999). "Progesterone via its receptor antagonizes the pro-inflammatory activity of estrogen in the mouse uterus." Biol Reprod 60(5): 1158-1165.
- Tiffany, J. M. (2008). "The normal tear film." Dev Ophthalmol 41: 1-20.
- Tran, M. T., R. N. Lausch, et al. (2000). "Substance P differentially stimulates IL-8 synthesis in human corneal epithelial cells." Invest Ophthalmol Vis Sci 41(12): 3871-3877.
- Tran, M. T., M. H. Ritchie, et al. (2000). "Calcitonin gene-related peptide induces IL-8 synthesis in human corneal epithelial cells." J Immunol 164(8): 4307-4312.
- Trifari, S. and H. Spits "IL-22-producing CD4+ T cells: middle-men between the immune system and its environment." Eur J Immunol 40(9): 2369-2371.
- Tutt, R., A. Bradley, et al. (2000). "Optical and visual impact of tear break-up in human eyes." Invest Ophthalmol Vis Sci 41(13): 4117-4123.
- Twa, M. D., J. J. Nichols, et al. (2004). "Characteristics of corneal ectasia after LASIK for myopia." Cornea 23(5): 447-457.
- Twigg, H. L., D. M. Soliman, et al. (1999). "Lymphocytic alveolitis, bronchoalveolar lavage viral load, and outcome in human immunodeficiency virus infection." Am J Respir Crit Care Med 159(5 Pt 1): 1439-1444.
- Uzel, G., D. E. Kleiner, et al. (2001). "Dysfunctional LAD-1 neutrophils and colitis." Gastroenterology 121(4): 958-964.

- Valladeau, J., O. Ravel, et al. (2000). "Langerin, a novel C-type lectin specific to Langerhans cells, is an endocytic receptor that induces the formation of Birbeck granules." Immunity 12(1): 71-81.
- van Setten, G. B., G. S. Schultz, et al. (1994). "Growth factors in human tear fluid and in lacrimal glands." Adv Exp Med Biol 350: 315-319.
- Varki, A. (1994). "Selectin ligands." Proc Natl Acad Sci U S A 91(16): 7390-7397.
- Vestweber, D. (2002). "Regulation of endothelial cell contacts during leukocyte extravasation." Curr Opin Cell Biol 14(5): 587-593.
- Vij, N., L. Roberts, et al. (2005). "Lumican regulates corneal inflammatory responses by modulating Fas-Fas ligand signaling." Invest Ophthalmol Vis Sci 46(1): 88-95.
- Walmer, D. K., M. A. Wrona, et al. (1992). "Lactoferrin expression in the mouse reproductive tract during the natural estrous cycle: correlation with circulating estradiol and progesterone." Endocrinology 131(3): 1458-1466.
- Walzog, B., K. Scharffetter-Kochanek, et al. (1999). "Impairment of neutrophil emigration in CD18-null mice." Am J Physiol 276(5 Pt 1): G1125-1130.
- Wang, J. H., D. M. Sexton, et al. (1997). "Intercellular adhesion molecule-1 (ICAM-1) is expressed on human neutrophils and is essential for neutrophil adherence and aggregation." Shock 8(5): 357-361.
- Wang, Q. and C. M. Doerschuk (2002). "The signaling pathways induced by neutrophil-endothelial cell adhesion." Antioxid Redox Signal 4(1): 39-47.

- Wang, Y., M. Sakuma, et al. (2005). "Leukocyte engagement of platelet glycoprotein Ibalphalpha via the integrin Mac-1 is critical for the biological response to vascular injury." Circulation 112(19): 2993-3000.
- Waterbury, L., E. A. Kunysz, et al. (1987). "Effects of steroidal and non-steroidal anti-inflammatory agents on corneal wound healing." J Ocul Pharmacol 3(1): 43-54.
- Watsky, M. A. (1995). "Keratocyte gap junctional communication in normal and wounded rabbit corneas and human corneas." Invest Ophthalmol Vis Sci 36(13): 2568-2576.
- Weibel, E. R. (1981). "Stereological methods in cell biology: where are we--where are we going?" J Histochem Cytochem 29(9): 1043-1052.
- Weill, F. S., E. M. Cela, et al. (2011). "Skin Exposure to Chronic But Not Acute UV Radiation Affects Peripheral T-Cell Function." J Toxicol Environ Health A 74(13): 838-847.
- Wenstrup, R. J., J. B. Florer, et al. (2004). "Type V collagen controls the initiation of collagen fibril assembly." J Biol Chem 279(51): 53331-53337.
- Whikehart, D. R., C. H. Parikh, et al. (2005). "Evidence suggesting the existence of stem cells for the human corneal endothelium." Mol Vis 11: 816-824.
- White, J. G. and R. D. Estensen (1972). "Degranulation of discoid platelets." Am J Pathol 68(2): 289-302.
- Wilson, R. W., C. M. Ballantyne, et al. (1993). "Gene targeting yields a CD18-mutant mouse for study of inflammation." J Immunol 151(3): 1571-1578.

- Wilson, S. E. (1998). "Everett Kinsey Lecture. Keratocyte apoptosis in refractive surgery." CLAO J 24(3): 181-185.
- Wilson, S. E. (2002). "Analysis of the keratocyte apoptosis, keratocyte proliferation, and myofibroblast transformation responses after photorefractive keratectomy and laser in situ keratomileusis." Trans Am Ophthalmol Soc 100: 411-433.
- Wilson, S. E., S. S. Chaurasia, et al. (2007). "Apoptosis in the initiation, modulation and termination of the corneal wound healing response." Exp Eye Res 85(3): 305-311.
- Wilson, S. E. and A. Esposito (2009). "Focus on molecules: interleukin-1: a master regulator of the corneal response to injury." Exp Eye Res 89(2): 124-125.
- Wilson, S. E., Y. G. He, et al. (1996a). "Epithelial injury induces keratocyte apoptosis: hypothesized role for the interleukin-1 system in the modulation of corneal tissue organization and wound healing." Exp Eye Res 62(4): 325-327.
- Wilson, S. E., Y. G. He, et al. (1994). "Effect of epidermal growth factor, hepatocyte growth factor, and keratinocyte growth factor, on proliferation, motility and differentiation of human corneal epithelial cells." Exp Eye Res 59(6): 665-678.
- Wilson, S. E. and J. W. Hong (2000b). "Bowman's layer structure and function: critical or dispensable to corneal function? A hypothesis." Cornea 19(4): 417-420.
- Wilson, S. E. and W. J. Kim (1998). "Keratocyte apoptosis: implications on corneal wound healing, tissue organization, and disease." Invest Ophthalmol Vis Sci 39(2): 220-226.

- Wilson, S. E., Q. Li, et al. (1996b). "The Fas-Fas ligand system and other modulators of apoptosis in the cornea." Invest Ophthalmol Vis Sci 37(8): 1582-1592.
- Wilson, S. E., R. R. Mohan, et al. (2001). "The corneal wound healing response: cytokine-mediated interaction of the epithelium, stroma, and inflammatory cells." Prog Retin Eye Res 20(5): 625-637.
- Wilson, S. E., R. R. Mohan, et al. (2002). "Apoptosis in the cornea in response to epithelial injury: significance to wound healing and dry eye." Adv Exp Med Biol 506(Pt B): 821-826.
- Wilson, S. E., R. R. Mohan, et al. (2001). "The wound healing response after laser in situ keratomileusis and photorefractive keratectomy: elusive control of biological variability and effect on custom laser vision correction." Arch Ophthalmol 119(6): 889-896.
- Wilson, S. E., R. R. Mohan, et al. (2003a). "Effect of ectopic epithelial tissue within the stroma on keratocyte apoptosis, mitosis, and myofibroblast transformation." Exp Eye Res 76(2): 193-201.
- Wilson, S. E., R. R. Mohan, et al. (2001). "The corneal wound healing response: cytokine-mediated interaction of the epithelium, stroma, and inflammatory cells." Prog Retin Eye Res 20(5): 625-637.
- Wolk, K., E. Witte, et al. "Biology of interleukin-22." Semin Immunopathol 32(1): 17-31.
- Xavier, A. M., N. Isowa, et al. (1999). "Tumor necrosis factor-alpha mediates lipopolysaccharide-induced macrophage inflammatory protein-2 release from alveolar epithelial cells. Autoregulation in host defense." Am J Respir Cell Mol Biol 21(4): 510-520.

- Xiao, Z., H. L. Goldsmith, et al. (2006). "Biomechanics of P-selectin PSGL-1 bonds: shear threshold and integrin-independent cell adhesion." Biophys J 90(6): 2221-2234.
- Xu, T., L. Zhang, et al. (2007). "P-selectin cross-links PSGL-1 and enhances neutrophil adhesion to fibrinogen and ICAM-1 in a Src kinase-dependent, but GPCR-independent mechanism." Cell Adh Migr 1(3): 115-123.
- Yang, H., P. S. Reinach, et al. (2000). "Fluid transport by cultured corneal epithelial cell layers." Br J Ophthalmol 84(2): 199-204.
- Yannariello-brown, J., C. K. Hallberg, et al. (1998). "Cytokine modulation of human corneal epithelial cell ICAM-1 (CD54) expression." Exp Eye Res 67(4): 383-393.
- Yoo, S. K. and A. Huttenlocher (2011). "Spatiotemporal photolabeling of neutrophil trafficking during inflammation in live zebrafish." J Leukoc Biol 89(5): 661-667.
- Yoshida, S., S. Shimmura, et al. (2005). "Serum-free spheroid culture of mouse corneal keratocytes." Invest Ophthalmol Vis Sci 46(5): 1653-1658.
- Yu, C. Q. and M. I. Rosenblatt (2007). "Transgenic corneal neurofluorescence in mice: a new model for in vivo investigation of nerve structure and regeneration." Invest Ophthalmol Vis Sci 48(4): 1535-1542.
- Zhao, J. and T. Nagasaki (2004). "Mechanical damage to corneal stromal cells by epithelial scraping." Cornea 23(5): 497-502.
- Zieske, J. D. (2004). "Corneal development associated with eyelid opening." Int J Dev Biol 48(8-9): 903-911.

Zieske, J. D., S. R. Guimaraes, et al. (2001). "Kinetics of keratocyte proliferation in response to epithelial debridement." Exp Eye Res 72(1): 33-39.

Zimmermann, D. R., B. Trueb, et al. (1986). "Type VI collagen is a major component of the human cornea." FEBS Lett 197(1-2): 55-58.

TABLES

Table 1: Platelet adhesion molecules and their associated ligands on PMNs and vascular endothelial cells

Platelet Adhesion Molecules	PMN Ligand	Endothelial Cell Ligand
P-selectin	PSGL-1	vWF
GP1b α	Mac-1 (CD11b)	N/A
ICAM-2	LFA-1 (CD11a)	N/A
JAM-A	JAM-A, LFA-1	JAM-A
JAM-C	Mac-1	JAM-C, JAM-B
PECAM-1 (CD31)	PECAM-1	PECAM-1

Table 2: List of primary, secondary antibodies, isotype controls used

Primary Antibody	CD Nomenclature	Clone	Host Isotype	Stock concentration (mg/ml)	Final concentration (µg/ml)	Company	Catalog Number	Application
Purified αMo E-cadherin	CD324	DECMA-1	Rt IgG1	0.5	10	eBioscience	14-3249-80	Keratocyte culturing
Purified αHu/Mo JAM-A	CD321	H202-106	Rt IgG	0.1	10	Genway	20-783-74155	Keratocyte culturing
PE αMo CD34	CD34	RAM34	Rt IgG2a	0.2	10	BD Bioscience	551387	Keratocyte culture characterization
Keratocan (serum)	N/A	N/A	Gt IgG	N/A	1:200 df	Dr. Liu, University of Miami	N/A	Keratocyte culture characterization
FITC αSmooth Muscle Actin (SMA)	N/A	1A4	Mo IgG2a	N/A	1:250 df	Sigma-Aldrich	F3777	Cultured myofibroblast characterization
PE αMo CD41	CD41	MWReg30	Rt IgG1	0.2	1	BD Bioscience	558040	Platelet marker
FITC αMo Ly6G	N/A	1A8	Rt IgG2a	0.5	2.5	BD Bioscience	551460	PMN marker
APC αMo PECAM-1	CD31	MEC 13.3	Rt IgG2a	0.2	1	BD Bioscience	551262	Limbal vessel marker
Purified ALDH3A1	N/A	H-76	Rb IgG	0.2	10	Santa Cruz Biotechnology	sc-67310	Keratocyte network marker
PE αMo ICAM-1	CD54	YN-1/1.7.4	Rt IgG2b	0.1	10	Abcam	ab25553	Keratocyte ICAM-1 marker
PE αMo Thy1.2	CD90.2	53-2.1	Rt IgG2a	0.2	1	BD Bioscience	553006	Fibroblast marker
PE αMoL-22R	N/A	496514	Rt IgG2a	N/A	1:200	R&D Systems	FAB42941 P	Keratocyte and vessel staining
PE P-selectin	CD62P	Wug.E9	Rt IgG1	N/A	1:250 df	Emfret Analytics	M130-2	Limbal vascular endothelium marker
FITC αMo β2 integrin (CD18)	CD18	C71/16	Rt IgG2a	0.5	2.5	BD Bioscience	553292	Leukocyte (β2 integrin) marker; keratocyte repopulation
FITC CD3e	CD3	145-2C11	Ar Ham IgG1	0.5	2.5	BD Bioscience	553061	T-cell marker; keratocyte repopulation
FITC CD45	CD45	30-F11	Rt IgG2b	0.5	2.5	BD Bioscience	553080	Pan leukocyte marker; keratocyte repopulation
FITC αMo γδ TCR	30C7	GL3	Ar Ham IgG2	0.5	2.5	BD Bioscience	553177	γδ T cell marker; keratocyte repopulation
FITC GR1	N/A	RB6-8C5	Rt IgG2b	0.5	2.5	BD Bioscience	553127	Mononuclear cell and PMN marker; keratocyte repopulation
Purified αMo ICAM-1	CD54	YN-1	Rt IgG	1	10	Made at Baylor College of Medicine	N/A	Functional PMN motility (blocking) assay

Purified αMo β2 integrin (CD18)	CD18	GAME46	RtIgG1	1	10	BD Bioscience	555280	Functional PMN motility (blocking) assay
FITC F4/80	N/A		MolG	N/A	1:250	Abcam	Ab60343	Macrophage/D C marker
Isotype Control	Clone	Stock concentration ((mg/ml)	Final concentration (μg/ml)	Company	Catalog Number	Application		
Rat IgG	N/A	1	10	N/A	N/A	Negative control for CD18 and ICAM-1 blocking assay		
Purified Goat IgG	N/A	27.5	10	Jackson Laboratories	005-000-003	Negative control for Keratocan		
Purified Rabbit IgG	N/A	11.3	10	Jackson Laboratories	011-000-003	Negative control for ALDH3A1		
PE Rat IgG1	R3-34	0.2	10	BD Bioscience	554685	Negative control for CD41, P-selectin		
PE Rat IgG2a	G155-178	0.2	10	BD Bioscience	553457	Negative control for CD34, Thy1.2, IL-22R		
PE Rat IgG2b	A95-1	0.2	10	BD Bioscience	553989	Negative control for (PE) ICAM-1		
FITC Rat IgG2a	R35-95	0.5	10	BD Bioscience	553929	Negative control for (FITC) CD18, Ly6G		
FITC Rat IgG2b	A95-1	0.5	10	BD Bioscience	556923	Negative control for GR-1, CD45		
FITC Mouse IgG	X39	0.1	10	BD Bioscience	349051	Negative control for α SMA		
Secondary Antibody	Stock concentration ((mg/ml)	Final concentration (μg/ml)	Company	Catalog Number	Application			
Gt α Rt IgG magnetic microbeads	N/A	1:5 df	Miltenyi Biotechnology	120-000-290	Cultured keratocyte isolation			
Gt α Rb Alexa 488	2	10	Invitrogen	A11008	Rb α ALDH3A1 2° labeling			
Dk α Gt Alexa 594	2	10	Invitrogen	A11058	Gt α Keratocan 2° labeling			

Table 3: Percent of PMN Surface in Close Contact (≤ 25 nm) with Keratocytes or Collagen in the Paralimbal Region of Injured Cornea

Genotype	Contact with Keratocytes (%)	Contact with Collagen (%)
Wild Type, n=5	39.9 \pm 3.5	51.3 \pm 3.4
ICAM-1 ^{-/-} , n=5	21.5 \pm 3.0*	59.1 \pm 2.0

*p < 0.05 compared to wild type.

Data are means \pm SEM.

Table 4: Percent of PMN Surface in Close Contact (≤ 25 nm) with Neighboring PMN(s) or Associated with Interlamellar Space (% Sv > 25 nm)

Genotype	PMN-PMN (% Sv ≤ 25 nm)	PMN-Interlamellar Space (% Sv > 25 nm)
Wild Type, n=5	0.4 \pm 0.4	8.4 \pm 2.8
ICAM-1 ^{-/-} , n=5	1.6 \pm 1.0	17.8 \pm 2.3*

*p < 0.05 compared to wild type.

Data are means \pm SEM.

Table 5: Total PMN numbers in the cornea as assessed by the area under the curve

Area under the curve is an indicator of total amount of the infiltrating PMN throughout 48 hours. (n=4 - 6, per region, per genotype)

Region	WT	ICAM-1 ^{-/-}	CD18 ^{mutant}
Limbus	588,122	885,690	434,200
Paralimbus	166,931	625,740*	149,533
Center	541,351	3,202,000*	359,911

*p < 0.05, 2-way ANOVA

Data are means ± SEM.

Table 6: Wild type anterior keratocyte network recovery

Anterior central keratocyte network surface area (SA) was significantly reduced 28 days after injury but posterior central SA recovered to baseline. Anterior and posterior central keratocyte network shape (Sv) did not differ from uninjured network Sv at 28 days post injury.

Time point	Anterior Central SA	Posterior Central SA	Anterior Central Sv	Posterior Central Sv
0 day, n=6	$2.13 \times 10^6 \pm 247553$	$1.94 \times 10^6 \pm 211149$	11.49 ± 0.68	10.19 ± 1.18
28 days, n=5	$1.41 \times 10^6 \pm 145989^*$	$1.31 \times 10^6 \pm 111311$	9.65 ± 2.08	10.70 ± 1.20

*p < 0.05, 1-way ANOVA

Data are means \pm SEM.

Table 7: Relationship between PMN infiltration, platelet accumulation, and keratocyte repopulation

Total PMN infiltration and extravascular platelet accumulation percentages are based on the assumption that WT values are normal (100%). Keratocyte repopulation percentages are based on recovery compared to the respective genotype baseline numbers. Description of keratocyte repopulation is a subjective determination based on percentage inflammatory cells infiltration versus percentage keratocyte repopulation at 4 days. This table merely summarizes the concept that enhanced inflammatory cell infiltration promotes keratocyte repopulation but it must be remembered that PMNs infiltrate in CD18^{mutant} at a later time while platelet numbers remain low, suggesting keratocyte repopulation is driven by early and enhanced platelet accumulation alone.

	WT	ICAM-1 ^{-/-}	CD18 ^{mutant}
Total PMN infiltration (L, PL, C)	100%	106%	42%
Extravascular platelet accumulation at 24h	100%	144%	2%
Keratocyte repopulation at 4d (% of baseline)	72%	100%	44%
Description of keratocyte repopulation	Incomplete	Enhanced	Depressed

FIGURES AND LEGENDS

Figure 1: Interaction between PMN CD18 and ICAM-1 (found on vascular endothelium and keratocyte)

Alpha subunits of the PMN $\beta 2$ CD18 interact with different domains of its known ligand, ICAM-1, a 5-domain transmembrane glycoprotein. CD11a/CD18 (LFA-1 or α_L) associates with domain 1 of ICAM-1 and CD11b/CD18 (Mac-1 or α_M) associates with domain 3 of ICAM-1.

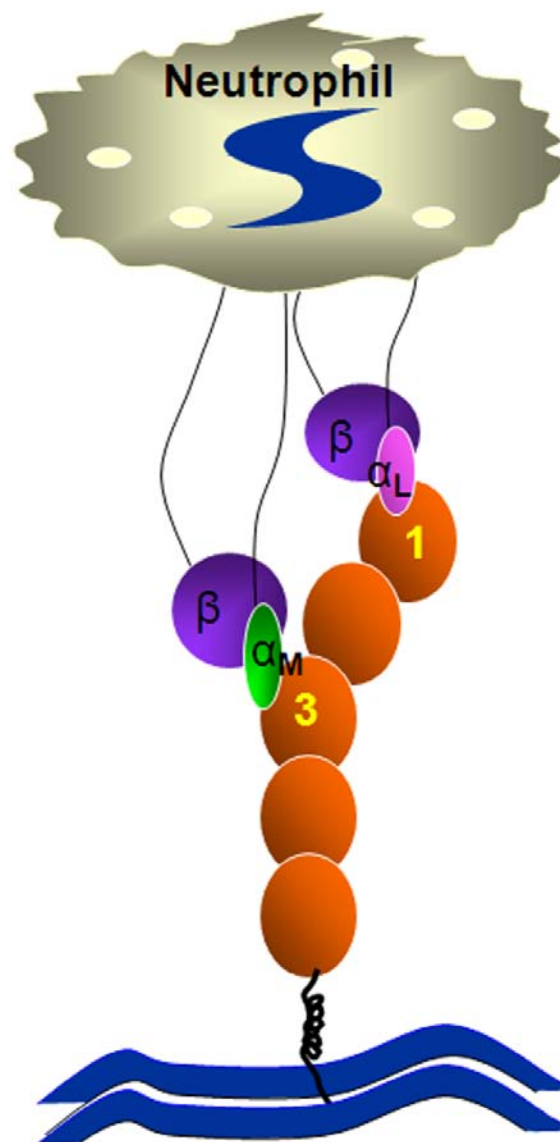


Figure 2: Diagram of the division of corneal regions

The diagram shows 9 regions of the flattened cornea, from limbus to center. Each region has a diameter of 0.4 mm, resulting in a 3.6 mm diameter in the flattened cornea. The 2mm wound region (pink) corresponds to the region where epithelium is debrided.

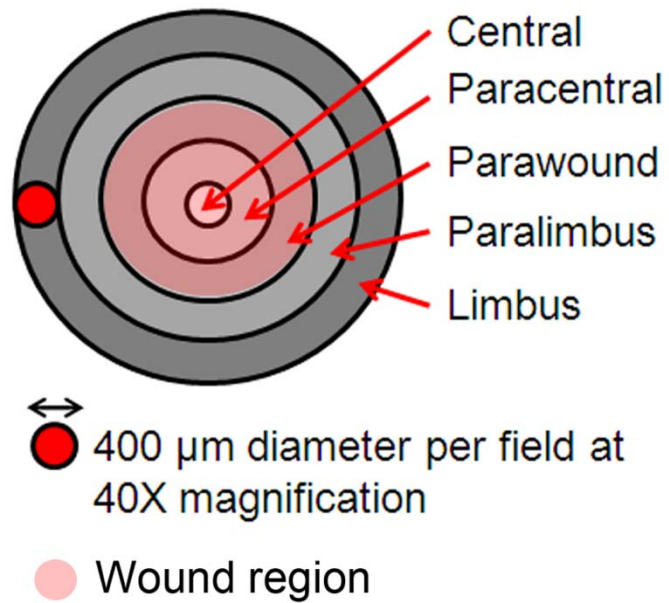


Figure 3: Eighteen hour Algerbrush injury versus Golf Club Spud injury in WT mice

PMN infiltration in WT mice 18 hours after Algerbrush injury appears feeble compared to golf club spud injured corneas at central (**A, E**), paralimbal (PL)(**B, F**), and limbal regions (**C, G**); (**A-D**, Algerbrush-induced epithelial abrasion; **E-H**, golf club spud-induced epithelial abrasion). Platelet infiltration in WT mice 18 hours after Algerbrush injury (**D**) is also visibly less than that observed in golf club spud injury (**H**). In 18 hour injured TCR $\delta^{-/-}$ mice, central (**I, M**), PL (**J, N**), and limbal (**K, O**) PMN infiltration is not different between Algerbrush and golf club spud injuries. However, clearly platelet accumulation is considerably greater in 18 hour Algerbrush-injured TCR $\delta^{-/-}$ mice (**L**) compared to 18 hour golf club spud-injured TCR $\delta^{-/-}$ mice (**P**). Scale bar = 20 μ m.

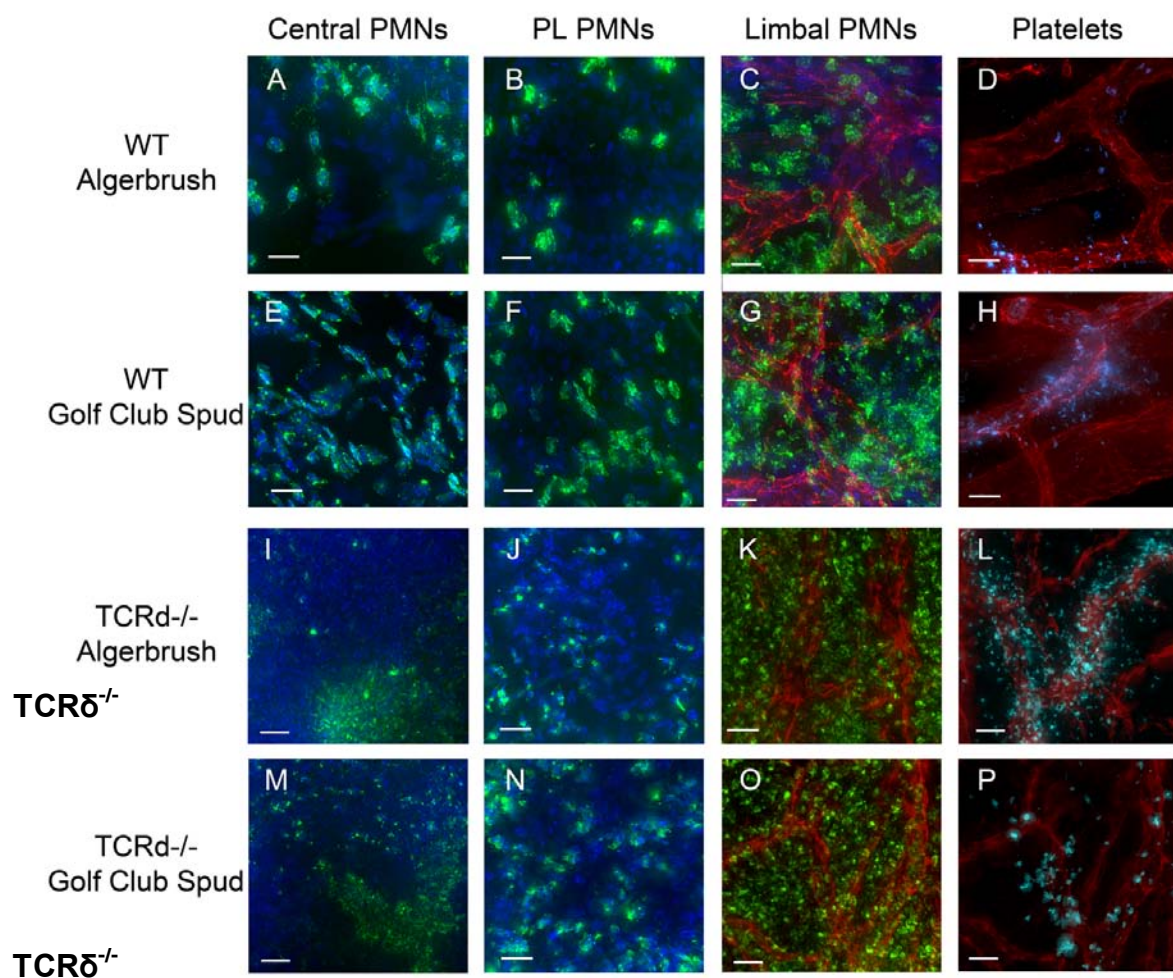


Figure 4: Mouse cultured keratocytes

Panel **A** shows cultured keratocytes 3 days after isolation (10X). Panel **B** shows the classic dendritic-like keratocyte morphology, 7 days after isolation (20X). Cultured keratocytes were used between 7-10 days after harvest.

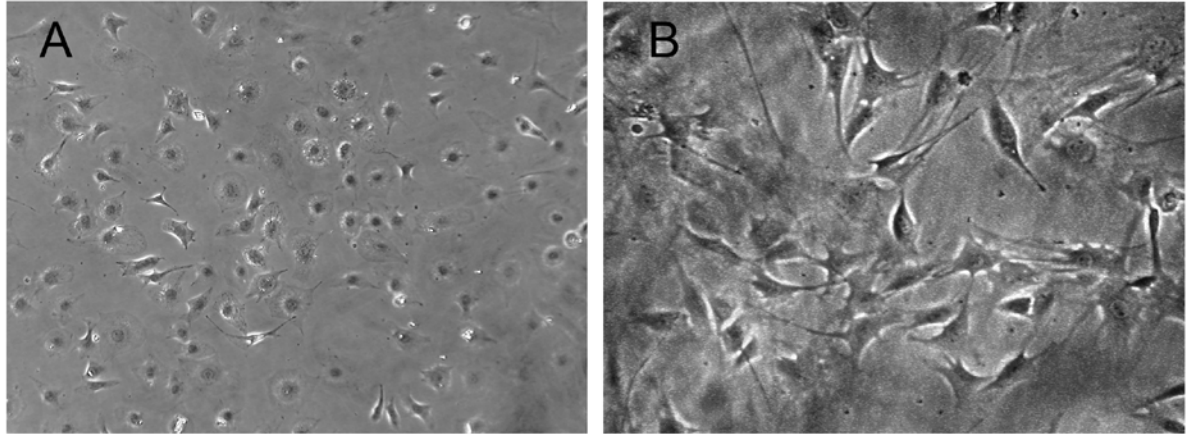


Figure 5: Tracking PMN migration over cultured mouse keratocytes

Extravasated PMN crawl along IL-1 treated keratocytes. (A) PMN motility on keratocytes prior to adding the antibody. IgG shows similar results as panel A. (B) There is a significant decrease of PMN motility 1min after adding antibody. PMNs are outlined in yellow.

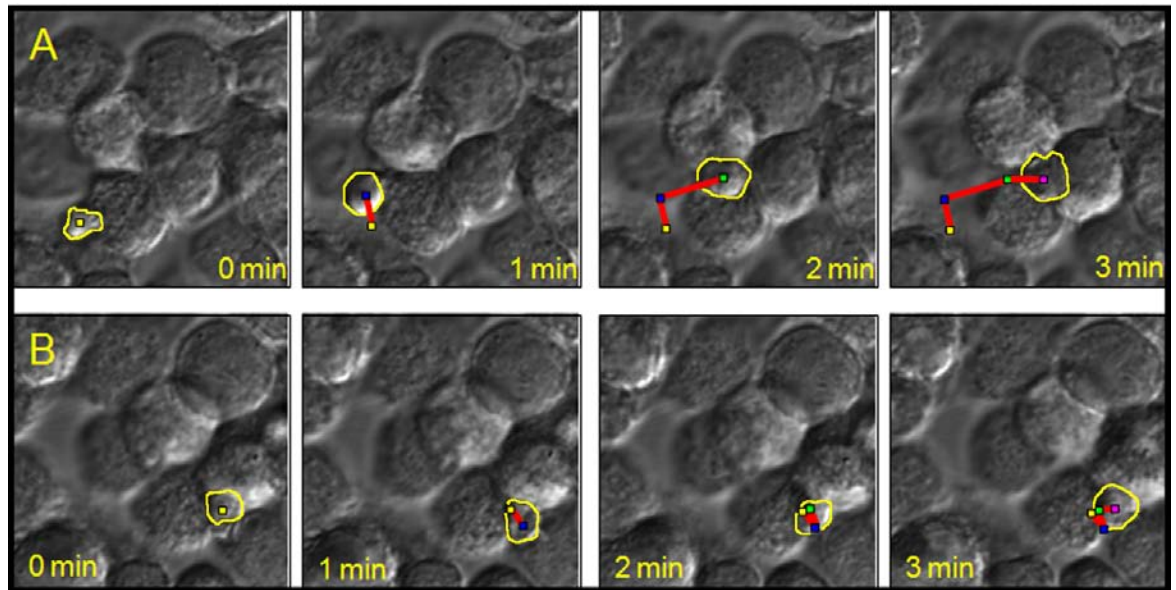


Figure 6: Morphometric number estimation grid for PMN density analyses

A 3X3 morphometric number estimation grid was used to determine PMNs/mm². Each grid square has an area of 625 μm². All PMN nuclei falling within the grid box or on the accepted line (denoted by white arrowheads) are counted and inserted into the following formula: $(n/9 * 10^6)/256$, where n equals total counted PMNs. PMNs falling outside of the grid boxes or on the forbidden lines are not included in the analyses (red asterisk).

Scale bar = 20 μm

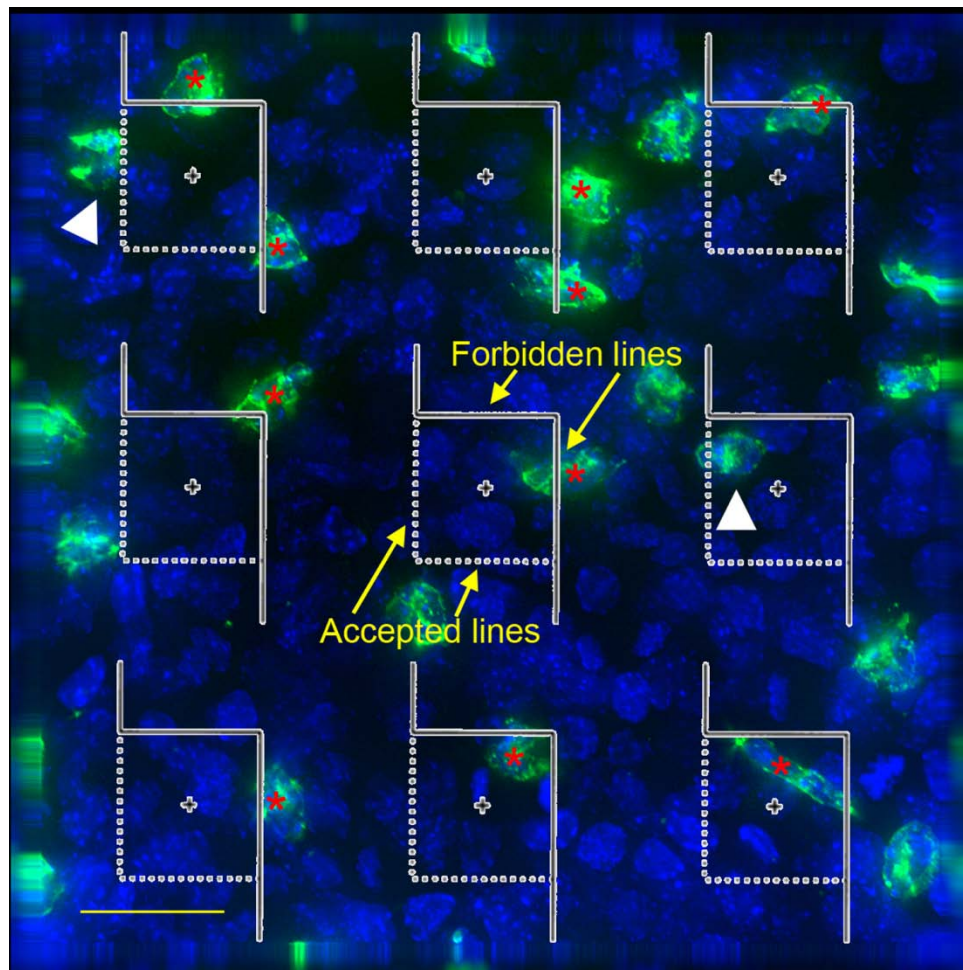


Figure 7: Morphometric number estimation grid for platelet density analyses

A 16X10-square number estimation grid is used to determine platelet density. The grid is orientated so the extending solid lines on the grid squared run perpendicular to the major axis (depicted by the white arrow) of the limbal vessels (**A**). The shaded region indicates the montage panel. Only grid squares falling completely within the montage are counted. A magnified image of this montage (**B**) shows platelets, in blue, inside and outside of vessels. Only platelets falling within the grid squares, whether inside or outside, are included in the analyses. Similar to the criterion set for PMN analyses, platelets falling on the forbidden lines are not counted while platelets falling on the accepted lines are counted. The white arrowhead indicates an example of a platelet that is counted. Platelets with a diameter less than 2 μm were not analyzed. Platelet counts (separated as inside of vessels or outside of vessels) and total grid squares falling within the area of the montage are inserted into the formula $[(\sum C / \sum S) / 3211] * 10^6$, where C is platelets counted and S is squares within the area of the montage. The constant 3211 is the area of each grid square. All calculations are expressed in platelets/ mm^2 . Scale bar = 25 μm .

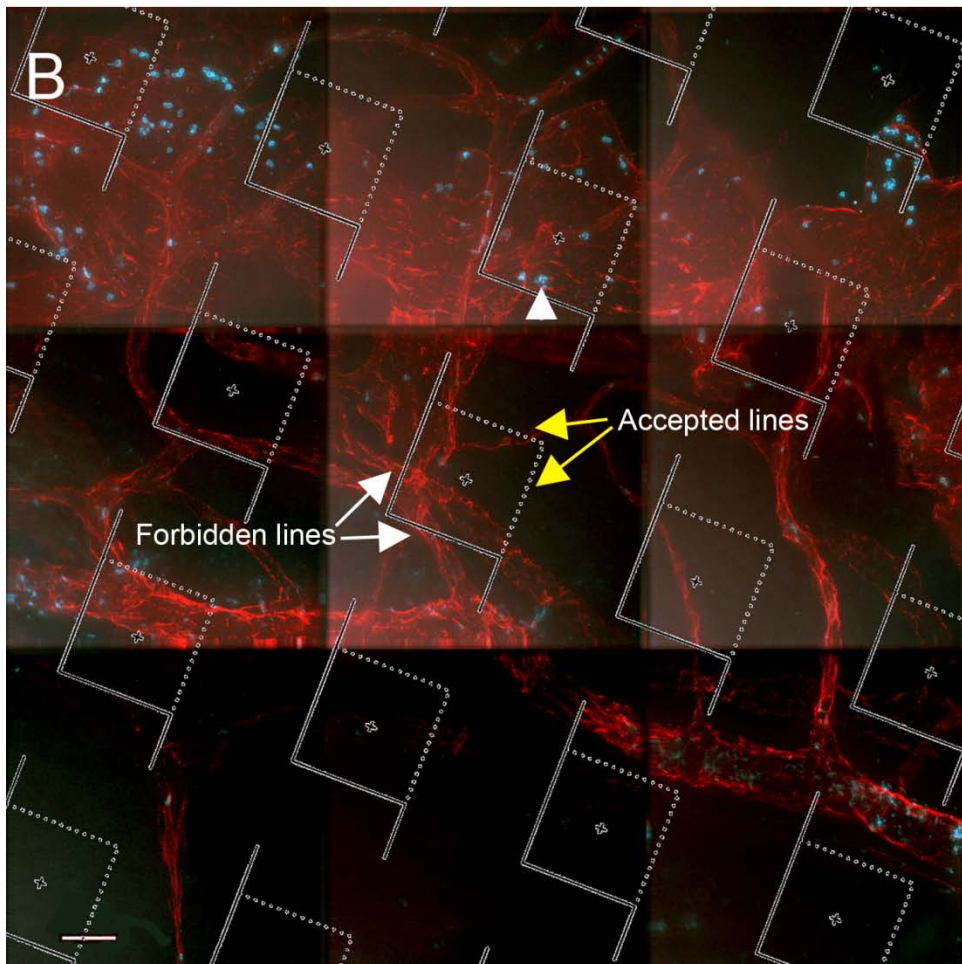
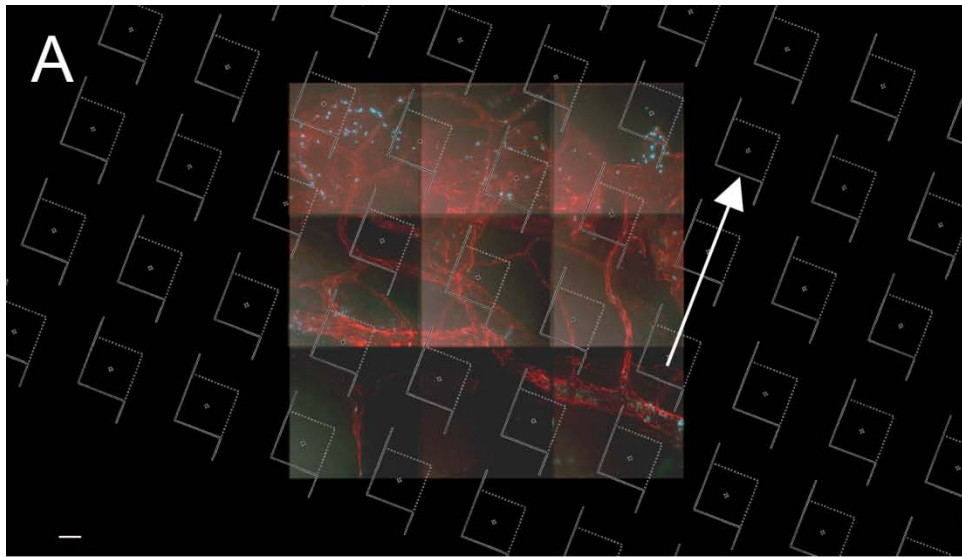


Figure 8: Morphometric analysis of keratocyte repopulation

Keratocyte nuclei are counted within a 125 μm X 125 μm morphometric number estimation frame. Only non-FITC-labeled nuclei falling within the area of the frame or on the accepted line are included in the analyses. These nuclei are counted through the thickness of the stroma, and divided into anterior and posterior regions. Counts are made at the central and paralimbal regions of the cornea and the kinetics of keratocyte repopulation is reported with respect to raw nuclei counts. Scale bar = 10 μm .

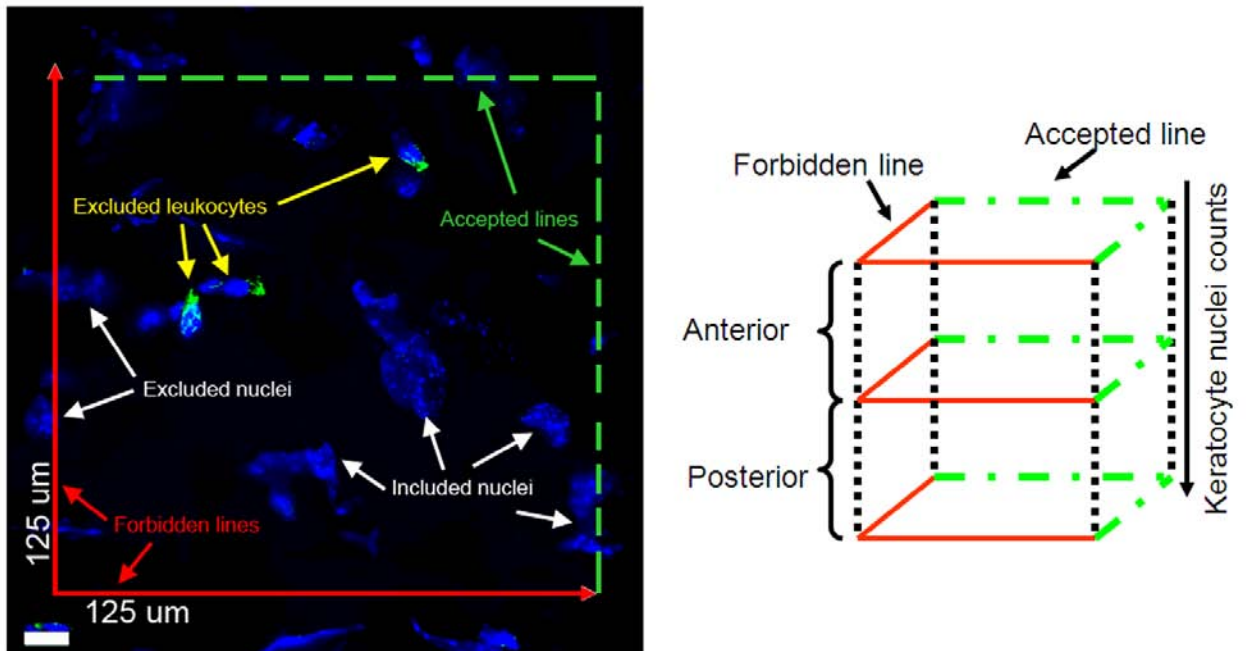


Figure 9: Morphometric analysis of PMN-keratocyte close surface interactions

Morphometric measurements of PMN-keratocyte interaction and keratocyte surface-to-volume ratio (Sv) using a cycloid grid. Panel **A** shows a systematically, randomly cast cycloid grid placed on top of a corneal cross section (WT 12 hours post-injury). The white arrow on the cycloid grid is oriented perpendicular to the longitudinally oriented collagen fibrils which run parallel to the orientation of the cycloid grid lines. Grid lines intersecting PMN-keratocyte membrane interfaces separated by distances of ≤ 25 nm are marked as close surface contacts (green points). Points falling within the PMN body are scored for volume measurements (blue points). PMN-collagen close interactions (≤ 25 nm) are indicated by red points. Panel **B** is a magnified image of panel **A** and shows areas of PMN close surface contact with keratocyte and collagen. Colored points are more easily appreciated at this magnification. Panel **C** shows a cycloid grid overlaid on top of uninjured WT anterior paralimbal keratocytes. Again, the white arrows on the cycloid grid are oriented perpendicular to the overall longitudinal orientation of the collagen fibrils. Here, the red points are placed at the intersections of grid lines and keratocyte membrane and blue points falling within the keratocyte body are used to calculate the keratocyte surface-to-volume ratio (Sv), an indirect measurement of shape. Panel **D** is a magnified image of panel **C** where the red points intersecting the grid line-membrane interface and blue points within the keratocyte body can be better appreciated. Additional symbols: N=PMN, K=keratocyte. Scale bar: 2 μ m (**A**, **C**), 0.5 μ m (**B**, **D**).

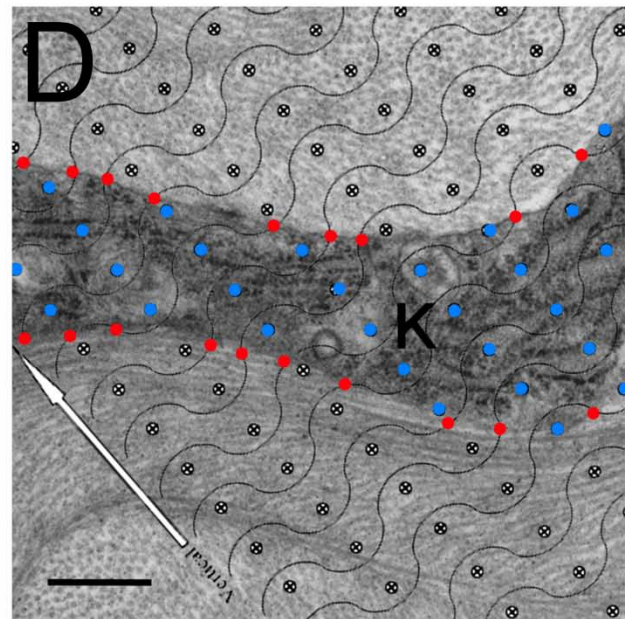
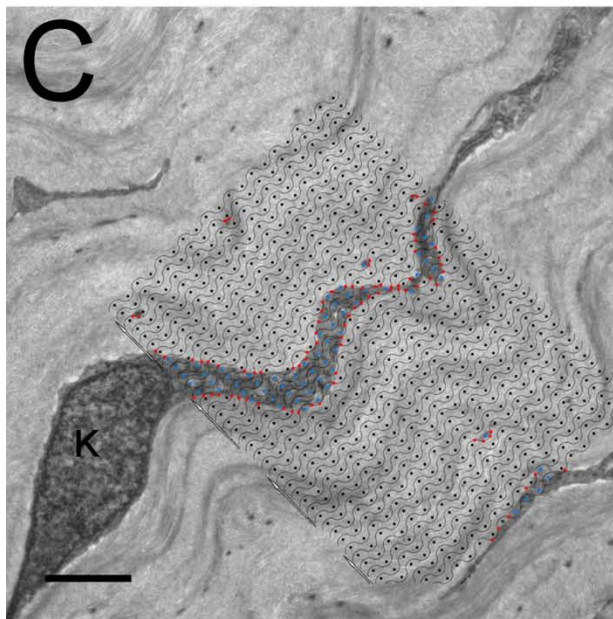
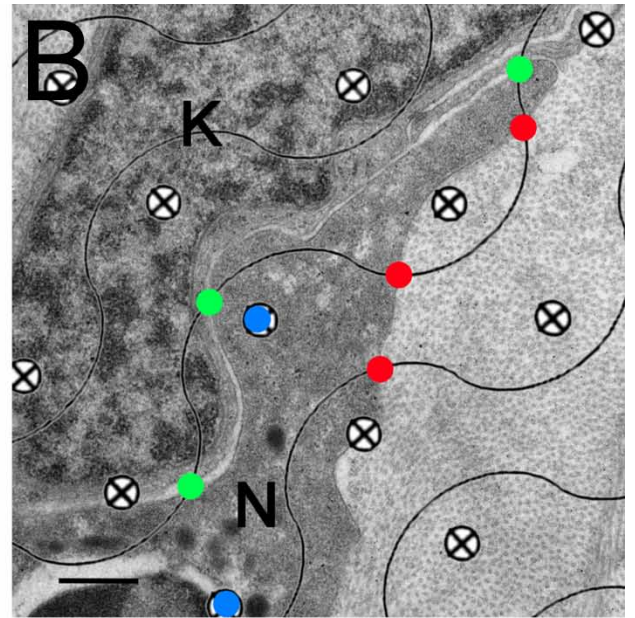
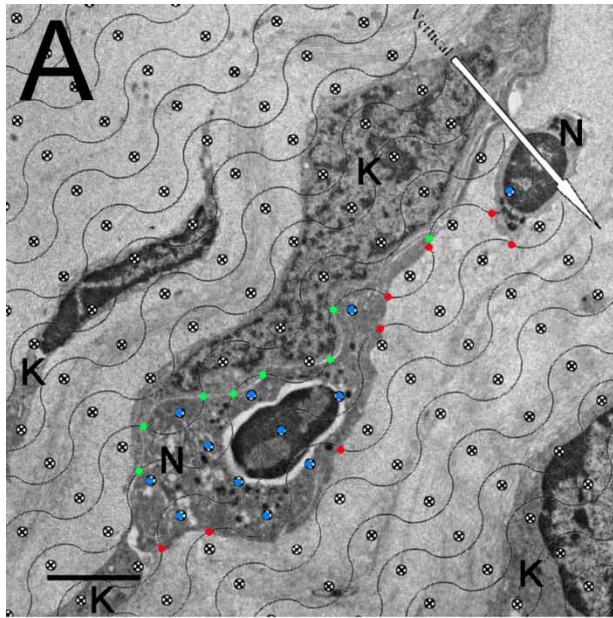


Figure 10: Paralimbal keratocyte ICAM-1 immunostaining

Expression of ICAM-1 on ALDH3A1 positive WT and ICAM-1^{-/-} mouse keratocytes.

DAPI nuclear stain show keratocyte nuclei in uninjured (Figs 2A and 2I) and differentiate keratocyte nuclei from PMN nuclei in 12 hour post-injured (Figs 2E and 2M) WT and ICAM-1^{-/-} mouse corneas. Paralimbal keratocytes in WT and ICAM-1^{-/-} corneas stain positively for ALDH3A1 (green, **B, F, G, N**). ICAM-1 staining (red) is detected at baseline levels on WT mouse keratocytes (**C**) and the merged image shows most ALDH3A1 positive cells are also ICAM-1 positive (**D**). Twelve hours after injury, ALDH3A1 positive paralimbal WT keratocytes (**F**) show increased staining for ICAM-1 (**G**) and the merged image confirms this increase occurs on ALDH3A1 positive keratocytes (**H**). PMNs stained with FITC-conjugated Ly6-G (pink) are seen in the injured cornea (white arrowheads). Keratocytes of uninjured and 12 hour injured ICAM-1^{-/-} mouse corneas express ALDH3A1 (**J** and **N**, respectively) but do not express ICAM-1 (**K** and **O**, respectively and merged images **L** and **P**), although FITC-stained PMNs (white arrowheads) are present in the tissue after injury. In all panels, nuclei are stained with DAPI (blue). Scale bars: 10 μ m (**A-P**).

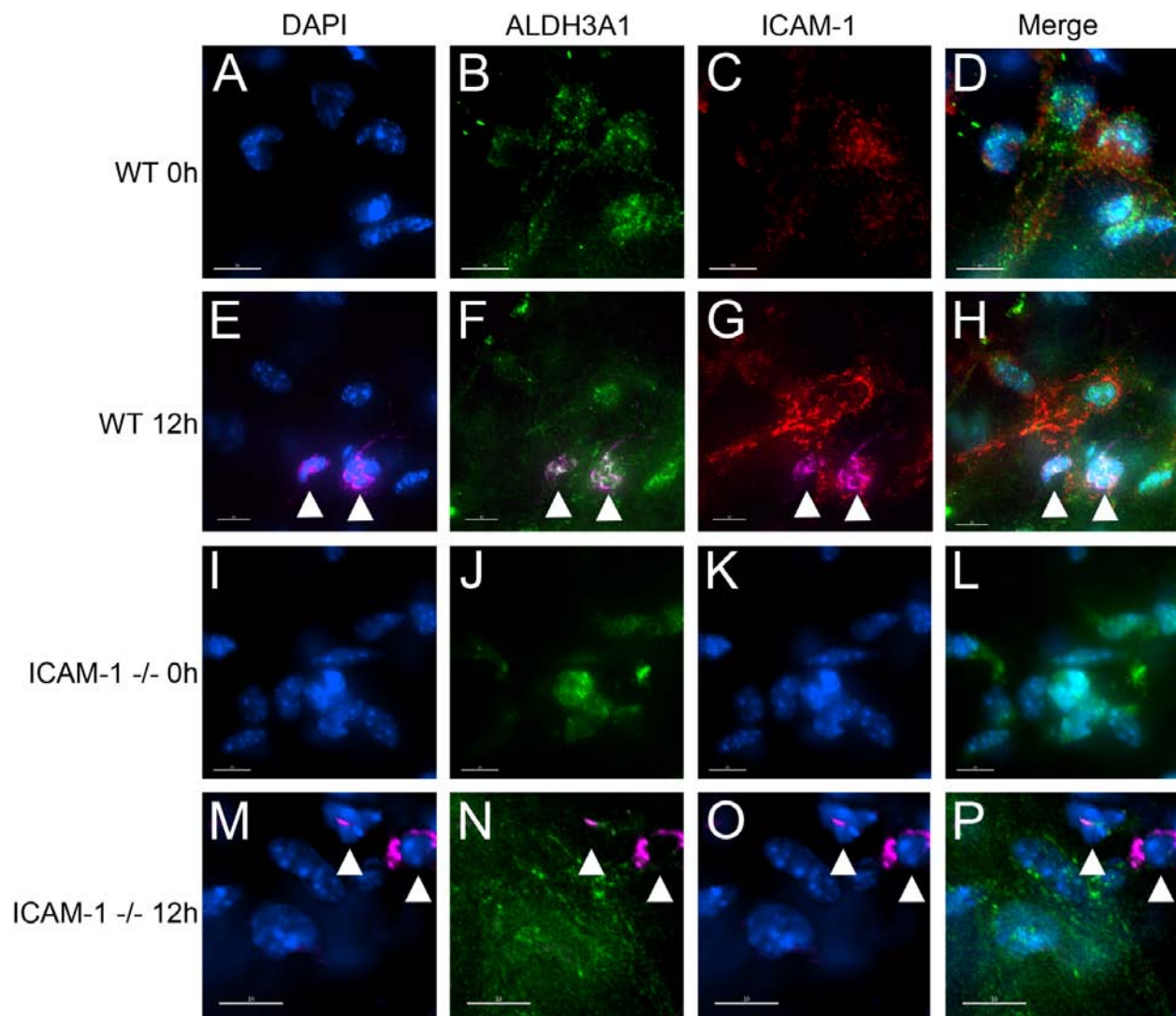


Figure 11: TEM of PMN-keratocyte close surface contacts in WT and ICAM-1^{-/-} mice

Transmission electron micrographs of 12 hour injured corneas in wild type (**A, B**) and ICAM-1^{-/-} (**C, D**) mice. (**A**) WT PMNs (12 hours post-injury) come into close contact with collagen (black arrowheads) and keratocytes (white arrowheads). Close contact is defined by any distance ≤ 25 nm between the surface of a PMN and an adjacent surface (e.g. collagen or keratocyte). (**B**) A magnified view of (**A**) shows close contact between PMN and keratocyte membrane surfaces. (**C**) In the ICAM-1^{-/-} cornea (12 hours post-injury), the PMN shows close surface contact with collagen (black arrowheads) but surface contacts with keratocytes (white arrowheads) are less evident and (**D**) the distance between PMN and keratocyte surfaces frequently exceeds 25 nm (black arrows). Additional symbols: N = PMN, K = keratocyte. Scale bars: 2 μ m (**A, C**), 0.5 μ m (**B, D**).

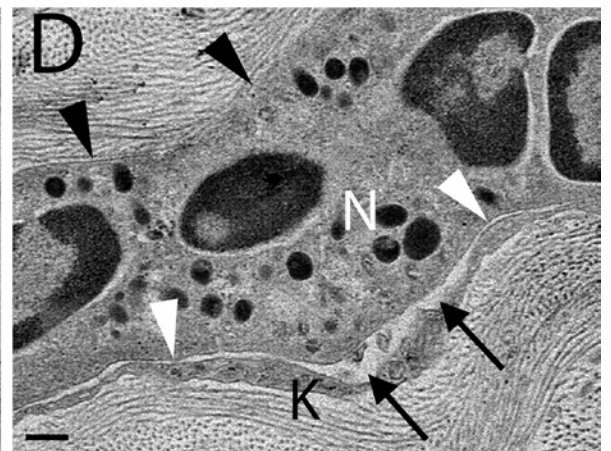
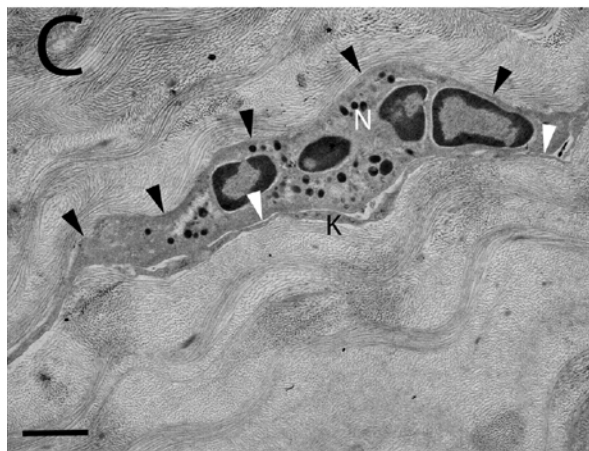
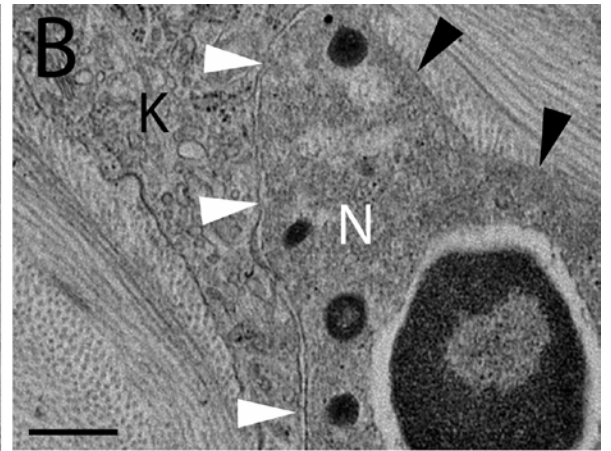


Figure 12: Keratocyte network surface-to-volume ratio (Sv) in WT and ICAM-1^{-/-} mice

Surface-to-volume ratio of paralimbal keratocytes of uninjured (**A**) and 12 hour injured (**B**) corneas. Both anterior and posterior regions of WT and ICAM-1^{-/-} corneas are evaluated. Data are means \pm SEM.

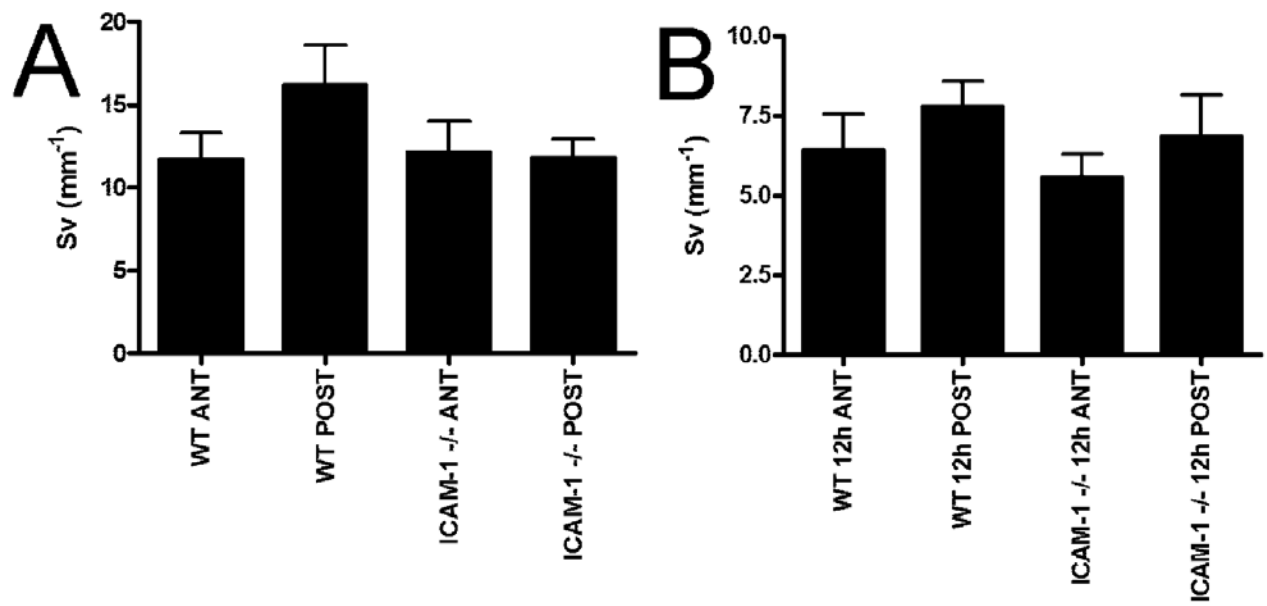


Figure 13: Keratocyte network surface area (SA) in WT and ICAM-1^{-/-} mice

Paralimbal keratocyte network surface area of uninjured (**A**) and 12 hour injured (**B**) corneas for WT and ICAM-1^{-/-} mice. Both anterior and posterior regions are evaluated.

Data are means \pm SEM.

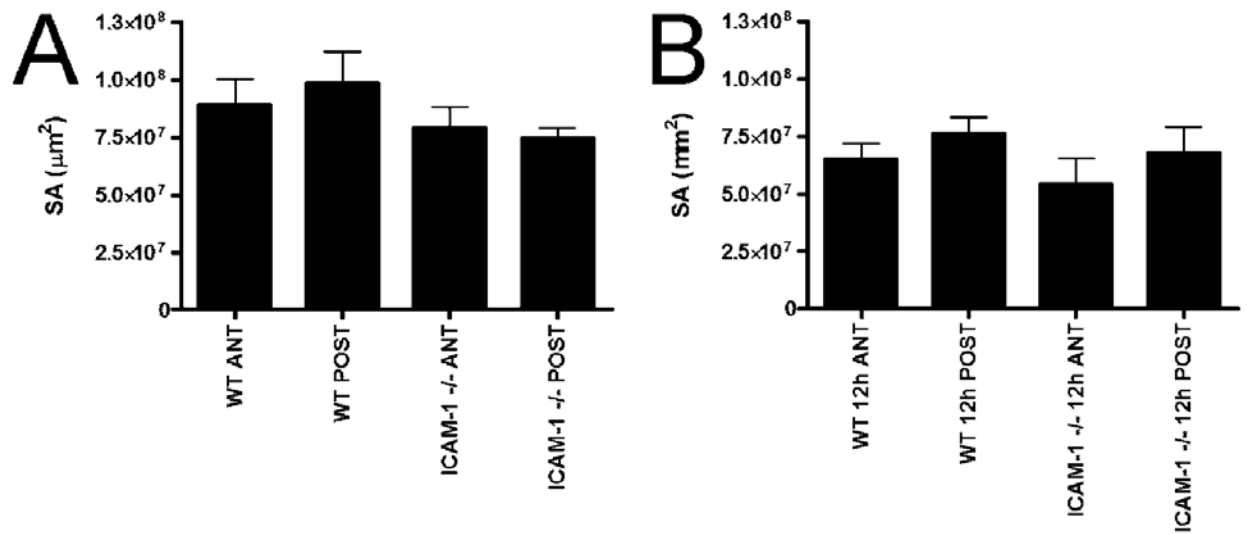


Figure 14: Stromal thickness in WT and ICAM-1^{-/-} mice

Paralimbal stromal thickness of uninjured and 12 hour injured WT and ICAM-1^{-/-} mice corneas. Data are means \pm SEM.

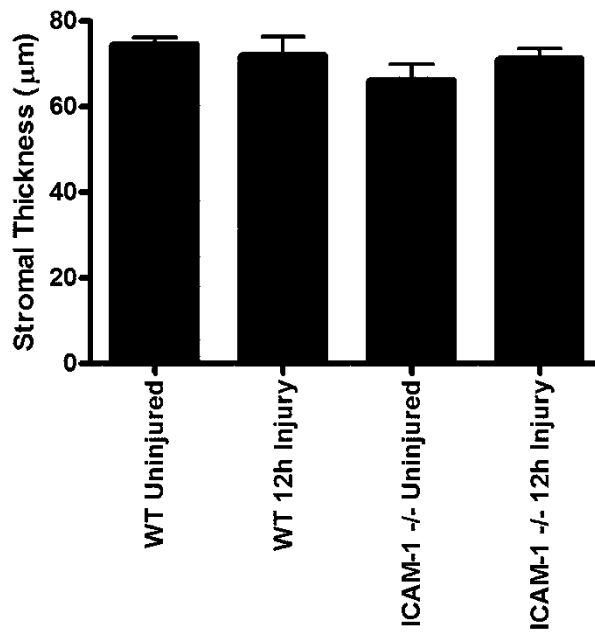


Figure 15: KSFM cultured mouse keratocytes retain their phenotype in culture

(A) CD34 positive and (B) Keratocan positive cells. (C) SMA negative keratocytes cultured in KSFM and (D) SMA positive keratocytes cultured in presence of 10% FBS.

Scale bar = 20 μ m.

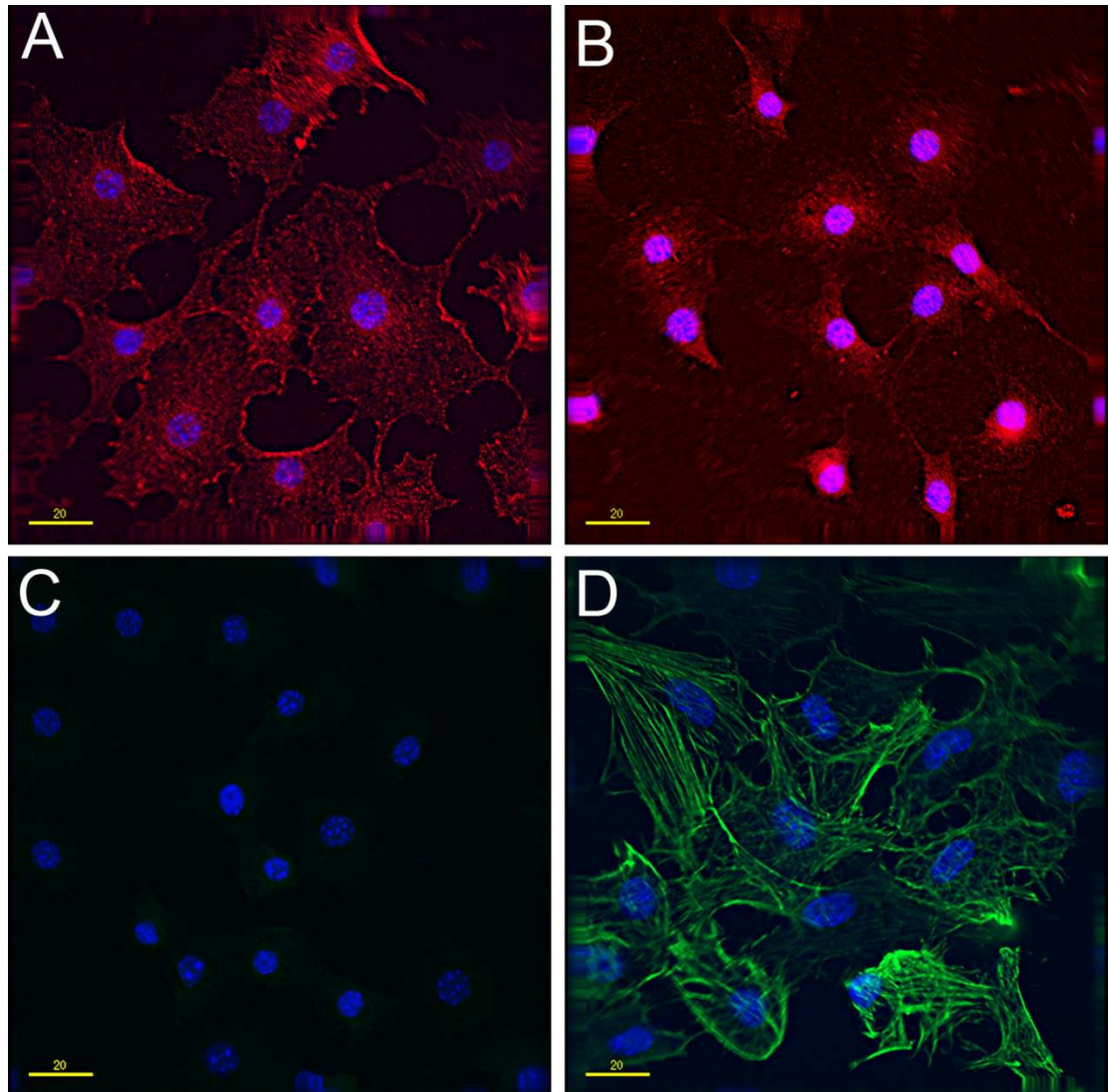


Figure 16: PMN migration on cultured mouse keratocytes

PMN migration on keratocytes is CD18 and ICAM-1-dependent. Addition of CD18 blocking antibody (GAME46) or ICAM-1 blocking antibody (YN-1) significantly reduces PMN motility.

* $p \leq 0.05$

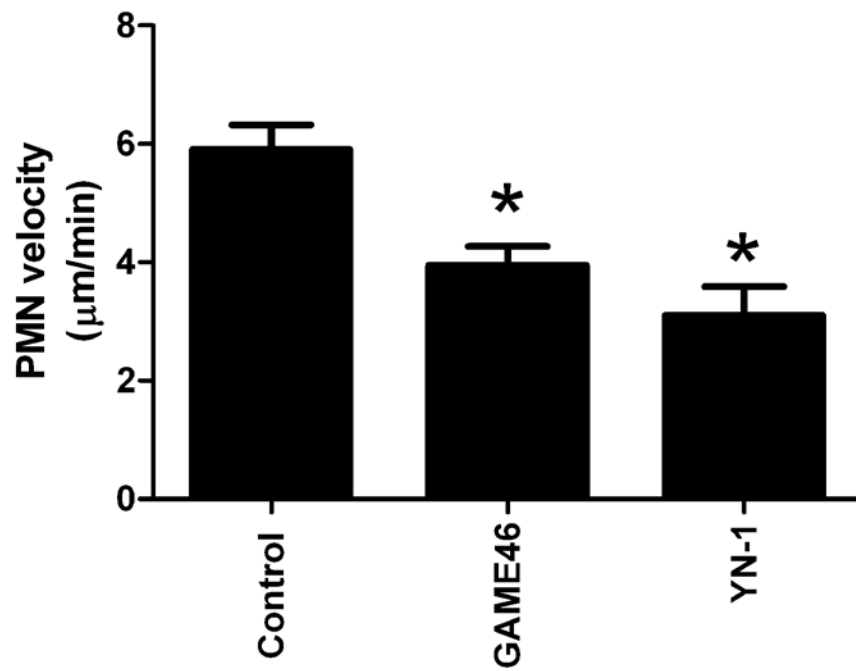


Figure 17: Kinetics of WT, CD18^{mutant}, and ICAM-1^{-/-} PMN infiltration following corneal epithelial abrasion with the Algerbrush

Central (A), paralimbal (B), and limbal (C) PMN infiltration in WT (red line), ICAM-1^{-/-} (blue line), and CD18^{mutant} (green line) mice. Y-axis scales for A, B, and C are not the same. This was done to represent the magnitude of individual regional responses. D, E, and F are the same graphs as A, B, and C but the paralimbal (E) and limbal (F) graphs' Y-axis have been scaled to match the central (D) Y-axis scale. This was done to demonstrate the magnitude of the central PMN response with respect to the paralimbal and limbal responses. * $p \leq 0.05$ ICAM-1 versus WT and CD18; # $p \leq 0.05$ ICAM-1 versus WT or CD18; $n = 4 - 6$ mice, per region, per genotype

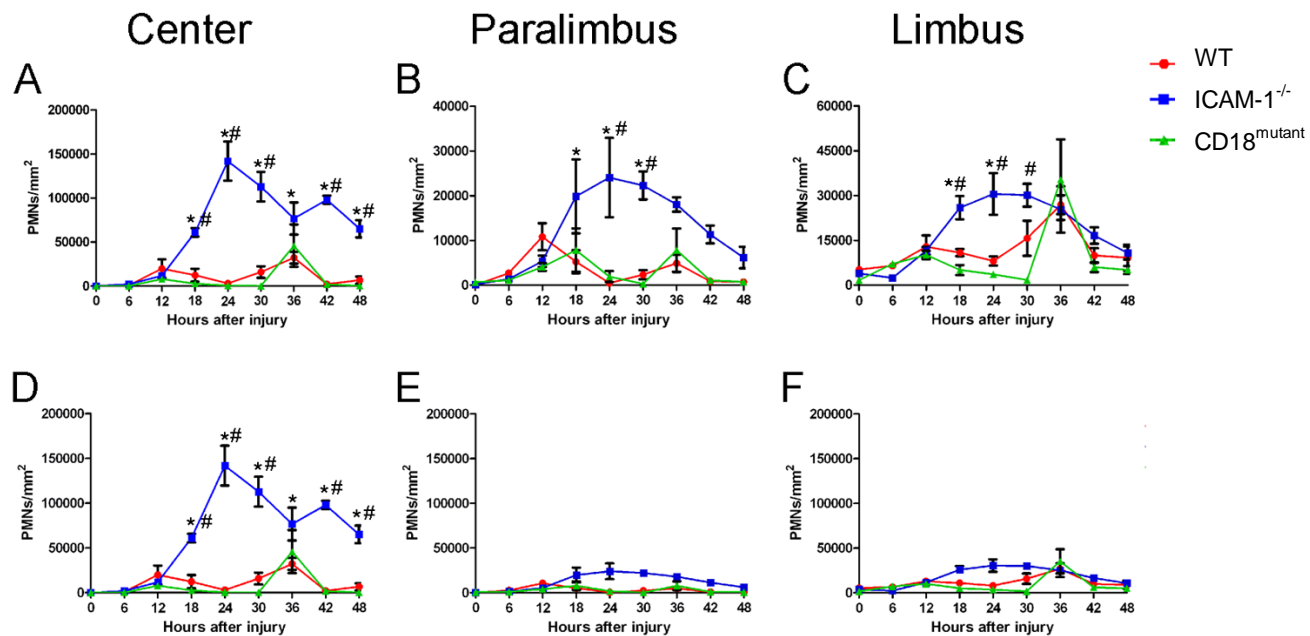


Figure 18: Kinetics of PMN infiltration in ICAM-1^{-/-} mice following diamond blade injury

Peak PMN infiltration in ICAM-1^{-/-} mice occurs 18 hours after epithelial abrasion using a diamond blade. (Courtesy of Dr. Zhijie Li, Baylor College of Medicine)

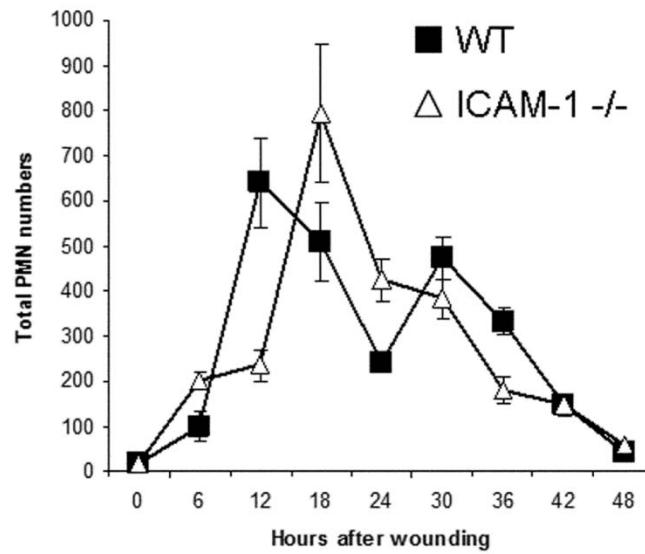


Figure 19: Kinetics of platelet infiltration following corneal epithelial abrasion with the Algerbrush

Platelets accumulation is separated into **A**) total platelets (inside and outside of vessels) and **B**) extravascular platelets (platelets outside of vessels). Panel **C** is a large-scaled version of **B**. While platelet accumulation in ICAM-1^{-/-} mice is significantly enhanced by 18 hours, peak platelet accumulation in WT mice does not occur until 24 hours post injury. Extravascular platelet accumulation in CD18^{mutant} mice remains depressed. * $p \leq 0.05$ ICAM-1^{-/-} mice versus WT and CD18^{mutant} mice; # $p \leq 0.05$ WT versus CD18^{mutant} mice. $n = 4 - 6$ mice, per genotype

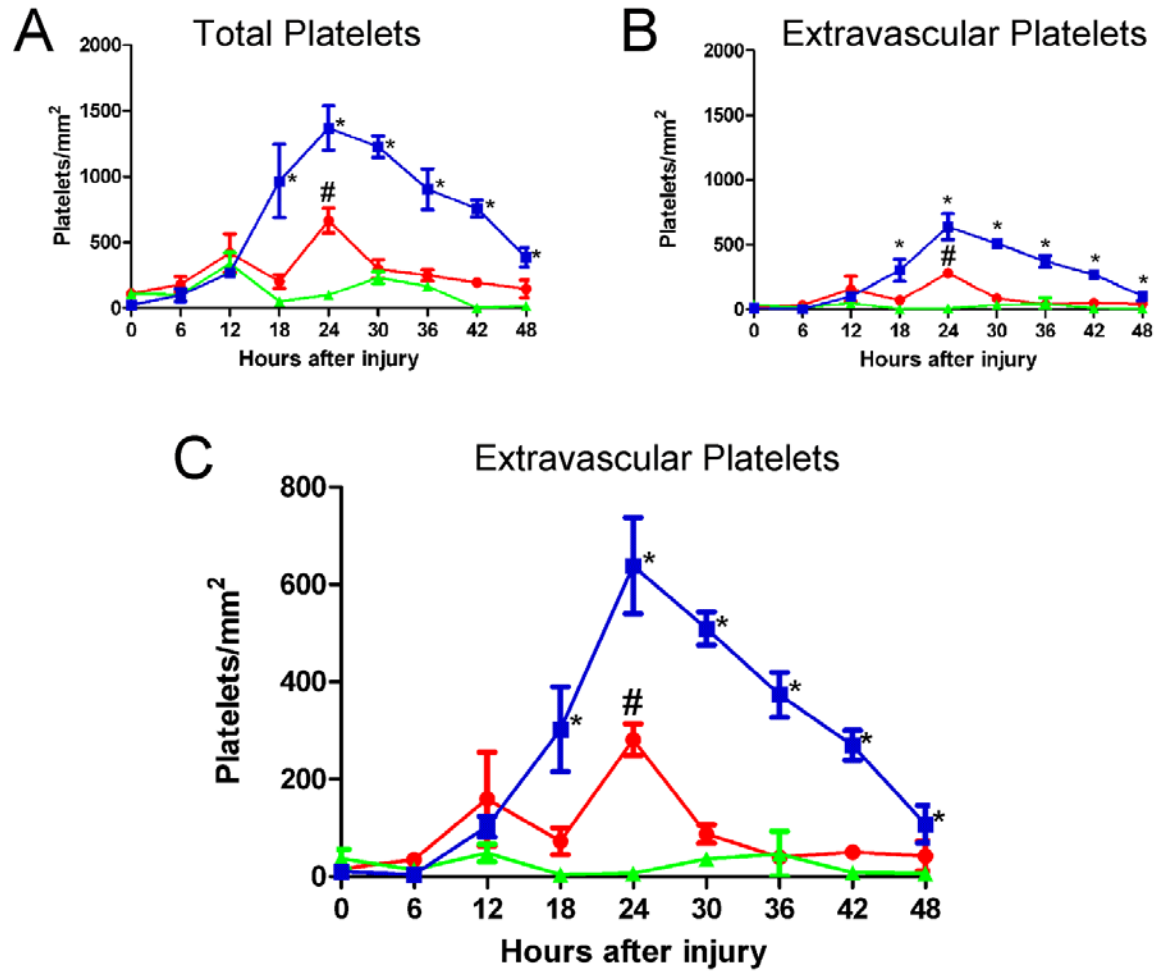
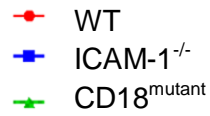


Figure 20: WT anterior central keratocyte repopulation

WT anterior central keratocytes do not recover to baseline values, up to 28 days.

Asterisk represents statistically significant comparisons with baseline anterior central keratocyte numbers.

* $p \leq 0.05$. $n = 5$ mice, per time point

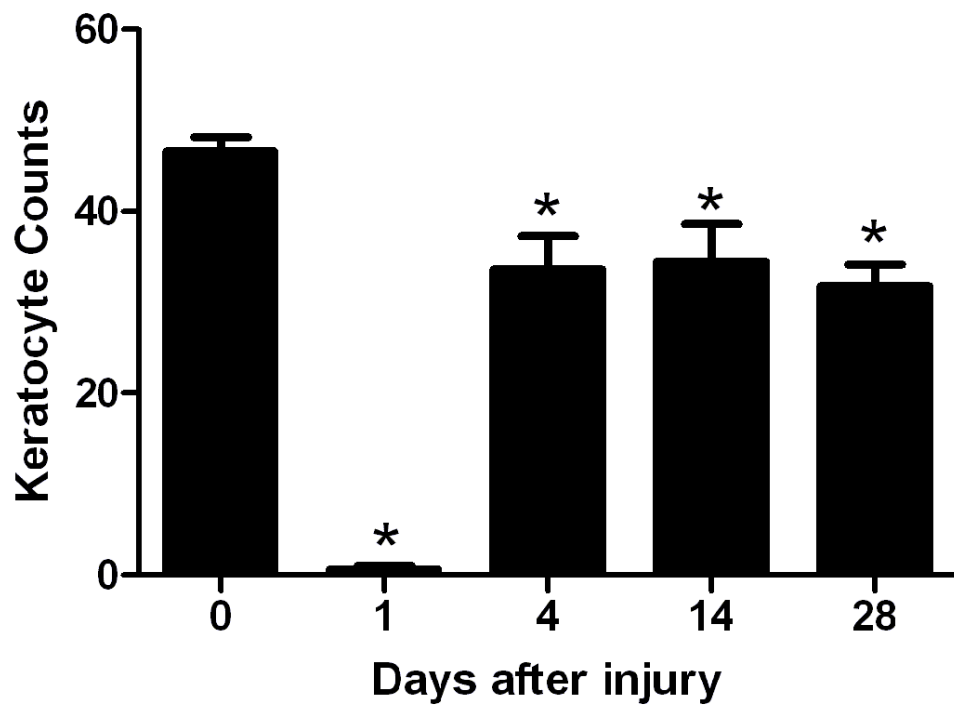


Figure 21: Keratocyte repopulation following corneal epithelial abrasion in WT, ICAM-1^{-/-}, and CD18^{mutant} mice

A large scale graph of anterior central keratocyte repopulation (**A**) shows keratocyte counts soon after injury but rapid recovery by 4 days. The Y-axis on graphs **B-E** are represented on a similar scale, to show the increases and decreases in keratocyte repopulation at the different regions: Anterior central (**B**), Anterior Paralimbal (**C**), Posterior Central (**D**), Posterior Paralimbal (**E**). Asterisks represent statistically significant values with respect to a specific genotypes' baseline number, using 1-way ANOVA. Number signs represent statistically significant genotype differences at a given time point calculated by 2-way ANOVA. Baseline values are extended to 28 days using dashed lines of representative color (WT = red, ICAM-1^{-/-} = blue, CD18^{mutant} = green)

*# $p \leq 0.05$.

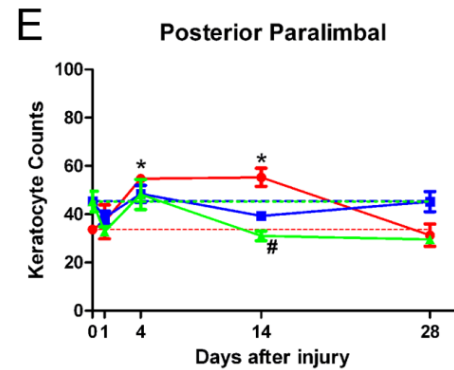
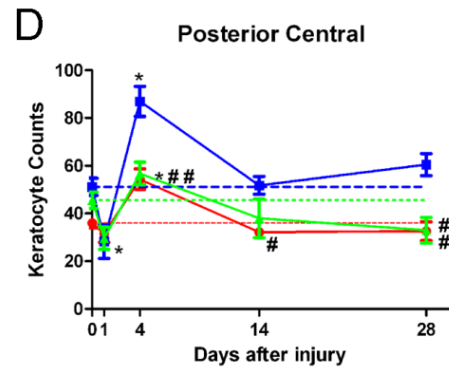
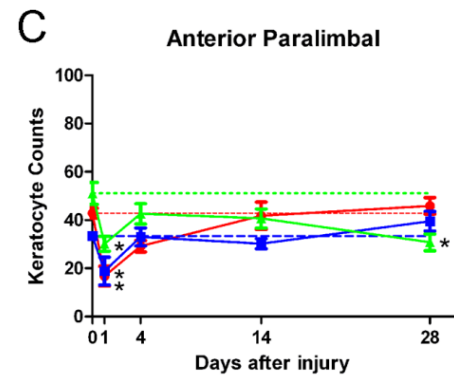
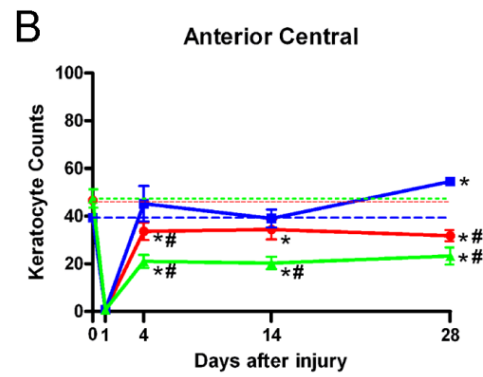
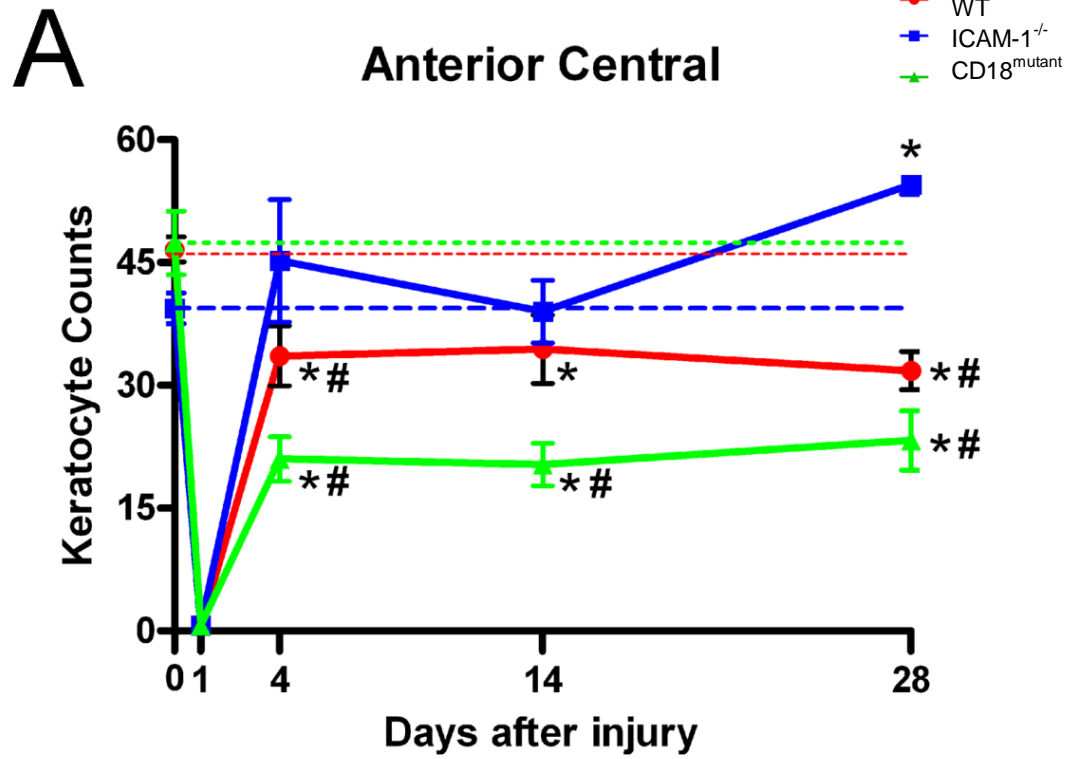


Figure 22: Anterior central keratocyte repopulation in platelet-depletion WT mice

Compared to baseline uninjured keratocyte numbers, 4 days post injury keratocyte numbers are depressed in untreated mice and blunted in platelet-depleted WT mice.

* $p \leq 0.05$. $n = 5$ mice per condition

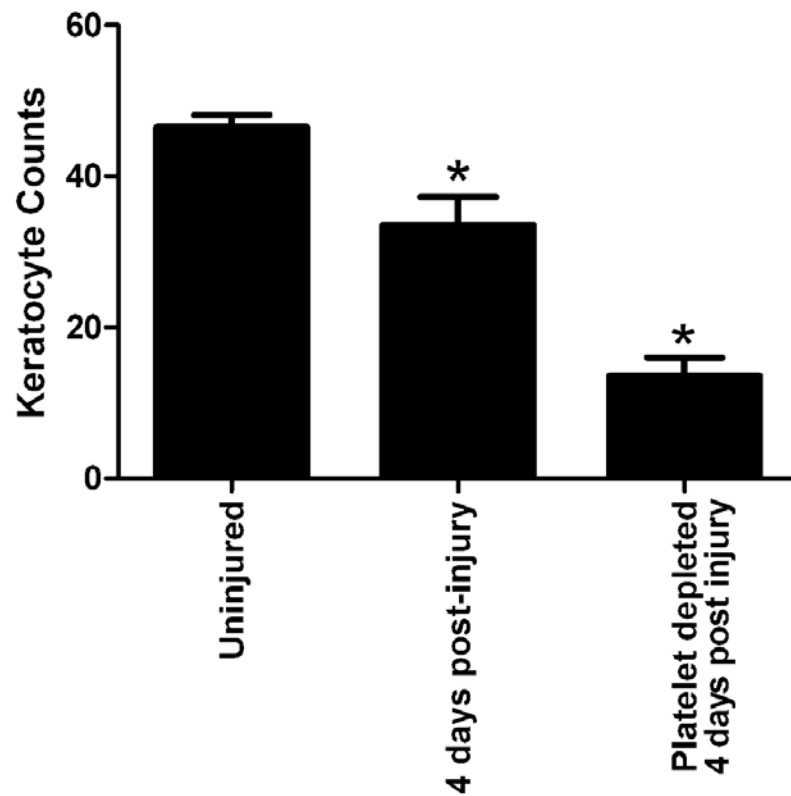


Figure 23: Four day anterior central keratocyte repopulation in TCR δ ^{-/-} mice

Anterior central keratocyte repopulation in TCR δ ^{-/-} mice is significantly lower than baseline 4 days after injury but posterior central numbers recover back to their respective baseline.

* $p \leq 0.05$. $n = 5$ mice per condition

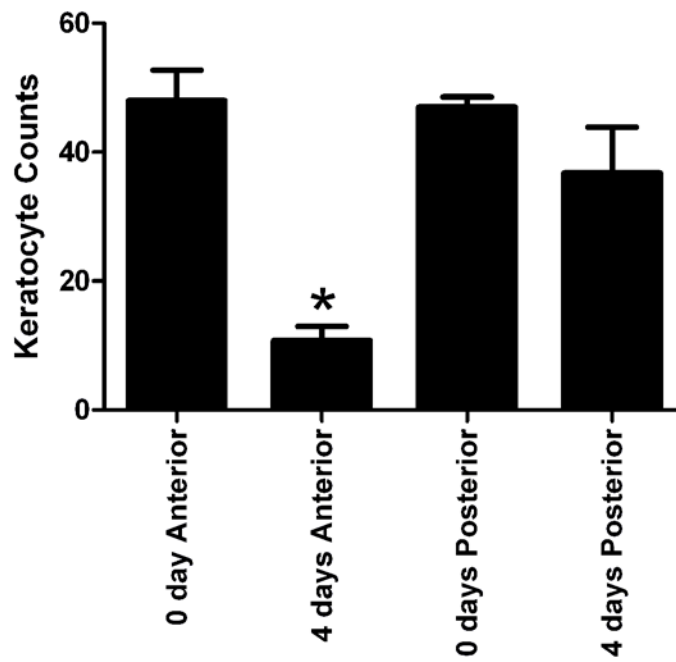


Figure 24: Anterior central keratocyte repopulation in P-selectin^{-/-} mice Keratocyte repopulation in P-selectin^{-/-} mice is significantly lower than its respective baseline counts and does not recover to its respective baseline. * $p \leq 0.05$. $n = 5$ per condition

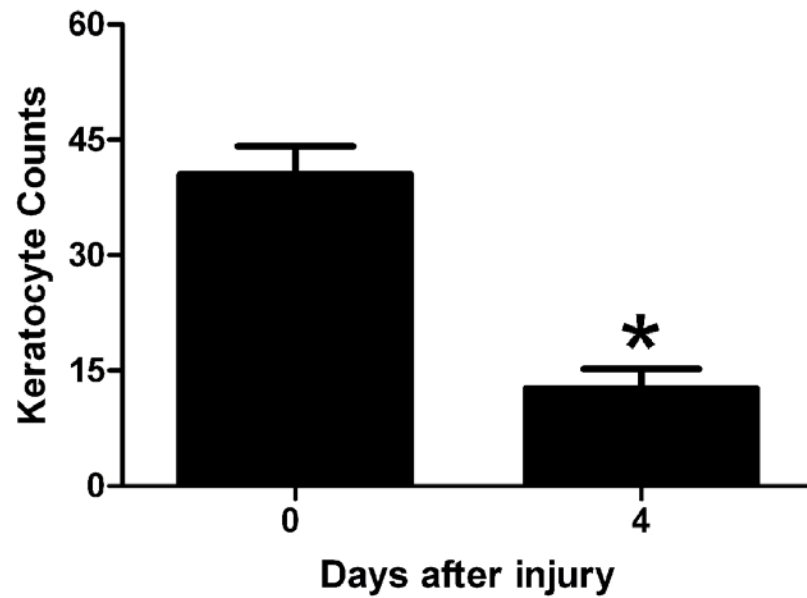


Figure 25: WT platelet infusion into P-selectin^{-/-} mice

Anterior central keratocyte numbers in P-selectin^{-/-} mice are restored following infusion of WT platelets. * $p \leq 0.05$, NS = not statistically significant. $n = 5$ (Uninjured and 4 day injured); $n = 10$ (+ WT platelet infusion)

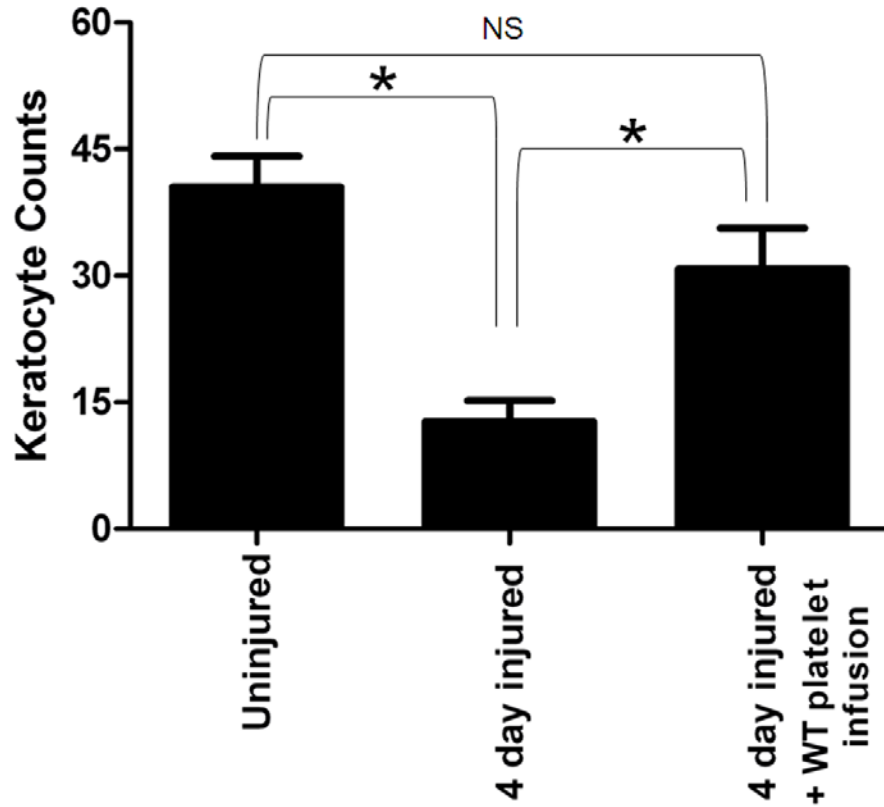


Figure 26: WT platelet infusion into WT mice

Infusion of WT platelets into WT mice does not rescue keratocyte repopulation. * $p \leq 0.05$, NS = not statistically significant. $n = 5$ (all)

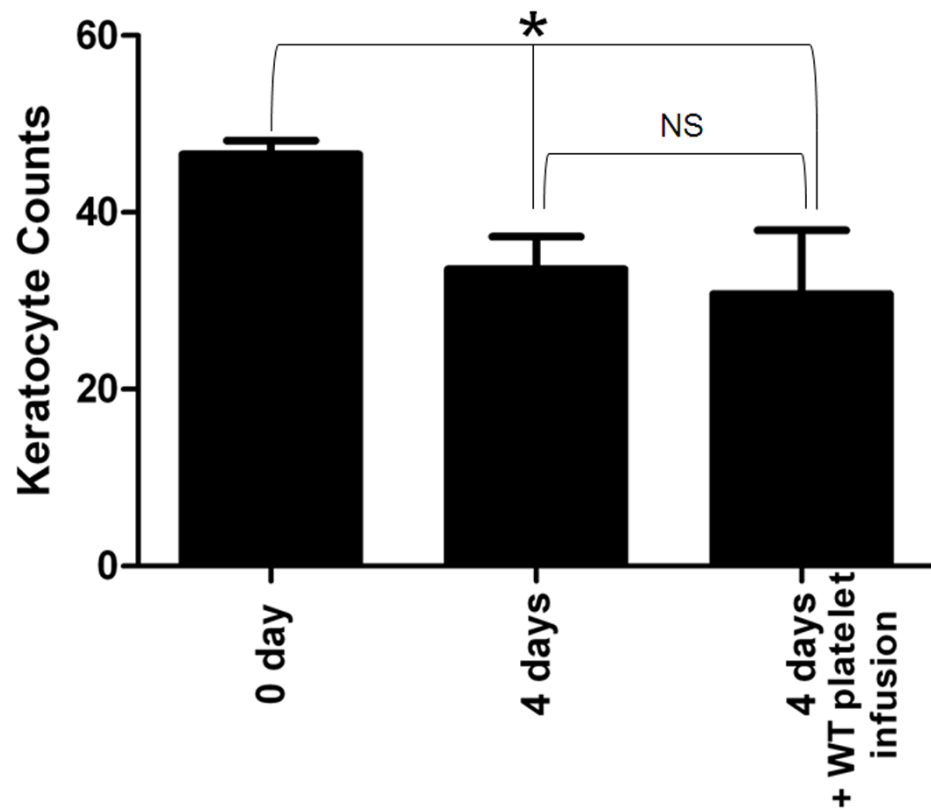


Figure 27: Twenty-four hour extravascular platelet density in WT and TCR $\delta^{-/-}$ mice

Extravascular platelet accumulation in TCR $\delta^{-/-}$ mice is significantly higher than that of WT. $p \leq 0.05$, $n = 4$ for WT, $n = 10$ for TCR $\delta^{-/-}$ mice

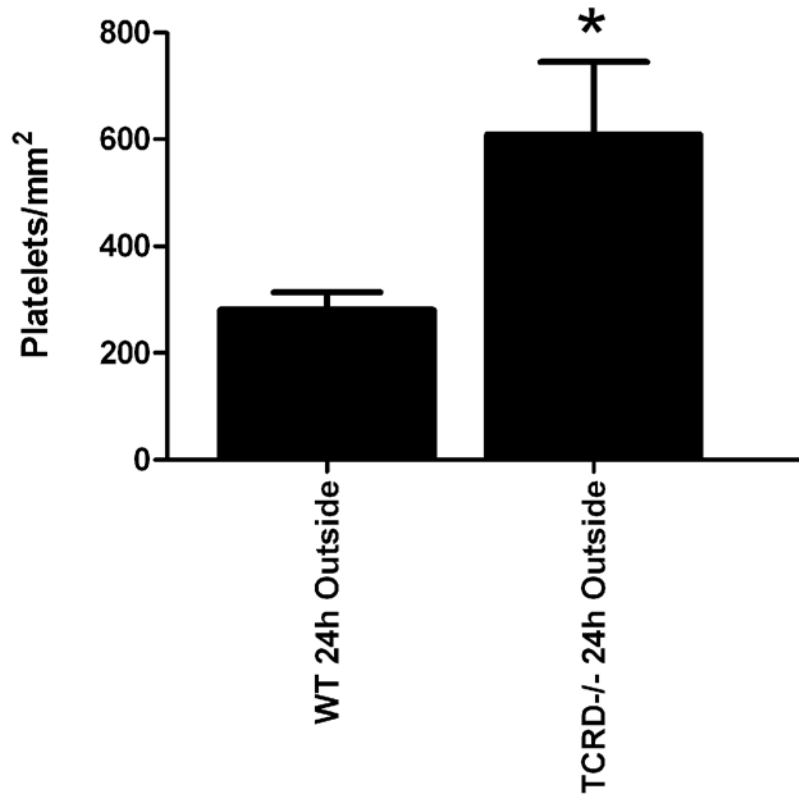


Figure 28: WT keratocyte IL-22R staining

IL-22R (red) staining is not detected in uninjured (0h) paralimbal (**A**) and central keratocytes (**E**). Twenty-four hours after injury, IL-22R staining is detected on paralimbal keratocytes (**B**) but not central keratocytes (**F**). Non-immune rat IgG staining did not show non-specific binding at 0h or 24h on paralimbal and central keratocytes (**C, D, G, and H**). green = Ly6G positive PMNs, blue = DAPI; asterisk = single PMN at paralimbal region.

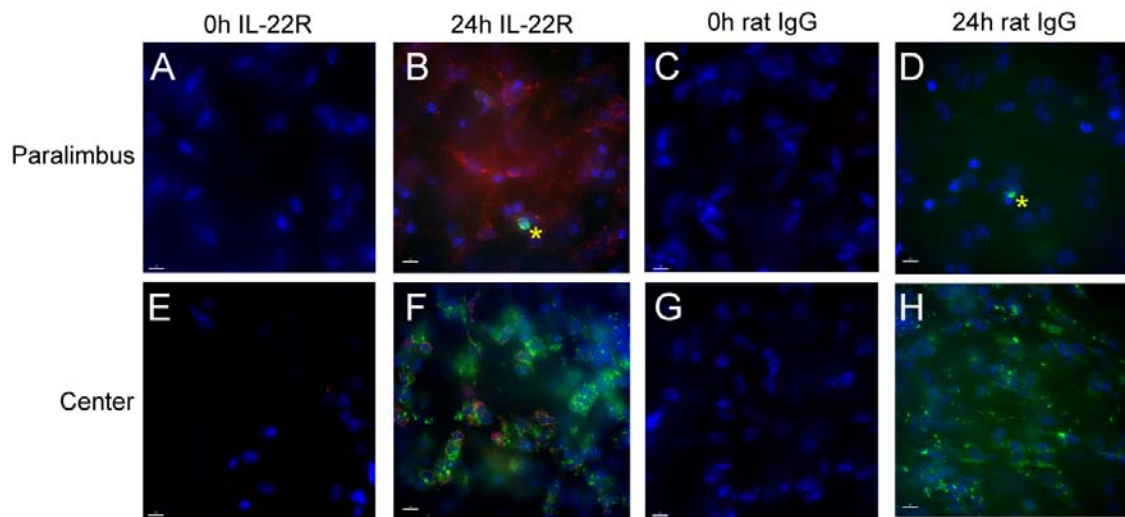


Figure 29: IL-22R staining at the corneal limbal region

IL-22R staining is not detected on uninjured vessels (**A**). IL-22R staining is detected on CD31-negative vessels 24 hours after injury, suggesting it stains lymphatic vessels and not limbal vessels (**C**). Non-immune rat IgG staining shows no non-specific binding on uninjured or 24h injured limbal region (**B, D**). CD31 limbal vessels are pseudo-colored yellow (**A-D**); IL-22R-positive vessels are pseudo-colored pink (**C**, white arrow).

Scale bars: A, C-D=20 μ m, B=10 μ m.

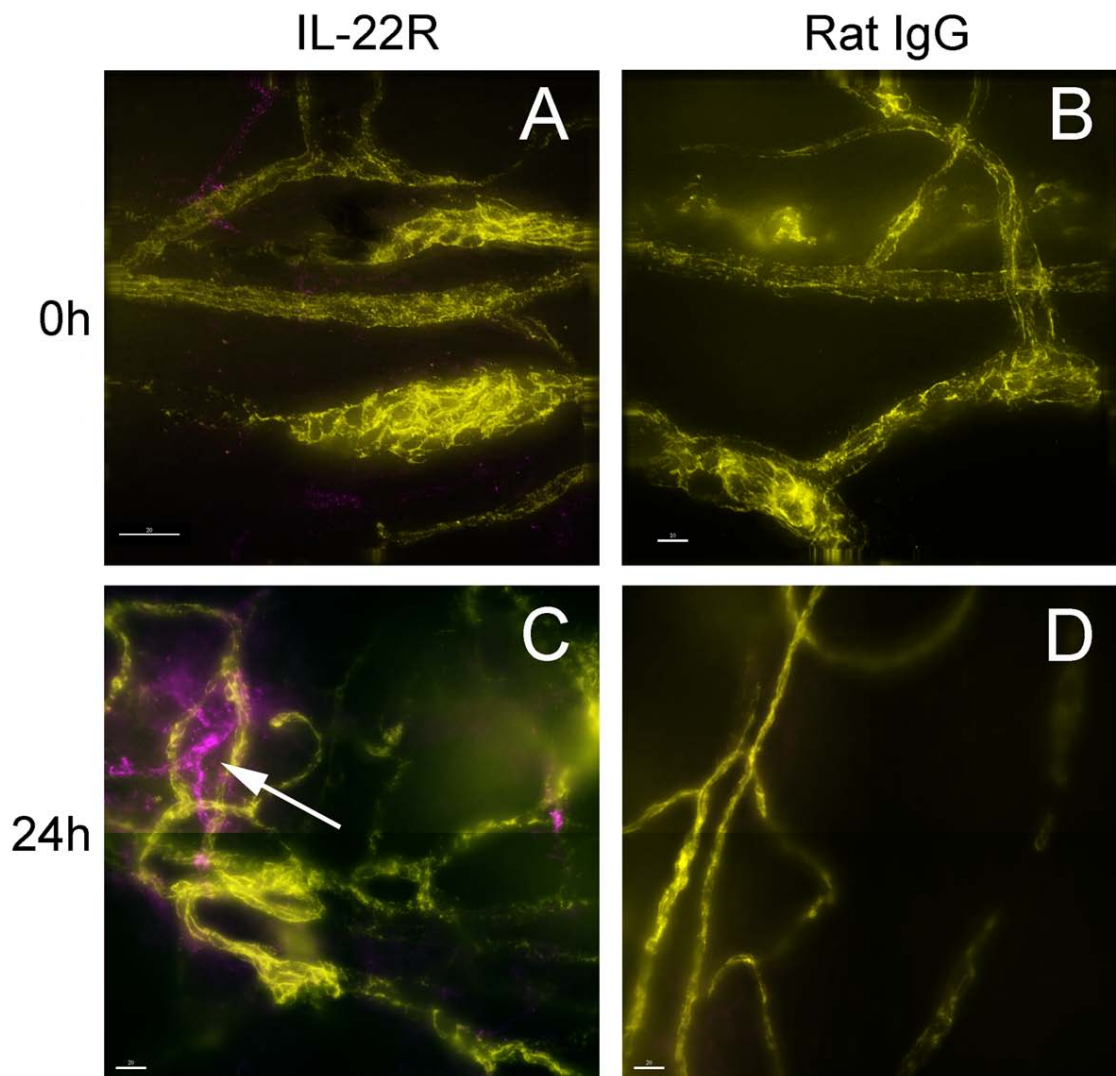


Figure 30: JAM-C protein and mRNA expression on cultured mouse keratocytes

Panel **A** shows a JAM-C positive cultured mouse keratocyte (in KSFM) and panel **B** shows increased JAM-C mRNA expression (relative to GAPDH) in freshly isolated mouse keratocytes.

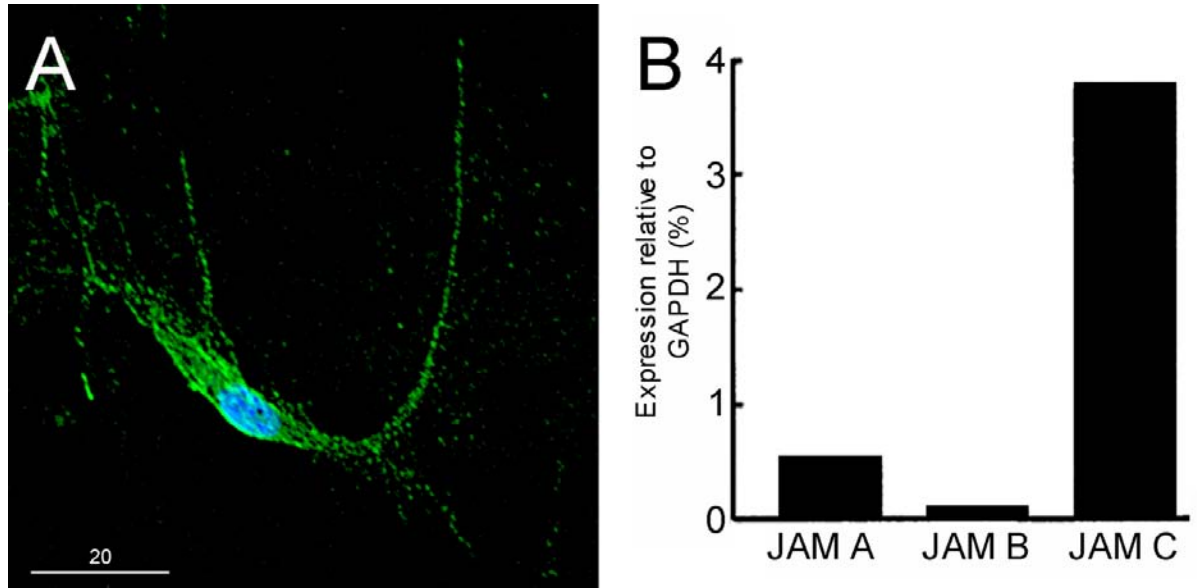


Figure 31: Inflammation induces endothelial cell activation and inflammatory cell infiltration

Inflammatory cells are not present inside or outside of the vessels of the uninjured cornea (**A-B**). Vascular endothelial cells are not ruffled and agitated. Panel **B** is a higher magnification of panel **A**. Twelve hours post injury (**C-D**) limbal vascular endothelial cells are inflamed and appear ruffled. PMNs and red cells are abundant inside of the vessels while PMNs, platelets (yellow arrow), and red blood cells (yellow arrow head) are seen outside of the vessels. Panel **D** is a magnified image of panel **C** showing the caveoli formation on the edges of the activated endothelial cell, giving it a “ruffled” appearance. IV=intravascular; EV=extravascular; EC=endothelial cell. Scale bars: **A**) 2 μ m, **B**) 1 μ m, **C**) 5 μ m, **D**) 1 μ m.

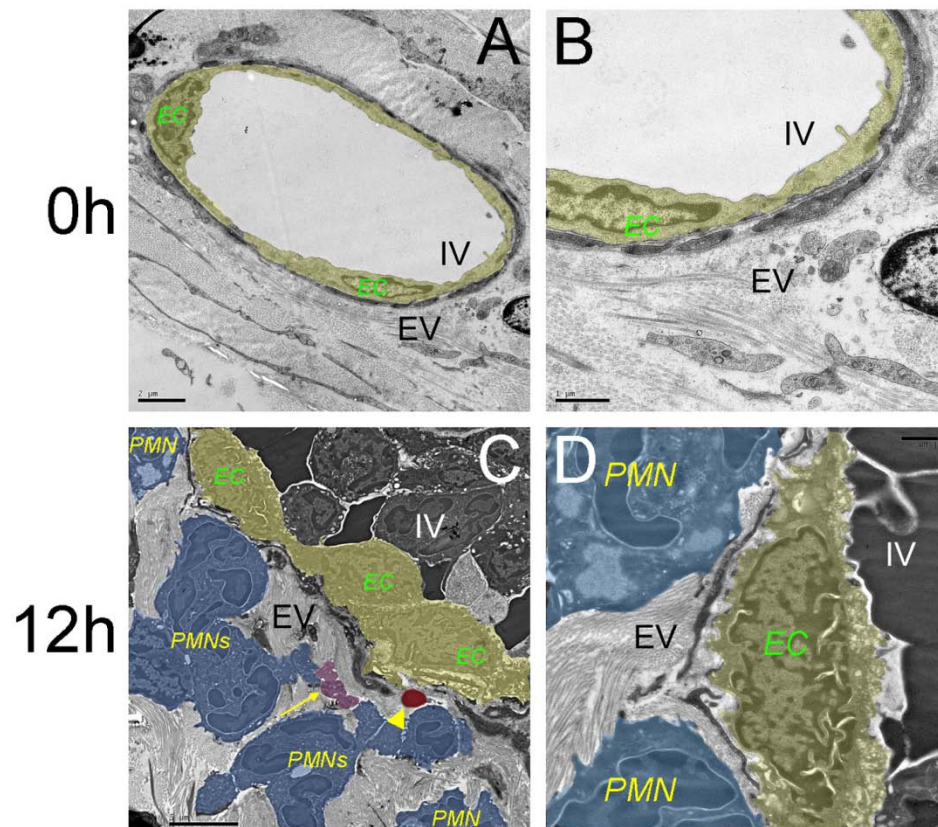


Figure 32: Unactivated appearance of $\text{TCR}\delta^{-/-}$ platelets

Eighteen hours after injury, WT platelets (**A**) do not appear round and platelet microparticles are noticeable outside of vessels (white arrows). Aggregated platelets are also detected inside and outside of vessels in WT mice (yellow arrows). Platelets in $\text{TCR}\delta^{-/-}$ mice (**B**) appear “unactivated” and round rather than shape-changed. Scale bar = 20 μm .

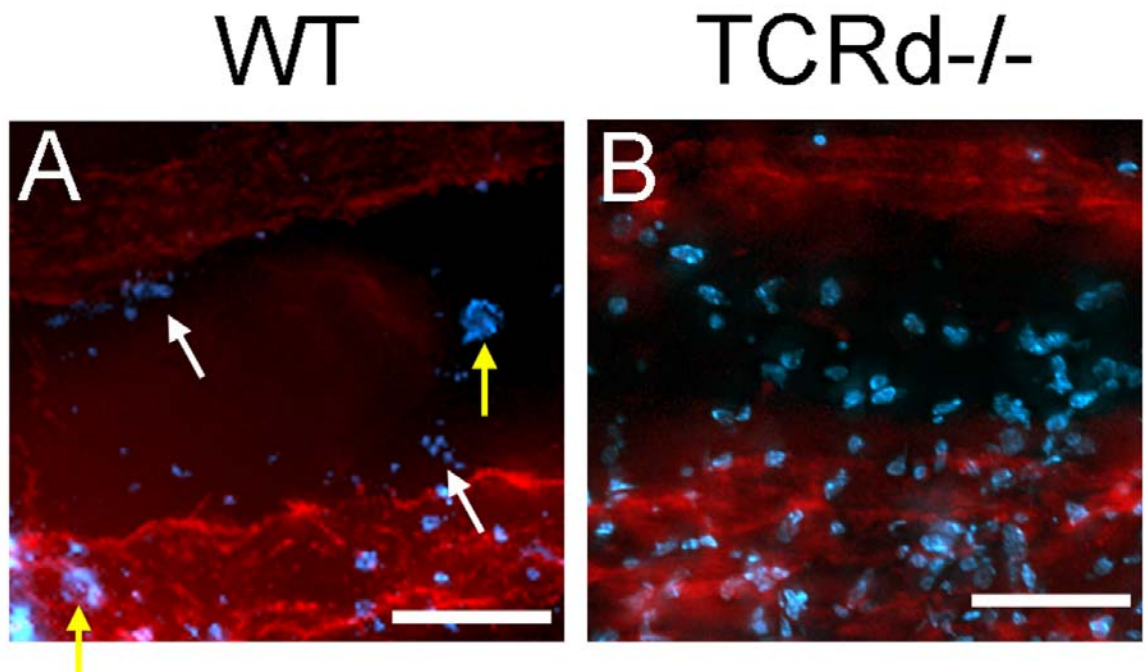
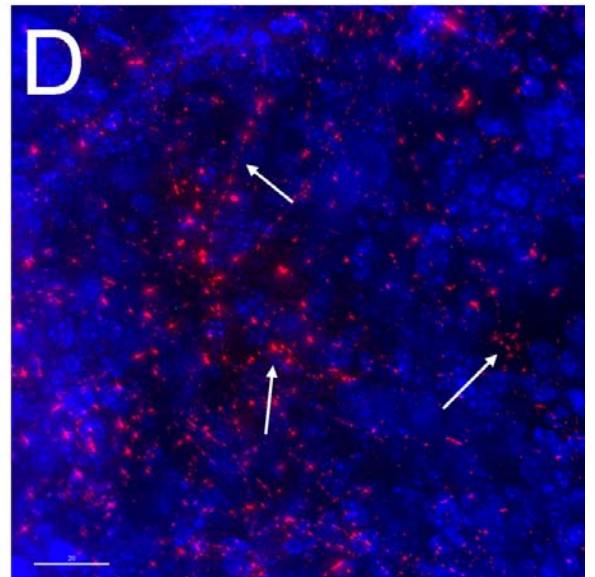
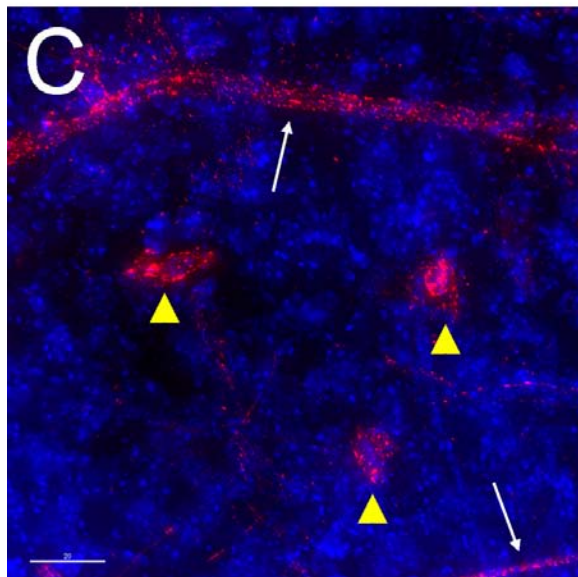
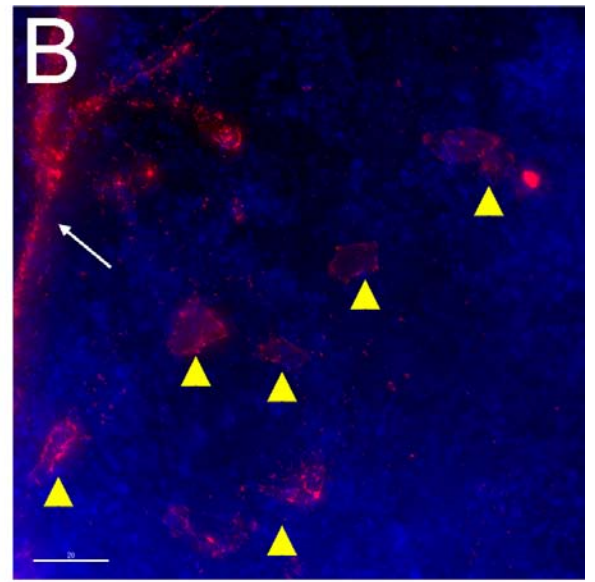
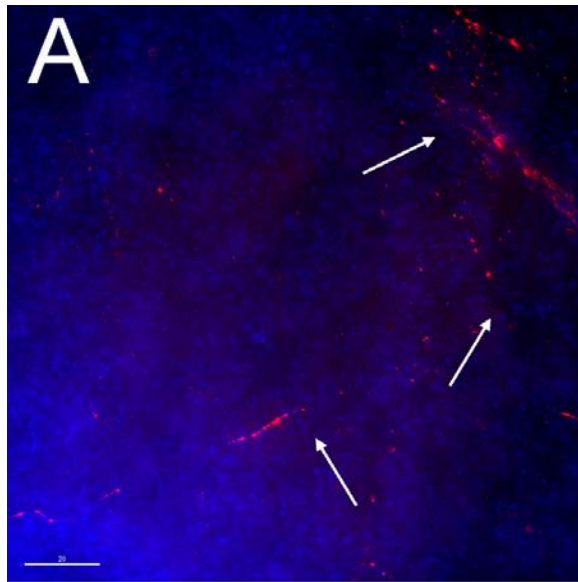


Figure 33: Thy1.2 Positive Stromal Cells in ICAM-1^{-/-} Mice

Twenty-four hours after corneal epithelial abrasion, no Thy1.2 positive cells are detected in the central stroma (**A**) but Thy1.2 positive nerves are observed (white arrows). By 42 hours, there is a dramatic increase in Thy1.2 positive cells (yellow arrow heads) as well as nerves (white arrows) in the central stroma (**B**). These central Thy1.2 positive cells are observed in fewer number 4 days post-injury (yellow arrow heads) (**C**) but are not present 4 weeks post injury (**D**), a time when anterior keratocyte counts have surpassed baseline values. At 4 weeks (**D**), only Thy1.2 positive vertical nerve endings, not nerve trunks, are detected (white arrows). Scale bar = 20 μ m



APPENDIX

Figure I: Cross section of mammal cornea

Panel **A** is a cartoon of human corneal cross section. The asterisk next to the ALL denotes the ALL is only in human corneas, not mouse corneas (**B**). B is a light micrograph of an uninjured WT mouse corneal cross section. ALL: Anterior Limiting Lamina (Bowman's Layer); PLL: Posterior Limiting Lamina (Descemet's membrane)

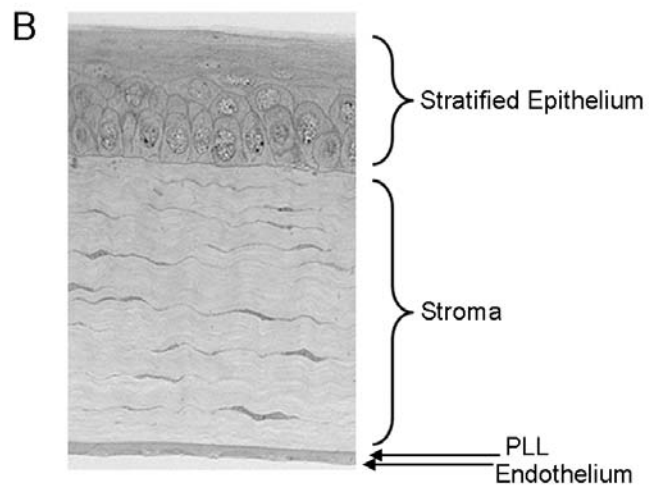
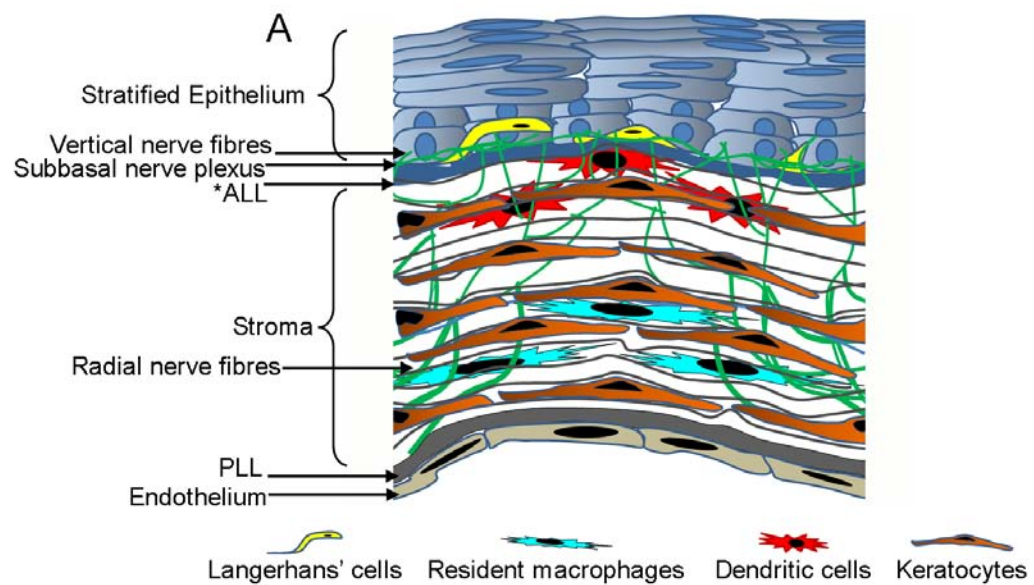


Figure II: CD18 expression on WT and CD18 hypomorphic mutant PMN infiltrating the cornea 36 hours after injury

WT (**A**) and CD18 hypomorphic mutant (**B**) mice PMNs labeled with PMN marker Ly6G (FITC) and CD18 (PE, clone GAME46). Yellow arrows identify Ly6G⁺ and CD18⁺ PMNs for both genotypes. **C** and **D** are the non-immune rat IgG negative controls for **A** and **B**, respectively. Scale bar = 20 μ m.

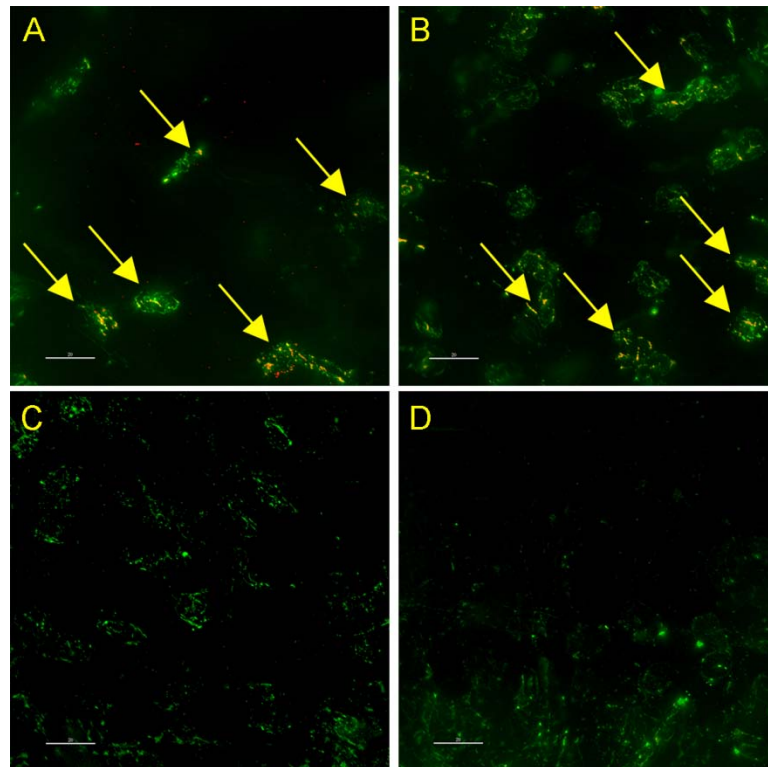


Figure III: Morphometric Analysis of Platelet Density: Intra-observer Comparisons

Analyses by two different observers of inside, outside, and total 24 hour platelet density in WT mice shows there is no difference in platelets/mm² among the two analyses. NS = Not statistically significant

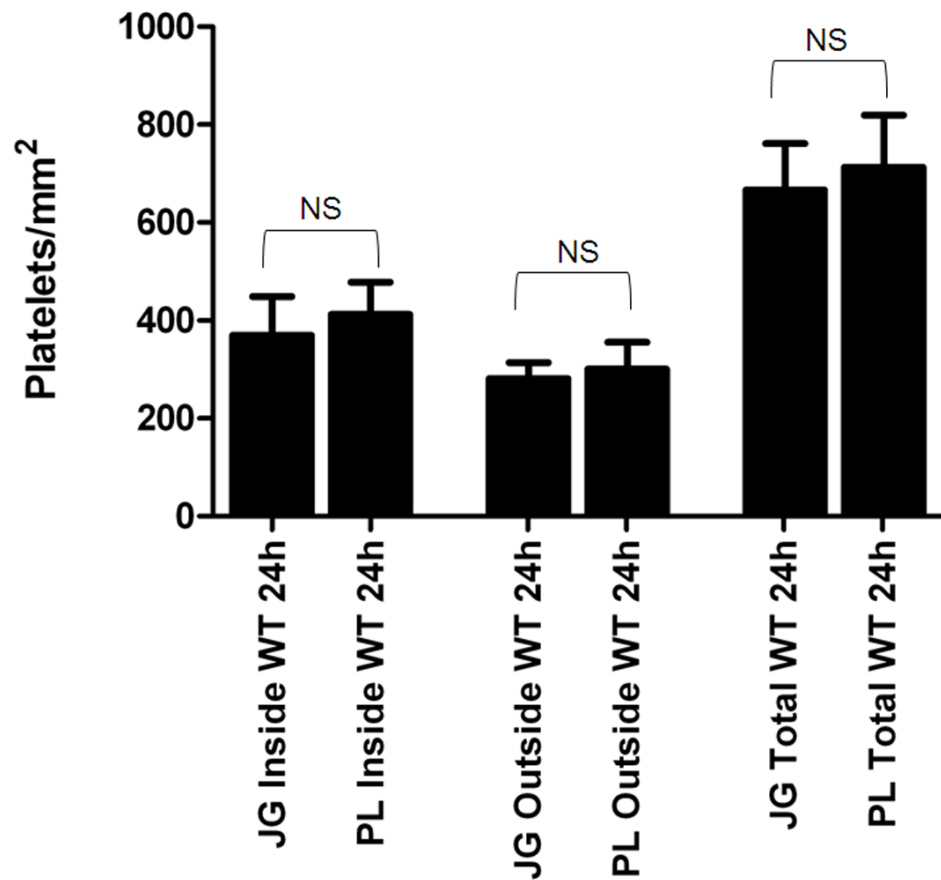


Figure IV: WT central corneal basal epithelial cell densities before and after epithelial abrasion

Central basal epithelial cells in uninjured mice appear tightly packed (**A**). One day after injury (**B**), central basal cell density appears to be lower than uninjured basal cell density. Central basal epithelial cell density appears similar to uninjured levels by 4 days post-injury (**C**). Scale bar = 20 μm

